

**Exploring complementary proteomic approaches for
biomarker discovery in renal cell carcinoma**

Rebecca Louise Shreeve

Submitted in accordance with the requirements for the degree of
Doctor of Philosophy

The University of Leeds

Faculty of Medicine and Health

January 2015

The candidate confirms that the work submitted is her own and that appropriate credit has been given where reference has been made to the work of others.

This copy has been supplied on the understanding that it is copyright material and that no quotation from the thesis may be published without proper acknowledgement.

The right of Rebecca Louise Shreeve to be identified as Author of this work has been asserted by her in accordance with the Copyright, Designs and Patents Act 1988.

© 2015 The University of Leeds and Rebecca Louise Shreeve

Acknowledgements

Firstly I would like to acknowledge the support, guidance, and continued assistance of my supervisors Roz Banks, Alexandre Zougman, Naveen Vasudev, and Peter Selby, who have provided guidance and direction throughout the duration of this degree. They have taught me invaluable lessons in the many facets of scientific research, each through their own ways, and I am indebted to their support.

Extra special thanks must also go to Rachel Craven, James Hornigold, and Michelle Hutchinson, who have not only given their expert knowledge and experience, but who have become very special friends throughout the process.

I would also like to thank David Cairns and Claire Taylor, both of whom have assisted in areas of the research that were outside of my expertise. Similarly, the histology lab (especially Filomena) and many other groups throughout the Leeds Institutes for Molecular Medicine have helped in too many ways to mention, and I am grateful for their support. I must also thank the sample processing team and the rest of the Clinical and Biomedical Proteomics Group, as the assistance they have provided has been paramount in the completion of this PhD.

Finally I would like to thank my family and friends. They have stood by my side throughout the many years of my education, and I would not be here today if it were not for their unfaltering love and support. So, to my mum and dad (Colin and Val Shreeve), brothers (Mark and Tim Shreeve), and my wonderful friends, thank you!

Abstract

Renal cell carcinoma (RCC) is one of the top ten most common malignancies worldwide. The field of clinical proteomics has seen successes in recent years, and advancements in technology is making ever more possible the ability to answer clinical questions. This study used proteomics to investigate two key clinical questions in RCC biology. Firstly, two comparative studies were performed to investigate biomarkers that may predict response to sunitinib, the predominant drug used to treat metastatic RCC. Serum (12 patients) and FFPE tissue (16 patients) samples from sunitinib responding and non-responding patients were analysed by liquid chromatography-tandem mass spectrometry (LC-MS/MS), to discover novel markers of response. Two candidate biomarkers were initially validated using Western blot or immunohistochemistry. Two serum (IGFBP5, CDH1) and two FFPE tissue (CD70, hCAP18) proteins were identified as promising candidate biomarkers, initial validation of CD70 and hCAP18 was performed. Secondly, furthering the understanding of RCC biology may improve rational drug design and biomarker identification. Five cell lines carrying mutations of VHL, the predominant tumour suppressor gene in RCC, were compared to investigate the proteomic impact of VHL mutation. The scaffold protein IRS2 was identified as highly expressed in the absence of VHL, and this protein was initially validated by Western blot in *in vitro* cell lines. The techniques used in this study revealed logical biological alterations, of which three proteins were validated using an independent technique. Further validation of the identified proteins is on-going, with the hope that they may impact upon patient care. The advantages and disadvantages of the proteomic analysis of serum, FFPE tissue, and *in vitro* cell lines is discussed.

Table of Contents

Acknowledgements	iii
Abstract	iv
Table of Contents	v
List of Tables	x
List of Figures	xii
Abbreviations	xiv
1. Introduction	17
1.1. Renal cancer	17
1.1.1. Aetiology.....	17
1.1.2. Pathology	18
1.1.3. Clinical Presentation and Diagnosis.....	20
1.1.4. Staging and Prognosis.....	20
1.2. Biology of RCC.....	23
1.2.1. VHL mutations in RCC.....	24
1.2.2. VHL functions in RCC.....	25
1.2.3. The hypoxic response.....	27
1.2.4. Alternative functions of VHL.....	29
1.3. RCC Therapeutics.....	31
1.3.1 Immunotherapy.....	31
1.3.2. Angiogenesis inhibitors	31
1.3.2.1 TKI inhibitors	32
1.3.2.2. mTOR inhibitors	35
1.3.2.3. Monoclonal antibodies.....	36
1.3.3. Emerging therapies.....	36
1.4. Biomarkers in RCC management	37
1.4.1. Diagnostic biomarkers	38
1.4.2. Prognostic biomarkers	39
1.4.3. Predictive and pharmacodynamic biomarkers.....	41
1.4.3.1. Protein biomarkers	42
1.4.3.2. Genetic markers.....	50
1.4.3.3. Clinical biomarkers.....	51
1.4.3.4. Imaging biomarkers.....	53
1.4.3.5. Circulating cells.....	54

1.4.4. Resistance to anti-angiogenic therapy	55
1.5. Clinical proteomics	57
1.5.1. RCC proteomics	58
1.5.2. Proteomic techniques	60
1.5.3. Proteomic analysis of different sample types	62
1.5.3.1. Serum proteomics	62
1.5.3.2. Tissue proteomics	64
1.5.3.3. Cell based proteomics	65
1.6. Study aims	66
2. Materials and Methods.....	68
2.1. Sample collection and preparation	68
2.1.1. Patients	68
2.1.1.1 Serum samples	68
2.1.1.2. Tissue samples	70
2.1.2. RCC cell lines	71
2.1.2.1 Cell culture	72
2.2. Protein Enrichment, Extraction, and Separation	72
2.2.1. Immunodepletion of serum with a MARS14 column.....	72
2.2.2. Generation of cell lysates from RCC cell lines	73
2.2.3 Protein extraction from FFPE tissue	74
2.2.4. Immunoprecipitation	74
2.2.5. 1D SDS-PAGE	75
2.3. Protein Assays	76
2.3.1. Bradford assay	76
2.3.2. Spectrofluorometer	76
2.4. Staining proteins.....	78
2.4.1. Colloidal Coomassie blue staining of 1D SDS-PAGE gels	78
2.4.2. Silver staining of 1D SDS-PAGE gels	78
2.4.3. Haematoxylin and Eosin staining of tissue sections	79
2.5. Tryptic digestion of proteins.....	79
2.5.1. On-membrane digestion of serum proteins	79
2.5.2. Filter Aided Sample Preparation (FASP) digestion of tissue extracted proteins	80
2.5.2.1. Peptide clean up using STAGE Tips	81
2.5.3. Suspension Trapping (STrap) digestion of cell lysate proteins.....	82

2.6. Protein Identification	83
2.6.1. LTQ-Orbitrap Velos Mass Spectrometry	84
2.6.2. Protein Identification using MaxQuant.....	85
2.7. Validation of protein expression profiles	85
2.7.1. Western Blotting	85
2.7.2. Immunohistochemistry	86
2.8. Data Analysis	88
2.8.1. Statistics	88
2.8.2. Bioinformatics	89
2.9. Genomic and transcriptomic methods	89
2.9.1. DNA sequencing.....	89
2.9.2. RT-PCR.....	92
3. The analysis of serum for the discovery of biomarkers predictive of response to sunitinib.....	94
3.1. Introduction	94
3.1.1. Aims	95
3.2. Patient selection.....	95
3.2.1. Patients selected for the baseline study.....	96
3.2.2. Patients selected for the longitudinal study	96
3.3. Using a MARS14 column to immunodeplete serum samples	101
3.4. Analysis of patient serum collected at baseline	103
3.4.1. Differential protein expression in the baseline serum of responders and non-responders	104
3.4.2. Bioinformatic analysis of baseline serum proteins.....	108
3.5. Analysis of patient serum collected longitudinally	109
3.5.1. Differential protein expression in longitudinal serum between responders and non-responders	111
3.5.2. Reproducibility of label-free mass spectrometry.....	114
3.5.3. Bioinformatic analysis of longitudinal serum proteins	115
3.6. Validation of differential serum protein expression.....	116
3.7. Discussion.....	117
3.7.1. Serum as a source of clinical biomarkers.....	118
3.7.2. Identification of serum biomarkers using mass spectrometry ...	120
3.7.2.1. Biomarker candidates identified from baseline serum ..	122
3.7.2.2. Biomarker candidates identified from longitudinal serum.....	127
3.7.3. Concluding remarks.....	130

4. Using <i>in vitro</i> cell lines to discover early markers of renal cell carcinoma pathogenesis	135
4.1. Introduction	135
4.1.1. Aims	136
4.2. Characterisation of VHL disease-specific cell lines	136
4.2.1. Confirmation of <i>vhl</i> mutations.....	137
4.2.2. Western blot confirmation of hypoxic phenotype	138
4.3. Comparison of plus/minus VHL proteome	140
4.3.1. Differentially expressed proteins between WTHAB6 and RCC4/T.....	143
4.3.1.1. Proteins upregulated in WTHAB6 versus RCC4/T.....	145
4.3.1.2. Proteins upregulated in RCC4/T versus WTHAB6.....	146
4.4. Investigation into IRS2 expression	151
4.4.1. Western blot examination of IRS2 expression.....	151
4.4.2. Investigation into IRS2 expression in clinical samples from RCC patients	153
4.4.3. Examination of IRS2 transcripts.....	153
4.5. Investigation into the binding partners of IRS2	155
4.6. Proteomic analysis of VHL disease mutant cell lines	160
4.6.1. Proteins differentially regulated in Type 1 and Type 2B	162
4.6.1.1. Heat map comparison of VHL disease-cell line proteomes	163
4.6.1.2. Comparison of data by filtering.....	166
4.6.2. Candidate early biomarkers in RCC pathogenesis.....	166
4.7 Discussion.....	169
4.7.1. Proteomic comparison of the plus/minus VHL cell lines WTHAB6 and RCC4/T	170
4.7.1.1. Insulin Receptor Substrate-2.....	171
4.7.1.2. Additional differentially expressed proteins.....	178
4.7.2. Proteomic comparison of the VHL disease-cell lines.....	183
4.7.3. Concluding remarks.....	187
5. Using FFPE tissue as a source for discovering predictive biomarkers	190
5.1 Introduction	190
5.1.1. Aims	191
5.2 Patient selection.....	191
5.2.1. Patient timelines	193
5.2.2. Pathological review of FFPE tissue blocks.....	195

5.3. Optimisation of sample injection number	196
5.4. Mass spectrometric analysis of FFPE samples	202
5.4.1. Proteins elevated in FFPE tissue from non-responders	205
5.4.2. Proteins elevated in FFPE tissue from the responders.....	212
5.4.3. Cross-over of candidate proteins between the FFPE and serum analyses.....	215
5.5. Validation of protein expression patterns	218
5.5.1. Candidate biomarkers.....	218
5.5.2. Validation of CD70 expression pattern.....	220
5.5.2.1. Analysis of the heterogeneity of CD70 expression	225
5.5.3. Investigation of hCAP18 and PRTN3 expression	227
5.6. Discussion.....	228
5.6.1. Mass spectrometry optimisation.....	230
5.6.2. Differentially expressed proteins in responders and non- responders.....	231
5.6.2.1. Elevated proteins in the FFPE tissue of non- responders	232
5.6.2.2. Elevated proteins in the FFPE tissue of responders	236
5.6.3. Concluding remarks and study limitations.....	241
6. Final Discussion	244
List of References.....	248
Appendix 1 List of Suppliers.....	290

List of Tables

Table 1.0.1: Heidelberg Classification of RCC	19
Table 1.0.2: 2009 TNM staging classification system	21
Table 1.0.3: TNM stage grouping	22
Table 1.0.4: Integrated staging systems for outcome prediction of RCC patients.....	23
Table 1.0.5: Subtypes of VHL disease and their neoplastic profile	25
Table 1.0.6: Potential serum biomarkers of clinical benefit in sunitinib treated patients	45
Table 1.0.7: Potential tissue biomarkers of clinical benefit in sunitinib treated patients	47
Table 2.0.1: RECIST criteria used to assess response to therapy in solid tumours	69
Table 2.0.2: Proteins immunodepleted by the MARS-14 column	73
Table 2.0.3: Antibodies used in Western blots of cell and tissue lysates	86
Table 2.0.4: Antibodies used in immunohistochemistry studies	88
Table 2.0.5: Forward and reverse primers used for PCR and sequencing of <i>VHL</i>	91
Table 3.0.1: Overview of patients used in both arms of the serum study	98
Table 3.0.2: Overview of differentially expressed proteins in baseline serum	105
Table 3.0.3: Baseline serum proteins selected as candidate biomarkers.....	106
Table 3.0.4: Overrepresented biological functions in the baseline dataset	109
Table 3.0.5: Proteins selected as candidate biomarkers in longitudinal serum	112
Table 3.0.6: Overrepresentation analysis of longitudinal serum samples.....	116
Table 4.0.1 VHL disease cell line models	137
Table 4.0.2: Numbers of differentially expressed proteins in WTHAB6 and RCC4/T	145
Table 4.0.3: Proteins upregulated in WTHAB6 versus RCC4/T.	148
Table 4.0.4: Proteins upregulated in RCC4/T versus WTHAB6	149
Table 4.0.5: Background VHL mutations present in three RCC cell lines.....	153

Table 4.0.6: Proteins enriched by IRS2 immunoprecipitation	159
Table 4.0.7: Proteins upregulated in the RCC forming cell lines	168
Table 4.0.8: Proteins downregulated in the RCC forming cell lines ...	168
Table 5.0.1: Characteristics of patients in the FFPE study.....	192
Table 5.0.2: Increase in number of identifications per injection number	199
Table 5.0.3: Increase in identifications between independent and combined MaxQuant analysis.....	201
Table 5.0.4: Number of protein fold changes in the non- responders	205
Table 5.0.5: Proteins upregulated in the non-responders	207
Table 5.0.6: Upregulated pathways in non-responder elevated proteins	210
Table 5.0.7: Number of protein fold changes in the responders.....	212
Table 5.0.8: Proteins upregulated in the FFPE tissue of responders	213
Table 5.0.9: Upregulated pathways amongst proteins elevated in responding patients.....	216
Table 5.0.10: CD70 staining intensity of responders and non- responders	222
Table 5.0.11: CD70 expression in different blocks in responders and non-responders	226

List of Figures

Figure 1.0.1: Histology of RCC subtypes	19
Figure 1.0.2: HIF and VHL in normoxia and pseudohypoxia.	28
Figure 2.0.1: Sunitinib cycles and sample collection.....	70
Figure 2.0.2: Location of VHL mutations in RCC4 transfectants	71
Figure 3.0.1: Chromatogram from a representative immunodepletion	102
Figure 3.0.2: 1D-PAGE analysis of depleted serum	102
Figure 3.0.3: Overlap of proteins identified in baseline serum in non-responders and responders	104
Figure 3.0.4: Baseline candidates chosen for downstream investigation	107
Figure 3.0.5: Overlap of proteins identified in longitudinal serum in responders and non-responders	110
Figure 3.0.6: Longitudinal candidates	113
Figure 3.0.7: Correlation of data acquired during separate label-free batches	115
Figure 4.0.1: Sanger sequencing of the VHL disease cell line mutations	138
Figure 4.0.2: Western blot characterisation of VHL disease-cell line phenotypes	140
Figure 4.0.3: Presence/absence analysis of proteins present in RCC4/T and WTHAB6	141
Figure 4.0.4: Upregulation of CA9, PLIN2, and HMOX1 in RCC4/T	142
Figure 4.0.5: Differential protein expression in RCC4/T and WTHAB6	147
Figure 4.0.6: IRS2 expression in RCC4/T and 786-0	152
Figure 4.0.7: Presence of IRS2 mRNA in RCC4/T and WTHAB6	155
Figure 4.0.8: SDS-PAGE analysis of immunoprecipitated IRS2	156
Figure 4.0.9: Western blot analysis of immunoprecipitated IRS2	157
Figure 4.0.10: Enrichment of IRS2 and YWHAQ in IRS2 immunoprecipitation	158
Figure 4.0.11: Shared proteins between the five VHL disease cell lines	161
Figure 4.0.12: Expression of known RCC markers in VHL disease transfectants	162

Figure 4.0.13: Heat maps of significantly different proteins in VHL transfectants of RCC4	164
Figure 4.0.14: Significantly different proteins in the Type 1 and Type 2B VHL disease cell lines.....	165
Figure 4.0.15: Differential protein expression in the RCC forming cell lines	167
Figure 5.0.1: Timelines for the responding and non-responding patients.	194
Figure 5.0.2: FFPE H&E stained sections for pathological review.....	196
Figure 5.0.3: Overlap in identifications between multiple LFQ injections	198
Figure 5.0.4: Correlation of quantitation values for 2 and 3 injections	200
Figure 5.0.5: Proteins unique and shared by responders and non-responders in FFPE tissue	203
Figure 5.0.6: Unique protein identifications in responders and non-responders based on peptide number	204
Figure 5.0.7: Elevated FFPE tissue proteins in the non-responders ..	206
Figure 5.0.8: Cell-to-cell signalling interaction network containing proteins elevated in non-responders	211
Figure 5.0.9: Proteins elevated in the FFPE tissue of responders.....	214
Figure 5.0.10: Cell-to-cell signalling interaction network containing proteins elevated in responders	217
Figure 5.0.11: Clinical features of patients and quantitative levels of target proteins.....	219
Figure 5.0.12: Antigen retrieval for CD70 staining on FFPE.....	221
Figure 5.0.13: IHC validation of CD70 staining in responders and non-responders.....	223
Figure 5.0.14: Western blot of hCAP18 in responders and non-responders	227

Abbreviations

ABC	Ammonium Bicarbonate
CA9	Carbonic Anhydrase 9
ccRCC	Clear cell (conventional) RCC
CI	Confidence Interval
CR	Complete Response
DTT	Dithiothrietol
ECM	Extracellular Matrix
ELISA	Enzyme Linked Immunosorbent Assay
FASP	Filter Aided Sample Preparation
FFPE	Formalin Fixed-Paraffin Embedded
H&E	Haematoxylin and Eosin
HIF	Hypoxia Inducible Factor
HPLC	High Performance Liquid Chromatography
HR	Hazard Ratio
IAA	Iodoacetamide
IHC	Immunohistochemistry
LC-MS/MS	Liquid Chromatography-Tandem Mass Spectrometry
LFQ	Label Free Quantitation
mRCC	Metastatic RCC
MRM	Multiple Reaction Monitoring
MWCO	Molecular Weight Cut Off

ORR	Objective Response Rate
OS	Overall survival
PBS	Phosphate Buffered Saline
PCR	Polymerase Chain Reaction
PD	Progressive Disease (check)
PFS	Progression Free Survival
PR	Partial Response
PS	Performance Status
pVHL	Protein VHL
RCC	Renal Cell Carcinoma
RT-PCR	Reverse Transcription Polymerase Chain Reaction
RTK	Receptor Tyrosine Kinase
SD	Stable Disease
SDS	Sodium Dodecyl Sulphate
SDS-PAGE	Sodium Dodecyl Sulphate – Polyacrylamide Gel Electrophoresis
SNP	Single Nucleotide Polymorphism
STAGE	STop And Go Extraction
STrap	Suspension Trapping
TBS	Tris Buffered Saline
TBST	Tris Buffered Saline – Tween
TKI	Tyrosine Kinase Inhibitor
TNM	Tumour Node Metastasis

TTP	Time to Progression
VEGF	Vascular Endothelial Growth Factor
VEGFR	Vascular Endothelial Growth Factor Receptor
VHL	Von Hippel Lindau

1. Introduction

1.1. Renal cancer

Kidney cancer represents one of the ten most common adult cancers. Over 320,000 new cases were diagnosed and over 140,000 people died, worldwide, in 2012 (Ferlay J, 2013). Incidence peaks in the sixth decade of life, and is higher in more developed regions of the world. Earlier onset (mid 40s) is more commonly associated with inherited forms of the disease. Kidney cancer prevalence has been steadily increasing for a number of decades (Mathew et al., 2002), an effect which has been only partially linked to improved early diagnosis through more liberal use of imaging techniques. Men are twice as likely to develop kidney cancer as women, with a global age standardised incidence rate of 6.0 per 100,000 individuals, compared to 3.1 in women, though a particular acceleration in female incidence has been observed in recent years (Mathew et al., 2002).

1.1.1. Aetiology

Although around 2-4% of renal cell carcinoma (RCC) is hereditary (Cairns, 2010), the majority of cases are sporadic. Established lifestyle and iatrogenic risk factors associated with RCC are smoking (Hunt et al., 2005), obesity (Renehan et al., 2008), pulmonary hypertension (Weikert et al., 2008), and acquired renal cystic disease (Port et al., 1989). Available data suggests an elevated risk of RCC with increased dietary fat and protein intake (Armstrong and Doll, 1975), and an inverse relationship with fruit and vegetable intake (Lee et al., 2009). Other suspected risk factors include level of exercise and alcohol consumption, which appear to demonstrate an inverse relationship with incidence (Chow et al., 2010).

1.1.2. Pathology

Approximately 90% of kidney cancers are RCC (Valera and Merino, 2011) and these manifest in a variety of histologies, of which the most common (60-80%) subtype is conventional (clear cell) RCC (ccRCC) (Brannon and Rathmell, 2010). The remainder is mostly made up by papillary (10-15%), chromophobe (5-10%), and collecting duct (<1%) subtypes (Table 1.0.1) (Kovacs et al., 1997), although variants within each subtype often results in an overlap in presentation. Benign renal oncocytomas are morphologically similar to chromophobe RCC and their differential diagnosis can be difficult, however they lack the genetic changes found in RCCs (Herbers et al., 1998). Clear cell RCC originates in the proximal tubules of the nephron and is so-called due to the clear appearance of the cytoplasm on inspection by light microscopy, following extraction of the intracellular lipid and glycogen deposits with organic solvents (Figure 1.0.1A). Histologically, a variety of architectural patterns may be observed in ccRCC including alveolar, solid, and acinar forms. The malignant epithelial cells are heavily interspersed with arborising vessels, and are easily distinguished from papillary RCC (pRCC), which also originates from the proximal tubules but is so called due to the papillary growth pattern observed in this renal tumour (Figure 1.0.1B). Chromophobe RCC, which originates in the intercalated cells of the distal tubules, is distinctive due to the eosinophilic cytoplasm (Figure 1.0.1C). Sarcomatoid changes, a histological progression associated with aggressive disease, may be observed in all histological subtypes and it is therefore no longer recognised as a unique histotype (Jiang et al., 1998).

Table 1.0.1: Heidelberg Classification of RCC

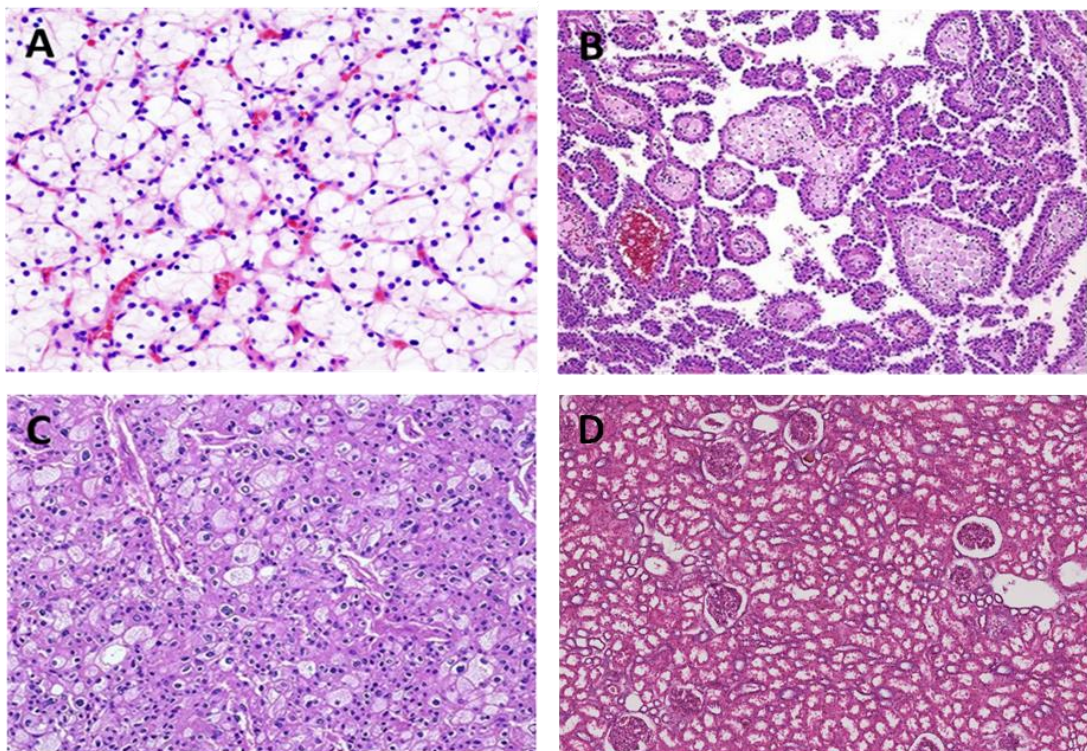
Subtype	Prevalence	Originating cells	Major genetic abnormalities
Conventional (clear cell)	60-80%	Proximal convoluted tubule	Loss of 3p, 6q, 8p, 9p, 14q. Gains at 5q22.
Papillary	10-15%	Proximal convoluted tubule	Trisomy of 3q, 7, 8, 12q, 16q, 17, 20q. Loss of 1p, 4q, 6q, 9p, 13q, X, Y
Chromophobe	5-10%	Intercalated cells of distal tubules	Loss of 1, 2, 6, 10, 13, 17, 21
Collecting duct	<1%	Medullary collecting duct	No consistent pattern
Unclassified	3-5%	NA	NA

Adapted from (Kovacs et al., 1997), (Jiang et al., 1998) and (Prasad et al., 2006).

NA, not available.

Figure 1.0.1: Histology of RCC subtypes

Clear cell (A), papillary (B), chromophobe (C), and normal renal cortex (D) tissue, as viewed by haematoxylin/eosin stained sections.



1.1.3. Clinical Presentation and Diagnosis

Early diagnosis of ccRCC can be difficult due to its frequent asymptomatic presentation; the classical triad of symptoms - haematuria, abdominal pain, and a palpable abdominal mass - are infrequently presented together. Amongst symptomatic patients, macroscopic or microscopic haematuria is most common, followed by abdominal pain and mass. Less common symptoms include fever, fatigue, coughing, and weight loss. Approximately 30% of patients present with locally advanced or metastatic disease; a further 30% with apparent localised disease at presentation will relapse after surgery (Hollingsworth et al., 2007). At present, many RCCs are incidentally detected due to imaging-based investigations of other symptoms (Ljungberg et al., 2010, Jayson and Sanders, 1998).

1.1.4. Staging and Prognosis

Following diagnosis, management of localised RCC usually involves surgical resection. Determination of prognosis is a crucial step in cancer management and a variety of parameters are used to assess this, including anatomical and clinical features. Stage, grade, platelet count, anaemia, localised symptoms, and patient performance status (European Cooperative Oncology Group (ECOG) performance status or the Karnofsky performance status) are the most widely used clinical features in determining a patient's prognosis. Tumour staging is performed using the tumour-node-metastasis (TNM) system (Tables 1.0.2 and 1.0.3), which assesses anatomical tumour features: size and extent of tumour invasion, lymph node involvement, and presence of metastases. Nuclear grading is commonly performed using the Fuhrman grading, which is a system based on histological characteristics of the tumour.

Table 1.0.2: 2009 TNM staging classification system

Anatomical staging of RCC tumours according to the Tumour Node Metastasis system. (Sobin et al., 2009)

Primary tumour (T)	
TX	Primary tumour cannot be assessed
T0	No evidence of primary tumour
T1	Tumour 7 cm or less in greatest dimension, limited to the kidney
T1a	Tumour 4 cm or less in greatest dimension, limited to the kidney
T1b	Tumour more than 4 cm but not more than 7 cm in greatest dimension
T2	Tumour more than 7 cm in greatest dimension, limited to the kidney
T2a	Tumour more than 7 cm in greatest dimension but less than 10cm
T2b	Tumours greater than 10 cm limited to the kidney
T3	Tumour extends into major veins or perinephric tissues, but not into the ipsilateral adrenal gland and not beyond Gerota's fascia
T3a	Tumour grossly extends into the renal vein or its segmental (muscle-containing) branches, or tumour invades perirenal and/or renal sinus (peripelvic) fat but not beyond Gerota's fascia
T3b	Tumour grossly extends into the vena cava below diaphragm
T3c	Tumour grossly extends into vena cava or its wall above the diaphragm or invades the wall of the vena cava
T4	Tumour invades beyond Gerota's fascia (including contiguous extension into the ipsilateral adrenal gland)
Regional lymph nodes (N)	
NX	Regional lymph nodes cannot be assessed
N0	No regional lymph node metastasis
N1	Metastasis in a single regional lymph node
N2	Metastasis in more than one regional lymph node
Distant metastasis (M)	
M0	No distant metastasis
M1	Distant metastasis

Table 1.0.3: TNM stage grouping

Staging of RCC tumours according to the Tumour Node Metastasis system. (Sobin et al., 2009)

Stage	T stage	N stage	M stage
Stage I	T1	N0	M0
Stage II	T2	N0	M0
Stage III	T3	N0	M0
	T1, T2, T3	N1	M0
Stage IV	T4	Any N	M0
	Any T	N2	M0
	Any T	Any N	M1

A number of nomograms integrating varying combinations of these and other features have been developed to aid prognostication (Sun et al., 2011) and these have been shown to be more effective in predicting prognosis than any of the independent prognostic features alone (Table 1.0.4). The most commonly used nomograms include the UCLA Integrated Staging System (UISS) (Zisman et al., 2001), the Stage, Size, Grade, and Necrosis (SSGN) system (Frank et al., 2002), and the postoperative Karakiewicz nomogram (Karakiewicz et al., 2007a). Staging systems using molecular markers, such as the Molecular Integrated Staging System (MISS) (Table 1.0.4) have also been developed, and a number of individual molecular biomarkers have been investigated for their prognostic potential, but as yet none have been shown to improve upon the current systems for determining prognosis.

Table 1.0.4: Integrated staging systems for outcome prediction of RCC patients

System	Histological subtype	Variable	Reference
UISS (UCLA Integrated Staging System)	RCC	TNM stage; performance status; Fuhrman grade	(Zisman et al., 2001)
SSGN (Stage, Size, Grade, and Necrosis score)	Conventional	TNM stage; Fuhrman grade; pathological size; necrosis	(Frank et al., 2002)
Postoperative Karakiewicz	Conventional, papillary, chromophobe	TNM stages; tumour size; Fuhrman grade; symptoms classification	(Karakiewicz et al., 2007a)
MISS (Molecular Integrated Staging System)	Conventional	UISS clinical variables; Ki-67; p53; gelsolin; CA9; CAXII; PTEN; EpCAM; vimentin	(Kim et al., 2005, Kim et al., 2004)

1.2. Biology of RCC

There are four hereditary forms of RCC. von Hippel-Lindau (VHL) disease, hereditary papillary RCC (HPRCC), and Birt-Hogg-Dubé (BHD) syndrome are the inherited forms of the clear cell, papillary type 1, and chromophobe subtypes, respectively (Linehan et al., 2009). The fourth familial RCC is hereditary leiomyomatosis and RCC (HLRCC), the renal tumours observed with this autosomal dominant familial syndrome tend to be of less common subtypes including papillary type 2, and collecting duct.

The most common genetic alteration in sporadic ccRCC is inactivation of the von Hippel Lindau (VHL) gene, which is located on chromosome 3p25 (Latif et al.,

1993). Biallelic somatic VHL inactivation occurs in the majority of non-familial ccRCC cases (Young et al., 2009, Nickerson et al., 2008), mostly through loss of heterozygosity (LOH) of chromosome 3p, point mutation, or through promoter hypermethylation. Other chromosomal abnormalities frequently observed in ccRCC include deletions at 6q, 8p, 9p, and 14q, and duplications at band 5q22 (Kovacs et al., 1997). Recently, large scale targeted and whole exome sequencing studies have revealed a number of other frequently mutated genes, with a marked prevalence for genes involved in chromatin biology. The most commonly mutated gene, after *VHL*, is polybromo 1 (*PBRM1*) (Varela et al., 2011). Other mutated genes include SET domain containing 2 (*SETD2*) (Dalgliesh et al., 2010), lysine (K)-specific demethylase 5C (*JARID1C*) (Dalgliesh et al., 2010), lysine (K)-specific demethylase 6A (*KDM6A*) (Dalgliesh et al., 2010), and BRCA1 associated protein-1 (*BAP1*) (Pena-Llopis et al., 2012). Interestingly, *PBRM1*, *BAP1*, and *SETD2* are all located at 3p21, and would therefore be lost alongside VHL in a 3p loss (Gossage et al., 2014). Oncogenes do not seem to be amplified in ccRCC; genotyping of 17 common oncogenes in 83 RCC samples revealed only one BRAF and one HRAS mutation (Thomas et al., 2007).

1.2.1. VHL mutations in RCC

Significant steps in the understanding of the genetic and functional landscape of RCC have come from studying patients with VHL disease. This autosomal recessive syndrome, which is characterised by germline inactivation of one *VHL* allele, predisposes the sufferer to a variety of malignancies which include, but are not limited to, pheochromocytomas, central nervous system haemangioblastomas, and RCCs. Loss of heterozygosity (LOH) of the second allele occurs in the majority of cases, and the resulting neoplasms that form are frequently multifocal in nature (Linehan et al., 2009). More than 150 germline VHL disease mutations have been

classified into four subtypes by correlation of genotype with clinical presentation of the disease (Kim and Kaelin, 2004) (Table 1.0.5). Type 1, which generally involves major VHL disruptions such as truncations, and Type 2B, which involves more minor VHL mutations, are the two subtypes that lead to the development of RCC (Maher et al., 2011).

Table 1.0.5: Subtypes of VHL disease and their neoplastic profile

VHL disease subtypes are characterised by their neoplastic predisposition to RCC, haemangioblastomas, and pheochromocytomas.

Subtype	Tumour predisposition
Type 1	RCC and haemangioblastomas
Type 2A	Haemangioblastomas and pheochromocytoma
Type 2B	RCC, haemangioblastomas and pheochromocytoma
Type 2C	Pheochromocytoma

1.2.2. VHL functions in RCC

The VHL protein is comprised of three exons, which together form two domains: alpha and beta. The alpha domain is formed from exon 3 and is responsible for elongin C binding. The beta domain is made up from exons 1 and 2, and is responsible for HIF, PKC, Jade1, Sp1, and microtubule binding. Exon 1 also contains an octaplex repeat of the motif GXEEX, which is of unknown function. The *vhl* gene (Latif et al., 1993) encodes a full length protein 213 amino acids in length, internal translation initiation gives rise to a truncated form lacking the first 53 amino acids (Iliopoulos et al 1998, Schoenfeld et al 1998; Blakeship et al, 1999). The smaller pVHL 18 isoform is found in both the nucleus and the cytoplasm, whereas the larger pVHL 24 isoform is found primarily in the cytoplasm (Iliopoulos 1998),

however both appear to retain tumour suppressor activity (Stebbins et al 1999). The protein product of VHL (pVHL) acts as the substrate recognition subunit of an E3 ubiquitin-ligase complex, which also contains cullin-2 (CUL2), RING-box protein (RBX) 1, elongin B, and elongin C.

VHL is perhaps most well-known for targeting members of the hypoxia inducible factor (HIF) family for destruction (Maxwell et al., 1999). HIF is a heterodimeric transcription factor consisting of a labile α subunit (HIF-1 α , HIF-2 α , and HIF-3 α) and a constitutively expressed, stable β subunit (HIF-1 β /ARNT) (Wang et al., 1995). VHL-defective cell lines have been shown to display a bias towards HIF-2 α expression (Maxwell et al 1999; Krieg et al 2000), and HIF-2 α has since been shown to have tumour promoting properties, in contrast to HIF-1 α which appears to repress tumour growth, in a xenograft model of renal cancer (Raval et al, 2005). Under normal conditions HIF is responsible for allowing cells to survive in a hypoxic environment (Semenza, 1998); over 100 survival related genes are under the control of this transcription factor (Ke and Costa, 2006), including proteins involved in glucose metabolism (e.g. GLUT-1), angiogenesis (e.g. VEGF), and apoptosis (e.g. NIP3). Upstream control of HIF is via the phosphatidylinositol-3-kinase (PI3K)/Akt/mTOR cascade, a pathway which has recently been identified as highly important in RCC pathogenesis (Weinstein et al., 2013, Ciriello et al., 2013). Downstream control of HIF is via proteasomal degradation; hydroxylation of HIF on two prolines and one asparagine, which occurs continuously in the presence of oxygen, allows VHL to recognise HIF (Figure 1.0.2) (Ohh et al, 2000). Ubiquitination and subsequent destruction via the proteasomal pathway prevents inappropriate inactivation of the hypoxic response. Loss of VHL during VHL pathogenesis creates a pseudohypoxic state, whereby HIF is stabilised and a plethora of tumour survival genes are switched on.

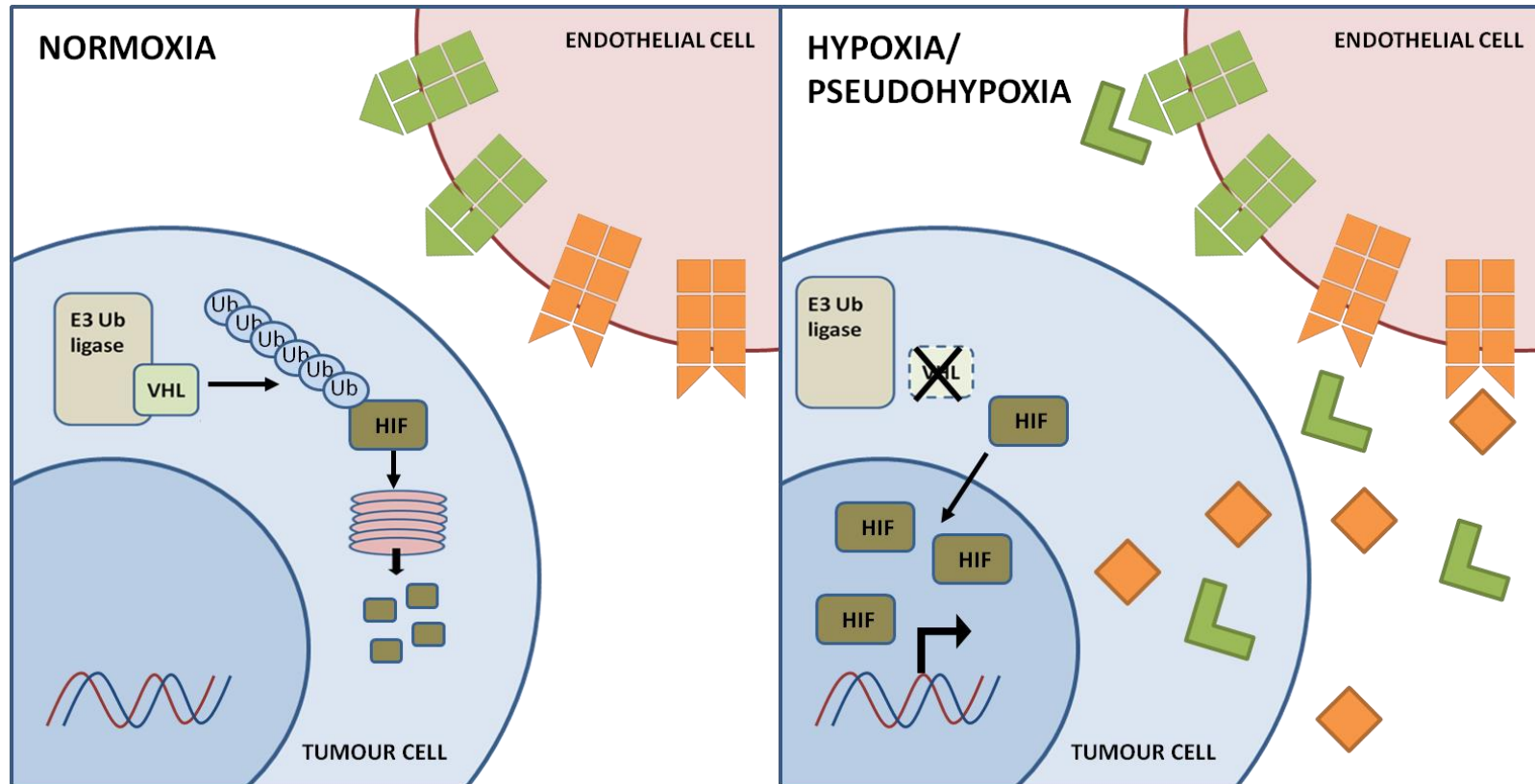
1.2.3. The hypoxic response

As the diffusion distance of oxygen in tissues is only around 100-200µm (Hoeben et al., 2004), angiogenesis is a key hurdle that must be achieved by the developing cancer to enable growth past the microscopic size (Folkman, 2007). Steps in the hypoxic response include a switch to glycolysis to allow anaerobic respiration, also known as the Warburg effect (Warburg, 1956), as well as neovascularisation and angiogenesis to enable a source of nutrients and oxygen, upregulation of anti-apoptotic proteins to avoid hypoxia-induced death, and upregulation of invasion pathways to allow hypoxic escape.

Angiogenesis is a multi-stepped process during which new blood vessels form from pre-existing vessels. VEGF is the most important growth factor in angiogenesis, and to date seven VEGF family members have been identified (Hoeben et al., 2004), of which VEGF-A is predominant. The VEGF receptors are receptor tyrosine kinases (RTKs) that signal via multiple pathways (Olsson et al., 2006), and include the members VEGFR-1, -2, -3, and flt-3. Sensing of VEGF by the VEGF receptors initiates the proliferation and migration of endothelial cells in neighbouring vessels towards the chemotactic signal. Stabilisation of the new vasculature is driven by the platelet derived growth factor (PDGF), which stimulates differentiation of the perivascular cells which surround the newly formed vascular endothelial cells.

Figure 1.0.2: HIF and VHL in normoxia and pseudohypoxia.

During normoxia HIF is targeted for destruction via the proteasome. The inactivation of VHL leads to the stabilisation of HIF, and the switching on of angiogenesis related proteins.



1.2.4. Alternative functions of VHL

Though the VHL-HIF axis has received the most attention, additional pVHL interactors have revealed roles other than proteasomal targeting and which support the role for VHL as a tumour suppressor. Restoration of VHL function is sufficient to suppress *in vivo* tumour formation (Iliopoulos et al., 1995, Schoenfeld et al., 1998, Gnarr et al., 1996), reinforcing its role as a tumour suppressor protein. The role of HIF-2 α in oncogenic transformation is disputed, whilst inhibition of HIF-2 α appears to be sufficient to prevent tumour growth (Kondo et al., 2002, Kondo et al., 2003), it seems that this does not inhibit all tumourigenic functions; expression of RCC markers and impaired extracellular matrix interactions are still observed despite HIF-2 α inhibition (Hughes et al., 2007), indicating that the molecular pathogenesis of RCC is far more complex than simple upregulation of HIF. Furthermore, the mutant pVHL found in patients with type 2C VHL disease is not defective in its ability to regulate HIF, yet these patients still go on to develop familial pheochromocytomas (Hoffman et al., 2001, Clifford et al., 2001). Finally, sufferers of Chuvash polycythemia harbour homozygous *VHL* mutations that result in a pVHL unable to regulate HIF, however these patients are not predisposed to tumour formation (Ang et al., 2002). All these points support additional, HIF independent, roles for VHL in the pathogenesis of RCC.

Many studies have investigated additional functions of VHL, including activities outside of its role as an ubiquitin ligase substrate recognition subunit. Aside from HIF, other degradation targets of VHL include proteins involved in transcription, translation, and regulation of protein degradation. The deubiquitinating enzymes VDU1 and VDU2 are substrates of VHL (Li et al., 2002a, Li et al., 2002b), their role is potentially directly antagonistic to that of the E3 ubiquitin ligase complex; they would therefore be important targets. Two further targets are the transcription factor

Sp1 (Mukhopadhyay et al., 1997) and atypical protein kinase C (Okuda et al., 2001). Interestingly these two proteins have been shown to be important in the activation of VEGF transcription (Pal et al., 1997, Pal et al., 1998) and are therefore important in the pathogenesis of RCC. VHL also ubiquitinates the RNA polymerase II subunits A (RPB1) and G (RPB7) (Kuznetsova et al., 2003, Na et al., 2003); RPB7 has been shown to be involved in translation initiation of VEGF (Na et al., 2003), explaining why this protein is a VHL target. Expression of RPB1 in RCC cells has been linked to tumourigenesis, and is regulated by VHL following oxidative stress-dependent hydroxylation by prolyl hydroxylase domain-containing protein 1 (PHD1) (Mikhaylova et al., 2008).

Non-ubiquitin based functions of VHL involve the stabilisation of the master tumour suppressor p53 (Roe et al., 2006) and also of the transcriptional co-activator Jade-1 (Panchenko et al., 2004, Zhou et al., 2004). Stabilisation of Jade-1 is VHL disease subtype dependent, with Type 1 and Type 2B mutations showing no stabilisation or partial stabilisation, respectively, whilst Type 2A mutations are not hindered in their ability to stabilise Jade-1 (Zhou et al., 2004). Jade-1 is a transcription factor which may have tumour suppressor activity; the inability of RCC forming VHL disease subtypes to stabilise Jade-1 may therefore suggest its role in the pathogenesis of RCC (Zhou et al., 2005). The epithelial-mesenchymal transition (EMT) is widely regarded as a crucial step in metastasis and cellular interactions with the ECM are extremely important in this process. Loss of VHL has been implicated in EMT (Pantuck et al., 2010), and in further support of this VHL has been shown to have important roles in cell-ECM interactions (Davidowitz et al., 2001), and in fibronectin deposition, the latter of which may have implications for tumour angiogenesis (Ohh et al., 1998). VHL can also impact upon cellular shape through its regulation of microtubule assembly. Microtubules fulfil roles in cell shape, motility, and assembly

of the mitotic spindle, and loss of VHL has therefore been linked to chromosomal instability (Hergovich et al., 2003, Thoma et al., 2009). All of the above supports a tumour suppressor role for VHL, and indicates that a complex interplay of protein interactions is likely to be involved in the VHL-dependent tumourigenesis of RCC.

1.3. RCC therapeutics

As renal cell carcinoma is notoriously resistant to conventional chemotherapy, radiotherapy, and hormonal therapy, an improved understanding of RCC biology has been necessary to allow the development of targeted therapies. The last decade has heralded a new era in the management of metastatic RCC, with the approval of seven new agents. Response to therapy is assessed using RECIST criteria, which is based upon changes in the tumour size, determined from CT scans of the tumour and any metastatic lesions (Eisenhauer et al., 2009).

1.3.1 Immunotherapy

Until the development of targeted therapies the only drugs found to have any effect against mRCC were the cytokines IFN- α and IL-2. Most patients receive no clinical benefit from these drugs; a retrospective Cochrane review found an average of only 12.9% of patients responded to cytokine therapy (Coppin et al., 2005). High dose IL-2 is still occasionally administered due to its ability to achieve complete responses in a subset of patients, however due to the severe toxicity profile of this drug it is reserved for patients who are assessed as having a favourable prognosis.

1.3.2. Angiogenesis inhibitors

The concept of targeting angiogenesis as a cancer therapy was first proposed by Judah Folkman (Folkman, 1971), and supported by research showing that a

reduction in tumour vascularity is associated with an increased progression free survival (PFS) and overall survival (OS) in metastatic RCC (mRCC) (Lamuraglia et al., 2006). The panoply of anti-angiogenesis drugs currently includes tyrosine kinase inhibitors (TKIs), mammalian target of rapamycin (mTOR) inhibitors, and antibody-induced VEGF blockade. These therapies have revolutionised patient care, and sequential therapy has been proposed to allow progression free survival up to 27 months, and overall survival up to 40 months (Escudier et al., 2009b).

1.3.2.1 TKI inhibitors

Tyrosine kinase inhibitors (TKIs) are a class of small molecule inhibitors designed to target receptor tyrosine kinases (RTKs). There are 58 known RTKs in humans, which include growth factor receptors and key modulators of intracellular signalling pathways, such as those involved in proliferation, metabolism, angiogenesis, and migration (Lemmon and Schlessinger, 2010). The principal target of anti-angiogenic TKIs are the VEGFR receptors, however many of the TKIs bind a number of other targets (Karaman et al., 2008), especially the PDGFRs, and are therefore often known as multi-tyrosine kinase inhibitors (MTKs). These non-specific interactions have been suggested to account for a variety of off-target effects leading to a wide variety of drug-induced toxicities (Bergers and Hanahan, 2008), which can be significant (Boehm et al., 2010). Currently four TKIs have been approved for clinical use in the UK, of which sunitinib and pazopanib are currently used in the front line setting.

Sunitinib

Sunitinib is an indoline ATP-mimetic directed against VEGFR-1, -2, and -3, PDGFR- α and - β , mast/stem cell growth factor receptor Kit (c-Kit/SCFR), fms-like

tyrosine kinase 3 (Flt-3), and colony stimulation factor-receptor 1 (csf-1) (Mendel et al., 2003, O'Farrell et al., 2003), though the inhibitory profile has been shown to be significantly broader than this (Karaman et al., 2008). By targeting both the VEGFRs and the PDGFRs, sunitinib is able to target both the vascular endothelium and the supporting pericytes, respectively (Erber et al., 2004). During a phase III trial whereby 750 RCC patients were randomised to either sunitinib or IFN- α , an improvement in median progression free survival (PFS) (11 months [95% CI 10-12] versus 5 months [95% CI 4-6]) and objective response rate (ORR) (31% versus 6%) was observed in the sunitinib arm (Motzer et al., 2007). Though these are clearly significant improvements, nearly a third of patients fail to see any clinical benefit, and many experience significant drug-induced toxicity. In a pooled analysis of two phase II studies, all grade gastrointestinal disorders were the most common adverse event including diarrhoea (49.1%), nausea (49.7%), and stomatitis (41.4%). Other reported toxicities included fatigue (60.4%), mucosal inflammation (17.8%), skin discolouration (32.0%), hypertension (16.6%), and palmar-plantar syndrome (12.4%) (Kollmannsberger et al., 2007). A retrospective analysis of 1059 patients from 6 clinical trials found that overall, 38% had an objective response, including 1% who displayed a complete response (Molina et al., 2014).

Pazopanib

Pazopanib is a recently approved synthetic indazolympyrimidine TKI, targeted against VEGFR-1, -2, and -3, PDGFR- α and - β , and c-Kit (Hamberg et al., 2010). In a placebo controlled phase III trial of 435 patients pazopanib was superior both in terms of median PFS (9.2 months versus 4.2 months; hazard ratio (HR) 0.46 [95% CI 0.34-0.62]; $P < 0.0001$) and ORR (30% versus 3%; $P < 0.001$) (Sternberg et al., 2010). A head-to-head comparison with sunitinib revealed that the two drugs have

a similar PFS (8.4 months versus 9.5 months; HR 1.05 [95% CI 0.90-1.22]), though pazopanib had a slightly improved ORR (31% versus 25%; P = 0.03), and appeared to be slightly better tolerated (Motzer et al., 2013b).

Sorafenib

Sorafenib is a second line MTK directed against VEGFR-1, -2, and -3, PDGFR- β , and Raf kinase. A placebo controlled trial of 903 patients who had progressed on previous systemic therapy saw an improvement in median PFS in the sorafenib arm (5.5 versus 2.8 months; HR 0.44 [95% CI 0.35-0.55]; P<0.01). Overall survival was similar (17.8 versus 15.2 months; HR 0.88 [95% CI 0.74-1.04], P = 0.146) however when data from placebo-assigned patients who crossed over was censored, the difference became significant (17.8 versus 14.3 months; HR 0.78 [95% CI 0.62-0.97]; P=0.029). Sorafenib was generally well tolerated, most adverse events were grade 1 or 2 (Escudier et al., 2007a, Escudier et al., 2009a).

Axitinib

Axitinib is a second generation small indazole TKI which is highly potent for VEGFR-1, -2, and-3, it also binds PDGFR- β and c-Kit (Escudier and Gore, 2011). A phase III trial of 723 randomised patients comparing axitinib to sorafenib in the second line setting, after progression on a previous systemic therapy, found no difference in median overall survival (20.1 months versus 19.2 months; HR 0.969 [95% CI 0.8-1.174]; P=0.3744), however an improved median PFS was achieved in the axitinib cohort (8.3 months versus 5.7 months; HR 0.656 [95% CI 0.522-0.779]; P<0.0001), establishing axitinib as a viable therapy for use in the second line setting (Motzer et al., 2013a).

1.3.2.2. mTOR inhibitors

mTOR inhibitors are rapamycin analogs that target the serine/threonine kinase mTOR. The mTOR protein is part of the PI3K/Akt/mTOR cascade and has important roles in cell growth, metabolism, proliferation, and motility. Furthermore, a downstream target of mTOR is the eukaryotic initiation factor 4E binding protein (4E-BP1), which in turn switches on the transcription of HIF, cyclin D, c-Myc, and other proteins implicated in cancer progression. Currently two mTOR inhibitors have been approved for clinical use in the second line setting.

Temsirolimus

Temsirolimus is a derivative of rapamycin which specifically prevents progression from G₁ to S phase by forming a complex with FKBP12 and preventing formation of the mTOR-raptor complex (Heng et al., 2010). Following retrospective stratification of 111 patients from a small phase III study into risk groups (Atkins et al., 2004), it was found to have unexpected benefit for prognostically poor risk patients. A subsequent phase III trial with 626 poor risk patients compared temsirolimus alone to IFN- α alone and combination therapy. The median overall survival times recorded were 10.9 months, 7.3 months and 8.4 months respectively; revealing that temsirolimus alone gives a better overall survival (temsirolimus alone versus IFN alone HR 0.73, 95% CI 0.58-0.92, P=0.008). An improvement in PFS (3.8 months versus 1.9 months versus 3.7 months, respectively) and ORR (8.6% versus 4.8% versus 8.1%, respectively) was also achieved (Hudes et al., 2007).

Everolimus

Everolimus is a specific partial inhibitor of mTORC1, which prevents formation of the activated mTOR complex. A phase III placebo controlled trial of 410 patients,

who had previously progressed on VEGF-targeted therapy, indicated an improvement in median PFS (4.9 months versus 1.9 months; HR 0.33 [95% CI 0.25-0.43]; $P < 0.001$), but no difference in median OS (14.8 months versus 14.4 months; HR 0.87 [95% CI 0.65-1.15]; $P = 0.162$) (Motzer et al., 2010).

1.3.2.3. Monoclonal antibodies

Using antibodies in cancer therapeutics offers a highly specific mechanism for neutralising the action of a protein. Currently only one monoclonal antibody has been approved for use in the treatment of RCC; bevacizumab is a humanised monoclonal antibody directed against VEGF. On its own Bevacizumab has shown disappointing results, however a phase III trial enrolling 649 patients found combination therapy with IFN- α gave improvements in PFS (10.2 months versus 5.4 months; HR 0.63 [95% CI 0.52-0.75]; $P = 0.0001$) over IFN- α plus placebo (Escudier et al., 2007b). A minor improvement in overall survival was found in a separate phase III study enrolling 732 patients to receive bevacizumab plus IFN- α , or IFN- α monotherapy (18.3 months versus 17.4 months; HR 0.86 [95% CI 0.73-1.01]; $P = 0.069$) (Rini et al., 2010b).

1.3.3. Emerging therapies

Tyrosine kinase inhibitors are the predominant therapy used in the management of metastatic RCC and a panoply of TKIs are now available, with many more in various stages of development or approval. Despite differences in toxicity profiles, significant improvements are yet to be made in efficacy, a scenario that is unlikely given their similar mode of action.

Other angiogenesis inhibitors in the research pipeline include inhibitors of other members of the PI3K/Akt/mTOR cascade, such as the PI3K inhibitor BKM120 and the dual PI3K-mTOR inhibitor NVP-BEZ235 (Figlin et al., 2013). Therapies involved in VEGF blockade such as ziv-aflibercept, a soluble decoy receptor that binds to VEGF, and ramcicirumab, a fully human immunoglobulin monoclonal antibody targeting VEGFR-2 are also under development (Kanesvaran and Tan, 2014). Recent studies suggest, however, that dual inhibition of mTORC1 and mTORC2 in mRCC has no clinical benefit over inhibition of mTORC1 alone (Powles, 2014).

A significant amount of research focus currently surrounds studies investigating how to harness the power of the immune system, for instance through controlling the action of immune checkpoint regulators. Examples include inhibitors of the immune system regulators PD-1 and PD-L1, and CTLA-4. These proteins have been found to be involved in immune evasion, and inhibitors of these targets include nivolumab, a PD-1 inhibitor currently in phase III trials; MPDL3280A, a PD-L1 monoclonal antibody currently in a phase II trial; and tremelimumab, a monoclonal antibody targeting the T cell inhibitor CTLA-4. Nivolumab has recently shown promising results in a dose-ranging phase II trial, which recorded an ORR of 20% and overall survival exceeding two years (Motzer, 2014). Furthermore, a phase I study investigating combination therapy of nivolumab with the CTLA-4 inhibitor ipilimumab achieved an objective response rate of 39% (Hammers HJ, 2014).

1.4. Biomarkers in RCC management

Biomarkers have the potential to impact on all areas of cancer management including diagnosis, prognosis, therapy selection, and response monitoring. Any

indicator of a change in biological behaviour may act as a biomarker as long as it is sufficiently sensitive and specific, cost effective, and easy to implement. Renal cell carcinoma is marred by a lack of useful clinical biomarkers, and despite hundreds of published candidate marker studies, none have made it into routine clinical use. Recently, a few biomarker initiatives have been undertaken to identify novel biomarkers for the management of RCC including the CAncer GENomics of the KIDney (CAGEKID) consortium, the Tumour Cancer Genome Atlas (TCGA) initiative, the National Institute for Health Research funded 'Biomarker pipeline', the TArgeted therapy in Renal cell cancer: Genetic and Tumour related biomarkers for response and toxicity (EuroTARGET) collaboration, the Personalised RNA interference to Enhance the Delivery of Individualised Cytotoxic and Targeted therapeutics (PREDICT) consortium, and the Scottish Collaboration on Translational Research into RCC (SCOTRRCC) (Vasudev et al., 2012).

1.4.1. Diagnostic biomarkers

Though protein biomarkers are starting to become more commonly used in determining the histogenesis of a renal neoplasm (Tan et al., 2013), we are still no closer to identifying a clinically validated ccRCC specific diagnostic biomarker, though recent genetic studies have made some headway in this field (Lasseigne et al., 2014). Potential biomarkers for diagnosis may include both serum/urine markers that would enable the screening of a population, and tissue markers that aid in the diagnosis of a suspected cancer. Unfortunately, although there is a survival advantage when RCC is detected early, due to the low overall incidence of RCC it would not be feasible to screen the population for this disease, except in high risk groups, as the marker would need to be both 100% sensitive and 100% specific to eliminate the risk in an incorrect diagnosis. However a marker that aids

in the tissue diagnosis of RCC would still be useful and several proteins have been investigated as potential molecular diagnostic tools. Previous studies have shown that ccRCC tissue is positive for vimentin, AE1/AE3 keratins, CD10, RCC marker, and carbonic anhydrase IX (CA9), and negative for CD117, kidney-specific cadherin, and parvalbumin (Truong and Shen, 2011). Other diagnostic suggestions include the tissue proteins Pax 2 and Pax 8 (Ozcan et al., 2012) and CD70 (Diegmann et al., 2005), and a three plasma protein panel comprising of N-methyltransferase (NNMT), L-plastin (LCP1), and non-metastatic cells 1 protein (NM23A) (Su Kim et al., 2013). Several genetic and epigenetic alterations have also been investigated, including changes in gene expression (Sanford et al., 2011), DNA methylation status (Costa et al., 2011), and miRNA expression (Youssef et al., 2011). As yet, no marker has improved upon the diagnostic accuracy of the pathological examination of tissue. Several factors are likely to be responsible for the failure to identify suitable diagnostic markers, of which the complex and heterogenous molecular landscape of the tumour is likely a significant contributor, along with limitations in equipment sensitivity and the ability to access sufficient samples to design properly controlled and well powered studies.

1.4.2. Prognostic biomarkers

A large number of proteins have been investigated for their prognostic utility, and these have been reviewed extensively elsewhere (Funakoshi et al., 2014, Eichelberg et al., 2009). Large scale validation is often missing from these studies, however a few of the more promising targets have been validated in relatively large clinical cohorts, including CA9, B7H1, IMP3, and Ki67, of which CA9 and Ki67 have both previously been integrated into a prognostic staging system (Kim et al., 2005, Kim et al., 2004). Though carbonic anhydrase 9 (CA9) has contradictory studies, the largest study to date investigated staining intensity in 321 patients (Bui et al.,

2003), where low staining was an independent poor prognostic factor for survival (HR 3.10; $P < 0.001$). B7H1 (PD-L1) has also been shown to be a powerful prognostic marker, in a study of 196 tissue specimens high expression was associated with increased risk of death (HR 4.53 [95% CI 1.94-10.56]; $P < 0.001$) (Thompson et al., 2004). Independent validation of insulin-like growth factor 2 mRNA-binding protein 3 (IMP3) in 716 patient specimens demonstrated that elevated tissue levels were associated with increased risk of death (HR 1.42; $P = 0.024$) and risk of metastasis (HR 4.71; $P < 0.001$) (Hoffmann et al., 2008). Likewise, a retrospective study of Ki-67 expression in 741 patient specimens found high expression was associated with a two-fold increase in the risk of death (HR 2.18 [95% CI 1.52-3.11]; $P < 0.001$). Multiple other proteins have been investigated including HIF, VEGF, MMP2, MMP9, CXCR3, CXCR4, and survivin (Eichelberg et al., 2009), however despite hundreds of studies no single protein has yet been found to outperform current clinical methods, and they are infrequently used in routine prognostication (Tan et al., 2013). Several studies have demonstrated the ability to improve upon the prognostic power of pre-existing nomograms when they are used in conjunction with molecular markers such as CA9 (Kim et al., 2004, Sim et al., 2012) and C-reactive protein (CRP) (Karakiewicz et al., 2007b, Jagdev et al., 2010). This is essential for a biomarker to be accepted, but these proteins have not yet made it into routine clinical use in this context.

In addition to prognostic nomograms, other nomograms have been developed to aid in assessing a patient's prognosis following therapeutic intervention. The two most commonly used nomograms in predicting survival in mRCC patients treated with anti-angiogenesis inhibitors are the MSKCC score and IMDC criteria (Heng score). The MSKCC score, which was originally developed to predict survival in cytokine treated patients (Motzer et al., 2002) uses the Karnofsky performance

status, lactate dehydrogenase concentration, haemoglobin concentration, corrected serum calcium level, and time from nephrectomy to diagnosis as predictors. This score has since been largely superseded by the IMDC criteria, which has been shown to be 73% accurate at predicting mortality in patients treated with angiogenesis inhibitors; external validation has shown it to have slightly improved discriminatory ability over the MSKCC score (Kwon et al., 2013). Factors measured in the Heng score are the Karnofsky performance status, haemoglobin concentration, corrected serum calcium, time from diagnosis to treatment, neutrophil count, and platelet count (Heng et al., 2009). Though other nomograms have been developed (Manola et al., 2011, Bamias et al., 2013), none have yet made a significant improvement on the Heng score, and molecular markers may therefore assist in increasing the predictive accuracy.

1.4.3. Predictive and pharmacodynamic biomarkers

With a modest clinical benefit, considerable associated toxicity and a high economic burden, the TKI inhibitors have come under considerable scrutiny since their introduction eight years ago. Survival or progression free survival benefits are limited and often measured in months (Kerbel, 2008). At present, no marker yet exists to predict or monitor response to sunitinib, and there is currently very little to guide selection of the most appropriate treatment for a patient. Generally, prognostic risk factors and nomograms are used, combined with knowledge of specific risk factors that may make a particular drug choice inappropriate. A large number of studies have investigated potential predictive biomarkers including both molecular and clinical characteristics; however most have not been sufficiently validated to enable the distinction between their predictive or prognostic capabilities to be confirmed. Successful examples of predictive markers in other cancers include amplifications of the HER2 gene or overexpression of the

oestrogen/progesterone receptors in breast cancer patients, which predicts sensitivity to trastuzumab or tamoxifen respectively (Sawyers, 2008). It must be noted here that Her2 expression is of mixed significance, with both predictive and prognostic implications (Weigel and Dowsett, 2010). Genetically, lung cancer patients with mutations in KRAS or in the kinase domain of EGFR display resistance (Pao et al., 2005) or sensitivity (Lynch et al., 2004, Paez et al., 2004) respectively, to erlotinib or gefitinib. Of note, in these examples the target of therapies involved are located on the tumour cells themselves, therefore their expression or mutation is more easily predictive of their therapeutic benefit.

1.4.3.1. Protein biomarkers

Molecular biomarkers have the potential to provide a rapid, objective test to determine the correct therapeutic intervention. Research into molecular biomarkers has covered a variety of samples types, with a particular emphasis on serum and tissue-derived markers of response. Hypothesis driven approaches have led the way, with considerable effort investigating proteins related to pathways which are biologically relevant to anti-angiogenic therapies, such as targets involved in angiogenesis, matrix remodelling, and hypoxia.

Serum

Studies investigating potential serum markers of response to sunitinib (Table 1.0.6) have been heavily focussed on angiogenic proteins. Conflicting results regarding the utility of VEGF-A have been observed, with two studies showing an improved outcome, and three showing poorer outcome (Deprimo et al., 2007, Kontovinis et al., 2009, Porta et al., 2010, Farace et al., 2011, Harmon et al., 2014). Furthermore, VEGF-A levels have been shown to characteristically rise and fall with cycles of therapy (Harmon et al., 2011, Deprimo et al., 2007), and may therefore be

indicative of a systemic response to the drug. The angiogenic factor showing most promise is perhaps VEGFR-3, with three studies demonstrating a correlation between serum protein levels and clinical response (Deprimo et al., 2007, Rini et al., 2008, Harmon et al., 2014). Harmon and colleagues conducted a two arm study which assessed baseline serum levels of VEGFR-3 in 33 sunitinib and 30 IFN treated patients from a phase phase III study. VEGFR-3 remained predictive for overall survival after multivariate analysis ($P = 0.037$), together with IL-8 ($P = 0.013$), which has been a subject of interest regarding its potential role in TKI-based resistance (Huang et al., 2010). Levels of circulating MMP-9 have been shown to be elevated in non-responders by two separate groups (Perez-Gracia et al., 2009, Miyake et al., 2014). In the study by Miyake, circulating levels of MMP-2, MMP-9, TIMP-1 and TIMP-2 in both sunitinib treated ($n = 52$) and healthy controls ($n = 30$) were compared, and the authors found the ratio of MMP-9 to TIMP-2 was significantly correlated with reduced progression free survival (HR 2.19, $P = 0.038$). Two independent studies have also found a link between elevated levels of CRP and poorer response, warranting further investigation of this protein (Miyake et al., 2014, Fujita et al., 2012). These serum studies are, however, generally hampered by a lack of sample numbers, and it will be difficult to fully assess the utility of any of these markers until larger studies have been conducted.

Tissue

There seems to be greater concordance between results in tissue-based studies (Table 1.0.7). Results for HIF-1 α are conflicting, however three independent studies have found a correlation between HIF-2 α levels and improved response, progression free survival, and overall survival (Patel et al., 2008, Saez et al., 2012, Garcia-Donas et al., 2013). Both VEGFR-2 and VEGFR-3 have multiple studies linking their expression with clinical benefit which may seem at odds with the results

found in serum (Table 1.0.6), however in both cases, whilst it appears that high expression in tissue is favourable, it also appears that presence of the receptor in the serum is unfavourable and it is possible that sVEGFR-3 may serve to 'mop up' circulating sunitinib. The hypoxia marker CA9 appears to be highly correlated with survival, and a recent study by Stewart et al looked at differences in both expression and variance between sunitinib treated (n = 23) and sunitinib naïve (n = 22) patients (Stewart et al., 2014). The authors also investigated tumour heterogeneity by looking at multiple tissue regions. Out of 55 proteins investigated, only CA9 was found to be significantly differentially expressed with treatment, whereby increased expression was associated with good overall survival (HR 0.26 [95% CI 0.11-0.61], P = 0.001), and intratumoural heterogeneity of expression increased with sunitinib therapy. Despite a number of promising studies, none of these have conclusively proven the predictive power of the biomarker in question in a sufficiently large study. Prospective studies are warranted to test these biomarkers further.

Table 1.0.6: Potential serum biomarkers of clinical benefit in sunitinib treated patients

Serum biomarkers investigated for their ability to predict clinical benefit in sunitinib treated patients. Reported P value and number of patients is shown.

Biomarker	Significance	Patients	Comment	Reference
VEGF-A	P < 0.05	63	Greater initial (cycle 1) increase in PR patients	(Deprimo et al., 2007)
	P = 0.01	42	Greater increase associated with worse PFS	(Kontovinis et al., 2009)
	P = 0.004	84	High baseline associated with worse PFS	(Porta et al., 2010)
	P = 0.02	46	Greater initial increase associated with worse OS	(Farace et al., 2011)
	P = 0.0108	63	Low baseline level associated with PFS	(Harmon et al., 2014)
VEGF-C	P = 0.0006	57	Low baseline associated with better PFS	(Rini et al., 2008)
sVEGFR-2	P < 0.05	63	Greater initial (cycle 1) decrease in PR patients	(Deprimo et al., 2007)
sVEGFR-3	P < 0.05	63	Greater initial decrease in PR patients	(Deprimo et al., 2007)
	P = 0.006	59	Low baseline associated with better PFS	(Rini et al., 2008)
	P = 0.037	63	Low baseline associated with OS	(Harmon et al., 2014)
TNF-a	P = 0.045	31	High level associated with worse OS	(Perez-Gracia et al., 2009)

	P = 0.009	31	Higher level in PD patients	(Perez-Gracia et al., 2009)
NGAL	P = 0.02	84	High baseline associated with worse PFS	(Porta et al., 2010)
SDF-1a	P = 0.002	46	Initial decrease (day 1-14) associated with worse PFS	(Farace et al., 2011)
	P = 0.007	46	Initial decrease (day 1-14) associated with worse OS	(Farace et al., 2011)
MMP-9	P = 0.027	31	Higher level in PD patients than PR or SD	(Perez-Gracia et al., 2009)
	P = 0.024	31	High levels associated with worse TTP	(Perez-Gracia et al., 2009)
	P = 0.042	31	Increased risk of PD	(Perez-Gracia et al., 2009)
MMP-9/ TIMP-2 ratio	P = 0.038	52	Elevated ratio associated with reduced PFS	(Miyake et al., 2014)
CRP	P = 0.027	52	Abnormal levels associated with reduced PFS	(Miyake et al., 2014)
	P = 0.016	41	Normal levels associated with objective response	(Fujita et al., 2012)
	P = 0.002	41	Normal levels associated with PR and SD	(Fujita et al., 2012)
	P = 0.036	41	Normal levels associated with PFS	(Fujita et al., 2012)
IL-8	P = 0.013	63	High baseline associated with poor response	(Harmon et al., 2014)
MMP-2	P = 0.018	74	Higher baseline associated with tumour response	(Motzer et al., 2014)
Ang-2	P = 0.0215	74	Lower baseline associated with tumour response	(Motzer et al., 2014)
NT-pro-BNP	P < 0.0001	36	Initial increase (<15 days) associated with worse response	(Papazisis et al., 2010)

P = 0.001	36	Greater increase associated with worse PFS	(Papazisis et al., 2010)
-----------	----	--	--------------------------

OS, overall survival; PFS, progression free survival; TTP, time to progression; PR, partial response; SD, stable disease; PD, progressed disease.

Table 1.0.7: Potential tissue biomarkers of clinical benefit in sunitinib treated patients

Tissue biomarkers investigated for their ability to predict clinical benefit in sunitinib treated patients. Reported P value and number of patients is shown.

Biomarker	Significance	Patients	Comment	Reference
HIF-1 α	P = 0.003	49	High expression associated with CR and PR	(Patel et al., 2008)
	P = 0.001	71	High expression associated with response rate	(Saez et al., 2012)
	P < 0.0001	71	High expression associated with PFS	(Saez et al., 2012)
	P < 0.0001	71	High expression associated with OS	(Saez et al., 2012)
	P = 0.001	65	Higher expression associated with worse PFS	(Muriel Lopez et al., 2012)
	P = 0.034	149	High expression associated with worse response	(Motzer et al., 2014)

	P = 0.011	41	High expression associated with PFS	(Dornbusch et al., 2013)
HIF-2 α	P = 0.001	49	High expression associated with CR and PR	(Patel et al., 2008)
	P = 0.04	71	High expression associated with better PFS	(Saez et al., 2012)
	P = 0.04	71	High expression associated with better OS	(Saez et al., 2012)
	P = 0.024	67	High expression associated with better response	(Garcia-Donas et al., 2013)
	P = 0.048	67	High expression associated with better OS	(Garcia-Donas et al., 2013)
VEGF-A	P = 0.0092	67	High expression associated with better OS	(Garcia-Donas et al., 2013)
VEGFR-2	P = 0.039	40	High expression associated with better response	(Terakawa et al., 2013)
	P = 0.0025	40	High expression associated with better PFS	(Terakawa et al., 2013)
	P = 0.016	58	High expression associated with tumour reduction	(You et al., 2014)
VEGFR-3	P = 0.012	67	High expression associated with better PFS	(Garcia-Donas et al., 2013)
	P = 0.026	41	High expression associated with better PFS	(Dornbusch et al., 2013)
CXCR-4	P = 0.026	62	High expression associated with worse response	(C et al., 2012)
	P = 0.027	62	High expression associated with worse PFS	(C et al., 2012)
CA9	P < 0.001	67	High expression associated with better response	(Muriel Lopez et al., 2012)
	P = 0.02	131	High expression associated with survival	(Stewart et al., 2014)

	P = 0.034	42	High expression associated with OS	(Dornbusch et al., 2013)
PTEN	P = 0.003	67	Positivity associated with response	(Muriel Lopez et al., 2012)
P21	P = 0.025	67	High expression associated with worse response	(Muriel Lopez et al., 2012)
PDGFR- β	P = 0.026	67	High expression associated with better response	(Garcia-Donas et al., 2013)
FSHR	P < 0.0001	50	Higher percent of FSHR positive vessels in PR pts	(Siraj et al., 2012)
P-VEGFR2	P = 0.01	48	Positivity associated with worse PFS	(del Puerto-Nevado et al., 2014)
	P = 0.02	48	Positivity associated with worse OS	(del Puerto-Nevado et al., 2014)
CD34	P = 0.033	41	High expression associated with PFS	(Dornbusch et al., 2013)
PDGFR- α	P = 0.005	42	High expression associated with worse OS	(Dornbusch et al., 2013)
VEGFR-1	P = 0.026	41	High expression associated with good OS	(Dornbusch et al., 2013)

OS, overall survival; PFS, progression free survival; TTP, time to progression; CR, complete response; PR, partial response; SD, stable disease; PD, progressed disease.

1.4.3.2. Genetic markers

A number of studies have also investigated genetic factors in predicting sunitinib response, including mRNA and microRNA expression, VHL mutation status, and a variety of single nucleotide polymorphisms (SNPs). A prospective study which assessed the association between 16 SNPs across 9 genes with sunitinib response (n=89) and toxicity (n=95) found two VEGFR-3 SNPs and a SNP in the high metabolising variant of the cytochrome P450 gene CYP3A5*1, which were associated with reduced PFS and an increased risk of dose reductions due to toxicity, respectively (Garcia-Donas et al., 2011). VEGFR-3 polymorphisms have been found to be associated with PFS and OS in at least two further genetic studies (Scartozzi et al., 2013, Beuselinck et al., 2013), reaffirming the notion that VEGFR-3 may have a role in the efficacy of sunitinib. A retrospective study investigating PFS and OS in 136 sunitinib treated patients found that carriers of polymorphisms in CYP3A5, NR1I3, or ABCB1 had improved PFS and OS. No association with VEGFR-3 was found in this study (van der Veldt et al., 2011), indicating a lack of reproducibility between studies. A more recent study of sunitinib treated patients (n = 91) investigating VEGFR1 SNPs found two polymorphisms, rs9582036 and rs9554320, which were associated with PFS, and OS (Beuselinck et al., 2014). Interestingly, rs9582036 has been found to be predictive for bevacizumab response in pancreatic cancer (Lambrechts et al., 2012), and therefore may be a pan-angiogenesis inhibitor effect.

MicroRNAs (miRNA) have been found to have numerous roles in cancer, and a few studies have investigated their role in assessing response to sunitinib. In a screen of 673 miRNAs using samples from 41 patients with marked response or resistance to sunitinib, 64 miRNAs were found to be differentially expressed. Of these, miR-

942, miR-628, miR-133a, and miR-484 were significantly associated with decreased time to progression and OS (Prior et al., 2014). Another miRNA study investigated the expression of 287 miRNAs, and two predictive models were generated, one for prolonged response (miR-410, miR-1181, miR-424) and one for poor response (miR-192, miR-193-5p, miR-501-3p) (Gamez-Pozo et al., 2012). Finally, the role of VHL mutation status has shown conflicting results. Two studies have shown an association between VHL mutation and improved clinical outcome, with carriers of mutant VHL either demonstrating a higher response rate (51% versus 32%, n=123, p=0.04) (Choueiri et al., 2008) or improved clinical outcome (Rini et al., 2006). However a third study demonstrated no link between VHL mutation status and sunitinib efficacy (Garcia-Donas et al., 2013), and more research is clearly needed to unravel this contradiction.

1.4.3.3. Clinical biomarkers

A variety of clinical features have been investigated for use as surrogate biomarkers for sunitinib efficacy including adverse events following therapy, and clinical features of the patient prior to therapy. The most widely researched adverse event is hypertension, with multiple studies reporting a link between hypertensive patients and improved progression free survival, overall survival, and objective response rate (Rixe et al., 2007, Rini et al., 2011a, Bono et al., 2011, Szmit et al., 2012). In a retrospective pooled study from three clinical trials (N = 544), patients who developed treatment-induced hypertension had improved PFS (12.5 months [95% CI 10.9-13.7] versus 2.5 months [95% CI 2.5-3.8]; P <0.001), improved OS (30.9 months [95% CI 27.9-33.7] versus 7.2 months [95% CI 5.6-10.7]; P<0.001), and an improved objective response rate (54.8% versus 8.7%). An association between hypertension and response has also been shown for other anti-VEGF therapies including axitinib (Rini et al., 2011b), tivozanib (Bhargava, 2010), and

bevacizumab (Rini et al., 2010a), suggesting hypertension may be a class effect of anti-angiogenesis inhibitors. Though hypertension seems like a promising clinical biomarker, it is important to remember that this feature is *post-hoc* and would not predict ahead of treatment, however it may assist in a decision on whether to continue therapy. Identifying surrogate markers that predict for the development of hypertension may help in this regard. A study of 255 patients investigating the association between single nucleotide polymorphisms (SNPs) and the development of hypertension found that an ACG haplotype in the VEGFA SNPs rs699947, rs833061, and rs2010963, and the presence of a C allele in the eNOS SNP rs2070744, were both associated with the development of grade 3 hypertension in a multivariate analysis ($P = 0.031$ and $P = 0.045$) (Eechoute et al., 2012). Another study found the VEGF SNP rs2010963 to be associated with the development and duration of sunitinib-induced hypertension ($P = 0.05$) (Kim et al., 2012b). A decrease in mean microvessel density may therefore be linked to clinical response in sunitinib treated patients (van der Veldt et al., 2010a, Vasudev et al., 2013). A further study has linked a decrease in active angiogenesis to improved clinical outcome (del Puerto-Nevado et al., 2014); these go hand in hand with sunitinib's mode of action and have rational biological explanations.

Other drug-induced adverse events investigated include leukopenia (Fujita et al., 2014), hypothyroidism (Kust et al., 2014, Wolter et al., 2008, Schmidinger et al., 2011), hyponatremia and neutrophilia (Kawashima et al., 2012), fatigue (Donskov et al., 2012, Davis et al., 2011), and the development of palmar-plantar syndrome (Donskov et al., 2012, Puzanov et al., 2011). Potential predictive clinical features include characteristics of the tumour, such as the initial tumour size (Yuasa et al., 2011, Basappa et al., 2011) or an early reduction in size (Abel et al., 2011) which have shown some promise in predicting PFS or OS.

1.4.3.4. Imaging biomarkers

The development of advanced imaging techniques such as dynamic contrast enhanced MRI (DCE-MRI) and ultrasound (DCE-US), and computed tomography (CT) has allowed for anatomical parameters such as tumour size and density, blood flow, and vessel density to be observed, and a number of studies have investigated their use in monitoring clinical outcome (O'Connor and Jayson, 2012). An early reduction in size and density has been associated with good clinical outcome in a number of studies (Abel et al., 2011, Thiam et al., 2010, Salem et al., 2014). In a study of 75 patients receiving sunitinib in a neoadjuvant setting, an early (≤ 60 days) reduction ($\geq 10\%$) in the size of the primary tumour was a significant predictor for overall survival (HR 0.26 95% CI 0.08-0.89; $p=0.031$) (Abel et al., 2011). Another study of 27 patients with unresectable tumours who received sunitinib, found that those who were later suitable for cytoreductive surgery demonstrated an early response to sunitinib and had improved response to sunitinib, compared to those who remained unsuitable for surgery ($p=0.005$) (Salem et al., 2014). Interestingly, a recent meta-analysis also found that early response to sunitinib was associated with improved PFS and OS (Molina et al., 2014).

Sunitinib targets the vasculature, and a predictable decrease in tumour vascularity following sunitinib treatment has been shown in *in vivo* studies (Hillman et al., 2009). A reduction in vascularity has also been linked to survival in TKI treated patients ($n=30$) whereby decreased attenuation, measured using contrast enhanced CT scanning following treatment with sunitinib or sorafenib, was associated with primary tumour response ($p=0.0053$) (Cowey et al., 2010). A similar study ($n=53$) found decreased attenuation in one or more metastatic lesion was associated with PFS (Smith et al., 2010a). A decrease in the rate of glucose uptake, and therefore metabolic activity of the tumour in sunitinib treated patients,

measured using positron emission tomography/computed tomography (FDG PET/CT) has been associated with survival (Namura et al., 2010) and has been used to classify patients into different response groups based on the change in tumour size and/or labelled glucose uptake (Ueno et al., 2012). Patients (n=35) treated with sunitinib were classified into three response groups based on these parameters; median PFS was 458 ± 146 , 131 ± 9 , and 88 ± 26 days for the good, intermediate, and poor response groups respectively (Ueno et al., 2012, Kakizoe et al., 2014).

Biomarkers based on imaging parameters are currently advantageous as tumour imaging is already routine in cancer management. However the techniques employed in many of these studies are highly specialised and it is not clear how they would be transferred into the NHS and routine clinical care. The most significant problem with these imaging studies is their size, without larger prospective studies it is difficult to fully determine the clinical utility of these markers. It is also not possible, from these studies, to determine if these markers are predictive or prognostic.

1.4.3.5. Circulating cells

The relationship between clinical benefit and changes to circulating cells, brought about by changes to the vasculature, has been investigated by a number of groups. In a study of circulating endothelial cells (CECs) in 26 patients, an elevation of CECs within 28 days of starting sunitinib was associated with a PFS above the study median ($p=0.0109$) (Gruenwald et al., 2010). A later study found no link with CECs, but instead found baseline levels of circulating progenitor cells (CPCs) to be predictive of PFS ($P=0.01$) and OS ($P=0.006$), in 46 patients treated with sunitinib (Farace et al., 2011). Another study found an increase in the number of apoptotic

circulating tumour cells (CTCs) was associated with better outcome ($P=0.01$) (Rossi et al., 2012). Furthermore, a decrease in the number of circulating regulatory T cells was correlated with overall survival ($P<0.05$) in a cohort of 28 sunitinib treated patients (Adotevi et al., 2010). A few studies have looked at the neutrophil-to-lymphocyte ratio (Dirican et al., 2013, Park et al., 2014, Keizman et al., 2011), all of which have found a lowered ratio to be predictive of clinical benefit. In a study of 109 patients, Keizman et al found a ratio of <3 was associated with overall survival (HR 0.3; $P=0.043$). Though most of these studies are fairly small, their findings warrant further investigation.

1.4.4. Resistance to anti-angiogenic therapy

Therapeutic resistance most likely explains the variation in response to sunitinib, and this may be intrinsic (no clinical benefit from the start of therapy) or acquired (the patient stops responding after an undetermined period of time). Understanding what causes resistance to sunitinib is important to allow improved cancer management, through monitoring potential resistance markers, and through rational design of tailored drug combinations to inhibit multiple signalling pathways. Many theories exist on the specific molecular and physiological factors that cause resistance, and these have been extensively reviewed elsewhere (Bergers and Hanahan, 2008, Vasudev and Reynolds, 2014, Sierra et al., 2010), however it is likely that it comes about either through the adaptation of a stress response, thus allowing survival in a more hostile environment, or through the activation of alternative signalling pathways to circumvent the blockage.

Though the VEGF cascade is the most prominent pro-angiogenic route, it is by no means the only mechanism through which angiogenesis can occur. Despite the

continued inhibition of VEGFR, the upregulation or pre-existence of alternative pro-angiogenic factors which are not targeted by sunitinib, such as angiopoietin-1 (Casanovas et al., 2005), interleukin-8 (IL-8) (Huang et al., 2010), and the delta-notch pathway (Li et al., 2011), can allow angiogenic escape in preclinical models treated with anti-angiogenesis inhibitors. IL-8 especially has been found to be an important mediator of sunitinib resistance in RCC (Huang et al., 2010), and has been found to be associated with poor clinical outcome both in sunitinib (Harmon et al., 2014) and pazopanib (Tran et al., 2012) treated patients. Other mechanisms that may allow the development of a new blood supply include the recruitment of bone marrow-derived cells, and modification of the existing vasculature. Bone marrow-derived vascular progenitors have been shown to allow neovascularisation in glioblastoma and, of relevance to RCC, this can be driven by a HIF-mediated mechanism (Du et al., 2008). Vascularisation by using pre-existing vessels, through mechanisms including intussusceptive microvascular growth (IMG), glomeruloid angiogenesis, vasculogenic mimicry, and looping angiogenesis have been proposed as additional methods for the tumour to secure a blood supply (Vasudev and Reynolds, 2014). Finally, increased tumour invasiveness may also play a role, through invasion of surrounding normal tissues and subsequent vessel co-option (Bergers and Hanahan, 2008), a mechanism which has been reported in a large number of tumours including primary and metastatic lesions (Vasudev and Reynolds, 2014). Increased aggressiveness has been reported following VEGF therapy (Paez-Ribes et al., 2009), moreover, sunitinib was found to upregulate the presence of pro-invasive proteins (Broutin et al., 2011), and cause a more metastatic phenotype in an *in vivo* model (Ebos et al., 2009).

The pre-existence, upregulation, or adaptation of factors allowing the tumour to secure an alternative vascular supply may represent an escape mechanism through which the tumour overcomes the hypoxia brought on by anti-angiogenic therapy. Supporting the pre-existing vasculature, for example through increased pericyte coverage of the endothelial cells, has been suggested as another route through which the tumour may adapt to vascular attack (Bergers and Hanahan, 2008). However as many TKIs also inhibit the platelet derived growth factor receptor (PDGFR) found on pericytes, this is an unlikely scenario in mRCC. TKIs have also been proposed to cause the destruction of mature vessels through their dependency on VEGF signalling, however as mature vessels may have differing dependencies on VEGF survival signals (Sitohy et al., 2012), VEGF blockade may only be targeting a subset of vessels. Survival signals may also come from infiltrating stromal cells, though the mechanism is not known a variety of cells have been proposed to provide support (Vasudev and Reynolds, 2014). Finally, the tumour may become resistant through a molecular mechanism such as point mutations of the inhibitor binding site, overexpression of the target receptor, or constitutive activation of downstream signalling pathways (Sierra et al., 2010).

1.5. Clinical proteomics

The technological advances made in recent years have significantly changed the landscape of cancer research, from the completion of the human genome project to the development of technologies allowing us to perform nucleic acid profiling experiments, expression analysis, and mutation detection; our ability to understand the molecular basis of carcinogenesis has reached unprecedented levels. There are, however, many questions that cannot be answered solely by genetic and

transcriptomic studies, such as the expression, activity, and interactions of the cellular proteins – the workhorses of the cell. Investigating the proteome for biomarkers and druggable targets provides a means to investigate a snapshot of the real-time activities of the cell. Furthermore, it is generally accepted that transcription of a gene does not guarantee its expression (Vogel and Marcotte, 2012); post translational modification can switch on, switch off, or target a newly synthesised protein for immediate destruction. The genetic and transcriptomic landscape may therefore not fully reflect the complexity of the cellular environment.

1.5.1. RCC proteomics

Proteomic analysis of renal cell carcinoma has mostly focussed on identifying new biomarkers, with multiple profiling studies completed on tissue, serum, urine, and cell lines, and these have been reviewed elsewhere (Craven et al., 2013b). Recent studies investigating the tissue proteome of RCC have profiled both primary and metastatic lesions. A label-free analysis of eight matched primary RCC mass and normal tissue identified 1761 proteins, and two differentially expressed proteins, Adipose differentiation-related protein and Coronin 1A, were further validated using immunohistochemistry (Atrih et al., 2014). This same study also used pathway analysis to identify a number of upregulated cancer-related pathways, a technique which is gradually being used with more frequency. A different study of twelve matched primary tumour and normal RCC tissue samples identified 213 dysregulated proteins, of which acyl-CoA acyltransferase 1 and manganese superoxide dismutase were validated in a further 6 matched pairs using Western blot (Zhao et al., 2014). Focussing on metastatic lesions, which can be very different to the primary tumour (Gerlinger et al., 2012), analysis of 6 metastatic and primary lesions by mass spectrometry found dysregulation of 29 proteins, of which profilin-1, 14-3-3 zeta, and galectin-1 were validated in an independent cohort of 22

primary and 26 metastatic lesions by Western blot (Masui et al., 2013). These are all small analyses, nevertheless these proteins have been validated on a small-scale, and further investigation of their expression is warranted.

Analyses of fluids have mostly focussed on serum, with other studies looking at tumour interstitial fluid, and urine. A recent study of serum from 58 ccRCC patients, 20 additional pre- and post-op ccRCC patients (40 samples), and 64 healthy volunteers identified peptides from RNA-binding protein 6 (RBP6), tubulin beta chain (TUBB), and zinc finger protein 3 (ZFP3) as upregulated in ccRCC, with levels in post-op ccRCC patients lowering towards normal levels (Yang et al., 2014). Though a few small studies have looked at using urinary peptide profiles to diagnose RCC (Wood et al., 2013), fewer studies have investigated the urinary proteome. Mass spectrometric analysis of 89 RCC patients and 76 normal controls identified a potential role for 14-3-3 beta/alpha, which was subsequently validated by Western blot (Minamida et al., 2011), however its upregulation in bladder cancer and cystitis means it may not be RCC-specific (Minamida et al., 2011). Finally, analysis of RCC tumour interstitial fluid revealed the differential expression of 539 proteins through spectral counting, of which 138 were found to be significantly different. Small-scale validation was completed for two proteins (NNMT and ENO2) by Western blot, and two by ELISA (ENO2 and TSP1) (Teng et al., 2011). Though early validation has been completed for many of these, large scale validation is generally missing. Nevertheless, renal proteomics has seen successes elsewhere, with the recent identification and validation of ACY1 as a predictor of delayed graft function in renal transplantation patients (Welberry Smith et al., 2013), providing confidence that this technology is starting to come of age.

As VHL appears to be lost very early on in pathogenesis (Zhuang et al., 1995, Lubensky et al., 1996), investigating the proteomic impact of VHL mutation may therefore be a feasible method to identify new biomarkers and drug targets that are present early in cancer development. Another means to investigate the RCC proteome is through the use of *in vitro* cell lines. Our labs and others have used cell lines to investigate VHL dependent changes, and this has revealed many alterations in the absence of VHL. In a proteomic 2D-PAGE study using the VHL defective cell line UMRC2 transfected with empty vector (-VHL) or wild type VHL (+VHL), 30 proteins were shown to change in the absence of VHL (Craven et al., 2006), including multiple mitochondrial proteins and the cytoskeletal GTPase septin 2 (SEPT2). The same cell lines were later enriched for membrane proteins and 19 differentially regulated proteins were revealed, including CD166 and CD147 (Aggelis et al., 2009). CD147 especially has roles in tumour growth, metastasis, and metabolism in multiple cancers (Kanekura and Chen, 2010).

1.5.2. Proteomic techniques

The proteomics field has developed significantly over recent years, with the most significant leap forward coming from the development of protein-suitable mass spectrometry. This technology allows identification of proteins within a sample by measurement of their mass-to-charge ratio and their abundance, identification is achieved by comparing the measured mass to a database of the known human proteome. Initial studies focussed on separation of proteins by 1D and 2D SDS-PAGE, with subsequent analysis of gel bands and spots by mass spectrometry. These techniques were limited mostly in their depth of coverage, with identifications limited to the most abundant proteins. Current methods allow mass spectrometric analysis of whole proteomes from both clinical and *in vitro* samples, allowing the comparison of different cell and disease phenotypes. Large-scale proteomic

profiling studies have recently identified over 10000 proteins in a single cell line (Nagaraj et al., 2011), furthermore, a recent publication reported the first draft of the human proteome (Kim et al., 2014, Wilhelm et al., 2014). It should be noted that these proof-of-concept studies often combine multiple fractionation technologies to improve the mining depth of current mass spectrometers, and would not currently be feasible in a medical research facility with many hundreds of samples requiring analysis. Other methods for identifying proteins in a sample include antibody array-based techniques, which require a hypothesis-driven approach to assess the type of proteins likely to be present in the sample. Following identification of a protein species, validation is essential and this is usually performed using an antibody-based technique such as Western blotting, enzyme linked immunosorbent assay (ELISA), or immunohistochemistry (IHC). However this can also be performed using the mass spectrometry-based technique multiple reaction monitoring (MRM), or using an array-based platform such as Luminex.

Despite these technical developments, there is still significant room for improvement in the proteomic field. Accurately quantifying protein amounts between samples in a reproducible fashion has not had the success of the genomic industry, and though many techniques are available there is, as yet, no gold standard for general protein quantification of a complex mixture. Current mass spectrometric quantification methods include both labelled and label-free experiments, each with their own advantages and disadvantages. Labelled techniques include stable isotope labelling by amino acids in cell culture (SILAC), isobaric tag for relative and absolute quantification (iTRAQ), isotope coded affinity tags (ICAT), and QConCAT. SILAC, iTRAQ and ICAT allow labelling of an entire sample, whereas QConCAT involves the creation of a labelled peptide specific to the protein of interest. Labelling techniques have the advantage of allowing low fold

changes to be identified, and greater confidence in the quantification of the identified proteins, however they are expensive processes which can be labour intensive. In contrast, label-free mass spectrometry, which relies on spectral counting or ion intensities to perform relative quantification are cheaper and quicker, however there is greater risk for technical error in the results, and high fold changes are generally required to improve confidence in the results. The difficulty in measuring highly complex samples is another problem for mass spectrometry, especially those samples with a large dynamic range of concentrations – such as serum. Methods to overcome this have focussed on pre-fractionation, and tools to perform this include chemical processes such as reverse phase chromatography which separates proteins based on their hydrophobicity, ion exchange (strong cation exchange (SCX)/ strong anion exchange (SAX)) and size exclusion chromatography (SEC), which rely on charge or size, respectively, on which to separate. Alternatively, affinity chromatography can be used, which separates based on a biological component of the sample. The dynamic changes of the proteome mean that there is a relatively high level of both spatial and temporal variability, even between cells of the same type. Nevertheless, the proteomic field is now starting to yield answers to clinically important questions (Mischak et al., 2012, Fuzery et al., 2013).

1.5.3. Proteomic analysis of different sample types

1.5.3.1. Serum proteomics

Serum has been estimated to contain tens of thousands of protein isoforms (Anderson, 2002, Archakov et al., 2007). The potential for tumour-made proteins to enter the blood through secretion or membrane shedding may enable this fluid to

contain disease-specific biomarkers. Serum is also an easily accessible fluid which can be obtained at any stage during a clinical intervention, thus giving the opportunity for longitudinal monitoring. Moreover, serum is not subjective to the spatial heterogeneity observed in tissue samples, although inter-individual variability can be very high. All of these features make serum a highly interesting clinical sample for proteomic studies. The most recent update of the human plasma proteome database reported 10,546 proteins, however only 3,784 of these have been found in two or more studies (Nanjappa et al., 2014), underlining two of the most significant problems of serum proteomics: depth of mining and reproducibility. The concentration of serum proteins spans ten orders of magnitude; this large range is problematic, due to the masking of low abundance proteins by high abundance proteins. The most comprehensive single study to-date confidently identified 2928 proteins, in this study the authors used two successive stages of fractionation to simplify the complex mixture and improve the discovery rate (Liu et al., 2007). Although this level of fractionation is not generally a feasible approach in clinical studies due to the significant amount of time necessary to undertake this level of mining, some prefractionation is essential. Many studies have investigated different types of fractionation, including the use of size exclusion, ion exchange, and reversed phase chromatography, however these generally require multiple fractions to achieve a significant depth of mining, thus increasing the analysis time. Removal of the most abundant proteins by immunodepletion has been shown to be a quick method to aid in unmasking lower abundance proteins. A 52.3% increase in the number of identifications, compared to neat serum, was achieved when using the MARS-14 column (Smith et al., 2011b), which selectively depletes the 14 most abundant proteins in human serum. Though there are concerns surrounding co-depletion when using this technique (Bellei et al., 2011), the one-step increase in identifications justifies this technique for clinical serum-based studies. Though

serum studies have poor reproducibility, performing repeat injections of the same sample may help alleviate this due to the selection of different peptides for fragmentation (Barnea et al., 2005). Downstream validation of putative targets using a sensitive and specific technique is essential to confirm the clinical utility of any identified targets; this was recently achieved with a panel of three serum biomarkers identified to predict response to bevacizumab (Collinson et al., 2013).

1.5.3.2. Tissue proteomics

A few thousand proteins can be identified from tissue studies without the need for any pre-fractionation; furthermore this sample does not suffer from the signal masking effects brought about by a few high abundance proteins, as seen in serum, unless the sample is particularly vascular. Acquiring tumour tissue is, however, a highly invasive process, thus removing the ability for multiple sampling. Moreover, due to an averaging out of the protein intensities within the sample, tissue studies are sensitive to infiltrating non-tumour cells, and all tissue blocks must therefore be pathologically reviewed prior to analysis to ensure the block is predominantly tumour. Tumour heterogeneity is another serious problem with tissue-based studies and significant protein, transcript, and genetic differences have been observed in different regions of the same tumour, and between different metastatic sites (Gerlinger et al., 2012). Finally, due to embedding of a significant amount of tumour tissue in formalin fixed-paraffin embedded (FFPE) blocks, very little – if any – sample may remain for storage as frozen sections, a sample type which requires significant infrastructure to bank properly which can make storage of this sample type problematic. Acquiring sufficient samples for an adequately powered study can therefore be challenging. The development of techniques to extract proteins from FFPE tissue blocks has helped alleviate one of these problems; with FFPE blocks routinely stored in pathology archives, access to multiple samples is now much

easier. Furthermore, these blocks have long term follow up data associated with them, enabling the clinical implications of the studies to be explored with greater depth. Studies in our lab have revealed there are comparable numbers of identifications between fresh frozen and FFPE stored blocks (Nirmalan et al., 2011), and that there is no loss in the number of protein identifications from specimens spanning up to a decade in age, with over 2000 proteins being identified per sample (Craven et al., 2013a).

1.5.3.3. Cell based proteomics

In vitro model systems have traditionally provided a platform on which to answer biological questions which may not otherwise be easily answered. Advantages of such a system include the ability to closely monitor and control the environment, the ability to genetically modify the cells to represent a variety of disease phenotypes, an essentially limitless supply of sample, and the homogenous nature of the resulting sample which removes complications from infiltrating non-tumour cells. Though the homogenous nature of *in vitro* samples allows for the detection of very low abundance proteins, it does not reflect the complexity of a tissue, and this oversimplification of the model may therefore bring results that do not translate into clinically valid findings. Furthermore, some of these immortalised cancer cell lines have been used for many years, and cell line validation is essential to ensure significant genetic and epigenetic alterations have not taken place. Finally, it is also unknown how sensitive many of these cell lines are to minor cell culture stressors, and how this may impact on the phenotype and thus the reliability of the cell line in question. Validation of findings in clinical samples is essential to truly determine the utility of any differential protein expressions identified. A cell-based mass spectrometry study can easily yield many thousands of proteins, indeed with

multiple levels of fractionation and a high speed mass spectrometer it is possible to identify over 10000 proteins (Nagaraj et al., 2011). The development of techniques such as Filter Aided Sample Preparation (FASP) (Wisniewski et al., 2009) and Suspension Trapping (STrap) (Zougman et al., 2014) have allowed for low quantities of cell lysate to be used to routinely identify over 3000 proteins. Furthermore, the potential for downstream studies investigating the functional aspects of a protein of interest, such as immunoprecipitation, make *in vitro* models an attractive method to investigate the proteome.

1.6. Study aims

The overall project aim was to identify clinically relevant markers that will assist with the management of renal cell carcinoma, focussing on (a) diagnosis of RCC and (b) prediction of the response to therapeutic intervention.

Predictive biomarker study

- To determine if baseline proteins could predict for response to sunitinib, by comparing baseline nephrectomised tissue of patients subsequently treated with sunitinib, in a non-hypothesis driven approach.
- To determine if quantifiable changes occur in protein profiles over time, and if markers of sunitinib response can be found in serum, by analysing baseline and longitudinal serum samples of responders and non-responders.
- To validate potential targets identified in the discovery patient set using Western blot, ELISA, and immunohistochemistry.

Early tumourigenesis study

- To find proteins specific to the VHL-mediated tumourigenesis of renal cell carcinoma by comparing the proteomes of isogenic cell lines carrying four clinically relevant VHL disease mutations, plus a wild type control.
- To validate potential markers using Western blot, immunoprecipitation, and RT-PCR.

A tripartite approach was used to investigate the utility of different samples for biomarker mining. Markers predictive of response to sunitinib were investigated using nephrectomised tissue and longitudinal serum collected from patients treated with sunitinib. Proteins that may shed light on the early tumourigenesis of RCC, and thus provide early biomarkers of disease, were investigated using cell lines carrying VHL disease relevant mutations. Potential candidates were validated using a variety of techniques including western blot, immunoprecipitation, and immunohistochemistry.

2. Materials and Methods

All solutions were made using Milli-Q ultrapure water (18M Ω resistance). Unless otherwise specified, all laboratory chemicals were purchased from Sigma.

2.1. Sample collection and preparation

2.1.1. Patients

An investigation into potential biomarkers to predict response to sunitinib was carried out using clinical samples. Both serum and renal tissue from patients with clear cell metastatic RCC treated with sunitinib at St. James' University Hospital were collected with informed consent and ethics approval (Ref.10/H1306/7). Sunitinib was administered at a starting dose of 50 mg once a day (p.o.) using a standard four weeks on/two weeks off repeating schedule. Best response was assessed by CT scan according to RECIST v1.1 criteria (Eisenhauer et al., 2009) (Table 2.0.1). Patients were selected for comparative analysis of response to sunitinib with the assistance of a renal oncologist. As far as possible, patients were matched for age, grade, gender, pathological stage, presence of metastases, and degree of toxicity. Follow up data including inpatient dose reductions and toxicities were recorded.

2.1.1.1 Serum samples

Longitudinal blood samples were collected from relapsed mRCC patients at baseline before treatment initiation, two weeks into the first cycle, then consecutively at the start of each treatment cycle (Figure 2.0.1). Venous blood samples were collected by the on-site sample processing team - according to

standard operating procedures - into 9 ml Z serum clot activator tubes (Greiner BioOne, Stonehouse, UK). Samples were left to clot for at least 45 minutes (max 2 hours) before being centrifuged at 2000 x g, for 10 minutes at room temperature. Serum was aliquotted and then stored at -80°C until further use.

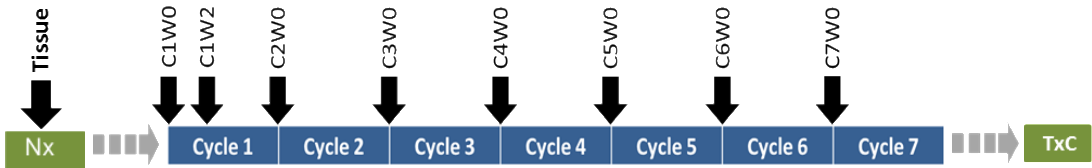
Table 2.0.1: RECIST criteria used to assess response to therapy in solid tumours

Response	Determination
CR	Disappearance of all target lesions. Any pathological lymph nodes (whether target or non-target) must have reduction in short axis to <10 mm.
PR	At least a 30% decrease in the sum of diameters of target lesions, taking as reference the baseline sum diameters.
SD	Neither sufficient shrinkage to qualify for PR nor sufficient increase to qualify for PD, taking as reference the smallest sum diameters while on study.
PD	At least a 20% increase in the sum diameters of target lesions, taking as reference the smallest sum on study. In addition to the relative increase of 20%, the sum must also demonstrate an absolute increase of at least 5 mm. (The appearance of one or more new lesions is also considered progression).

PD, progressive disease; SD, stable disease; PR, partial response; CR, complete response. Adapted from (Eisenhauer et al., 2009)

Figure 2.0.1: Sunitinib cycles and sample collection

Tissue was taken at nephrectomy (Nx). Blood samples were collected at baseline - before treatment initiation (C1W0), two weeks into the first cycle (C1W2), and at the start of every cycle thereafter, until treatment cessation (TxC). C, cycle number; W, week number within cycle. Broken arrow indicates an unspecified period of time.



2.1.1.2. Tissue samples

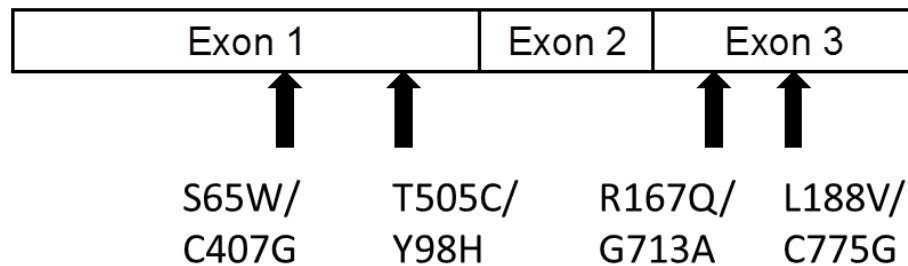
Formalin Fixed-Paraffin Embedded (FFPE) tissue blocks from the pathology archive were requested and carefully reviewed by an expert urological pathologist. As far as possible, all patients were matched for age, grade, gender, pathological stage, presence of metastases, and degree of toxicity. Multiple blocks were requested for each patient, and the age of the blocks spanned a range of 1-11 years. Pathological review allowed for the histological type to be confirmed and a representative region from a single block per patient to be marked for subsequent analysis; most blocks required macrodissection. Representative blocks were chosen to maximise tissue recovery and minimise contamination from necrosis, normal tissue, and inflammatory areas. Following review, 10µm sections were cut (total surface area approx 5 cm²) onto glass slides, oven dried, and then heated on a hot plate at 60°C for 30 minutes.

2.1.2. RCC cell lines

To investigate the proteomic changes brought about by mutation of VHL, four subtypes of VHL disease, generated as previously described (Clifford et al., 2001) from stable transfections of the parental cell line RCC4 were compared. The RCC4 renal cancer derived cell line carries the C194G loss-of-function mutation in exon 1 of *vhl*, causing a switch from serine to tryptophan at position 65 (Ser65Trp). Five stable transfectants were previously generated from this parental line which had the following modifications introduced via a pcDNA3.1 vector: full length wild type VHL (WTHAB6), empty vector (RCC4/T), and three mutations representative of VHL disease types 2A, 2B and 2C (RCC4/2A, RCC4/2B, RCC4/2C, respectively). The RCC4 *VHL* mutation (C407G/S65W) and the type 2A (T505C/Y98H) mutations are both located in exon I, the type 2B (R167Q/G713A) and type 2C (L188V/C775G) mutations are both in exon III (Figure 2.0.2). All five cell lines were kindly donated by Professor Eammon Maher (Abdulrahman et al., 2007). All VHL-disease cell lines were Short Tandem Repeat (STR) profiled to confirm their lineage.

Figure 2.0.2: Location of VHL mutations in RCC4 transfectants

Location of *VHL* mutations in RCC4/T (S65W/C407G), RCC4/2A (T505C), RCC4/2B (G713A), and RCC4/2C (C775G).



2.1.2.1 Cell culture

Three replicates of each cell line were routinely passaged at 85-90% confluence by washing with PBS+0.1% w/v EDTA and incubating for 3-4 minutes with 0.5 ml trypsin-versene. The five VHL cell lines were grown in MEM- α culture medium (Life Technologies, Paisley, UK) supplemented with 10% v/v FCS and 2 mM glutamine. The first passage following revival from liquid nitrogen storage contained 1 mg/ml Geneticin to select for plasmid-carrying cells, and the cells were passaged five times prior to downstream analysis. Cells were grown in triplicate to provide independent replicates, and maintained at 37°C, 5% CO₂.

2.2. Protein enrichment, extraction, and separation

2.2.1. Immunodepletion of serum with a MARS14 column

Immunodepletion was performed using a MARS14 column (4.6 x 100 mm) (Agilent Technologies, Wokingham, UK), which uses antibodies to capture 14 of the most abundant proteins from human serum (Table 2.0.2). Proteins not bound by the antibodies on the column ('peak 1') constituted the lower abundance fraction, proteins recognised and bound by the column ('peak 2') formed the high abundance fraction. Samples were depleted and analysed as previously described (Smith et al., 2011a). Briefly, depletion was performed on an Agilent 1200 series HPLC using the proprietary buffers for the MARS14 column: Buffers A and B. The column was operated at room temperature and stored at 4°C in between uses, the autosampler and fraction collector were operated at 4°C. Samples were diluted 1:3 in Buffer A and filtered through a 0.22 μ m centrifugal Spin-X filter (Corning, Amsterdam, NL) to remove large aggregates. A total of 160 μ l was injected onto the column, containing

40 µl neat serum (average concentration of neat serum, 76 µg/µl; range, 52.86-103.52 µg/µl) per depletion. A single depletion was performed per sample. The column was operated at maximum 60 MPa with the following programme: 0-21 minutes 100% Buffer A, 0.125 ml/min; 21-23 minutes 100% Buffer A, 1 ml/min; 23-30 minutes 100% Buffer B, 1 ml/min; 30-41 minutes 100% Buffer A, 1 ml/min. Fractions were collected in 1 minute intervals. The peak 1 and peak 2 fractions were individually pooled and frozen at -80°C until further use. An identical programme, using Buffer A as the sample, was performed between samples to wash the column and minimise protein carry-over.

Table 2.0.2: Proteins immunodepleted by the MARS-14 column

Albumin	α2-macroglobulin
IgG	IgM
Transferrin	Apolipoprotein A1
α1-antitrypsin	α1-acid glycoprotein
Fibrinogen	Complement C3
IgA	Apolipoprotein A2
Haptoglobin	Transthyretin

The 14 serum proteins depleted by the MARS14 column.

2.2.2. Generation of cell lysates from RCC cell lines

Cells were grown to 85-90% confluence in T150 flasks, the media was aspirated off and the cells were washed five times in ice-cold PBS. Excess liquid was removed using a stripette. Cells were lysed into 1.5 ml 5% w/v SDS/50 mM Tris-HCl, pH 7.6 and sonicated for 1 minute using a Soniprep 150 (MSE, London, UK) to disrupt the DNA. DTT (15 mM) was added and the samples were heated to 95°C for 5 minutes to denature the proteins and reduce the disulphide bonds. The lysate was clarified

by centrifugation in a microfuge at 14,000 x g for 10 minutes, then the supernatant was aliquotted and stored at -80°C until further use.

2.2.3 Protein extraction from FFPE tissue

FFPE tissue sections were first dewaxed and rehydrated using five sequential incubations of organic solvents: (1) five minutes in 100% xylene; (2) five minutes in 100% xylene; (3) five minutes in 100% ethanol; (4) five minutes in 90% ethanol; (5) five minutes in 70% ethanol. The sections were macrodissected with a sterile scalpel as necessary and the required regions were scraped into 400 µl sample buffer (5% w/v SDS/50 mM Tris-HCl pH7.6), vortex mixed and heated to 105°C for 45 minutes to extract, and denature the proteins. The extracts were cooled on ice for five minutes and then the DNA was sheared using a Soniprep 150 (MSE, London, UK). DTT (15 mM) was added to the extracts, followed by heating to 95°C for 5 minutes to break and reduce the disulphide bonds. Extracts were clarified by centrifugation for 10 minutes at 4°C, and then aliquots were stored at -80°C until further use.

2.2.4. Immunoprecipitation

RCC4/T cells were grown in T150 flasks and allowed to reach 85% confluence, then cell monolayers were scraped into PBS + 0.1% w/v EDTA, pelleted, and washed twice in PBS. The cells were centrifuged, the supernatant was removed, and the cells were lysed into a modified RIPA buffer (150 mM NaCl, 50 mM Tris-HCl pH 7.4, 1% v/v NP40, 0.2% w/v sodium deoxycholate, protease inhibitor cocktail tablet). Cell lysis was allowed to occur on a spinner at room temperature for 15 minutes. The lysate was clarified by centrifugation at 14,000 x g for 10 minutes, filtered through a 0.45µm Acrodisc® filter (Pall Life Sciences, Portsmouth, UK), and either frozen at -20°C or used immediately. Immunoprecipitation was performed at

room temperature using capture antibody at 4 µg/ml, or an equal concentration of species-matched normal IgG, which was added directly to the cell lysate and incubated on a spinner at room temperature for 45 minutes. Magnetic protein G coupled Dynabeads® (Life Technologies, Paisley, UK) were prepared by washing once in the modified RIPA buffer, resuspended in the same buffer, and added to the protein-antibody mix (20µl/100µl sample). The mix was allowed to incubate at room temperature on the spinner for 45 minutes. The magnetic beads were captured using a strong magnet and the supernatant was retained. The bead pellet was washed once in modified RIPA buffer, and then resuspended in Laemmli buffer (62.5 mM Tris-HCl (pH 6.8), 10% v/v glycerol, 2% w/v SDS, 15 mM DTT), and heated at 95°C for 5 minutes. The magnetic beads were captured using a magnet and the supernatant was kept for downstream analysis.

2.2.5. 1D SDS-PAGE

Protein samples were diluted in Laemmli buffer, denatured and reduced by heating to 95°C for 5 minutes, allowed to cool, then separated (10 µg/lane) on 12% acrylamide gels cast in-house, or 8-16% Criterion tris-glycine gels. A Tris-glycine running buffer was used (25 mM Tris, 192 mM glycine, 0.1% w/v SDS) and the gels were run at 120V for 60-90 minutes in a Mini-Protean II gel electrophoresis kit (Bio-Rad, Herts, UK), or Criterion™ Cell gel tank (Bio-Rad, Herts, UK), respectively. For very low or very high molecular weight proteins, a Bis-Tris gel (Life Technologies, Paisley, UK) was used. Proteins were diluted in a modified Laemmli buffer (62.5 mM Tris-HCl (pH 6.8), 10% v/v glycerol, 2% w/v SDS, 20 mM DTT), denatured and reduced by heating to 95°C for 5 minutes, allowed to cool, then separated (10 µg/lane) on 10% or 12% NuPAGE® Bis-Tris gels (Life Technologies, Paisley, UK). MES (Life Technologies, Paisley, UK) or MOPS (Life Technologies, Paisley, UK) running buffer was used to assist in the resolution of very low, or very

high, molecular weight proteins respectively. Gels were run at 150V for 60-90 minutes in a Novex® electrophoresis tank (Life Technologies, Paisley, UK).

2.3. Protein assays

2.3.1. Bradford assay

Protein concentrations of serum samples were determined using a modified microplate Bradford assay. Reactions were set up in sample tubes using PBS as the diluent (1/50 dilution). Standards (range: 1.0-20.0 µg/ml) were made using 1 mg/ml BSA diluted in PBS. Samples and standards were transferred to a 96-microwell plate in duplicate (200 µl/well), and then 50 µl of Bradford reagent (Bio-Rad, Herts, UK) was added to each well and mixed thoroughly with a multichannel pipette. The plates were incubated for 20 minutes before reading the absorbance at 620nm using a MultiSkan Ex (Thermo, Hemel Hempstead, UK). PBS + Bradford reagent was used as the background, which was subtracted during analysis. Microsoft Excel 2007 was used to plot a standard curve and calculate concentrations.

2.3.2. Spectrofluorometer

To determine protein concentration by spectrofluorometry, the tryptophan autofluorescence of the protein samples was measured, and then this intensity was multiplied by an assay-determined normalisation factor to account for the average amount of tryptophan found in the human proteome. Protein samples in lysis buffer (2.5% w/v SDS/50 mM Tris-HCl pH 6.8, 15 mM DTT) were heated to 95°C to denature the proteins and reduce disulphide bonds. Protein intensity was measured

using a Jasco Spectrofluorometer (Jasco, Dunmow, UK) controlled using the proprietary software. Briefly, a background of 8M urea was used to maintain a denaturing environment, and the amino acid tryptophan (0.1 µg/µl) was used as the amino acid standard. Peak intensities were measured at a wavelength of 285 nm, in increments of 1nm. The peak intensity for the urea background was measured, and the intensity for tryptophan was determined by adding 1 µl, mixing, and measuring, and this step was then repeated to give two tryptophan measurements. Samples were then measured by sequentially adding 1µl of each sample, mixing thoroughly, and recording the intensity. The equation used to determine the concentration of each of the samples is shown in Equation 1. The urea background (U) was subtracted from the first (W1) and second (W2) tryptophan samples, and from each of the test samples (S). To determine the concentration of each test sample, the difference in intensity between the two tryptophan values was determined, and this was divided by the amount of tryptophan (A) used in micrograms (0.1 µg used here), to determine an assay specific standard normalisation factor. Next, the intensity measured for each test sample was divided by the assay specific normalisation factor, and multiplied by a global normalisation factor of 70. The global normalisation factor was determined assuming that tryptophan accounts for 1.3% of the human protein amino acid composition (Kulak et al., 2014).

Equation 1: Determining sample concentration from spectrofluorometry

Determination of sample concentration using spectrofluorometer-determined intensities. S, sample intensity; U, urea background intensity; W1, first tryptophan intensity reading; W2, second tryptophan intensity reading; A, tryptophan standard, μg .

$$\left\{ \frac{S-U}{\left[\frac{(W2-U)-(W1-U)}{A} \right]} \right\} 70$$

2.4. Staining proteins

2.4.1. Colloidal Coomassie blue staining of 1D SDS-PAGE gels

Gels were first fixed in 50% ethanol/10% acetic acid overnight, to wash out SDS and precipitate the proteins into the gel. Colloidal Coomassie staining was performed using Brilliant Blue G – Colloidal Coomassie concentrate (Sigma, Dorset, UK), diluted 4:1 with methanol prior to use. Staining was allowed to continue for at least 1 hour. Gels were destained for 1 minute with destain 1 (25% v/v methanol, 10% v/v acetic acid), then further destained using destain 2 (25% v/v methanol) until an optimal protein pattern was observed.

2.4.2. Silver staining of 1D SDS-PAGE gels

Gels were fixed as described above (Section 2.4.1.), and silver staining was performed using the ProteoSilver™ Silver Stain Kit (Sigma, Dorset, UK) according to the manufacturer's instructions. The gels were allowed to develop until an

optimum protein pattern was observed, then halted according to the manufacturer's instructions.

2.4.3. Haematoxylin and Eosin staining of tissue sections

FFPE tissue sections were haematoxylin and eosin (H&E) stained prior to pathological review. Sections were dewaxed in xylene (4 x 3 minutes), and rehydrated through 100% ethanol (4 x 3 minutes), 90% ethanol (1 x 3 minutes), and 70% ethanol (1 x 3 minutes). Sections were washed in running tap water (2 minutes), stained with Mayer's haematoxylin (2.5 minutes), and rinsed in running tap water again. The Mayer's pigment was blued with Scott's tap water (2 minutes), then slides were washed in running tap water (1 minute) and stained with eosin (2 minutes). Slides were washed once more with running tap water (1 minute), blotted dry, and dehydrated through four changes of 100% ethanol (15 seconds, 1 minute, 5 minutes, 5 minutes). Sections were cleared in xylene (3 x 3 minutes) and mounted with DPX mounting medium.

2.5. Tryptic digestion of proteins

2.5.1. On-membrane digestion of serum proteins

Depleted serum samples were concentrated using a 0.5 ml 10kDa molecular weight cut off (MWCO) Amicon filter (Millipore, Watford, UK). Concentration from a total starting volume of approximately 2ml was performed at 4°C, 14000 x g for approximately 30 minutes, to 150µl. The samples were frozen at -80°C in a fresh sample tube until further use. All centrifugation steps were performed at 14000 x g at 4°C. The unbound (Peak 1) samples were heated to 95°C for 5 minutes with DTT

to denature and reduce the proteins (final concentration 50 mM), centrifuged for 5 minutes, and then transferred to a 0.5 ml 30 kDa MWCO Amicon filter (Millipore, Watford, UK). Samples were washed with 300 µl 50mM ammonium bicarbonate (ABC), centrifuged for 10 minutes to clarify the solution, then incubated in the dark for 10 minutes with 80 µl 100 mM iodoacetamide to alkylate the cysteines. The solution was centrifuged for a further 5 minutes, then the proteins were washed on the filter with 250 µl 50 mM ABC five times and a fresh collection tube was attached. Digestion was performed in a wet chamber at 37°C overnight using sequencing grade modified porcine trypsin at a 1:50 enzyme:protein w/w ratio (Promega, Southampton, UK). Peptides were extracted with 140 µl MilliQ by centrifugation, and the peptides were pooled from two extractions. The concentration was measured using a NanoDrop 8000 (Thermo, Hemel Hempstead, UK) and the solution was concentrated to approximately 10µl using a Concentrator Plus (Eppendorf, Stevenage, UK) vacuum centrifuge.

2.5.2. Filter Aided Sample Preparation (FASP) digestion of tissue extracted proteins

Due to the presence of SDS in the tissue lysates, it was necessary to use the Filter Aided Sample Preparation (FASP) protocol to process these samples, which was carried out using a modified version of the published method (Wisniewski et al., 2009). In this method, the chaotropic agent urea was used to break the SDS micelles and wash SDS out of the sample. Urea was then washed out with ABC. Samples were diluted into lysis buffer (5% w/v SDS 100 mM Tris-HCl, 10 mM dithiothreitol (DTT), lysed using a Soniprep 150 (MSE, London, UK), clarified by centrifugation at 14000 x g, and denatured at 95°C for 5 minutes. Due to the heat labile nature of urea, all the following centrifugation steps were performed at 20°C,

14000 x g. The lysates were diluted with 8M urea to reduce the SDS concentration (final concentration 0.4%), transferred into a 30kDa MWCO Amicon filter (Millipore, Watford, UK), and centrifuged for 10 minutes. Proteins were washed three further times with 400µl 8M urea to remove SDS and centrifuged for 20 minutes each time. The cysteine residues were alkylated for 10 minutes in the dark using 100 mM iodoacetamide (IAA), followed by centrifugation for 10 minutes. Excess IAA was then washed away with 400µl 8M urea, by centrifugation for 20 minutes. The urea was then diluted out with four washes of 50mM ABC, followed by 20 minutes of centrifugation each time. The MWCO filters were transferred to new collection tubes, 45µl 50mM ABC was added and then sequencing grade modified porcine trypsin (Promega, Southampton, UK) was added (enzyme:protein ratio 1:50). The tryptic digests were incubated in a wet chamber at 37°C overnight. Peptides were extracted in two steps with 140µl MilliQ, the extractions were pooled and their concentrations were measured using the NanoDrop (Thermo, Hemel Hempstead, UK).

2.5.2.1. Peptide clean up using STAGE Tips

Samples that were digested using FASP were cleaned prior to mass spectrometric analysis using the STop And Go Extraction (STAGE) tips method (Ishihama et al., 2006). To prevent damage to the packed tip, all centrifugation steps were performed at 5000 x g, at room temperature. Packed tips were made using five plugs of Empore™ C18 octadecyl discs (Sterlitech, Washington, USA) pushed down into a P200 tip and inserted into the top of a sample tube. The STAGE Tip was wetted with 50 µl methanol and centrifuged for 1 minute, then the tip was activated with 80 µl Velos Buffer B (80% v/v acetonitrile (ACN), 0.1% v/v formic acid, 0.01% v/v trifluoroacetic acid). The tip was washed with 100 µl Velos Buffer A (5% v/v ACN, 0.1% v/v formic acid, 0.01% v/v trifluoroacetic acid). The sample was

loaded onto the top of the tip (maximum 10 µg/plug), then centrifuged for 3-4 minutes, washed with 100 µl of Velos Buffer A and then centrifuged for a further 3-4 minutes. Proteins were eluted into a fresh collection tube with 80 µl Velos Buffer B, the eluate was collected then added onto the top of the tip and centrifuged through the tip once more. The concentration was measured using a NanoDrop (Thermo, Hemel Hempstead, UK) and the solution was concentrated to approximately 10µl using a Concentrator Plus (Eppendorf, Stevenage, UK) vacuum centrifuge.

2.5.3. Suspension Trapping (STrap) digestion of cell lysate proteins

In this combined protein digestion and peptide clean up protocol (Zougman et al., 2014), a pipette tip is packed with both a quartz matrix and a C18 resin. The SDS is washed out with other contaminants whilst the undigested proteins are trapped in a suspension held by the quartz matrix. The proteins are digested, and as the peptides pass through the C18 resin they are desalted and concentrated. Briefly, the STrap tip (S-tip) was assembled by inserting 3 plugs of C₁₈ Empore resin, followed by 11 plugs of MK360 quartz fiber (Munktell Filter Ab, Falon, Sweden), into a P200 pipette tip, then the plugs were gently compacted down. To the S-tip, 120 µl of STrapping buffer (90% v/v methanol, 100 mM Tris/HCl pH 7.1) was added, and the tip was allowed to sit for 1 minute. The S-tip was inserted into a 1.5 ml microcentrifuge tube with a hole punctured in the lid; the two components together created the 'spin-unit'. To prepare the sample, 60 µg of cell lysate - prepared as previously described (Section 2.2.2.) - was concentrated to 30 µl, alkylated with 150 mM IAA (stock 0.9 M in H₂O) for 15 minutes in the dark, and acidified with phosphoric acid (final concentration, 1.2% v/v). The alkylated and acidified sample was slowly added into the S-tip, and the spin-unit was centrifuged at 2800 x g for 2 minutes, and the flow through disposed of. Next, 70µl of STrapping buffer was added into the S-tip and it was placed into a fresh microcentrifuge tube, the device

was centrifuged at 2800 x g for 45 seconds. To wash out the methanol, 30 µl of 50 mM ABC was added to the S-tip and centrifuged through for 30 seconds at 2800 x g. To enable digestion, 22µl of trypsin was added to the top of the spin-unit (0.033 µg/µl, in 50mM ABC) and pushed into the filter stack with the aid of a syringe. The Spin-unit was closed off using a 10 µl filter tip, and incubated at 47°C for 60 minutes. After incubation, 50 µl of ABC was added and the device was centrifuged for 1 minute at 2300 x g. To wash out impurities, 100 µl of 0.5% v/v trifluoroacetic acid (TFA) in H₂O was added and centrifuged through the spin-unit for 90 seconds at 2500 x g. The STRap-tip was once again placed into a fresh microcentrifuge tube and 80 µl of elution buffer (70% v/v acetonitrile, 0.5% v/v formic acid, in H₂O) was added, the device was briefly centrifuged for 5 seconds at 2500 x g to allow the buffer to enter the matrix, then incubated at room temperature for 30 seconds. Finally the spin-unit was centrifuged for 1 minute at 2500 x g to elute the peptides. The eluate was concentrated to approximately 10 µl using a Concentrator Plus (Eppendorf, Stevenage, UK) vacuum centrifuge.

2.6. Protein identification

Protein identification was performed by reverse-phase fractionating and injecting the digested peptides onto the mass spectrometer, where they were ionised using a nano-electrospray ionisation source, before being focussed and passed through to the Orbitrap for the first analysis. During this stage the m/z of the ions is determined; this is carried out by using a fourier transform to deconvolute each ions signal, which is generated by their speed and tangent as they move around the central coaxial spindle-like electrode, and is dependent on their mass. A highly accurate fingerprint of their mass – a peptide mass fingerprint – is generated, and the top most abundant ions are selected for further analysis. Fragmentation by

collision-induced dissociation ensues (MS/MS), and the fragments are measured in the linear ion trap (LTQ) quadrupole cell, which uses four electrodes with oscillating radio and electrical fields to trap the ions and measure their m/z value. Three sets of data are thus achieved using this technique: the retention time of the peptides on the C_{18} column, the peptide mass fingerprint as measured by the Orbitrap, and the peptide fragmentation pattern as measured by the ion trap. The mass peak lists were then compared to the UniProt database using the MaxQuant software suite (Cox and Mann, 2008a), to analyse the proteins in the sample.

2.6.1. LTQ-Orbitrap Velos Mass Spectrometry

Digested peptides were separated by online reversed-phase capillary liquid chromatography (LC) and analyzed by electrospray tandem mass spectrometry (MS) using either two or three injections per sample. The sample concentrations were normalised to one another within an experiment (total amount of protein injected varied between experiments; see individual studies) and injected onto an in-house prepared 20 cm reversed phase fused-silica capillary emitter column (inner diameter 75 μm , packed with 3.5 μm Kromasil C_{18} media) using a Dionex UltiMate 3000 RSLCnano nanoflow system (Thermo, Hemel Hempstead, UK), or a Thermo EasyNano system (Thermo, Hemel Hempstead, UK). The LC setup was connected to a linear quadrupole ion trap-orbitrap (LTQ-Orbitrap) Velos mass spectrometer (Thermo, Hemel Hempstead, UK) equipped with a Proxeon nanoelectrospray ion source (Thermo, Hemel Hempstead, UK). The total acquisition time was 240 min per injection, the major part of the gradient (from 10 to 210 min) being 4–25% v/v ACN in 0.1% v/v formic acid at a flow rate of 400 nl/min. Survey MS scans were acquired in the Orbitrap with the resolution set to 60000. Up to 20 most intense ions per scan were fragmented and analyzed in the linear trap.

2.6.2. Protein Identification using MaxQuant

The raw Xcalibur files were searched against either an IPI or Uniprot human protein sequence database with the MaxQuant suite of software (Cox et al., 2009, Cox and Mann, 2008b). The initial maximal mass tolerance for the MS scan was set to 10 ppm, the fragment mass tolerance for MS/MS was set to 0.5 Thomson. The maximum false protein and peptide discovery rates were set to 0.01. Default settings were kept except (i) 'Label Free Quantitation' and (ii) 'second peptides' were switched on, and (iii) 'fast LFQ' and (iv) 'match between runs' were switched off. ProteinGroups files from MaxQuant were filtered to remove proteins that were identified from the decoy database, known contaminants, and proteins that were identified with only one peptide.

2.7. Validation of protein expression profiles

2.7.1. Western Blotting

Proteins were separated by 1D SDS-PAGE and then transferred onto Hybond™-C Super membranes (GE Healthcare LifeSciences, Little Chalfont, UK) in transfer buffer (250 mM Tris, 192 mM Glycine, 10% v/v methanol) using a Mini Protean II (Bio-Rad, Hemel Hempstead, UK) at 100V for 1 hour, or using a Criterion™ Blotter (Bio-Rad, Hemel Hempstead, UK). Following transfer, blots were stained with Ponceau S solution (Sigma, Dorset, UK), allowing the quality of the transfer to be checked. The Ponceau S was washed off using MilliQ, then the blot was blocked using blocking buffer (TBS + 0.1% v/v Tween-20 + 10% w/v skimmed milk powder) for 1-2 hours. Blots were washed in TBST (TBS + 0.1% Tween-20) for 3 x 5 minutes and incubated with the primary antibody for a defined period (antibodies were titrated to determine optimal concentrations and incubation conditions) (Table

2.0.3). The blots were washed in TBST three times for five minutes each to remove excess primary antibody, and then incubated with the appropriate EnVision secondary HRP-labelled antibody (Dako, Ely, UK), diluted 1/100. Excess secondary antibody was washed off with three x five minute TBST washes and then the blots were incubated with the luminol substrate, SuperSignal® West Dura Extended Duration Substrate (Thermo, Hemel Hempstead, UK) for five minutes. Blots were visualised using Kodak BioMax MS film (Sigma, Dorset, UK) on a Medical Film Processor (Konica Minolta, Banbury, UK).

Table 2.0.3: Antibodies used in Western blots of cell and tissue lysates

Antigen	Species	Clone	Clone	Conc/dil	Source	Cat No.
VHL	Rabbit	pAb	-	1/100	SDIX	2319.00.02
HIF1a	Mouse	pAb	-	1/100	Sigma	SAB1405933
CA9	Mouse	mAb	M75	1/80000	(Oosterwijk et al., 1986)	NA
IRS2	Rabbit	mAb	EP976Y	1/200	Abcam	ab52606
Cathelicidin	Mouse	mAb	OSX12	1/1000	Abcam	ab87701
CD70	Mouse	mAb	2F2	2.5µg/ml	Abcam	ab51664

NA, not applicable. Dilution provided where a concentration was not available. pAb, polyclonal; mAb, monoclonal.

2.7.2. Immunohistochemistry

To determine the most appropriate antibody concentration to use, immunohistochemistry protocols were first optimised using OCT-embedded frozen tissue, before analysing FFPE sections. Sections (3-5µm) were cut onto slides (FFPE, or OCT-embedded frozen). FFPE sections were first dewaxed in xylene (3 x 5 minutes) and rehydrated in 100% ethanol (3 x 1 minute). Antigen retrieval was undertaken using proteinase-K. Briefly, proteinase-K was resuspended in

resuspension buffer (10 mM Tris-HCl pH 7.5, 20 mM CaCl₂, 50% v/v glycerol) and diluted in PBS (100 µl/50ml). Sections were incubated with the proteinase K solution at 37°C for 25 minutes, then rinsed in TBS. OCT-embedded frozen sections were allowed to thaw and fully dry at room temperature, then were fixed in acetone for 2 minutes, and air dried fully again. For all sections, endogenous peroxidase was blocked for 20 minutes using 0.6% v/v hydrogen peroxide made fresh in methanol, and the slides then washed in running water for 10 minutes. The slides were next mounted onto Shandon coverplates with TBS, and loaded into the Sequenza (Thermo, Hemel Hempstead, UK). The sections were blocked for 20 minutes using casein (Vector Laboratories, Peterborough, UK), diluted 1/10 in Zymed antibody diluent (Life Technologies, Paisley, UK). Primary antibody (Table 2.0.4) was diluted in Zymed antibody diluent (Invitrogen, Paisley, UK), and incubated at room temperature for 1 hour. Slides were washed twice in TBS (4 minutes, then 5 minutes), then incubated with Novolink™ post-primary block (Leica Biosystems, Newcastle Upon Tyne, UK) for 30 minutes. Slides were washed twice more in TBS (4 minutes, then 5 minutes), and incubated with the Novolink™ HRP Polymer secondary antibody (Leica Biosystems, Newcastle Upon Tyne, UK) for 30 minutes. Slides were washed twice in TBS (4 minutes, 5 minutes), removed from the Sequenza, and incubated with ImmPACT™ DAB Peroxidase Substrate (Vector Laboratories, Peterborough, UK) for 5-10 minutes. The reaction was stopped by placing the slides into tap water, and the slides were rinsed in running tap water for 1 minute. Counterstaining was performed using Meyer's haematoxylin for 20 seconds, then slides were rinsed in tap water (1 minute), Scott's tap water (1 minute), and tap water (1 minute). Slides were dehydrated through three changes of absolute ethanol (3 x 1 minute), air dried for 5 minutes, then through four changes of xylene (4 x 1 minute). Coverslips were mounted with DPX mounting medium.

Table 2.0.4: Antibodies used in immunohistochemistry studies

Antigen	Species	Clonality	Clone	Conc	Source	Cat No
CD70	Mouse	mAb	2F2	2.5 µg/ml	Abcam	ab51664
CD31	Mouse	mAb	JC70A	15 µg/ml	Dako	102870

mAb, monoclonal

2.8. Data analysis

2.8.1. Statistics

Statistical analyses were performed by Dr David Cairns and Michelle Wilson (with the Clinical and Biomedical Proteomics Group). Principal components analysis and hierarchical cluster analysis were used as multivariate methods of exploratory data analysis to examine the data for outliers and check for visible groupings in the data. Differential expression of proteins between patient groups, cell lines, and time points for longitudinal analyses was assessed using non-parametric statistical tests on the changes in peptide values, intensity, and LFQ intensity, considering each protein separately. Analyses of longitudinal time points were performed using the Friedman test. Cell lines were assessed using Kruskal Wallis to determine if there was a significant difference between any pair of data. Pairwise comparisons for all studies were performed using the Wilcoxon Mann Whitney test. The false discovery rate was calculated using the q-value method (Storey, 2002). Heat maps were generated by determining the Z-score for each protein, and colour coded per sample depending on the determined score. Clustering was performed to enable an optimal pattern of expression to be determined, based on grouping similar expression patterns between responders and non-responders. Exploratory comparisons of mass spectrometric injections were performed, by generating Venn

diagrams and boxplots to enable data visualisation and comparison of statistical parameters. All analysis was undertaken in the R environment for statistical computing (Team, 2011).

2.8.2. Bioinformatics

Uniprot identifiers were extracted from the list of identified proteins. Protein functions were determined using a combination of UniProt and SwissProt, Gene Ontology, and literature searching. Uniprot identifiers were converted into ENSEMBL gene IDs using UniProt's ID mapping service (<http://www.uniprot.org/mapping/>). Pathway analysis was performed using Ingenuity Pathways Analysis (Qiagen, Crawley, UK) and a variety of online tools, including DAVID (david.abcc.ncifcrf.gov/), GeneMania (www.genemania.org/), and KOBAS (kobas.cbi.pku.edu.cn/).

2.9. Genomic and transcriptomic methods

2.9.1. DNA sequencing

Sequencing was performed over the *vhl* mutations in the five RCC4 cell lines to ensure only the expected mutations were present. Cells from 80% confluent flasks were washed once with PBS + 0.1% w/v EDTA, then lifted with 0.5ml trypsin-versene as described above (Section 2.1.2.1.). Cells were resuspended in PBS + 0.1% w/v EDTA, transferred to a 15 ml Falcon tube, washed twice, then frozen at -20°C. DNA was recovered using the mini QIAprep kit (Qiagen, Crawley, UK), according to the manufacturer's directions, and quantified using the NanoDrop 8000

(Thermo, Hemel Hempstead, UK). Recovered DNA was frozen at -80°C until required.

All PCR and sequencing reactions were performed by Dr. Claire Taylor, St James's University Hospital. The cDNA transgene was amplified from WTHAB6, RCC4/2A, RCC4/2B, and RCC4/2C using the PCR primer pair V3/V6 (Table 2.0.5). The endogenous VHL at the site of the inactivating mutation was amplified using the PCR primer pair M3529/M3538 in all five cell lines and wild type VHL. PCR was carried out using the HotStarTaq PCR Master Mix kit (Qiagen, Crawley, UK). Reactions contained 20ng of total DNA, (11.25 pmol) forward primer, (11.25 pmol) reverse primer, 10ul HotStarTaq master mix, and, for primer set M3529/M3538, 10% of v/v DMSO in a total volume of 20 µl. For both primer sets the cycling conditions were: denaturation at 95°C for 15 minutes, and 40 cycles of denaturation at 95°C for 30 seconds, annealing at (50-65°C) for 30 seconds, and extension 72°C for 60 seconds, followed by a final extension at 72°C for 10 minutes. PCR products (5 µl) were cleaned up using 2 µl ExoSAP-IT (Affymetrix, High Wycombe, UK).

Sequencing over the inactivating RCC4 mutation in the genomic copies of this gene was performed using both the primer pair M3529/M3538 and M3533/M3536 (Table 2.0.5). Primer pair M3529/M3538 were located in the 5'untranslated region (UTR) and intron 1 respectively, to ensure endogenous VHL was amplified and not the transgene. Primer pair M3533/M3536 were used to sequence over the mutation. Primer pairs for sequencing over the respective cell line specific mutations were picked to give the best possible view of the known mutation site. Sequencing was performed using the M3537/V6 pair (WTHAB6), V5/V6 (RCC4/2A) and M3541/V6 (RCC4/2B and RCC4/2C). Sequencing reactions were performed using the

BigDye® ready reaction mix (Life Technologies, Paisley, UK). Reactions contained 1 µl of cleaned PCR product, 0.5 µl of BigDye Terminator v3.1 (Applied Biosystems, Warrington, UK), 3.5 µl Half Big Dye reagent (Molecular Devices, California, USA), and 0.5 µl of 3.2 µM primer in a total volume of 10 µl. Sequencing conditions were 25 cycles of 96°C for 10 sec, 60°C for 5 sec and 60°C for 4 min. Unincorporated nucleotides and primers were removed by ethanol precipitation. Sequencing products were resuspended in 20 µl of formamide and run on an Applied Biosystems 3130 genetic analyser (Life Technologies, Paisley, UK) using POP7 polymer and 36 cm well-to-read capillaries. Data analysis was carried out by visual inspection of electropherograms and using Mutation Surveyor software (SoftGenetics, Pennsylvania, USA).

Table 2.0.5: Forward and reverse primers used for PCR and sequencing of *VHL*

Primer pairs were selected to cover both the endogenous *VHL* and to enable the best view of the mutation. Primers pairs for PCR (PCR) and sequencing (S) are shown.

Target	Pair	Forward primer	Reverse primer
cDNA – PCR	V3/V6	Agtacggccctgaagaagac	tgcgctcctgtgtcagccgctccaggt
gDNA – PCR	M3529/M3538	Cccgggtggtctggatcg	accgtgctatcgccctgct
gDNA – S	M3533/M3536	Agtcgggcccaggagt	aggcggcagcgttgggtag
gDNA – S	M3529/M3538	Cccgggtggtctggatcg	accgtgctatcgccctgct
WTHAB6 – S	M3537/V6	Cgtcgtgctgccgtatg	tgcgctcctgtgtcagccgctccaggt
505 – S	V5/V6	catcttctgcaatcgcagtcgcgcgct	tgcgctcctgtgtcagccgctccaggt
713 – S	M3541/V6	ccaaactgaattattgtgccatc	tgcgctcctgtgtcagccgctccaggt
775 – S	M3541/V6	ccaaactgaattattgtgccatc	tgcgctcctgtgtcagccgctccaggt

2.9.2. RT-PCR

Transcript levels may be investigated through the use of quantitative RT-PCR, by measuring the appearance of product over time through successive cycling. The TaqMan system involves the use of a probe, which is specific to a sequence between the primer pair, and has a fluorescent label together with a quencher attached (Gibson et al., 1996, Livak et al., 1995). The probe binds to the cDNA during the annealing step, and when polymerase extends over the probe the quencher is released, allowing the fluorescent signal to be measured. Successive cycling results in an increase of the signal, which may be used in a relative comparison of target gene mRNA presence in the samples tested.

Cells were grown to 85% confluence, washed, and mRNA was extracted using the Qiagen RNeasy kit, according to the manufacturer's guidelines. The concentration of mRNA was determined using the NanoDrop 8000 (Thermo, Hemel Hempstead, UK). Total RNA was reverse transcribed into cDNA using SuperScript™ First Strand Synthesis System (Invitrogen, Paisley, UK). Reaction mixtures were set up in triplicate, and included 3 ng total RNA, 4 µl First Strand buffer, 2 µl dNTP mix (10 mM), 1.6 µl MgCl₂ (100 mM), 1 µl oligo(dT) primers (Eurogentec, Southampton, UK), 1 µl DTT (100 mM), 0.5 µl RNasin (Invitrogen, Paisley, UK), and 1 µl SuperScript III, in a total volume of 20 µl. RNA was boiled at 95°C for 5 minutes, before adding to the reaction mixture. Reverse transcription was carried out by incubation at 50°C for 1 hour to allow primer extension, followed by incubation at 72°C for 15 minutes to terminate the reaction. TaqMan primers were selected, based on best coverage, for IRS2 (Hs00275843_s1) and ACTB (Hs01060665_g1) (Applied Biosystems, Warrington, UK) and included a FAM-MGB labelled probe. Quantitative PCR was set up in triplicate for the target and for the endogenous

control. A triplicate reaction volume included 50 μ l TaqMan Universal master mix (Applied Biosystems, Warrington, UK), 5 μ l of TaqMan probe mix, 20 μ l of PCR reaction mix, in a volume of 100 μ l. A total of 25 μ l was transferred to each of three wells of a PCR reaction plate (Life Technologies, Paisley, UK). Quantitative PCR was carried out using a 7500 real time PCR machine (Applied Biosystems, Warrington, UK), using the $\Delta\Delta C_t$ method (Livak and Schmittgen, 2001).

3. The analysis of serum for the discovery of biomarkers predictive of response to sunitinib

3.1. Introduction

Around a third of metastatic RCC patients fail to see any clinical benefit from sunitinib, and despite a plethora of publications on putative biomarkers none have yet made it into clinical use. As serum contains a snapshot of all proteins – both intracellular and extracellular – due to low level tissue leakage (Anderson, 2002), this fluid may hold the key to finding a protein, or proteins, that can predict response to sunitinib. Furthermore, obtaining a blood sample from a patient is less invasive than acquiring a tissue sample, and this also raises the potential for procuring multiple longitudinal samples to monitor patient response to the drug. Finally, the averaging across spatial location of all the serum proteins means intra-patient heterogeneity – a significant issue in tissue based profiling – is not a problem in serum studies. Serum is therefore an attractive source for biomarker mining, and this experiment aimed to investigate the potential for using this fluid for biomarker discoveries in a non-hypothesis driven manner.

Serum-based research is problematic in a mass spectrometry setting due to the large concentration range of the proteins found within this sample, which spans ten orders of magnitude. The most clinically useful biomarkers are likely to be found in the pg-ng/ml range (Anderson, 2002), but these are masked by the more abundant proteins when using standard mass spectrometry techniques. Prefractionation of serum is essential to improve the chances of observing the less abundant proteins. In this study serum samples were immunodepleted using a MARS14 column, which selectively depletes the 14 most abundant proteins in human serum.

Immunodepleted serum from sunitinib-responding and non-responding patients were compared, using mass spectrometry, at baseline and longitudinally during the course of therapy, to investigate if proteins could be identified that predicted response to sunitinib, either prior to therapy or soon after treatment initiation.

3.1.1. Aims

- Investigate if differences in protein expression could be found between sunitinib responders and non-responders in a pilot scale study, using serum collected at baseline.
- Analyse protein changes over the course of therapy to determine if protein profiles could be used to monitor response.
- Identify a set of putative biomarkers of response to sunitinib, for downstream multiplexed validation in a large patient cohort.

3.2. Patient selection

Patients with metastatic clear cell RCC treated in the first line setting with sunitinib were selected based on best response according to RECIST 1.1 criteria (Eisenhauer et al., 2009). Those with partial response as best response were designated 'responders', and those with progressive disease were designated 'non-responders'. Patients were matched as much as possible for age, gender, grade, pathological stage, presence of metastases, and drug-related toxicity. Patients were selected independently for the baseline and longitudinal arms of the study.

3.2.1. Patients selected for the baseline study

Five responders (PR1-PR5) and five non-responders (PD1-PD5) were selected for analysis at baseline (Table 3.0.1), using serum samples taken prior to treatment initiation. Patients were similar for gender, age, grade, and stage, however non-responding patients were found to have poorer performance status, and higher Heng and MSKCC scores, compared to the sunitinib responding patients. In addition, more non-responding patients had metastatic disease at the time of presentation. Dose reductions of sunitinib were more common in the non-responding group, this was mostly due to toxicity and may have resulted in the patients receiving sub-optimal doses. Finally, four out of five responders and two out of five non-responders received nephrectomies following diagnosis.

3.2.2. Patients selected for the longitudinal study

Patients were chosen based on best response and availability of longitudinal samples, and were matched as much as possible for all other factors (Table 3.0.1). Four responders (PR1, PR2, PR6, PR7) and three non-responders (PD1, PD3, PD4) were selected for longitudinal analysis; two of the responders (PR1 and PR2) and all three non-responders were also analysed in the baseline study. As with the baseline study, the two patient groups were similar for age, gender, stage, and grade. A difference was observed between the groups when performance status, MSKCC score, IMDC criteria (Heng score) and the presence of metastases at presentation were considered, with the non-responding patients scoring more poorly in all these aspects (Table 3.0.1). All four responders, compared to only one out of the three non-responders, received a nephrectomy. Longitudinal samples were frequently available for responders spanning many months and these patients were analysed across 5-6 time points: baseline before treatment initiation, two

weeks into the first cycle, and the start of alternating cycles up to one-year post initiation of therapy. Non-responders generally did not remain on therapy for long periods and consequently had fewer samples available, these patients were therefore analysed across baseline before treatment initiation, two weeks into the first cycle, and the start of the second or third treatment cycle depending on sample availability. The samples were numbered sequentially, from T1 to T6, to indicate the time point they were associated with.

Table 3.0.1: Overview of patients used in both arms of the serum study

Overview of the patients used in the baseline and longitudinal serum studies. Patients were picked based on best response, and matched as much as possible thereafter. Absolute numbers of patients are provided, with percent of the within group population shown in brackets. MSKCC (Motzer et al., 2002) and IMDC (Heng) (Heng et al., 2009) scoring, 0 = favourable, 1-2 = intermediate, 3+ = poor. PR, partial response; PD, progressive disease. Unknown – data was not available on these patients. Fuhrman grade 2 is not shown as no patients with this grade were present in the study.

		Baseline study		Longitudinal study	
		Responders (PR)	Non-responders (PD)	Responders (PR)	Non-responders (PD)
Outcome, n (%)	<i>PR</i>	5 (100)	0 (0)	4 (100)	0 (0)
	<i>PD</i>	0 (0)	5 (100)	0 (0)	3 (100)
Gender, n (%)	<i>Male</i>	3 (60)	4 (80)	2 (50)	2 (67)
	<i>Female</i>	2 (40)	1 (20)	2 (50)	1 (33)
Age, y	<i>Median (range)</i>	76 (54 - 77)	67 (54 - 76)	73 (62 – 82)	58 (54 – 76)
Duration on sunitinib, y	<i>Median (range)</i>	1.91 (0.81 - 2.74)	0.42 (0.22 - 0.77)	2.7 (1.90 - 3.38)	0.42 (0.22 - 0.54)
	<i>Average (± SE)</i>	1.93 (± 0.36)	0.46 (± 0.09)	2.67 (± 0.3)	0.39 (± 0.09)

Prior nephrectomy, n (%)	Yes	4 (80)	2 (40)	4 (100)	1 (33)
	No	1 (20)	3 (60)	0 (0)	2 (67)
Fuhrman grade, n (%)	1	1 (20)	1 (20)	0 (0)	0 (0)
	3	1 (20)	2 (40)	2 (50)	2 (67)
	4	1 (20)	0 (0)	1 (25)	0 (0)
	Unknown	2 (40)	2 (40)	1 (25)	1 (33)
Pathology stage, n (%)	T1a/T1b	1 (20)	0 (0)	2 (50)	0 (0)
	T2a/T2b	0 (0)	0 (0)	0 (0)	0 (0)
	T3a/T3b	1 (20)	1 (20)	2 (50)	1 (33)
	T4	1 (20)	1 (20)	0 (0)	0 (0)
	Unknown	2 (40)	3 (60)	0 (0)	2 (67)
MSKCC score, n (%)	Favourable	3 (60)	0 (0)	3 (75)	0 (0)
	Intermediate	2 (40)	4 (80)	1 (25)	3 (100)
	Poor	0 (0)	1 (20)	0 (0)	0 (0)
Heng score, n (%)	Favourable	3 (60)	0 (0)	3 (75)	0 (0)
	Intermediate	2 (40)	3 (60)	1 (25)	2 (67)

	<i>Poor</i>	0 (0)	2 (40)	0 (0)	1 (33)
Metastases, n (%)	<i>Synchronous</i>	2 (40)	5 (100)	0 (0)	3 (100)
	<i>Metachronous</i>	3 (60)	0 (0)	4 (100)	0 (0)
Performance status, n (%)	<i>0</i>	3 (60)	1 (20)	1 (25)	0 (0)
	<i>1</i>	2 (40)	3 (60)	3 (75)	3 (100)
	<i>2</i>	0 (0)	1 (20)	0 (0)	0 (0)
Dose reduction, n (%)	<i>Yes</i>	1 (20)	4 (80)	1 (25)	2 (67)
	<i>No</i>	4 (80)	1 (20)	3 (75)	1 (33)

3.3. Using a MARS14 column to immunodeplete serum samples

Depletion of baseline and longitudinal serum samples was performed using a MARS14 column, which depletes the 14 most abundant proteins found in human serum, using a protocol previously optimised in our laboratory (Smith et al., 2011a). Neat serum (40 μ l) was diluted and depleted using a MARS14 column on an Agilent 1200 series HPLC. A representative HPLC chromatogram from a MARS14 depletion is shown in Figure 3.0.1. The 'Peak 1' fraction, which contained the unbound proteins, was eluted first. The 'Peak 2' fraction, which consisted of high abundance proteins bound by the column, was eluted separately. Analysis of the fractionated samples indicated that the proportion of the peak 1 proteins averaged $5.35\% \pm 0.28$ (SE) of the starting injected material. Analysis of neat serum and peak 1 by SDS-PAGE was performed to check the quality of the depletion (Figure 3.0.2). A noticeable difference in the gel banding pattern was observed between depleted (D) and neat serum (S) samples; with few, more abundant proteins present in the neat serum samples, compared to the depleted samples which appeared to have a greater number of less abundant proteins.

Figure 3.0.1: Chromatogram from a representative immunodepletion

Representative chromatogram from a MARS14 immunodepletion. Unbound proteins were eluted in peak 1, high abundance proteins were eluted separately in peak 2. Green and red lines indicate the collection of a fraction, protein abundance was measured in milli absorbance units (mAU).

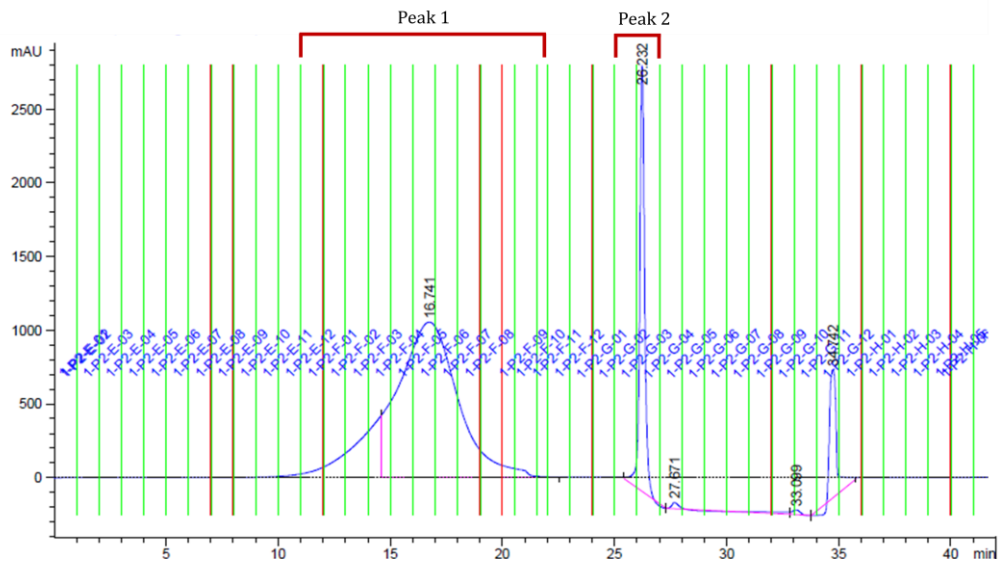
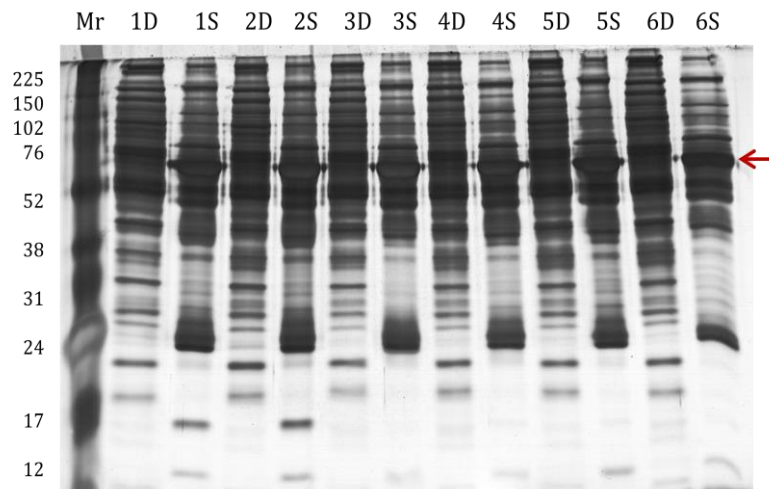


Figure 3.0.2: 1D-PAGE analysis of depleted serum

Representative SDS-PAGE gel of six peak 1 (1D-6D) and six neat serum (1S-6S) samples. Molecular weight markers are shown on the left, arrow indicates albumin.



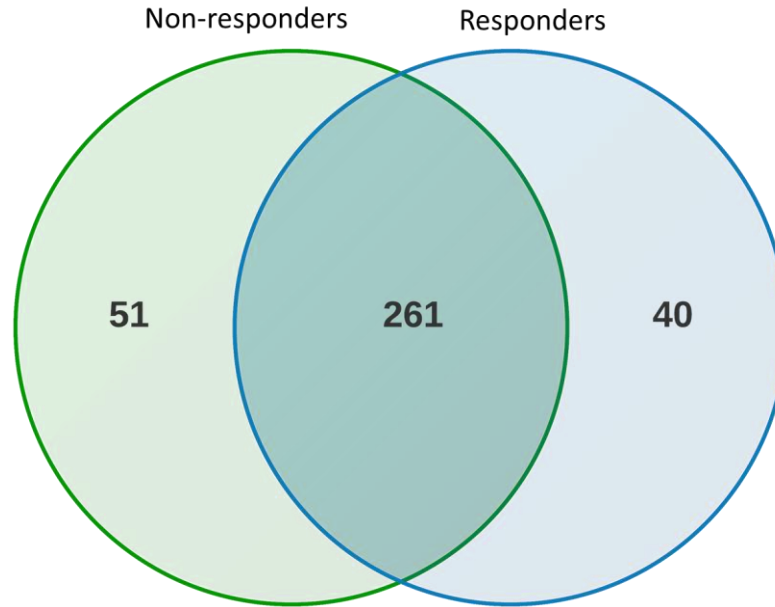
Of note, consistent with previous studies (Tu et al., 2010, Smith et al., 2011a), mass spectrometric analysis of the depleted serum samples revealed that immunodepletion was not complete; most of the depleted proteins remained detectable in all of the patient samples. The number of peptides identified ranged from 1.20 ± 0.37 for transthyretin, to 57.40 ± 3.28 for $\alpha 2$ -macroglobulin. Using the intensity of all the identified proteins to assess the contribution of the depleted proteins to the total protein ion intensity, it was found that the proteins targeted for removal accounted for 5.6% of the total measured mass spectrometry protein intensity, with individual proteins accounting for between 0.002% and 2.54% of the total measured mass spectrometry protein intensity (data not shown). No association was found between the intensity of depleted proteins remaining in each sample (range 2.8-12.2%), and the number of protein identifications in each sample (range 253-335); a regression analysis between protein number and total intensity accounted for by depleted proteins revealed no correlation ($r^2=0.04$) (data not shown), indicating the incomplete removal of the proteins intended for depletion did not impact upon the number of identifications.

3.4. Analysis of patient serum collected at baseline

Serum samples, collected at baseline from five responders and five non-responders, were analysed by mass spectrometry following immunodepletion as previously described, and data were analysed using the MaxQuant software suite. The total number of identifications was different depending on the quantification method used: 404 and 352 proteins were identified based on peptide and LFQ data, respectively. Of those identifications based on LFQ data, 74.1% were common to both patient groups (Figure 3.0.3). The complete set of raw and analysed data can be found on supplementary data files S4, S5, and S6.

Figure 3.0.3: Overlap of proteins identified in baseline serum in non-responders and responders

Overlap between responders (blue) and non-responders (green), indicating 74.1% of proteins were common to both groups, based on LFQ data.



3.4.1. Differential protein expression in the baseline serum of responders and non-responders

As expected, most proteins did not show significant differences in their levels between responders and non-responders. The number of significantly different proteins differed according to the quantitation method used, with five, six, seven, and eight significant proteins identified through peptide number, intensity, LFQ, and MSMS count respectively (Table 3.0.2). Not all proteins that demonstrated a present/absent pattern were significantly different; those that failed to reach significance were absent from many patients in both groups. Most of these were significant through only one quantitation method, with 20 proteins significant through at least one quantitative method, four proteins significant across two

quantitative methods, one protein (RNASE4) significant across three quantitative methods, and no proteins significant across all four methods (data not shown). When peptide data was analysed, five proteins demonstrated a significant change, of which only one of these had a fold change ≥ 5 (PRG2). Although 23 proteins demonstrated a present/absent pattern at the peptide level, 22 of these were identified with ≤ 3 peptides and were therefore close to the limit of detection. A greater number of proteins demonstrated present/absent changes, or large fold differences, when LFQ data was considered (Table 3.0.2). In the LFQ dataset, 91 proteins demonstrated an on/off response in either group, however only one of these, MRC1, was significantly different, with three further proteins approaching significance (DPP4, CDH1, PLA2G7).

Table 3.0.2: Overview of differentially expressed proteins in baseline serum

The number of differentially expressed proteins between responders and non-responders at different fold changes, based on peptides and LFQ data. Sig, total number of significantly different proteins ($P < 0.05$).

		Sig	On/off	≥ 10 fold	≥ 5 fold	≥ 2.5 fold
Peptides	Responders	1	9	0	2	7
	Non-responders	3	14	0	5	7
LFQ	Responders	4	40	3	3	17
	Non-responders	3	51	2	7	21

Data were filtered based on their significance level and fold changes, and visually inspected for their number of peptides and LFQ intensity. Both peptide and LFQ values were used to calculate fold changes (LFQ fold changes not shown). Ten proteins of interest were chosen based on both peptide and LFQ data (LFQ data

not shown), and biological interest (Table 3.0.3), and included both significantly different and non-significantly different proteins. Six proteins were chosen that were upregulated in the non-responders, these were OIT3, S100A8, CTSZ, hCAP18, MSN, and GOLM1. Four proteins that were upregulated in the responders were chosen, these were PRG2, HEG1, PLA2G7, and CDH1. Of these ten targets, OIT3, S100A8, CTSZ, PRG2 and HEG1 demonstrated significant differences between the responders and non-responders (Figure 3.0.4). Interestingly, S100A8 was also found to be upregulated in the non-responders of the longitudinal study.

Table 3.0.3: Baseline serum proteins selected as candidate biomarkers

Proteins selected for downstream investigation in responders (↑PR) and non-responders (↑PD). Fold values are based on the mean number of peptides identified. P values are shown for LFQ, intensity (inten), peptides (pept), and MSMS. * significant, according to Wilcoxon rank-sum test. NC, not calculated; uncalculated fold values due to presence/absence differences.

Gene	Uniprot	R/NR	Fold	Peptides	Pept	Inten	LFQ	MSMS
OIT3	Q8WWZ8	↑NR	9.00	1.8	0.071	0.025*	0.424	0.025*
S100A8	P05109	↑NR	2.00	5.6	0.034*	0.032*	0.095	0.073
CTSZ	Q9UBR2	↑NR	NC	1.0	0.023*	NC	NC	NC
hCAP18	P49913	↑NR	2.00	3.2	0.133	0.151	0.131	0.090
MSN	P26038	↑NR	NC	1.2	0.072	0.072	0.424	0.072
GOLM1	Q8NBJ4	↑NR	NC	0.8	0.071	0.072	0.433	0.071
PRG2	P13727	↑R	8.00	1.6	0.038*	0.075	0.180	0.057
HEG1	Q9ULI3	↑R	3.00	1.2	0.146	0.045*	0.424	0.057
PLA2G7	Q13093	↑R	3.67	2.2	0.083	0.091	0.072	0.089
CDH1	P12830	↑R	2.67	1.6	0.072	0.205	0.072	0.134

3.4.2. Bioinformatic analysis of baseline serum proteins

Analysis by DAVID of the full baseline dataset revealed an overrepresentation of proteins from the extracellular region, as expected for proteins identified from serum. Biological functions identified as overrepresented included response to wounding, defence response, proteolysis, and inflammatory response (Table 3.0.4). Upregulated proteins were investigated further using DAVID's Functional Annotation Clustering; three clusters were found to be significantly enriched in the non-responders; secreted proteins (2.77 enrichment score), inflammatory proteins (2.58 enrichment score), and membrane location (1.58 enrichment score). Only one cluster, secreted proteins (2.82 enrichment score), was found to be significantly enriched in the responders. A GeneMania analysis also indicated that inflammatory proteins were enriched in the non-responders ($P=0.0005$), as well as proteins related to bacterial defence ($P=0.0002$) and neutrophil chemotaxis ($P=0.03$). No functions were found to be significantly enriched in the responders.

Table 3.0.4: Overrepresented biological functions in the baseline dataset

Gene Ontology_FAT terms, assigned by DAVID v6.7, on 278 recognised IDs.

Term	Proteins	P value	Benjamini
Extracellular region	208	5.4E-114	1.3E-111
Secreted	182	1.8E-123	3.5E-121
Response to wounding	86	1.5E-57	3.0E-54
Defence response	74	1.4E-39	5.0E-37
Proteolysis	59	1.8E-14	1.1E-12
Inflammatory response	58	5.6E-40	2.3E-37
Plasma membrane	58	4.9E-2	2.5E-1
Immune response	56	6.2E-21	5.8E-19
Cell adhesion	50	3.4E-16	2.3E-14
Carbohydrate binding	44	2.1E-24	4.2E-22

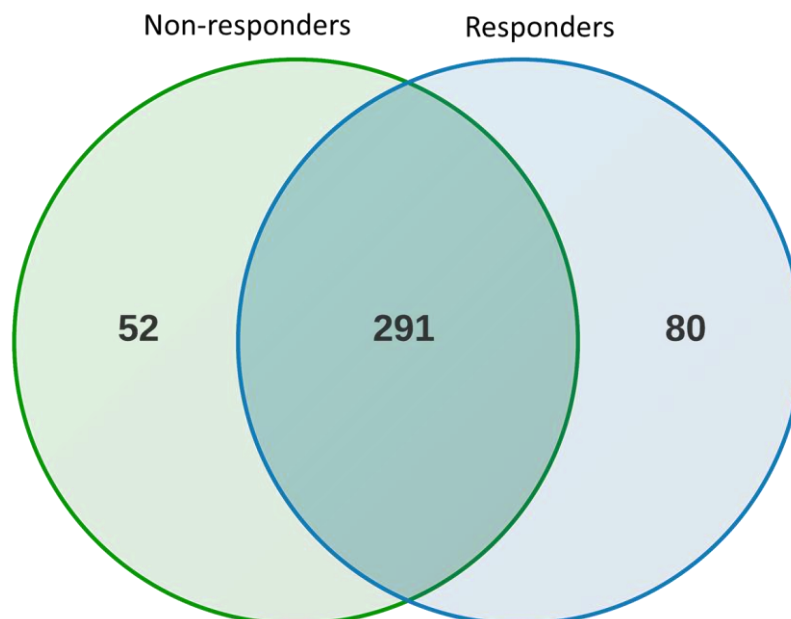
3.5. Analysis of patient serum collected longitudinally

Longitudinal immunodepleted serum samples from four responders and three non-responders were concentrated, digested with trypsin, and separated over four hours by reversed phase liquid chromatography coupled online to an Orbitrap Velos mass spectrometer. Each sample was injected three times, for a total of 12 hours analysis time per sample. Due to limitations in the number of samples that could be analysed concurrently, samples from the responding and the non-responding patients were analysed independently in two separate batches; a sample from one responding patient was analysed alongside the non-responding samples to act as a control across the two batches. Data from the two studies were combined and peak lists were searched against the human IPI database, using the MaxQuant software suite. In total, 371 and 343 proteins were identified in the responders and non-

responders respectively, with an overlap of 68.8% (Figure 3.0.5). Pairwise comparisons were performed using LFQ values between responders and non-responders at each time point. Due to the low number of biological samples and therefore the high amount of technical and biological variability, between group comparisons did not reach significance. The lowest P value achieved was 0.125, at this probability value 42 proteins demonstrated a difference between responders and non-responders across all three time points, and 164 proteins demonstrated a difference between responders and non-responders at any one time point, including 112, 79, and 104 proteins at time points T1, T2, and T3 respectively. The complete set of raw and analysed data can be found in supplementary data files S1, S2, and S3.

Figure 3.0.5: Overlap of proteins identified in longitudinal serum in responders and non-responders

Overlap between responders (blue) and non-responders (green), indicating 68.8% of proteins were common to both groups, based on LFQ data



3.5.1. Differential protein expression in longitudinal serum between responders and non-responders

Using peptide and LFQ data, protein profiles were visually inspected for pattern of response, quantification level, and inter- and intra-patient variability. Table 3.0.5. shows eight proteins that demonstrated a difference between responders and non-responders at the peptide and LFQ level, most of these were elevated in the responders, probability values were calculated using LFQ values. Patterns of protein response were generally acute; the largest difference between responders and non-responders frequently occurred during time points T1 and/or T2. ALDOA, IGFBP5, LDHA, and S100A8 all show an acute response, with measured levels generally peaking at T2. A more chronic change was demonstrated by CECR1, CNTN1, ICAM2, and MAN2A1, with levels changing more consistently towards T3. Figure 3.0.6 shows the protein abundance profiles for all eight longitudinal targets, based on LFQ values (peptide data not shown).

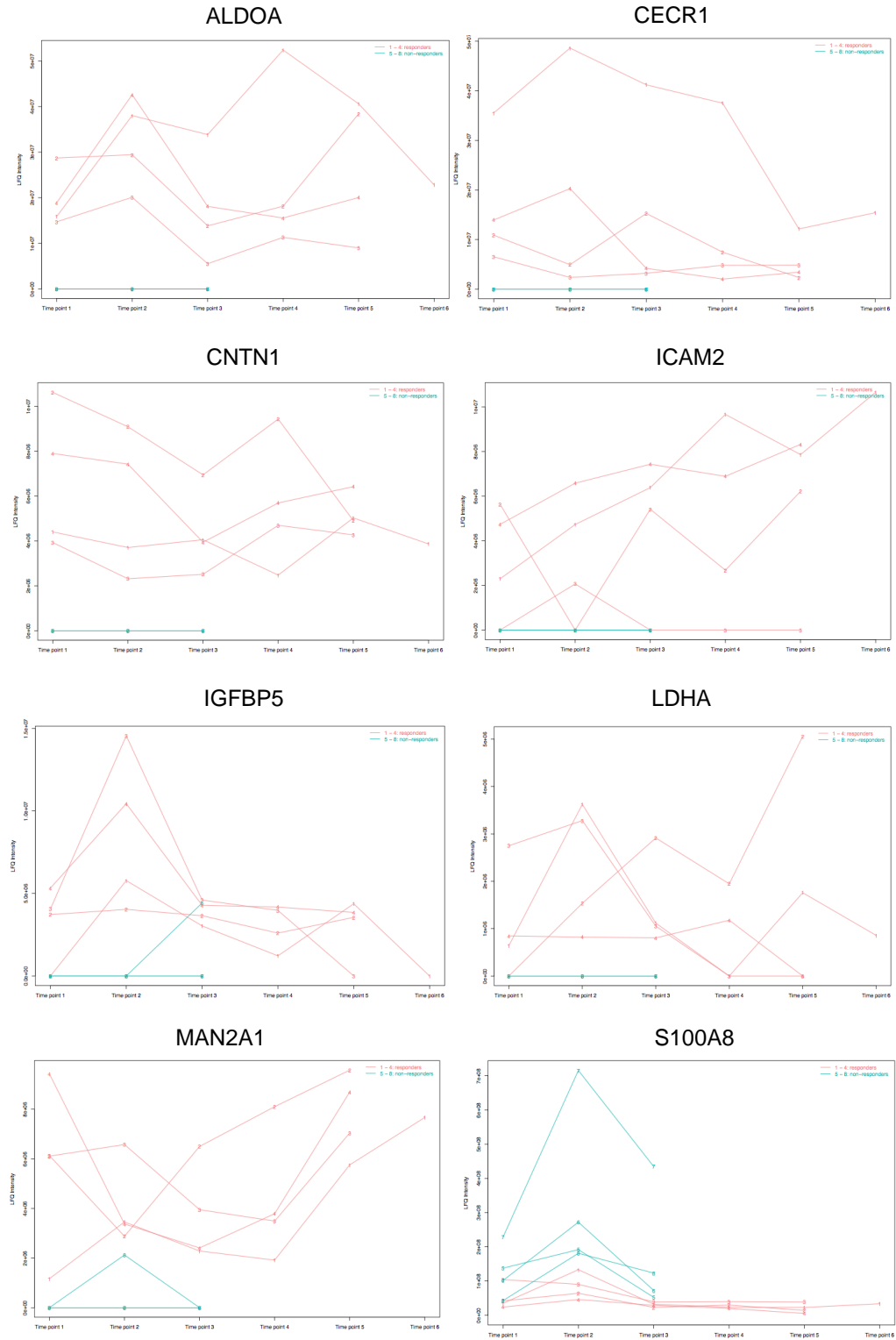
Table 3.0.5: Proteins selected as candidate biomarkers in longitudinal serum

The probability (Pval) of a difference between responders and non-responders at time points T1, T2 and T3 are provided. 'Peptides' refers to the total number of peptides used to identify the protein species of interest.

Protein	UniProt	T1 Pval	T2 Pval	T3 Pval	Peptides	R/NR
ALDOA	P04075	0.125	0.125	0.125	5	↑R
CECR1	Q9NZK5	0.125	0.125	0.125	6	↑R
CNTN1	Q12860	0.125	0.125	0.125	6	↑R
ICAM2	P13598	0.181	0.181	0.181	4	↑R
IGFBP5	P24593	0.181	0.125	0.250	4	↑R
LDHA	P00338	0.181	0.125	0.125	4	↑R
MAN2A1	Q16706	0.125	0.125	0.125	7	↑R
S100A8	P05109	0.125	0.125	0.125	10	↑NR

Figure 3.0.6: Longitudinal candidates

Longitudinal targets upregulated in responding and non-responding patients, based on LFQ data. Y axis, LFQ intensity, X axis, time points T1-T6. Blue lines, responders, red lines, non-responders.

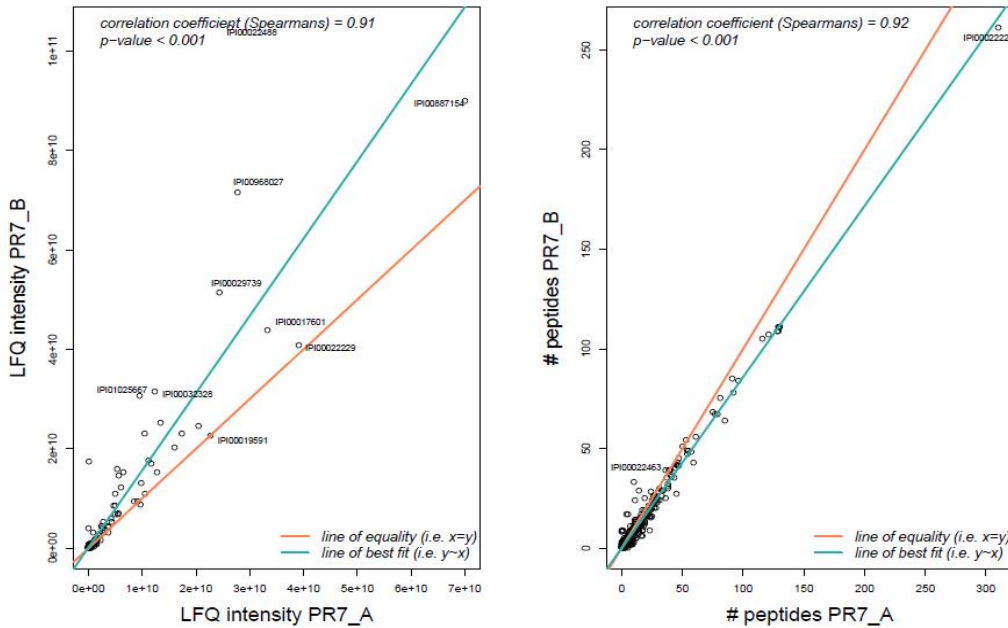


3.5.2. Reproducibility of label-free mass spectrometry

As the responders and the non-responders were analysed in separate mass spectrometry analyses, it was necessary to investigate the level of reproducibility between the two batches. On inspection of the data for individual proteins, the measured LFQ levels appeared to be frequently higher in the responders group as compared to the non-responders group, raising the possibility that differences between patient groups were due to inter-batch variability. Regression analysis of the control sample from a responding patient, which was processed and re-analysed alongside the non-responder samples, was performed. The quantitative values for peptides, intensity, and LFQ from both analyses were also compared. All quantitative values were found to be highly correlated between the two runs ($r^2 \geq 0.9$) (Figure 3.0.7). For both of the peptide and intensity values, the line of equality ($x=y$) indicated the original data was typically higher than the re-run data, suggesting these values were generally elevated overall in the responder analysis. Interestingly the opposite was found for the LFQ data, with the line of equality falling below the line of best fit indicating the non-responder protein levels were generally higher. This difference with the intensity and peptide values as compared to the LFQ values may be due to normalisation of the LFQ value during the MaxQuant analysis. Nevertheless, the high levels of correlation between the two separate batches indicate there is a high level of reproducibility between label-free mass spectrometry analyses completed at separate times, providing confidence in the ability to directly compare the two separate batches.

Figure 3.0.7: Correlation of data acquired during separate label-free batches

Correlation of the repeated sample in the first batch (PR7_A) and second batch (PR7_B). The line of equality (orange) and line of best fit (green) is shown. The first batch included the responder samples, the second batch included the non-responder samples.



3.5.3. Bioinformatic analysis of longitudinal serum proteins

Analysis of the combined responders and non-responders dataset by DAVID v6.7 indicated that there were a significant number of secreted proteins. Protein functions that were significantly overrepresented included response to wounding, cell adhesion, and carbohydrate binding (Table 3.0.6). The data achieved by DAVID analysis was corroborated by analysis of the responders by Ingenuity Pathways Analysis, which indicated that the majority of the proteins were from the plasma membrane or the extracellular space. The predominant protein types in these two locations were transmembrane receptors and peptidases, respectively.

Table 3.0.6: Overrepresentation analysis of longitudinal serum samples

Top overrepresented Gene Ontology annotations as determined by DAVID v6.7, from a list of 1274 overrepresented records, based on 356 protein IDs that were recognised by DAVID.

Term	Genes	P value
Extracellular region	245	3.5E-123
Plasma membrane	114	6.5E-02
Response to wounding	97	2.9E-60
Defence response	77	6.2E-35
Proteolysis	68	1.4E-14
Inflammatory response	61	2.2E-37
Cell adhesion	58	3.2E-17
Carbohydrate binding	52	6.1E-27

3.6. Validation of differential serum protein expression

It was not possible to validate serum proteins levels in responders and non-responders using antibody based techniques due to the absence of suitable and specific antibodies. A collaboration was established to take these proteins forward using multiple reaction monitoring (MRM), but unfortunately due to staffing issues at the external lab this was not achieved. However analysis of one protein (CDH1) is now going to be undertaken using a commercially available ELISA, and analysis of another protein (IGFBP5) will be performed using an Illuminex assay. Levels will initially be checked in the discovery set of patients, and analysis of baseline and longitudinal samples will be performed, focussing on the two week (T2) and end of first cycle (T3) samples, as most of the candidate proteins demonstrated changing levels in this time frame. Following this, putative candidates will be validated in a

larger patient cohort, using a case-controlled set of patients to allow the assessment of their predictive over their prognostic value to be assessed.

3.7. Discussion

Despite significant improvements in the range of available therapeutics to treat mRCC patients, median overall survival remains in the order of two years. Though some studies have hypothesised on an ability to reach much longer survival times (Escudier et al., 2009b), these are yet to be realised. The predominant TKI used to treat mRCC patients, sunitinib, has variable response rates and significant drug-induced toxicity. Whilst some patients do achieve partially durable responses, ultimately most patients acquire resistance and subsequently relapse. Further, there is evidence to suggest that TKI therapies can drive a more aggressive phenotype by positive selection of resistant cell populations (Paez-Ribes et al., 2009, De Bock et al., 2011). It is paramount that we understand why only a percentage of patients respond to therapy and why the majority of patients stop responding after an undetermined period of time. Predicting response to sunitinib is therefore an urgent requirement of cancer management in mRCC.

Though many studies have investigated potential biomarkers, these have generally been hypothesis-driven approaches that have focussed on validation of pre-selected targets, chosen through biological reasoning. Further, none of these have yet made it into clinical use. The cytokine IL-8 has so far shown promise in predicting sunitinib response (Harmon et al., 2014, Huang et al., 2010) and has also been found to be predictive of pazopanib efficacy (Tran et al., 2012). Soluble VEGFR-3 has also shown reasonable consistency between studies (Deprimo et al., 2007, Rini et al., 2008, Harmon et al., 2014) and larger studies are necessary to

investigate these markers further. However, using a non-hypothesis driven approach to mine patient samples may allow for the identification of protein targets that would not otherwise have been considered. This study therefore aimed to compare patients with semi-durable sunitinib responses ('responders') to those who received no clinical benefit ('non-responders'). A non-hypothesis driven approach was used, which focussed on profiling of the serum proteome of patients, both at baseline, and longitudinally during the course of therapy.

3.7.1. Serum as a source of clinical biomarkers

The constant perfusion of tissues by peripheral blood means that serum may harbour tumour-specific proteins, and it has therefore received increasing attention as a source of biomarkers in recent years. With improved chromatographic and mass spectrometric methods the number of proteins identified in serum is constantly increasing; the most recent update from the Human Plasma Proteome project reported data on 10546 proteins, of which 3784 had been identified in at least two studies (Nanjappa et al., 2014), although it must be noted that many of these come from a study whereby many of the IDs did not reach significance due to the high false discovery rate (Liu et al., 2007). However the complexity of serum is such that, despite an effective mining range of 10^5 by current mass spectrometers, additional fractionation methods such as immunodepletion are essential to allow identification of the lower abundance proteins.

The Agilent Multiple Affinity Removal System (MARS) method has previously been shown by our group to be highly effective in reducing complexity, with a 52.3% increase in the number of protein identifications compared to neat serum (Smith et

al., 2011a). Although this technique routinely allows mining of 350-450 proteins (Smith et al., 2011a, Millionini et al., 2011), a number which is consistent with this study, it must be remembered that this is still a very low number in comparison to tissue and cell based profiling studies, which routinely profile over 3000 proteins. The MARS14 column depletes serum of the top 14 most abundant proteins from human serum, which equates to around 94% of the total serum proteins, with around 98-99% efficiency. Due to the abundance of the MARS14 targets proteins in neat serum they remain detectable by mass spectrometry (Tu et al., 2010). Most of the MARS14 target proteins were identified in the depleted serum analysed in this study, however the presence of these proteins did not appear to correlate with the number of identifications made, suggesting they were not the largest contributor to limiting the number of sample identifications (as compared to cell and tissue studies). Furthermore, analysis of the neat serum and depleted samples by 1D-PAGE indicated that these proteins were greatly reduced in concentration when compared to neat serum. Even after depletion of these MARS14 targeted proteins there is still a high number of classical serum proteins that are considerably more abundant than the low abundance proteins, such as tissue leakage products and cytokines (Anderson, 2002), and these most likely contribute significantly to reducing the mining depth in this study.

A concern of immunodepletion studies is the risk of co-depleting proteins of interest bound to carrier proteins such as albumin (Mehta et al., 2003). The 'depletome' and 'albuminome' have been coined to describe these co-depleted proteins, and investigations into the number of proteins co-depleted with albumin vary from 24 - 67 depending on the method used to isolate these proteins (Scumaci et al., 2011, Gundry et al., 2007). It is probable that some proteins were co-depleted with

albumin in this study, and a future investigation could focus on investigating the 'depletome', to determine if it contains any potential biomarker candidates.

3.7.2. Identification of serum biomarkers using mass spectrometry

Using mass spectrometry to capture a phenotypic protein snapshot of the sample allows for proteins to be identified that could not be predicted solely through genomic or transcriptomic profiling (Kim et al., 2014). Furthermore, when applied to biomarker studies the proteomic profiling of clinical samples also removes the need to pre-emptively predict proteins of interest. In this study proteins that could be expected to demonstrate a dynamic profile in response to TKI therapy include tumour-derived proteins, inflammatory proteins, and proteins related to angiogenesis such as cytokines, proteases, and cell adhesion molecules (Carmeliet and Jain, 2011). Additionally, proteins and peptides derived from stromal-epithelial interactions, immune cell MHC (major histocompatibility complex) presentation, apoptosis, cytokines, and other tissue leakage products may passively diffuse into the circulation (Scumaci et al., 2011), and these are likely to provide a source of clinically useful biomarkers. Changes in these proteins would indicate both a systemic response to therapy and a direct impact on the vasculature, and perhaps even the tumour itself. Even though we are now routinely observing cell adhesion molecules and cytokine receptors, the abundance of many of these would likely be too low to detect in a serum study with current technologies. Analysis using Ingenuity Pathways Analysis, and DAVID indicated that many of the identified proteins were from the plasma membrane and the extracellular space, representing two of the predominant locations from which plasma proteins derive. The types of protein identified included transmembrane receptors, and proteins involved in proteolysis, wound healing, immune response, and cell adhesion - those that one would expect to find in a serum sample. It is important to note here that many of the

proteins identified in this study have previously been identified in cancer tissue, and published studies about their function may not have relevance in a serum setting, considering the proteins identified in this study have been either shed or released into the serum through another mechanism.

One drawback to mass spectrometry based research is the difficulty in accurate protein quantification. Currently the most effective tools are labelling-based methods, though the implementation of a labelling study when handling clinical samples can be prohibitive due to the high cost, impracticability of the sample type, or the difficulty in multiplexing. By contrast, label-free quantitation is a quick and cheap method to gauge the relative protein levels in any sample. However, due to the absence of labels, the samples are not analysed in tandem, and the quantitation is therefore more sensitive to technical and systematic sources of variation. On an Orbitrap Velos, label-free quantitation is performed using the peptide precursor ion signal intensity as a measurement of its relative abundance in the sample. Following analysis of the data using MaxQuant a number of quantitative values are reported, including peptide number, intensity, label free quantitation (LFQ) intensity, and MS/MS values (Cox and Mann, 2008a). The run-specific LFQ value, which is calculated from the intensity value, is determined using a number of in software-calculated normalisations to try and minimise the effects of technical variation amongst the samples. The LFQ value risks over- or de-amplifying a change, as the value is inferred based on assumption of average protein intensities. By contrast, the peptide value is an unmodified representation of the presence of a protein in the sample; however it does not account for differences in loading, and is biased towards larger proteins with more peptides. Both peptide and LFQ values have positive and negative consequences, and without a more in-depth analysis of the quantitative power of each technique both methods should be considered when

making decisions about putative biomarker targets. A further consideration of label-free techniques is the reproducibility. A previous study found the reproducibility of label-free LC-MS/MS analysis of serum proteins to be fairly high (Smith et al., 2011a) and similar results were observed here, nevertheless comparisons of relative levels between patient groups must be viewed cautiously and validated extensively. This is especially important for the longitudinal study, for which the two study arms were independently analysed, and differences between patient groups could therefore be due to technical variance as opposed to a real difference. The forthcoming validation of the candidate proteins identified in this study will resolve this question.

3.7.2.1. Biomarker candidates identified from baseline serum

Ideally response to sunitinib would be predicted at baseline, thus saving the patient any unnecessary drug associated side effects. A comparison of serum from responding and non-responding patients collected at baseline resulted in the identification of a wide range of proteins, and a number of proteins appeared to be differentially expressed between the responders and non-responders. Analysis using DAVID indicated there was over representation of proteins involved in inflammation in the non-responders, a clinical manifestation which has been associated with the progression of cancer (Rakoff-Nahoum, 2006); this inflammatory upregulation may be involved in promoting invasion and metastasis, which in turn may assist in intrinsic and acquired resistance to anti-angiogenic therapy.

Focussing on the proteins that demonstrated the greatest differences in relative concentration, a number of these were involved in the promotion or prevention of

invasion and metastasis, depending on whether they were identified in the non-responders or responders, respectively. (Bergers and Hanahan, 2008). The most highly upregulated proteins in the non-responders were cathelicidin (hCAP18), cathepsin Z (CTSZ), moesin (MSN), golgi membrane protein 1 (GOLM1), calgranulin A (S100A8), and oncoprotein induced transcript protein 3 (OIT3). All of these, except for OIT3, have been shown to be upregulated in various cancers and four of these have roles in tumourigenesis and promoting metastasis. Interestingly, the inflammatory protein calgranulin A was also found to be upregulated in the non-responders in the longitudinal arm of the study.

Human cathelicidin (hCAP18) is an antimicrobial propeptide, the active peptide LL-37 is upregulated during inflammation and wound repair (Chow et al., 2013). This inflammatory protein has also been shown to be upregulated in lung (von Haussen et al., 2008), breast (Heilborn et al., 2005), and epithelial ovarian cancers (Coffelt et al., 2008), and also appears to aid in driving tumourigenesis through promotion of proliferation and invasion. Interestingly LL-37 has also demonstrated an ability to induce apoptosis, and these seemingly contrasting roles may well be explained by LL-37's ability to cause double stranded DNA breaks: at low peptide levels this promotes tumourigenesis, and at high concentrations this encourages apoptosis (Chow et al., 2013). Cathepsin Z (CTSZ) also promotes metastasis, this is a cysteine protease located at 20q13.3, a region which has been associated with metastatic potential in many cancers (Hidaka et al., 2000). The cysteine proteases are frequently implicated in cancer and CTSZ was associated with invasiveness in gastric cancer (Krueger et al., 2005), and with driving metastasis in hepatocellular carcinoma (Wang et al., 2011), and breast cancer (Sevenich et al., 2010). The pro-metastatic capability of CTSZ has been linked to its ability to interact with integrins (Akkari et al., 2014). Moesin (Membrane Organising Extension Spike Protein),

which is a member of the ERM (Ezrin, Radixin, Moesin) family and of the band 4.1 superfamily, is involved in membrane-cytoskeletal linkage, and therefore has a role in cell shape, adhesion, and motility. Levels of this protein have been shown to be upregulated in breast cancer (Charafe-Jauffret et al., 2007), papillary thyroid carcinoma (Brown et al., 2006), and oral squamous cell carcinoma (Kobayashi et al., 2004). In vitro studies using 3D matrices also found that moesin plays a role in invasion (Estechea et al., 2009). The presence of these proteins at baseline may therefore provide the tumour with an intrinsic mechanism to encourage co-option of normal vessels, and invasion into normal tissue, thus enabling escape of the drug-induced hypoxia.

Though its functional role in cancer is yet to be determined, Golgi membrane protein 1 (GOLM1) was identified as one which was commonly dysregulated in 20 cancer types, including kidney, by QRT-PCR analysis (Lu et al., 2007). Serum levels were found to be upregulated in hepatocellular carcinoma (Bachert et al., 2007, Marrero et al., 2005), and urine levels have been investigated for prostate cancer diagnosis (Varambally et al., 2008). Though multiple studies have demonstrated an upregulation of this protein its exact role is yet to be determined (Kim et al., 2012a), however it is possible that it promotes tumour pathogenesis and may therefore support the innate resistance of the tumour. Very little is known about oncoprotein Induced transcript protein 3 (OIT3). Early studies indicated it was present specifically in liver and it appeared to be downregulated in hepatocellular carcinoma (Xu et al., 2003), recent studies however suggest it may have a role in normal kidney physiology, where it has been proposed to be involved in uric acid excretion (Yan et al., 2012). None of these functions have an obvious tie to drug resistance, and the exploratory nature of proteomic profiling means that novel proteins with an as yet undetermined function may be identified as potential

biomarkers. Interestingly, a slight elevation of C-reactive protein (CRP) was found in the non-responders in the baseline study, a protein that has previously been linked with poor response to sunitinib (Miyake et al., 2014, Fujita et al., 2012).

In contrast to the metastasis-promoting proteins found to be upregulated in the non-responders, the proteins found at higher levels in the responders may function to limit the invasive capability of the tumour and therefore prevent metastatic escape as a means of drug resistance. The most highly upregulated proteins in this group of patients were cadherin 1 (CDH1), platelet-activating factor acetylhydrolase (PLA2G7), protein HEG homolog 1 (HEG1), and bone marrow proteoglycan (PRG2). Interestingly, CDH1 and PLA2G7 have both previously been shown to have roles in preventing tumour formation through limiting metastatic spread. Cadherin 1 (CDH1), also known as E-cadherin, is a highly conserved adhesion molecule which is involved in the formation and maintenance of cell-cell junctions, and is crucial in the development of epithelia (Pecina-Slaus, 2003). Loss of CDH1 expression has been reported in multiple cancers (Berx and van Roy, 2009), including RCC – an IHC study of 131 ccRCC tissue specimens found positive staining in only 5% of these cases (Langner et al., 2004). Changes to the adhesive properties of cells are associated with tumourigenesis, and the loss of CDH1 is characteristic of a switch from a benign to a metastatic lesion (Birchmeier and Behrens, 1994). It is therefore regarded as a suppressor of invasion, although following metastasis it is possible that E-Cadherin expression is switched back on again (Bukholm et al., 2000). The absence of this protein from the non-responders may therefore be linked to a more metastatic phenotype, tying in with the apparent upregulation of metastasis-associated proteins observed in the non-responders. Importantly however, this study detected soluble levels of CDH1, rather than tissue

levels, and it may have a different role in this setting. A recent *in vitro* study on murine skin cells suggested soluble CDH1 may be oncogenic, through its ability to activate the PI3K/Akt/mTOR pathway (Brouxhon et al., 2014). Platelet-activating factor acetylhydrolase (PLA2G7) is a secreted enzyme that degrades the platelet activating factor (PAF). PAF has been shown to have a variety of roles in cancer with most studies suggesting a tumour-promoting role, such as the promotion of oncogenic transformation (Kume and Shimizu, 1997) and metastasis (Braeuer et al., 2011). PAF also seems to have a role in angiogenesis (Kim et al., 2011) and in increasing vascular permeability, however as this is via a VEGF-based route it is unlikely that the absence of PLA2G7 in the non-responders allows angiogenic escape, and it is more likely that PLA2G7 exerts its effects through decreasing metastasis in the responders. PLA2G7 itself appears to be upregulated in both prostate (Vainio et al., 2011) and hepatocellular carcinoma (Smith et al., 2003), and it is possible that the effects of PLA2G7 and PAF are both tissue specific (Xu et al., 2013).

Further links to potential limitation of invasive capacity were found in the responders, with a differential regulation of bone marrow proteoglycan (PRG2). PRG2 is the pro-form of the cytotoxic eosinophilic major basic protein (MBP), which comprises the major constituent of eosinophil granules. Interestingly PRG2 has been shown to have proteinase inhibitor capability; by complexing with pregnancy-associated plasma protein-A (PAPP-A) it abrogates the action of this protein (Overgaard et al., 2000), one function of which is to degrade IGFBP-5 (Laursen et al., 2001), which was found to be elevated in the serum of responders in the longitudinal arm of this serum study, and may have a role in preventing metastasis (Sureshbabu et al., 2012). PRG2 may therefore have a role in increasing the levels of the anti-metastatic IGFBP-5. The last protein identified as an interesting

biomarker candidate was HEG1. As with GOLM1 and OIT3, no defined function has yet been ascribed to HEG1, which is a homolog of the Zebrafish heart of glass gene and which shows limited similarity to other human proteins. It was shown to be significantly underexpressed in malignant serous epithelial ovarian cancer tissue samples (Birch et al., 2008), and HEG1 null mice demonstrate serious deformities of the heart, blood vessels and lymphatic vessels (Kleaveland et al., 2009) indicating that HEG1 has an important role in vessel formation and integrity. Its apparent links to vascular integrity make this an interesting differentially expressed protein, and it is possible that improved vessel integrity may aid drug delivery in the responders.

3.7.2.2. Biomarker candidates identified from longitudinal serum

Monitoring protein changes over time in a longitudinal study opens up the possibility of looking for dynamic temporal changes in response to therapy. In this way it might be possible to predict response or to observe a change in response before a radiologically confirmed progression. Eight proteins were identified as putative biomarker candidates for longitudinal monitoring of response, of which seven were upregulated in the responders. These included proteins upregulated in an acute phase setting, and may be indicative of an early response to therapy or an early marker of a reduction in tumour vascularity; although the median time to an observed partial response has been stated as 2.3 months (Motzer et al., 2006), a reduction in tumour vascularity can be observed within three weeks (Lamuraglia et al., 2006). A few proteins demonstrated a more gradual chronic change, which may reflect physiological changes to the tumour itself. Validation of these protein changes is essential, and although initial plans for MRM validation have not been realised, steps have now been taken to validate two of these proteins using

alternative techniques: IGFBP5 will be validated using Luminex, CDH1 will be validated using ELISA.

Proteins changing acutely were aldolase A (ALDOA), lactate dehydrogenase (LDHA), insulin-like growth factor binding protein-5 (IGFBP5), and Calgranulin A (S100A8). The glycolytic proteins ALDOA and LDHA were both acutely upregulated in the two week on-treatment sample in the responders, both of these proteins have been implicated in response to hypoxia and their upregulation in responders during therapy may be associated with a reduction in tumour vascularity and the accompanying tumour hypoxia. Many groups have investigated the role of LDHA in cancer (Miao et al., 2013) and contrary to previous opinion, recent studies indicate that elevated levels of lactate – the product of the LDHA enzyme – accompany less metastatic breast cancer tumours, with more highly metastatic breast cancers producing less (Xu et al., 2014). Furthermore, elevated levels of lactate dehydrogenase were found to be associated with better response to therapy in mRCC patients treated with the mTOR inhibitor temsirolimus (Armstrong et al., 2012). In contrast to these results, ALDOA mRNA has been associated with metastasis and worse prognosis in lung adenocarcinoma (Du et al., 2014), and the ALDOA protein has been found to be upregulated in the tissue (Pfleiderer et al., 1975) and serum (Takashi et al., 1992) of renal cell carcinoma patients. However importantly, these studies were tumour-normal comparisons, whereas this study was a tumour-tumour comparison. The fact that LDHA and ALDOA are both elevated during hypoxia may instead indicate that the anti-angiogenic therapy is working efficiently, without escape via an alternative method of angiogenesis (Bergers and Hanahan, 2008).

Another acutely upregulated protein was IGFBP5. This protein is one of a group of proteins involved in the regulation of insulin-like growth factors (IGFs). The IGFs are involved in the promotion of proliferation and IGFBP5 has therefore been anticipated to reduce the metastatic potential of tumour cells (Sureshbabu et al., 2012). It is possible that elevated levels in the responders may be involved in mopping up IGF and reducing metastasis, whereas its absence in the non-responders may allow for continued signalling through the IGF axis and increased invasive capability. In contrast to these effects, the inflammatory mediator Calgranulin A (Kerkhoff et al., 1998) was found to have a greater acute upregulation in the non-responders when compared to the responders. This protein has been found to be upregulated in multiple cancers (Cross et al., 2005), and has been implicated in attracting circulating tumour cells following upregulation by premetastatic tissues (Hiratsuka et al., 2006). The elevated levels in all patients suggest this effect may be due to treatment-induced inflammation, however the higher levels in non-responders could be due to a secondary mode of expression in these patients, perhaps brought about by premetastatic conditioning and increased metastatic potential in these patients, as the ability to invade normal tissues and to migrate along normal vessels through co-option has been proposed as a method of drug resistance in anti-angiogenics (Bergers and Hanahan, 2008).

A more chronic change in protein levels was demonstrated by the proteins contactin-1 (CNTN1), adenosine deaminase (CECR1), intercellular adhesion protein 2 (ICAM2), and alpha mannosidase 2 (MAN2A1), all of which demonstrated changing levels in the responders, with low or absent expression in the non-responders. The cell adhesion protein CNTN1 demonstrated a consistent decrease between baseline and the two week sample in all responding patients. CNTN1 has previously been shown to be overexpressed in glioblastoma and lung

adenocarcinoma, where it has also been implicated in tumour invasiveness and metastatic capacity (Su et al., 2006, Eckerich et al., 2006). A decrease in levels may therefore reflect a reduction in tumour burden, and a decrease in metastatic potential; CNTN1 could potentially aid in response to drug by preventing metastatic escape. Another protein that may assist in this regard is CECR1. Undetected in the non-responders, levels of this protein tended to decrease over time in the responders. CECR1 is secreted by monocytes undergoing proliferation, and may have a regulatory role in proliferation. Importantly, plasma levels were shown to decrease following treatment with chemotherapy, and a reduction in levels was correlated with tumour regression in different cancer types (Roberts and Roberts, 2012). CECR1 may therefore have a similar role in this study, and a decrease may also correlate with tumour response.

Due to the exploratory nature of this work, it may not be immediately obvious why certain proteins demonstrate their observed response. The upregulation of alpha mannosidase 2 (MAN2A1) in the responders does not have an obvious explanation, but may be due to some, as yet, unknown mechanism of drug sensitivity. MAN2A1, which is a key protein involved in the N-glycosylation pathway, was elevated in the responders and detected at only low levels in the non-responders. Complex carbohydrate structures are known to be important in cancer signalling and metastasis, and various studies have investigated inhibiting MAN2A1 in cancer treatment (van den Elsen et al., 2001).

3.7.3. Concluding remarks

The proteins found to be upregulated in the non-responders have links to tumourigenesis and metastasis, and may therefore represent escape mechanisms

that the tumour has in place to avoid the toxic effects of therapy. Whilst other studies investigating response to sunitinib have identified proteins linked to angiogenesis and invasion, very few of these proteins were identified in this study (data not shown), and this is likely due to the technical limitations of the study; those proteins are too low in abundance to be easily detected by these techniques. Profiling serum using mass spectrometry remains a difficult task. This study has potentially found some interesting targets that are supported by biological reasoning, and therefore warrant further investigation, but the number of identifications is still low when compared to the thousands that are identified in cell and tissue samples. Even with MARS14 depletion there is still a significant amount of masking of low abundance proteins (Tu et al., 2010), and to get to the very low abundance proteins greater levels of fractionation may be required. Other methods such as SCX, or a supermix column, may assist with improving the depth of mining, though the latter has been implicated in depleting known disease biomarkers, this is a particular risk of this column as the targeted proteins have not been fully evaluated (Patel et al., 2012). It may not be necessary to mine to the full depths of serum, comparisons of extreme phenotypes may reveal proteins in high enough abundance to be detected by current means, but validation of these targets is essential to confirm this. Many of the chosen targets were different between the baseline and longitudinal studies as they were chosen for separate reasons, with the longitudinal study focussing on protein changes over time as opposed to solely at baseline.

The main limitations of the study are in the low sample numbers used, and the inability to validate the targets using in-house techniques. Due to the significant amount of time it takes to profile clinical samples, proteomic mining studies are frequently designed to compare the extreme phenotypes of a limited number of

'discovery' patients, with subsequent validation in a wider cohort. This strategy has been successfully used in other studies (Collinson et al., 2013, Welberry Smith et al., 2013), but confirmation of the clinical utility of the potential markers cannot be verified until validation has been carried out, first in the discovery set of patients and then in a larger cohort using a complementary technique. Certainly in a study as small as this, these findings can only be viewed as exploratory until confirmation of their differential expression pattern has been achieved. Limited sample numbers has a knock-on effect on the variation of the study, between-patient variation is considerable and it is important to control for as many factors as possible to try and limit the impact of this potential source of error. Numerous factors must be accounted for, including gender, age, pathological stage, nuclear grade, chronicity of disease, amongst others. Though every care was taken to try and normalise these factors, inevitably, due to a low sample population from which to choose (n=50 at the time of the study) it was not possible to fully match these patients. It cannot therefore be ruled out that the proteins identified in this study are markers of variation, or of prognosis, as opposed to predictive of sunitinib treatment. Finally, concern has been raised over use of the RECIST method of evaluating tumour response (Eisenhauer et al., 2009, Therasse et al., 2000), especially when considering therapies known to cause extensive necrosis such as sunitinib (Faivre SJ and S, 2007) as this can mimic progressive disease. Concern is focussed on the potential underestimation of responders, and alternative methods that have been suggested include the Choi criteria (van der Veldt et al., 2010b, Choi et al., 2007), and the Mass, Attenuation, Size, and Structure (MASS) criteria (Smith et al., 2010b). A change in the method of assessing response may therefore have a knock-on effect on the number of samples available as a few SD patients may become PR patients, for example decreasing the percentage change required for a partial response from a 30% decrease to 10%, and classifying all others as non-

responders (Thiam et al., 2010). This could increase sample numbers in both studies, making it easier to normalise other factors.

It may be that no single marker has the necessary sensitivity and specificity to allow for accurate prediction of response to sunitinib. Differential expression between the responders and non-responders in this study was fairly low, with no very large fold changes observed between the responders and non-responders. This may be due to a difficulty in measuring protein levels using a label-free technique, which has a higher level of technical variation at low fold changes. Alternatively it could be due to diminished differences in a tumour versus tumour comparison, or perhaps it may be reflective of the real situation, whereby there are many small differences between the responders and non-responders. In this situation a nomogram may have a greater predictive power than any single protein, whereby measurement of multiple targets are combined into a panel of protein markers, which may provide greater predictive power than any one protein alone. Early studies for pazopanib (Tran et al., 2012) and bevacizumab (Collinson et al., 2013) have shown promise in this area. Either way, proper validation is critical. Many studies investigating predictive markers do not properly test the predictive nature of the marker, whereby levels are measured in both a treated and untreated population, and their prognostic utility cannot therefore be ruled out. These samples in the numbers required only come from large trials, and the validation study must therefore be designed prospectively, alongside the trial. Another purpose of validation is to ensure the measured effects are due to response, and not a systemic effect to sunitinib itself. Sunitinib has been shown to inhibit a range of kinases far beyond its target range (Karaman et al., 2008), which may explain the wide-ranging toxic side effects seen with this drug. Furthermore, previous studies in non-tumour bearing mice have shown that sunitinib has a considerable systemic effect, with

upregulation of many proteins including osteopontin and stem cell factor (Ebos et al., 2007). This must be considered for the longitudinal arm of this study, but this would not impact upon the baseline study, which used serum from patients who had not yet been exposed to sunitinib. Therefore, in the same way that VEGF and VEGFR-2 have treatment related peaks and troughs (Deprimo et al., 2007), verifying which proteins are directly an on-treatment response is essential, and this could potentially be done by collecting and analysing an additional on-treatment sample.

Finally, recent serum studies have yielded markers that have shown promise in their field (Collinson et al., 2013, Welberry Smith et al., 2013), and both of these studies used similar techniques to those used here. The responses demonstrated by these putative markers are distinct and biologically relevant. Many of the proteins identified here have previously been identified in tissue, and it must be considered that their function in a serum setting may be different, nevertheless they may potentially pave the way to validating a baseline predictor of response, or a longitudinal pharmacodynamic monitoring marker. A critical next step in this study would be to validate these findings with a larger cohort of patient samples using a sensitive and specific technique; the putative targets discussed already have been selected for further investigation, and steps are currently being taken to pursue validation of these targets using Luminex and ELISA.

4. Using *in vitro* cell lines to discover early markers of renal cell carcinoma pathogenesis

4.1. Introduction

The management of RCC is marred by a lack of reliable biomarkers. Though it is understood that VHL inactivation is a key step in the pathogenesis of the majority of sporadic RCCs, it is not fully known what impact the different VHL mutations have on the functioning of the cell. VHL has many documented functions, which includes, but is not limited to the targeting of HIF for degradation and the downstream repercussions of this. Inactivation of VHL is known to allow the accumulation of HIF and the destabilisation of the tumour suppressor Jade-1, amongst others. VHL disease is an inherited disorder with a prevalence of 1 in 36,000 live births, and predisposes the sufferer to a variety of benign and malignant tumours, including RCC (Kim et al., 2010). Genotype studies of cancers arising from both sporadic and familial RCC (resulting from VHL disease) have revealed an array of VHL mutations. Those arising from familial RCCs have been categorised based on genotype-phenotype studies into four different VHL disease subtypes: type 1, type 2A, type 2B and type 2C (Kim et al., 2010). Each subtype predisposes to a different combination of renal cell carcinoma, haemangioblastoma, or pheochromocytoma (Table 4.0.1), with type 1 and type 2B giving rise to RCC. RCC is not seen in type 2C, and infrequently seen in type 2A. In this investigation, the impact of VHL disease-specific mutations on the proteome were investigated, using five isogenic cell lines carrying mutations clinically relevant in VHL disease, and corresponding to the different VHL disease subtypes. A comparative analysis looking at VHL specific proteomic changes was carried out first, using two cell lines with and without

functional VHL. A further study investigated the impact of renal cell carcinoma-specific VHL mutations, by comparing the proteomes of all five cell lines.

4.1.1. Aims

The specific aims of this chapter were:

1. To investigate proteomic changes brought about by VHL inactivation using an *in vitro* model
2. To investigate VHL-dependent changes using cell lines carrying RCC forming and non-RCC forming mutations.
3. To validate expression of target proteins in cell lines and clinical samples.

4.2. Characterisation of VHL disease-specific cell lines

Using the RCC4 cell line – which carries a VHL inactivating C194G mutation in exon 1 – five cell lines were generated by stably transfecting RCC4 with a pcDNA3.1 vector carrying full length wild type VHL (WTHAB6); empty vector (RCC4/T); or full length VHL with one of three VHL mutations relevant to type 2A, type 2B, and type 2C VHL disease (Table 4.0.1). Cell lines were kindly donated by Professor Eammon Maher (University of Cambridge). The wild type control (WTHAB6) carries the RCC4 mutation in its genome, but also carries wild type VHL to replace any lost function. The type 1 disease cell line (RCC4/T) carried only an empty vector; the RCC4 phenotype of an inactive VHL was maintained in this cell line. The type 2A disease cell line (RCC4/2A) carries a T505C point mutation in exon 1, the type 2B disease cell lines (RCC4/2B) carries a G713A point mutation in exon 3, and the type 2C disease cell line (RCC4/2C) carries a C775G point mutation in exon 3.

Table 4.0.1 VHL disease cell line models

Cell lines used in this study are shown. The mutation* numbering used throughout this study is consistent with that used in the original publication of these cell lines (Clifford et al., 2001). RCC, renal cell carcinoma; HB, haemangioblastoma; PH, pheochromocytoma.

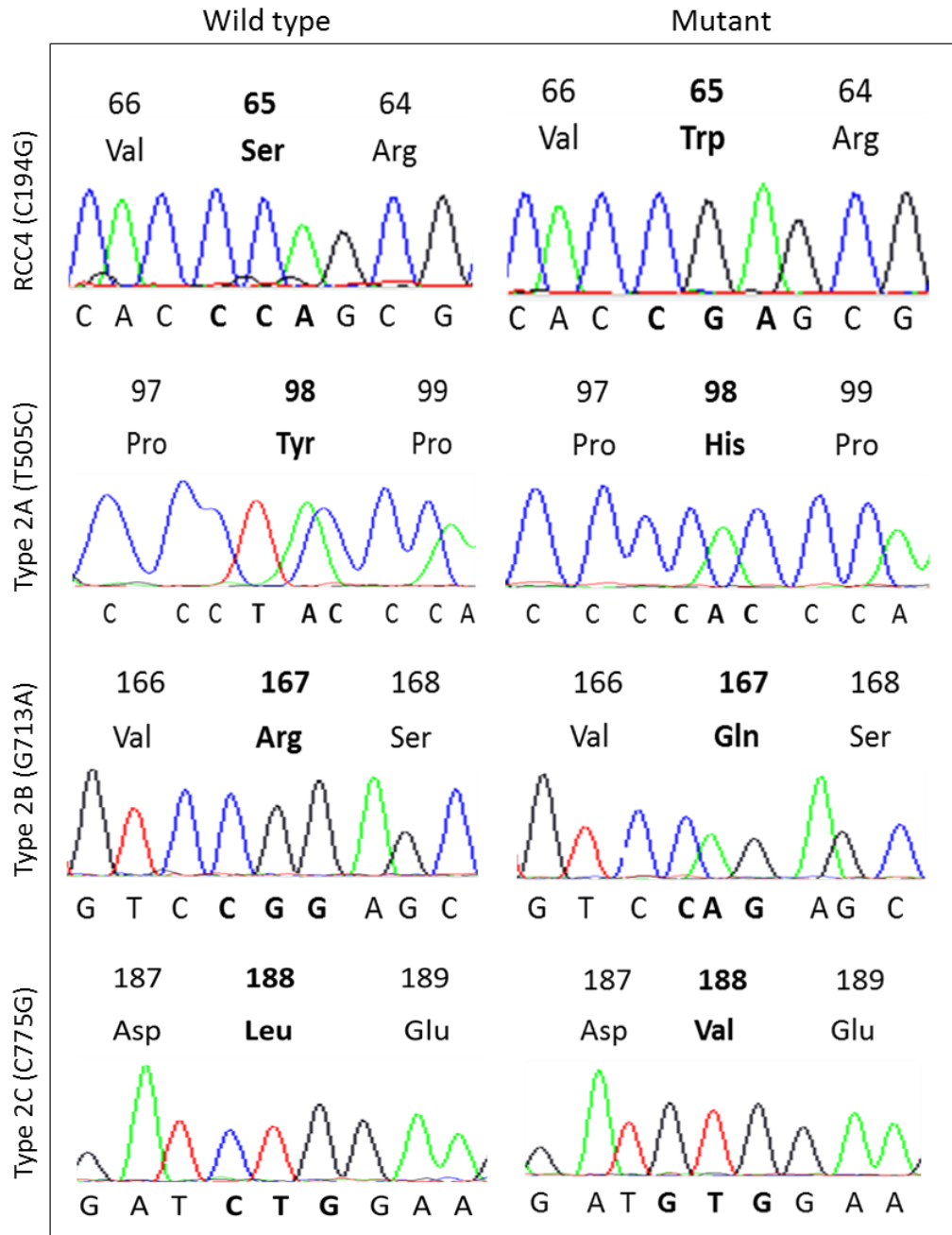
Cell Line	Disease subtype	Mutation*	WT codon	Mutant codon	Protein	Cancer
WTHAB6	Wild type	-	-	-	-	-
RCC4/T	Type 1	C407G	TCG	TGG	Ser65Trp	RCC/HB
RCC4/2A	Type 2A	T505C	TAC	CAC	Tyr98His	HB/PH
RCC4/2B	Type 2B	G713A	CGG	CAG	Arg167Gln	RCC/HB/PH
RCC4/2C	Type 2C	C775G	CTG	GTG	Leu188Val	PH

4.2.1. Confirmation of *vhl* mutations

Sanger sequencing was performed to ensure the expected mutations were present, both for the somatic RCC4 mutation and the three disease-specific mutations. The cells were grown to 85% confluence and DNA was recovered using the QIAamp DNA mini kit. Sanger sequencing was kindly performed by Dr Claire Taylor. The expected RCC4 germline C194G mutation was confirmed in all cell lines (data not shown). For cDNA sequencing of VHL mutations carried on the plasmid, primer pairs that spanned exons were used to ensure genomic DNA was not amplified. The type 2A, type 2B, and type 2C mutations, as detailed in the Table 4.0.1, were found in the expected cell lines (Figure 4.0.1), and were absent from both the WTHAB6 and RCC4/T cell lines.

Figure 4.0.1: Sanger sequencing of the VHL disease cell line mutations

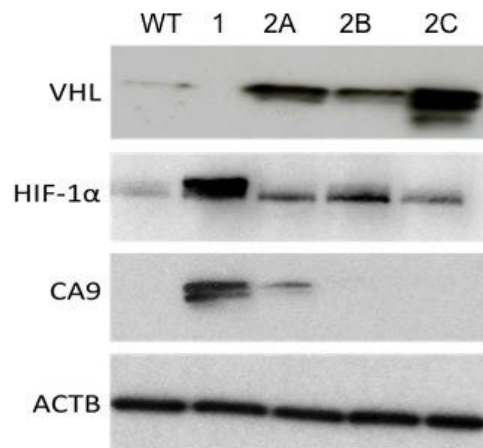
VHL mutations present in the five RCC4-derived cell lines. Wild type is shown in the left hand panel, and the mutant is shown in the right hand panel. All five cell lines were confirmed to have the expected mutations.



The phenotype of the cell lines was checked by performing Western blots probing for VHL, the VHL target hypoxia inducible factor 1-alpha (HIF-1 α), and the hypoxic-regulated protein carbonic anhydrase 9 (CA9) (Figure 4.0.2). A dominant band of 24kDa, corresponding to the larger VHL p24 isoform, was observed in WTHAB6, RCC4/2A, RCC4/2B, and RCC4/2C, though WTHAB6 appeared to express lower levels. No VHL bands were observed in RCC4/T, which was not transfected with any form of VHL. Two further bands at 19kDa and 18kDa, corresponding to the VHL p19 and VHL p18 respectively which are missing the first 53 amino acids of the *VHL* gene, were visible in the 775 cell line, which appeared to express larger amounts of VHL than the other cell lines. In the HIF-1 α blots a band of 92kDa, corresponding to the expected size for HIF-1 α , was observed in all five cell lines. RCC4/T displayed considerably higher levels than all the other cell lines, and the amount present in WTHAB6 was very low, as expected. CA9 was absent from the WTHAB6 cell line, and was found in the RCC4/T, RCC4/2A, RCC4/2B, and RCC4/2C cell lines, with a doublet at the expected location of 52kDa. Considerably higher levels of CA9 were found in RCC4/T than any of the remaining cell lines, 505 was the next highest expressing cell line, very low levels were detected in RCC4/2B and RCC4/2C. No specific binding was observed in the control Western blots (data not shown).

Figure 4.0.2: Western blot characterisation of VHL disease-cell line phenotypes

Cell lysates were probed with antibodies specific to VHL, HIF-1 α , and CA9, as detailed in materials and methods. Membranes were probed for β -actin (ACTB) as a loading control. WT, WTHAB6; 1, Type 1 (RCC4/T); 2A, RCC4/2A; 2B, RCC4/2B; 2C, RCC4/2C.



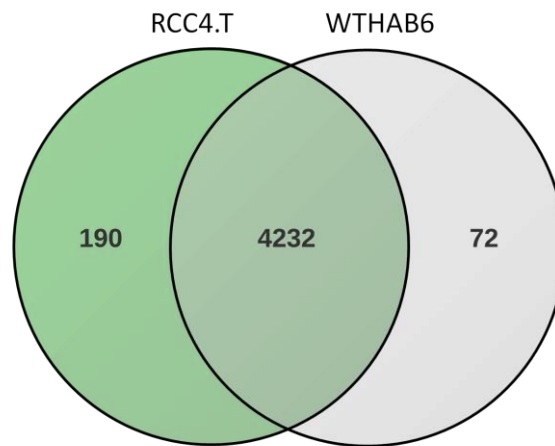
4.3. Comparison of plus/minus VHL proteome

VHL is frequently lost in sporadic RCC (Young et al., 2009, Nickerson et al., 2008) and therefore the initial experiment focussed on investigating the proteomic differences brought about by VHL inactivation. Three replicates of the wild type VHL-transfected cell line (WTHAB6) and the VHL negative cell line (RCC4/T) were compared by LC-MS/MS, as described in materials and methods (Zougman et al., 2014). In total, 4494 proteins were identified (with at least two peptides, including one unique) across both cell lines. An analysis of the overlap of protein identifications found that 4.2% and 1.7% of the proteins were unique to either RCC4/T or WTHAB6 respectively, and 94.2% proteins were common to both cell

lines (Figure 4.0.3). The complete set of raw data can be found in supplementary data files S7 and S8.

Figure 4.0.3: Presence/absence analysis of proteins present in RCC4/T and WTHAB6

Overlap of protein identifications. A presence/absence comparison for RCC4/T and WTHAB6, demonstrated that 94.2% of all protein identifications were common to both cell lines.

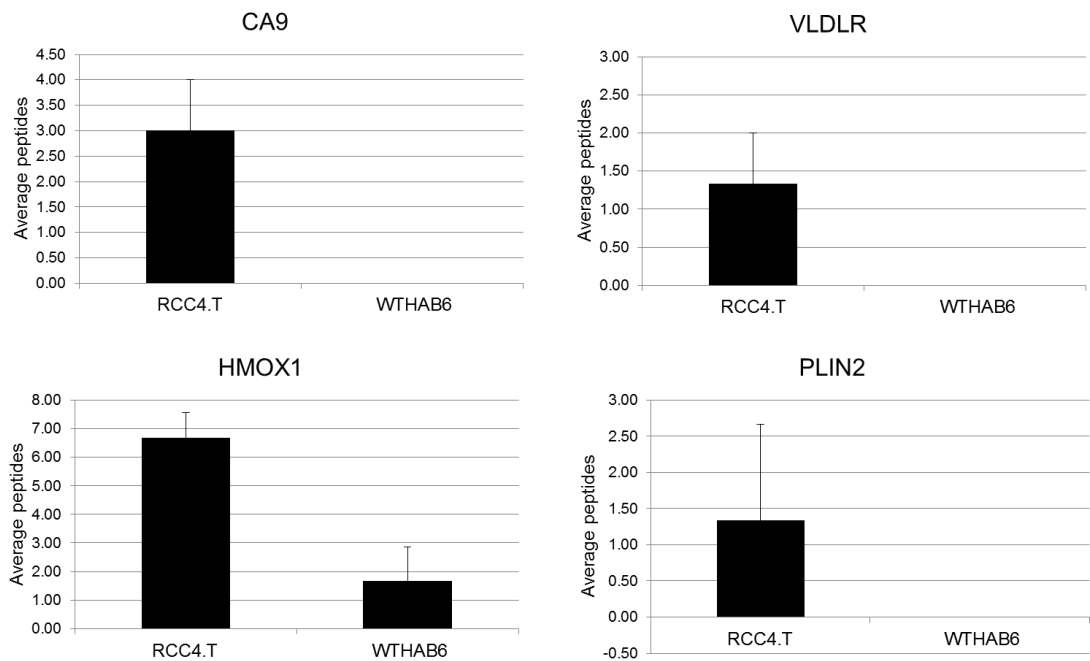


To investigate the validity of the dataset, the expression of known RCC markers was investigated. Two proteins known to be regulated by VHL, carbonic anhydrase-9 and hemoxygenase-1 (HMOX1), plus perilipin-2 (PLIN2) which is upregulated in RCC, were found to be upregulated in RCC4/T versus WTHAB6 at the peptide level (Figure 4.0.4) and the LFQ intensity level (data not shown). Both CA9 and PLIN2 were detected only in RCC4/T, and HMOX1 was upregulated 2.3 fold in RCC4/T versus WTHAB6 (Figure 4.0.4). PLIN2, which is involved in lipid storage, may be involved in the fatty appearance of conventional RCC (Yao et al., 2007, Yao et al., 2005). Another protein which has been linked to this morphology is the very low-density lipoprotein receptor (VLDLR), which was also found at a similar level to

PLIN2. Proteins that were not expected to change, such as β -2-microglobulin and β -actin, were found to have a similar level of expression between the two cell lines (data not shown).

Figure 4.0.4: Upregulation of CA9, PLIN2, and HMOX1 in RCC4/T

Bar graphs show the upregulation of carbonic anhydrase-9 (CA9), heme oxygenase 1 (HMOX1), perlipin-2 (PLIN2), and very low density lipoprotein receptor (VLDLR) in Type 1 (RCC4/T) versus wild type VHL (WTHAB6) disease cell lines. Bars show average number of peptides identified by LC-MS/MS from a triplicate experiment, error bars show SEM.



4.3.1. Differentially expressed proteins between WTHAB6 and RCC4/T

Differentially expressed proteins were identified by first comparing present/absent proteins, followed by comparisons of protein fold changes. Proteins that were unique to RCC4/T included insulin receptor substrate 2 (IRS2), perilipin-2 (PLIN2), brefeldin A-inhibited guanine nucleotide-exchange protein 3 (ARFGEF3), and protein jagged-1 (JAG1). Proteins that were unique to WTHAB6, and were therefore lost with VHL-transfection, included carbonic anhydrase 2 (CA2), Echinoderm microtubule-associated protein-like 2 (EML2), and thymidine phosphorylase (TYMP). Following visual inspection of the data IRS2, CA2, and EML2 were shortlisted as interesting candidates for potential downstream investigation in further samples (Tables 4.0.3-4.0.4, Figure 4.0.5). Analysis by DAVID (Huang et al., 2009a, Huang et al., 2009b) of the RCC4/T unique proteins (≥ 2 peptides) indicated that there were 80 statistically significant overrepresented clusters, the top five of these were phosphoprotein ($p=0.000012$), acetylation ($p=0.000022$), t-SNARE ($p=0.000065$), mitochondrion ($p=0.00023$), and GTPase regulator activity ($p=0.0065$). There were 25 significantly overrepresented clusters in the WTHAB6 unique protein (≥ 2 peptides) list. The top 5 upregulated pathways were carbohydrate biosynthetic process ($p=0.0061$), N-glycan biosynthesis ($p=0.0068$), cell division ($p=0.0078$), mitochondrion organisation ($p=0.0012$), and glycosyltransferase ($p=0.0026$). As DAVID sources pathways from multiple databases, there was a lot of redundancy in the pathways identified.

A further method to looking at unique proteins involved filtering the dataset set based on significance values and fold changes. Analysis of the data revealed 31 proteins were significantly ($P < 0.05$) different between WTHAB6 and RCC4/T, when comparing peptide data. No proteins were found to be significant through analysis of LFQ data. These 31 proteins included 27 that were unique to either WTHAB6 or

RCC4/T, however these were identified with only 1 peptide and were thus below the threshold for confident identification. The remaining four proteins demonstrated a ≤ 2 fold change, which is not outside the level of technical variability in a label-free study. No proteins were calculated to have a probability value below 0.047 due to the power limitations of the study, as only three replicates were used. Proteins were therefore identified that had a trend towards significance, by raising the threshold to $p < 0.077$. At this threshold, and with a requirement for a minimum 2.5 fold change, 156 and 64 proteins were identified by inspecting peptide and LFQ data respectively. In the peptide analysis, this included 33 upregulated by RCC4/T, 54 upregulated by WTHAB6, and 69 proteins demonstrating an on/off response (Table 4.0.2). In the LFQ data this included 21 proteins upregulated by RCC4/T, 18 proteins upregulated by WTHAB6, and 25 proteins demonstrating an on/off response (Table 4.0.2). There was some concordance between the data with some proteins being found upregulated in both datasets, however these proteins were infrequently regulated at the same fold level. Of the WTHAB6 upregulated proteins, 12 proteins were found in both datasets; 18 proteins upregulated by RCC4/T were found to be upregulated in both datasets.

Table 4.0.2: Numbers of differentially expressed proteins in WTHAB6 and RCC4/T

Number of proteins (IDs) differentially expressed in WTHAB6 and RCC4/T, with ≥ 2.5 fold change, or were found in only one cell line, based on peptide data and LFQ intensities.

	$\geq 2.5 - < 5$ fold		$\geq 5 - < 10$ fold		≥ 10 fold		On/off	
	WT	RCC4/T	WT	RCC4/T	WT	RCC4/T	WT	RCC4/T
Peptide	35	21	14	10	5	2	29	40
LFQ	3	3	14	10	1	8	10	15

4.3.1.1. Proteins upregulated in WTHAB6 versus RCC4/T

Proteins upregulated by WTHAB6 were shortlisted based on fold change, average number of peptides, and visual inspection of the data to identify potential candidates for downstream investigation. Both peptide and LFQ data were taken into consideration. The eleven proteins with the greatest upregulation were shortlisted (Table 4.0.3). The greatest upregulation was shown by protein niban (FAM129A), carbonic anhydrase 2 (CA2), TBC1 domain family member 4 (TBC1D4), neurofilament medium polypeptide (NEFM) (Figure 4.0.5), dipeptidyl peptidase 4 (DPP4), and fibronectin (FN1).

The upregulated proteins with $p < 0.077$ were investigated using DAVID v6.7 (Huang et al., 2009a, Huang et al., 2009b), KOBAS v2.0 (Xie et al., 2011a), and GeneMania (Warde-Farley et al., 2010). Different annotations were achieved for proteins identified through analysis of peptide and LFQ intensities, the candidate proteins identified through both methods were therefore combined to give an

overview for both datasets, giving 99 WTHAB6 proteins, and 91 proteins for RCC4/T. Functional annotation clustering using DAVID v6.7 revealed multiple overrepresented annotations in the wild type cell line, these included Mitochondrion (enrichment score (ES) = 3.25, $P = 1.6 \times 10^{-4}$), Nucleotide binding (ES = 1.04, $P = 2.9 \times 10^{-2}$), Cellular amino acid catabolic process (ES = 1.12, $P = 4.7 \times 10^{-2}$), and Response to oxygen levels (ES = 1.03, $P = 3.5 \times 10^{-2}$). Analysis using DAVID's functional annotation chart also indicated that multiple proteins annotated with acetylation ($P = 1.1 \times 10^{-3}$) and phosphoprotein ($P = 6.2 \times 10^{-3}$) were present. No significantly upregulated functions were identified through either KOBAS 2.0 or GeneMania analysis.

4.3.1.2. Proteins upregulated in RCC4/T versus WTHAB6

The fifteen most upregulated proteins in RCC4/T compared with WTHAB6 were shortlisted (Table 4.0.4) based on the same criteria as used for the wild type cell line, these proteins included insulin receptor substrate (IRS2), spermatogenesis-associated serine-rich protein 2 (SPATS2), Myc box-dependent-interacting protein 1 (BIN1), tensin-1 (TNS1), and prolow-density lipoprotein receptor-related protein 1 (LRP1) (Figure 4.0.5). In the DAVID analysis of the Type 1 VHL transfectant, mitochondrial proteins also appeared to be enriched (ES = 1.9, $P = 8.2 \times 10^{-3}$), other enriched processes included Fatty acid metabolic process (ES = 1.65, $P = 1.6 \times 10^{-2}$), Nuclear lumen (ES = 1.58, $P = 8.0 \times 10^{-4}$), and response to hypoxia (ES = 1.34, $P = 2.8 \times 10^{-2}$). A high number of proteins annotated with acetylation ($P = 1.7 \times 10^{-7}$) and phosphoprotein (6.9×10^{-5}) were also found in this dataset, these annotations were therefore not unique to either set of data and were more likely pan annotations. Analysis by GeneMania indicated several functions were listed as upregulated, these were very similar to those identified by DAVID and included response to

hypoxia, mitochondrial matrix, and fatty acid metabolic process. No functions were found to be significantly upregulated in the KOBAS analysis.

Figure 4.0.5: Differential protein expression in RCC4/T and WTHAB6

Upregulated proteins in RCC4/T and WTHAB6. Average number of peptides across three replicates is shown. Bars show SEM.

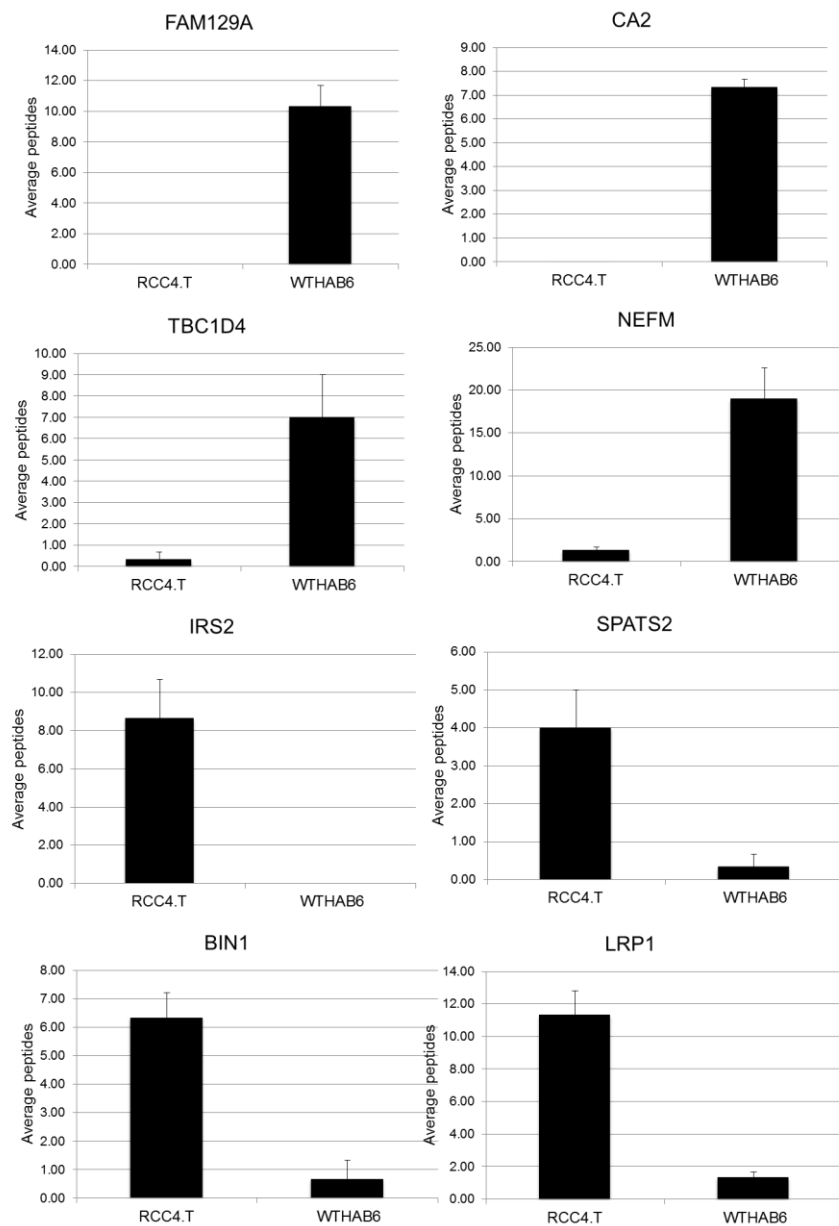


Table 4.0.3: Proteins upregulated in WTHAB6 versus RCC4/T.

Proteins with the largest fold changes in WTHAB6 versus RCC4/T are shown based on peptide data. Fold change proteins are shown for those with ≥ 8 fold change. NC, not calculated, due to presence/absence expression pattern.

Protein name	Gene name	Uniprot	Fold (peptides)	P value (peptides)	Fold (LFQ)	P value (LFQ)	Average peptides
Protein Niban	FAM129A	Q9BZQ8	NC	0.059	NC	0.064	10.33
Carbonic anhydrase 2	CA2	P00918	NC	0.059	NC	0.064	7.33
Echinoderm microtubule-associated protein-like 2	EML2	O95834	NC	0.064	NC	0.197	3.33
TBC1 domain family member 4	TBC1D4	O60343	21.00	0.072	NC	0.064	7.00
Neurofilament medium polypeptide	NEFM	P07197	14.25	0.077	NC	0.064	21.00
Dipeptidyl peptidase 4	DPP4	P27487	12.00	0.077	NC	0.064	4.00
Pyruvate dehydrogenase phosphatase regulatory subunit, mitochondrial	PDP-1	Q8NCN5	11.00	0.072	NC	0.064	3.67
Fibulin 1	FBLN1	P23142	9.00	0.077	-	-	3.00
Fibronectin	FN1	P02751	6.57	0.100	38.82	0.100	65.67

Tissue factor pathway inhibitor 2	TFPI2	P48307	4.50	0.077	NC	0.064	3.00
Splicing factor 3B subunit 4	SF3B4	Q15427	3.33	0.059	NC	0.064	3.33

Table 4.0.4: Proteins upregulated in RCC4/T versus WTHAB6

Largest fold changes in RCC4/T versus WTHAB6, On/off changes are shown for proteins with an average number of peptides ≥ 3 . NC, not calculated, due to presence/absence expression pattern

Protein name	Gene name	Uniprot	Fold (peptides)	P value (peptides)	Fold (LFQ)	P value (LFQ)	Average peptides
Insulin receptor substrate 2	IRS2	Q9Y4H2	NC	0.064	NC	0.064	8.67
Spermatogenesis-associated serine-rich protein 2	SPATS2	Q86XZ4	12.00	0.072	NC	0.064	4.00
Butyryl-CoA dehydrogenase	ACADS	P16219	10.00	0.072	NC	0.064	3.33
Myc box-dependent-interacting protein 1	BIN1	O00499	9.50	0.077	16.13	0.077	6.33
Prolow-density lipoprotein receptor-related protein 1	LRP1	Q07954	8.50	0.077	16.39	0.077	11.33
Tensin-1	TNS1	Q9HBL0	8.00	0.077	11.78	0.077	10.67
Adenosine deaminase	ADA	P00813	6.49	0.077	NC	0.064	4.33

Nuclear receptor corepressor 2	NCOR2	Q9Y618	5.32	0.077	7.15	0.077	5.33
Nuclear-interacting partner of ALK	ZC3HC1	Q86WB0	4.67	0.077	NC	0.064	4.67
Pseudouridine-5-monophosphatase	HDHD1	Q08623	4.50	0.077	NC	0.064	3.00
E3 ubiquitin-protein ligase listerin	LTN1	O94822-3	4.50	0.059	NC	0.064	3.00
Peptidase M20 domain-containing protein 2	PM20D2	Q8IYS1	3.75	0.077	11.19	0.077	5.00
Fumarylacetoacetase	FAH	P16930	3.66	0.077	9.10	0.077	3.67
Alpha N-terminal protein methyltransferase 1A	METTL11A	Q9BV86	3.33	0.077	NC	0.064	3.33
Inositol 1,4,5-trisphosphate receptor type 3	ITPR3	Q14573	3.25	0.077	7.04	0.077	8.67

4.4. Investigation into IRS2 expression

Due to the differential expression between the plus and minus VHL cell lines, IRS2 was chosen for further initial downstream investigation. This protein is a scaffold protein with links to metastasis in other studies. Furthermore, it is involved in PI3K signalling, and may be controlled by hypoxia.

4.4.1. Western blot examination of IRS2 expression

Expression levels of IRS2 in RCC4/T and WTHAB6 were first confirmed by Western blot, and they were found to corroborate the mass spectrometry data (Figure 4.0.6), with high levels in RCC4/T as observed by a band at approximately 160kDa, higher than the predicted molecular weight of 130kDa but consistent with the literature-reported size during Western blot analysis. A considerably lower level of expression was found in WTHAB6 after an extended exposure (data not shown). To ensure the expression pattern was not due to any potential slowing of growth at 85% confluence, the experiment was repeated with cells grown to 50% confluence. No difference in expression pattern was observed (data not shown).

To confirm the differential expression pattern of IRS2 in RCC4/T and WTHAB6, and to investigate whether the difference in expression of IRS2 was present in other VHL-transfected RCC cell lines with different genetic backgrounds, the expression of IRS2 was investigated in two further plus/minus VHL cell line pairs. UMRC2 and 786-0, RCC cell lines that both carry a defective VHL, have previously been stably transfected with a plasmid carrying full length, wild type VHL, to replace lost VHL function. IRS2 was found to be highly expressed in the RCC4/T and 786-0/-VHL cell lines, and absent from WTHAB6 and the VHL positive 786-0/+VHL cell line, i.e.

following VHL transfection (Figure 4.0.6). No detectable expression was observed in either of the UMRC2 cell lines. The three *vhl* mutations in these three cell lines all occur in exon I (Table 4.0.5), with the UMRC2 point mutation lying between the RCC4 point mutation and the 786-0 frameshift mutation. Therefore the difference in IRS2 stability may not be solely explained by the exonic location of the mutation, however there are multiple binding sites of different moieties on exon I of *VHL*, and there is likely an explanation for the difference in IRS2 expression in the disruption of these binding sites.

Figure 4.0.6: IRS2 expression in RCC4/T and 786-0

Cell lysates were probed with anti-IRS2 (EP976Y). Gels were checked for normalisation using a parallel coomassie staining (data not shown).

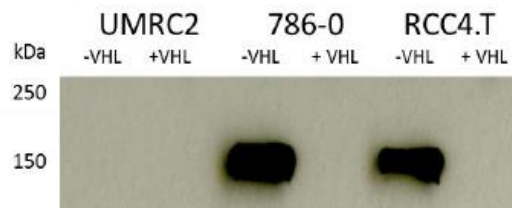


Table 4.0.5: Background VHL mutations present in three RCC cell lines

The VHL specific mutations that are present in RCC4, UMRC2, and 786-0. Point mutations are present in RCC4 and UMRC2, a frameshift (fs) mutation is present in 786-0. The polypeptide mutation is also shown.

Cell line	Genomic mutation	Protein mutation
RCC4	C194G	S65W
UMRC2	G245C	R82P
786-0	311delG	G104fs

4.4.2. Investigation into IRS2 expression in clinical samples from RCC patients

Protein levels of IRS2 were investigated by Western blot in matched frozen tissue acquired from nephrectomised RCC patients, with the intention of determining the clinical significance of IRS2 expression. However it was not possible to determine any difference in IRS2 expression between the tumour and normal tissues, due to the high amount of non-specific binding of the IRS2 antibody to multiple bands in the tissue samples.

4.4.3. Examination of IRS2 transcripts

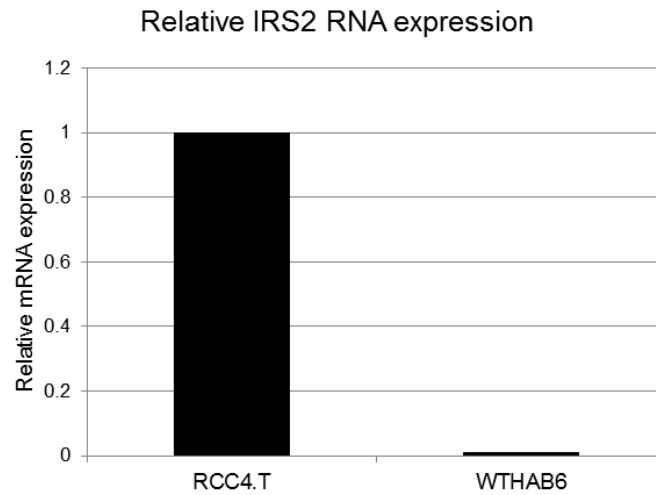
Protein expression levels reflect the dynamic phenotype of the functioning cell, however investigating transcript levels can also provide useful information on how a protein's expression is controlled. Although the absence of a transcript would confirm the absence of a protein product, the presence of the transcript does not confirm the presence of an active protein, as the protein may be rapidly degraded, or may be the target of inactivating post-translational modifications.

An endogenous control ('housekeeping' gene) was chosen through a combination of literature searching and proteomic data from the RCC4/T and WTHAB6 cell lines. Desirable attributes were a similar level of expression between the RCC4/T and WTHAB6 proteomes, a low standard error, and a high a number of average peptides. There were 14 literature-identified endogenous controls that were also present in the data set, and seven further novel candidates were also identified. Five potential candidates were chosen based on ≥ 3 average number of peptides, and ≤ 0.5 standard error (data not shown), including three already known endogenous controls, ACTB, HPRT1, and B2M (Jung et al., 2007, Glenn et al., 2007), and two novel genes, RPL37A and RPL30. ACTB was found to have the highest expression with the lowest standard error. ACTB had also been investigated in other studies (Jung et al., 2007, Glenn et al., 2007) and it was therefore chosen as the endogenous control for this study; all qRT-PCR experiments were performed using this control.

To check for detectable levels of IRS2 RNA, a titration (range 0.04-80ng/ul) was performed using RCC4/T. The cells were grown to 85% confluence; mRNA was harvested using the RNeasy kit and then reverse transcribed to cDNA. IRS2 and ACTB specific TaqMan probes were used in the qRT-PCR analysis. IRS2 mRNA was detected in all RNA dilutions (data not shown); a starting RNA amount 0.8ng/ μ l was chosen for future analyses. Next, the amount of IRS2 mRNA in RCC4/T and WTHAB6 was compared. RCC4/T was used as the control sample, and the level of IRS2 mRNA in WTHAB6 was determined as a proportion of the mRNA level observed in RCC4/T. A 100-fold lower amount of IRS2 mRNA was observed in WTHAB6 as compared to RCC4/T, suggesting IRS2 expression may be controlled at the transcript level (Figure 4.0.7.).

Figure 4.0.7: Presence of IRS2 mRNA in RCC4/T and WTHAB6

Relative levels of IRS2 mRNA in WTHAB6 as a function of RCC4/T. Values were calculated using the delta-delta-Ct method (Livak and Schmittgen, 2001).

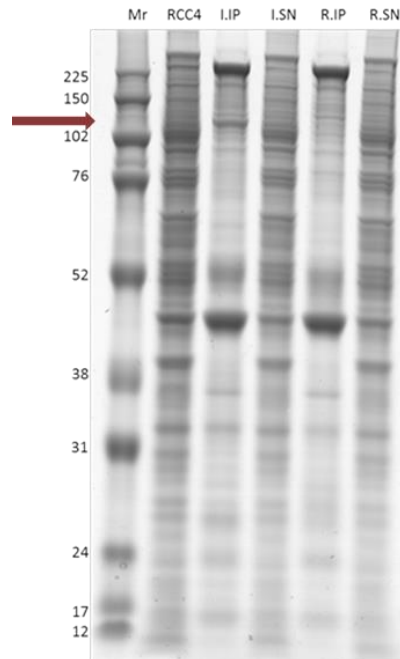


4.5. Investigation into the binding partners of IRS2

IRS2 is known to interact with a number of proteins and, through its role as a scaffold protein, it functions to relay messages downstream. To this end it was hypothesised that an immunoprecipitation of IRS2 may shed light on novel interaction partners of IRS2 and serve to provide further information on the role this protein plays in RCC pathogenesis. SDS-PAGE analysis of the immunoprecipitated proteins and the supernatant revealed a complex mixture of proteins in the immunoprecipitated fractions; a large number of proteins were brought down non-specifically by IgG (Figure 4.0.8). A strong band around 130kDa was observed in the IRS2 antibody lane, which was absent from the control antibody lane, and a few other bands were present in the IRS2 immunoprecipitation lane that appeared to be absent from the rabbit IgG immunoprecipitation lane, which may be IRS2-specific interactors.

Figure 4.0.8: SDS-PAGE analysis of immunoprecipitated IRS2

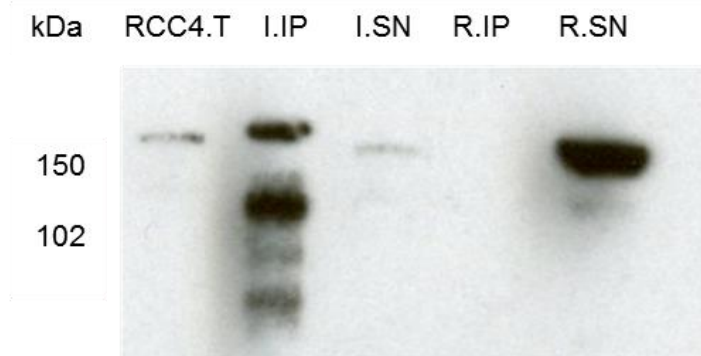
Proteins associated with IRS2 were immunoprecipitated using anti-IRS2 (EP976Y). A control immunoprecipitation was performed using anti-Rabbit IgG. I.IP, IRS2 immunoprecipitation; I.SN, IRS2 supernatant; R.IP, Rabbit IgG immunoprecipitation; R.SN, Rabbit supernatant. Arrow indicates the location of IRS2.



To confirm the IRS2 immunoprecipitation did precipitate the target protein, a Western blot of the recovered proteins was performed (Figure 4.0.9). The Western blot revealed that high levels of IRS2 were brought down by the immunoprecipitation (I.IP lane), but precipitation was not complete, as some remained in the supernatant (I.SN lane). The presence of IRS2 in the rabbit IgG supernatant lane (R.SN) and its concomitant absence from the rabbit IgG immunoprecipitate (R.IP) lane indicates that rabbit IgG did not precipitate IRS2. Interestingly, multiple bands were observed in the IRS2 immunoprecipitation lane, which were not observed in the other lanes, and may be fragments of IRS2.

Figure 4.0.9: Western blot analysis of immunoprecipitated IRS2

Proteins associated with IRS2 were immunoprecipitated using anti-IRS2 (EP976Y), a control immunoprecipitation was performed using anti-Rabbit IgG. I.IP, IRS2 immunoprecipitation; I.SN, IRS2 supernatant; R.IP, Rabbit IgG immunoprecipitation; R.SN, Rabbit supernatant IRS2 (I) versus rabbit IgG (R), pull-down (IP) and supernatant (SN).



To investigate the interaction partners of IRS2, immunoprecipitated proteins were analysed by mass spectrometry. Proteins were recovered as described above, digested using the modified FASP-based procedure, and analysed in a two hour gradient on the Orbitrap Velos. In this analysis 879 proteins were confidently identified, most proteins were common to both precipitations and therefore represented the non-specifically bound fraction, 8.8% (77) of the identifications were unique to IRS2, and 6.6% (58) were only found in the rabbit IgG fraction. In the IRS2 precipitation, the target protein IRS2 was identified with 24 peptides (Figure 4.0.10). IRS2 was also found in the control pull-down, indicating some non-specific binding of IRS2 had occurred, though intensity, and sequence coverage were all considerably lower in this pull down (data not shown). By filtering for proteins identified with a minimum four fold change in the number of peptides identified, and a minimum of three peptides required for identification, 46 proteins were found to be unique or upregulated in the IRS2 pull-down. The proteins with the

greatest fold change, and which are therefore more likely to be true interactors, are listed in Table 4.0.6. Proteins immunoprecipitated with IRS2 include the RNA binding proteins Heterogeneous nuclear ribonucleoproteins C1/C2 (HNRNPC) and RNA-binding protein (RALY), the nuclear matrix protein matrin-3 (MATR3), and the 14-3-3 theta (YWHAQ) protein, which has previously been shown to interact with IRS2 (Figure 4.0.10). Analysis of the 46 co-immunoprecipitated proteins by DAVID indicated an overrepresentation of RNA binding ($P=8.5 \times 10^{-16}$), phosphoproteins ($P=2.9 \times 10^{-9}$), RNA splicing (1.4×10^{-6}), and spliceosome (2.8×10^{-6}) proteins.

Figure 4.0.10: Enrichment of IRS2 and YWHAQ in IRS2 immunoprecipitation

IRS2 and YWHAQ were found to be enriched in the IRS2 immunoprecipitation versus the rabbit IgG immunoprecipitation, based on number of peptides identified.

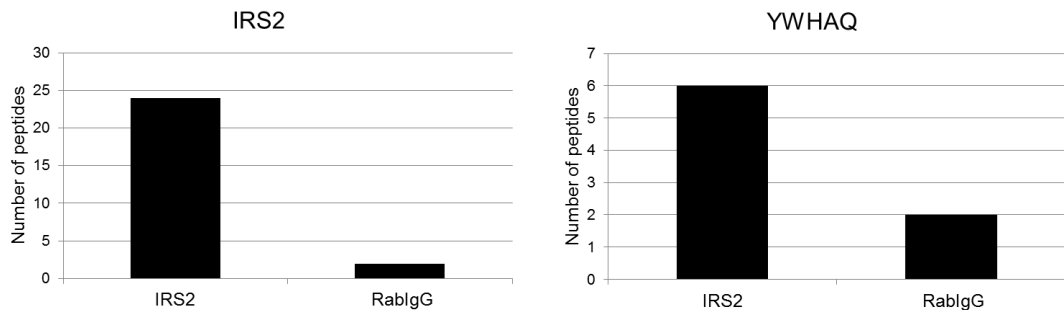


Table 4.0.6: Proteins enriched by IRS2 immunoprecipitation

Proteins with a fold change ≥ 4 , and with ≥ 4 identified peptides.

Gene names	Protein names	IRS2	RablgG	Fold
HNRNPC	Heterogeneous nuclear ribonucleoproteins C1/C2	10	1	10.0
MATR3	Matrin-3	9	1	9.0
RALY	RNA-binding protein Raly	9	1	9.0
UPF1	Regulator of nonsense transcripts 1	13	2	6.5
CDC5L	Cell division cycle 5-like protein	6	1	6.0
MRPL37	39S ribosomal protein L37, mitochondrial	6	1	6.0
SRRM2	Serine/arginine repetitive matrix protein 2	9	2	4.5
HNRNPUL2	Heterogeneous nuclear ribonucleoprotein U-like protein 2	13	3	4.3
RBMX	RNA-binding motif protein, X chromosome	12	3	4.0
IGF2BP2	Insulin-like growth factor 2 mRNA-binding protein 2	8	2	4.0
CEP250	Centrosome-associated protein CEP250	11	0	-
NOP14	Nucleolar protein 14	7	0	-
CDKN2AIP	CDKN2A-interacting protein	7	0	-
PARN	Poly(A)-specific ribonuclease PARN	6	0	-
GADD45GIP1	Growth arrest and DNA damage-inducible proteins-interacting protein 1	5	0	-
MRPL24	39S ribosomal protein L24, mitochondrial	5	0	-
PRPF31	U4/U6 small nuclear ribonucleoprotein Prp31	4	0	-
LDHB	L-lactate dehydrogenase B chain	4	0	-
EXOSC10	Exosome component 10	4	0	-
ZFR	Zinc finger RNA-binding protein	4	0	-

IRS2 immunoprecipitated proteins identified with ≥ 4 fold change, or an on/off change with a minimum of 3 peptides for identification (46 IDs), were submitted for analysis by Ingenuity Pathways Analysis (IPA). This analysis revealed a significant upregulation of RNA processing proteins. Top upregulated networks were 'RNA post-transcriptional modification; Hereditary disorder' and 'RNA damage and repair; Protein Synthesis; Gene Expression', with 18 and 12 proteins involved in these networks respectively. The top upregulated molecular pathways were also dominated by mechanisms involving RNA processing and protein synthesis proteins (data not shown). The top disease was identified as Cancer, with 43 proteins attributed to this, indicating many of the proteins involved may support the growth of the RCC4 cells.

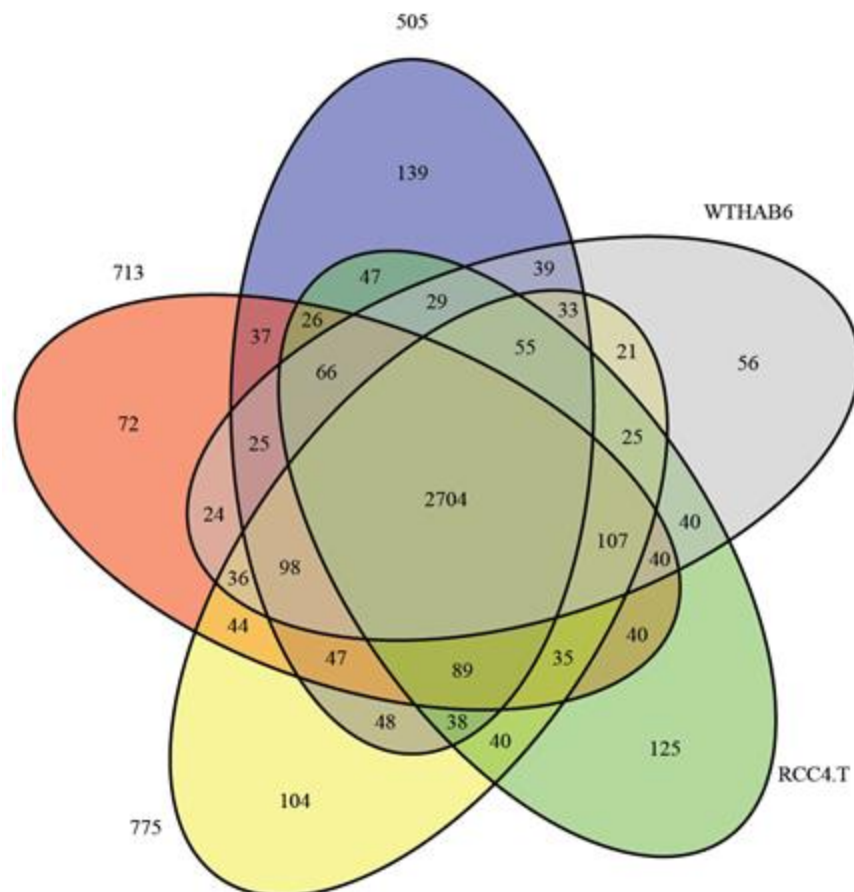
4.6. Proteomic analysis of VHL disease mutant cell lines

To investigate the impact of VHL disease-specific *VHL* mutations on the cellular proteome, an exploratory mass spectrometry study of four cell lines carrying *VHL* mutations plus a wild type control was conducted. The mutations carried by the Type 1 (RCC4/T) and Type 2B (RCC4/2B) cell lines lead to the development of RCC, and as such differences in these two cell lines were of particular interest. In total, 4680 proteins were confidently identified, with at least two peptides (including one unique). The cell lines were very similar to one another; 62.5% of proteins were common to all five cell lines (Figure 4.0.11), with 11.5%, 8.8%, 7.7%, and 9.6% found in any one cell line, two cell lines, three cell lines, or four cell lines respectively. The percentages of unique proteins identified in each cell line were fairly similar with 1.3%, 2.9%, 3.2%, 1.7%, and 2.4% unique proteins found in WTHAB6, RCC4/T, RCC4/2A, RCC4/2B, and RCC4/2C respectively. All possible pairwise comparisons found that 255 proteins demonstrated a significant difference

($p < 0.05$) between any cell line pair. Nine proteins were significant at the $p < 0.01$ level, however eight of these were upregulated in a single cell line, with the remaining protein upregulated in both the Type 1 and wild type cell lines, and it was therefore not of clinical interest to the development of RCC. The complete set of raw and analysed data can be found in supplementary data files S9, S10, and S11.

Figure 4.0.11: Shared proteins between the five VHL disease cell lines

Shared proteins between the five cell lines, based on peptide data, with a threshold cut off of at least 1 peptide.

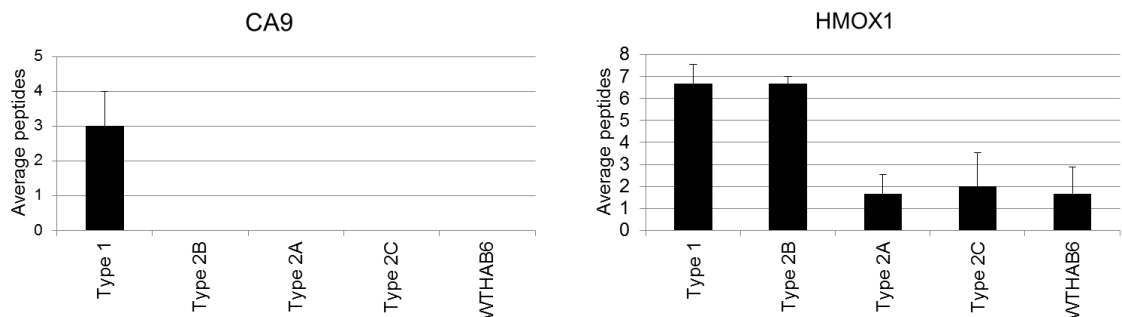


4.6.1. Proteins differentially regulated in Type 1 and Type 2B

Type 1 and type 2B VHL disease predisposes the sufferer to the development of multifocal RCC, and as such these two cell lines were of particular interest for proteomic mining. Data were analysed to allow comparison of these two cell lines with the remaining three cell lines, to hopefully identify proteins that may be involved in the development of RCC. Previous analysis of the gene expression microarray profile of these five cell lines revealed 19 differentially expressed genes (Abdulrahman et al., 2007). Five of these 19 genes were identified in this dataset; ACTA2, ALDH9A1, SEC31A, SNRPN, and PALLD, however none of these were found to be differentially expressed in this proteomic analysis. The known RCC markers CA9 and HMOX1 were both found in the current analysis (Figure 4.0.12), with upregulation of CA9 found in RCC4/T and upregulation of HMOX1 found in both the RCC forming transfectants.

Figure 4.0.12: Expression of known RCC markers in VHL disease transfectants

Expression of known RCC markers in *vhl* mutant cell lines. Values shown are average peptides across three replicates \pm SEM.

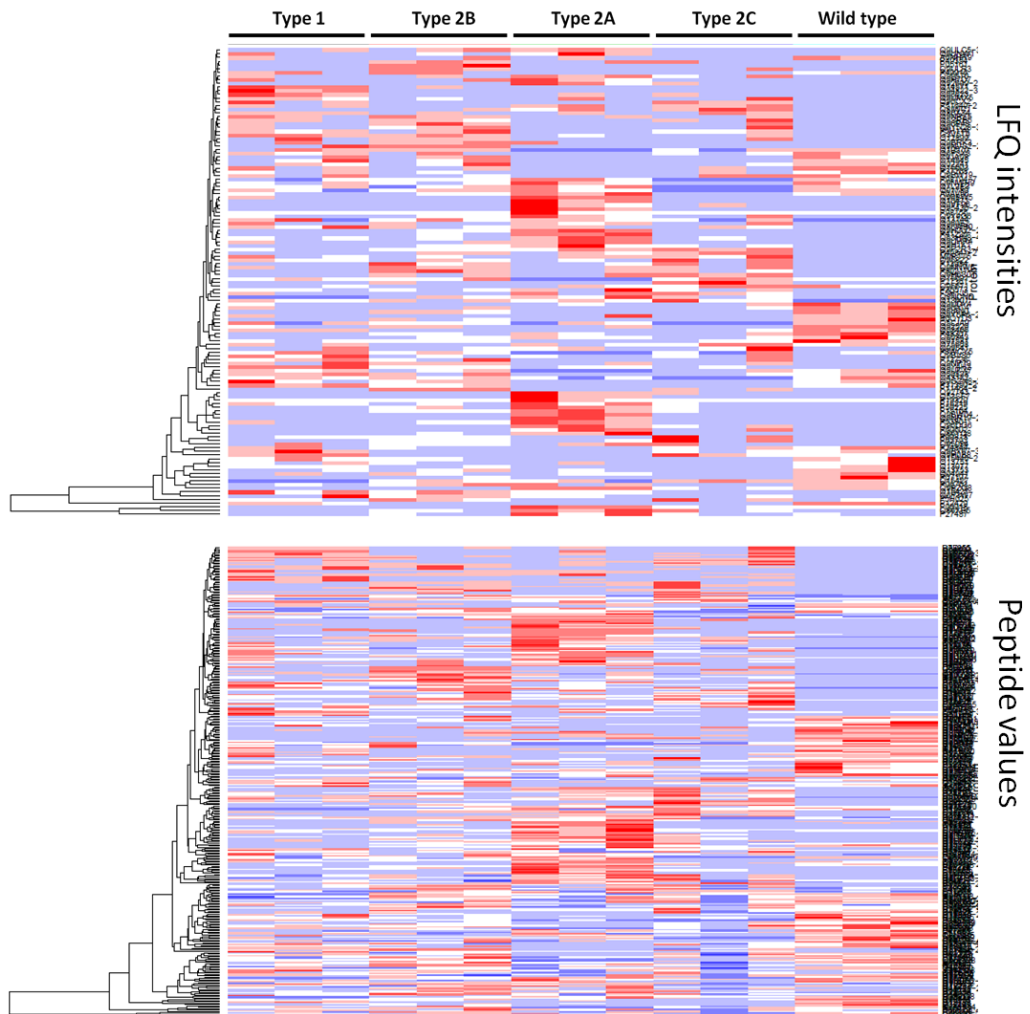


4.6.1.1. Heat map comparison of VHL disease-cell line proteomes

Deciding a suitable method through which to analyse the data was a significant problem in this analysis. As there were five cell lines to consider, a simple pairwise comparison was not feasible. The data were first analysed using heat maps to allow graphical representation of the differential expression, and to hopefully identify a characteristic pattern of expression. Visualising mass spectrometric data using heat maps, whilst a less traditional method for viewing proteomic data, is a method which is increasingly being used as it allows for patterns in the data to be quickly observed. The heat maps were constructed by comparing the Z-score for each cell line replicate to the protein's average, considering each protein separately, and colour coded based on the Z-score value. Heat map analysis of all the identified proteins revealed no pattern of expression, as most of the proteins did not show a significant difference across the cell lines. Next, the represented proteins were limited to those that were determined to be significantly different from the wild type cell line, based on pairwise comparisons for each of peptide values, LFQ intensities, and intensity values. Data were clustered to give an optimal pattern of expression revealing significant differences between the wild type cell line and any other cell line (Figure 4.0.13).

Figure 4.0.13: Heat maps of significantly different proteins in VHL transfectants of RCC4

Proteins were colour coded and grouped according to their Z-score away from the mean for all cell lines, then clustered compared to the wild type cell line. Values range -3 Z-score (dark blue), -2 Z-score (mid blue), -1 Z-score (light blue), 0 Z-score (white), +1 Z-score (light red), +2 Z-score (mid red), +3 Z-score (dark red).



Due to the high amount of variation observed in the peptide heat maps, subsequent maps focussed on the LfQ intensities due to the inbuilt normalisation with this value, thus limiting the bias caused by focussing on the simpler peptide value, and

4.6.1.2. Comparison of data by filtering

Another method to identify differentially expressed proteins involved filtering the proteins in Excel, based on the average number of peptides or average LFQ intensity across the three replicates. Using this technique allowed the identification of proteins that were not necessarily significantly different between the cell lines but nevertheless demonstrated a pattern of expression that was worthy of further investigation. By filtering the data to identify proteins upregulated or downregulated in RCC-forming cell lines according to peptide data, three different proteins were identified, including two downregulated, and one upregulated. Absent in melanoma 1 (AIM1) and mRNA turnover protein 4 homolog (MRTO4) were found to be downregulated in the RCC forming cell lines, whereas Cyclin-dependent kinase 4 (CDK4) was found to be upregulated in these two cell lines. Of these, CDK4 and AIM1 were also differentially expressed based on LFQ data. By filtering the LFQ data using the same criteria as for the peptide data, three further candidates were identified, including one upregulated (GNE) and two downregulated (CLCC1, NRP1) in the RCC forming cell lines (Tables 4.0.7-4.0.8, Figure 4.0.15). The RCC4/T upregulated protein IRS2 was also found to be elevated in the RCC forming cell line RCC4/2B, these levels were only slightly elevated compared to the remaining two *VHL* mutants (Tables 4.0.7-4.0.8, Figure 4.0.15.).

4.6.2. Candidate early biomarkers in RCC pathogenesis

By using two different methods to analyse the data, seven potential candidates were identified (Tables 4.0.7-4.0.8, Figure 4.0.15). Data analysed included both peptide (data not shown) and LFQ values. The heat maps were reliant on significance values and allowed for powerful computer-based identification of potential candidates, whereas filtering using Excel allowed non-significant proteins

to be identified by eye. The two techniques were thus complementary to one another, and allowed the best visualisation of the data when combined together. The shortlisted proteins may be involved in the pathogenesis of early RCC and validation of their expression level is warranted.

Figure 4.0.15: Differential protein expression in the RCC forming cell lines

Average LFQ values \pm SEM are shown. Cell lines represented are RCC4/T (Type 1), 713 (Type 2B), 505 (Type 2A), 775 (Type 2C), and WTHAB6 (wild type).

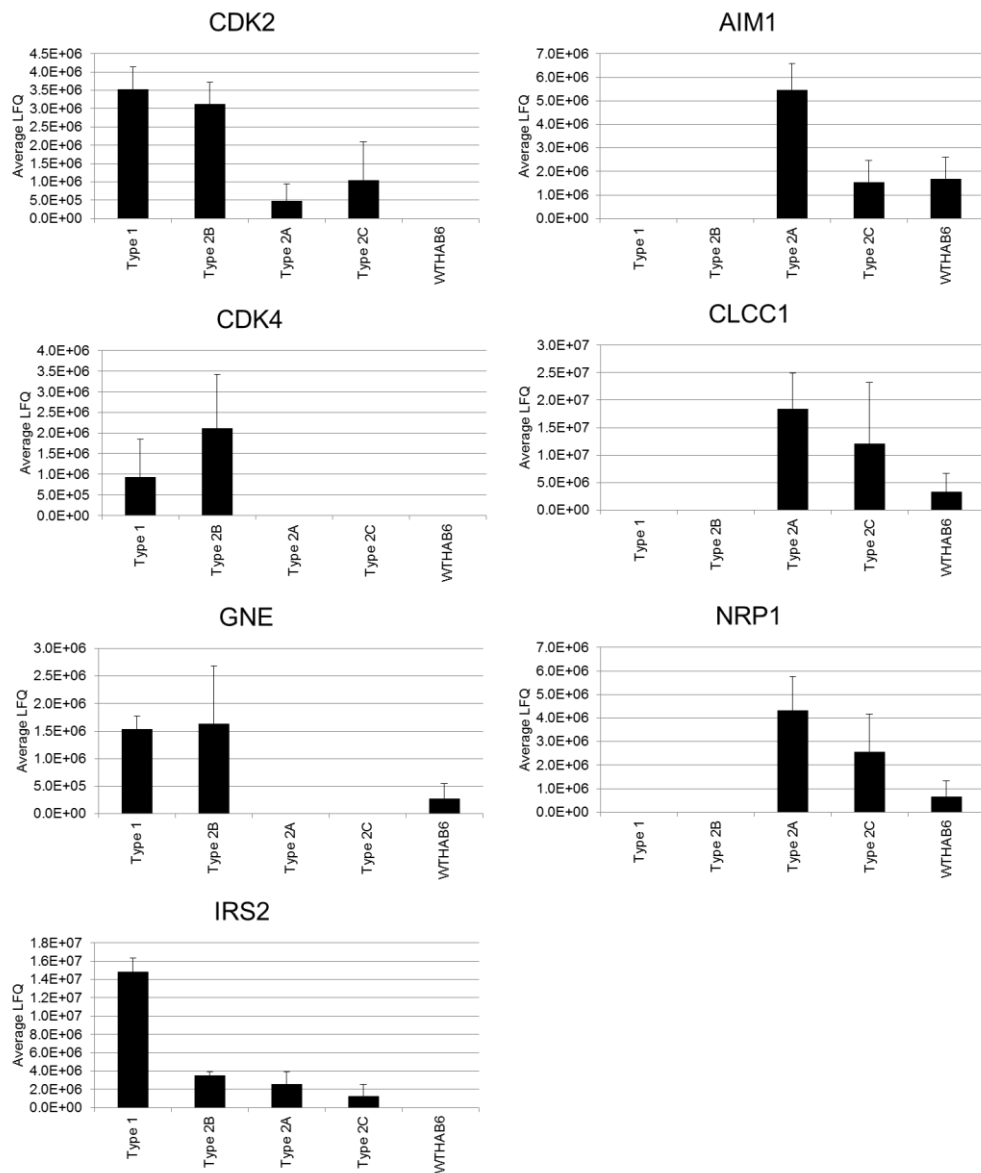


Table 4.0.7: Proteins upregulated in the RCC forming cell lines

Average LFQ values \pm SEM are shown

	Type 1		Type 2B		Type 2A		Type 2C		Wild type	
CDK2	3.5E+06	\pm 6.1E+05	3.1E+06	\pm 6.0E+05	4.7E+05	\pm 4.7E+05	1.0E+06	\pm 1.0E+06	0	\pm 0
CDK4	9.3E+05	\pm 9.3E+05	2.1E+06	\pm 1.3E+06	0	\pm 0	0	\pm 0	0	\pm 0
GNE	1.5E+06	\pm 2.3E+05	1.6E+06	\pm 1.0E+06	0	\pm 0	0	\pm 0	2.7E+05	\pm 2.7E+05
IRS2	1.5E+07	\pm 1.5E+06	3.5E+06	\pm 4.0E+05	2.5E+06	\pm 1.4E+06	1.3E+06	\pm 1.3E+06	0.0E+00	\pm 0.0E+00

Table 4.0.8: Proteins downregulated in the RCC forming cell lines

Average LFQ \pm SEM are shown

	Type 1		Type 2B		Type 2A		Type 2C		Wild type	
AIM1	0	\pm 0	0	\pm 0	5.5E+06	\pm 1.1E+06	1.5E+06	\pm 9.3E+05	1.7E+06	\pm 9.3E+05
CLCC1	0	\pm 0	0	\pm 0	1.8E+07	\pm 6.4E+06	1.2E+07	\pm 1.1E+07	3.3E+06	\pm 3.3E+06
NRP1	0	\pm 0	0	\pm 0	4.3E+06	\pm 1.4E+06	2.6E+06	\pm 1.6E+06	6.6E+05	\pm 6.6E+05

4.7 Discussion

The early stages of RCC development are poorly understood; delineating the molecular pathogenesis of this disease is a crucial step in improving the clinical progression of RCC, and for the identification of new druggable targets. In recent years our knowledge of the genetic landscape of RCC has been significantly improved, with the understanding that a variety of genes become deregulated during the pathogenesis of RCC, the predominant of which is VHL. Involvement of VHL has been found in the majority of sporadic RCC cases (Young et al., 2009, Nickerson et al., 2008) and mutation of this gene is also responsible for the development of VHL disease, the familial form of renal cell carcinoma. Previous studies have investigated the proteomic and transcriptomic impact of *VHL* inactivation (Aggelis et al., 2009, Craven et al., 2006). A genomic screen of the same cell lines used in this study, found 19 differentially regulated genes between the RCC forming RCC4/T and RCC4/2B, versus the non-RCC forming RCC4/2A and RCC4/2C cell lines. Two of these proteins, thymosin beta-15A and proteinase-activated receptor 2 were implicated in RCC pathogenesis when investigated at the *in vitro* level (Abdulrahman et al., 2007). Furthermore, analysis of conditioned media from 786-0 and A498 cells transfected with empty vector, wild type VHL, or one of three Type 2C VHL disease mutations, revealed downregulation of the chaperone protein Clusterin in Type 2C and VHL negative cell lines (Nakamura et al., 2006).

To enable a greater understanding of the proteomic changes brought about by *VHL* mutation, five cell lines carrying mutations relevant to VHL disease were analysed by mass spectrometry. This study focussed predominantly on the

proteomic changes brought about by *vhl* mutation, by comparing the VHL wild type and VHL negative cell lines WTHAB6 and RCC4/T (VHL disease type 1), respectively, followed by an exploratory study comparing the proteomes of all five cell lines. Of note, the type 1 disease mutation (S65W) lies in the alpha domain of VHL, and the type 2B mutation (R167Q) lies in the elongin C binding region of the beta domain. Both mutations would potentially impact upon VHLs ability to target proteins for ubiquitination. The type 2A (Y98H) and type 2C (L188V) mutations lie in the beta and alpha domains respectively.

4.7.1. Proteomic comparison of the plus/minus VHL cell lines WTHAB6 and RCC4/T

The impact of VHL inactivation was investigated by proteomically comparing RCC4/T with WTHAB6. In total, 4494 proteins were identified and most of these were common to both cell lines. The dataset was checked for the expression of the known VHL targets CA9 and HMOX1. The hypoxic protein CA9 is involved in the reversible hydration of carbon dioxide and it is a well-documented marker for RCC (Bui et al., 2003, Tostain et al., 2010). In this study CA9 was found to be present in RCC4/T, and completely absent from WTHAB6, which supported the results observed by Western blot. Hemeoxygenase (HMOX1), though not switched off in WTHAB6, appeared to be expressed at higher levels in RCC4/T, which is consistent with previous reports (Banerjee et al., 2012). Hemeoxygenase 1 has been proposed to be an anti-inflammatory protein involved in tumour survival, and is activated by HIF (Yang and Zou, 2001). Perilipin-2 was also found to be upregulated in RCC4/T, indicating it might be controlled by VHL. This protein is involved in lipid storage and has been shown to be upregulated in renal cell carcinoma

tissue (Yao et al., 2007, Yao et al., 2005) and urine (Morrissey et al., 2010, Morrissey et al., 2014), its presence may contribute to the clear appearance of ccRCC. Another protein which has been associated with lipid storage in ccRCC is the very low-density lipoprotein receptor (VLDLR) (Sundelin et al., 2012), which was also found at higher levels in the RCC4/T cell line.

To identify proteins controlled by VHL, proteins that were upregulated or unique to either RCC4/T or WTHAB6 were investigated. By looking for differential protein expression based on both LFQ and peptide data, 26 proteins were shortlisted for potential further investigation; 15 that were upregulated by RCC4/T, and 11 that were downregulated by RCC4/T (upregulated in WTHAB6).

4.7.1.1. Insulin Receptor Substrate-2

The insulin receptor substrate -2 (IRS-2) demonstrated the largest differential expression between RCC4/T and WTHAB6, it demonstrated an on/off response at both the peptide and LFQ level, and was therefore selected for further investigation as a potential protein involved in early pathogenesis of RCC. IRS2 comes from the insulin receptor substrate family of adaptor proteins that includes five other members, IRS-1, IRS-3, IRS-4, IRS-5 (DOK4), and IRS-6 (DOK5). The IRS proteins share some similarity in structure, with N-terminal pleckstrin homology (PH) and phosphotyrosine binding (PTB) domains, and a less conserved C-terminal site of tyrosine and serine/threonine phosphorylation (Sun et al., 1995, White, 2002). The pleckstrin homology domains allow for lipid and/or protein-protein interactions, with the C-terminal phosphorylated residues mediating interaction with other

proteins through their SH2 domains. The IRS proteins have no intrinsic kinase activity, and instead function as important adaptors of intracellular signalling by recruiting other signalling proteins. They are widely expressed and have a prominent role in the insulin signalling cascade; insulin signalling has a prominent role in growth and metabolism, and can activate a number of downstream pathways involved in these mechanisms (White, 2002). Binding of insulin to the insulin receptor (IR) tyrosine kinase stimulates auto phosphorylation and docking of a variety of intracellular scaffold proteins, including IRS-1 and IRS-2. Subsequent phosphorylation of the scaffold proteins allows activation and interaction with other cellular components, including PI3K, Grb-2, and SHP2 (White, 1998, Yamauchi et al., 1998). Various signalling pathways are downstream of IRS2, and IRS2 is therefore an important mediator of intracellular signalling. Although IRS1 and IRS2 share significant sequence homology (Sun et al., 1995), their respective roles have been found to be non-redundant (Bruning et al., 1997, Sesti et al., 2001); whereas IRS1 has been associated with increased proliferation, IRS2 has instead been linked to motility and metastasis (Byron et al., 2006, Hoang et al., 2004), which occurs through a PI3K mediated mechanism (Shaw, 2001). Furthermore IRS2 is activated by hypoxia (Mardilovich and Shaw, 2009), and was shown to be induced by HIF-2 α , but not HIF-1 α (Wei et al., 2013). Aside from propagating insulin signalling and promoting metastasis, other ccRCC tumourigenic roles that IRS2 may be involved in include assisting glycolysis through upregulation of GLUT1 (Pankratz et al., 2009), and enhancing abnormal lipid retention (steatosis) (Rametta et al., 2013).

VHL mutation occurs early in RCC pathogenesis (Zhuang et al., 1995, Lubensky et al., 1996), and the proteomic changes brought about as a result

of this mutation could be reflective of early changes in RCC tumourigenesis. IRS2, like many other signalling adaptors, assists in cellular oncogenic transformation (Dearth et al., 2007). Elevated levels of IRS proteins have been found in many cancers, with upregulation of IRS2 found in hepatocellular carcinoma (Boissan et al., 2005) and pancreatic cancer (Kornmann et al., 1998), as well as many breast cancer cell lines (Dearth et al., 2007). Upregulation of IRS2 mRNA was also found in 6/10 renal tumours in a small study (Al-Sarraf et al., 2007). Furthermore, a study investigating polymorphisms in insulin cascade proteins found a IRS2 G1057D polymorphism that was associated with reduced colorectal carcinoma risk (Slattery et al., 2004). Suppression of IRS2 signalling may therefore aid in preventing early tumourigenesis.

In this study IRS2 was found to be highly upregulated in RCC4/T, this is possibly due to the induction of HIF-2 α and subsequent upregulation of IRS2. Confirmation of the mass spectrometry data was achieved through Western blotting of WTHAB6 and RCC4/T, which revealed high levels of IRS2 in the RCC4/T cell line. Very low levels of IRS2 were detected in the WTHAB6 cell line after an extended Western blot exposure (data not shown), indicating that IRS2 is constitutively expressed in this cell line. IRS2 was also found to be expressed in the VHL negative 786-0 cell line, but not in the VHL negative UMRC2 cell line. It was not clear what caused the difference in IRS2 expression between these cell lines, however it is unlikely that this difference is due to HIF α isoform expression, as HIF-2 α induces IRS2 (Wei et al., 2013) and all three-cell lines express this HIF isoform. The *VHL* mutations for these three cell lines all lie in exon I of *VHL*, with the 786-0 frameshift mutation occurring downstream of the UMRC2 point mutation. Both the 786-0 and

UMRC2 mutations lie in the HIF binding domain of VHL, however it is possible that the two mutations do not have equivalent effects on HIF interaction. Furthermore, although the RCC4/2A cell line expresses IRS2, the levels are much lower than the levels observed in RCC4/T; the RCC4/2A mutation is also located in the HIF binding domain of *VHL* exon 1. Alternatively, as other protein moieties also interact with exon 1 of VHL, the difference in IRS2 expression may be due to disruption of one of these.

Analysis of IRS2 transcript levels by qRT-PCR found a greater than 100 fold upregulation in RCC4/T, as compared to WTHAB6. Although the transcript levels appeared to correlate well with the protein levels, additional control of IRS2 at the posttranslational level cannot be ruled out. Chronic signalling through the serine/threonine kinase mTOR was shown to induce phosphorylation of IRS2, which led to its proteosomal-mediated destruction in a negative feedback loop (Briaud et al., 2005). Furthermore, both IRS1 and IRS2 appear to be regulated by the SOCS box proteins SOCS1 and SOCS3 (Rui et al., 2002). The SOCS box proteins are a group of proteins that contain the SOCS box domain, a conserved sequence which allows interaction with the Elongin BC complex (Kamura et al., 1998) of E3 ubiquitin ligases, for which they have been proposed to act as the substrate recognition component (Thomas et al., 2013). Importantly, VHL contains a SOCS box domain (Kamura et al., 1998, Zhang et al., 1999), and therefore VHL could be involved in the posttranslational control of IRS2.

IRS2 is a large protein with multiple phosphotyrosine sites; it interacts with a wide number of proteins via SH2 and PTB recognition modules, and functions

to activate multiple downstream proteins. A recent study investigating the phosphotyrosine interactome of IRS1 and IRS2 indicated a large number of common interactors, including PI3K (which activates the Akt cascade) and the adaptor protein Grb2 (which signals along the Ras-MAP cascade). Other common interactors include the Ras inhibitor RasGAP, the tyrosine phosphatase SHP2, the lipid phosphatase SHIP2, the WD repeat-containing protein 92 (WDR92), and septins 2, 7, 9, and 11 (Hanke and Mann, 2009). Interestingly, Septin-2 has previously been found to be upregulated in a VHL negative cell line (Aggelis et al., 2009). A number of proteins involved in fatty acid catabolism were also found to be interactors of both proteins, including acyl-CoA dehydrogenases (ACADs) with long, and very-long chain specificity, supporting IRS2's role in lipid metabolism (Taniguchi et al., 2005). Interactors unique to IRS2 were also identified, including DOCK6, and DOCK7, the adaptor protein Shc, the phospholipase PLCY, and the E3 ubiquitin ligase complex protein cullin-5 (Hanke and Mann, 2009). Due to these interesting interactions the interactome of IRS2 was investigated in the RCC4/T cell line in this study, to investigate potential new interactors of this protein. SDS-PAGE analysis of the immunoprecipitated lysate revealed a band at approximately 130kDa, which was observed in the IRS2 immunoprecipitation but was absent from the control immunoprecipitation. Furthermore Western blot analysis of the immunoprecipitated lysates revealed a band of the expected 180kDa size in the IRS2 immunoprecipitation and the rabbit IgG supernatant, however three other bands were also observed in the IRS2 immunoprecipitate. These bands were all smaller than the 180kDa band, the largest of which corresponded to the 130kDa size band observed by SDS-PAGE. Although IRS2 is 137kDa in size, on a gel it usually runs at around 180kDa. A similar phenomenon is demonstrated by IRS1, and extensive

phosphorylation has been suggested as a causative factor in this (Sun et al., 1991); due to their similar structure it is possible that this also contributes to the large apparent size of IRS2. It is therefore possible that the smaller, 130kDa size band corresponds to the dephosphorylated form of IRS2, if this is the case it cannot be known if this is loss of the activating phosphotyrosines, or deactivating phosphoserines. The bands lower than 100kDa in size may be fragments of IRS2, however it is not clear why these are absent from the other IRS2 containing lanes. Analysis of the IRS2 immunoprecipitated proteins by mass spectrometry revealed 46 co-immunoprecipitated proteins, only one of which is a previously reported interactor of IRS2; 14-3-3 theta protein (YWHAQ) has previously been shown to interact with residues 300-600 of IRS2 through a strictly conserved region (Neukamm et al., 2012). A large number of RNA binding proteins were identified, most specifically three members of the heterogeneous nuclear ribonucleoproteins (hnRNPs): hnRNPC, hnRNPUL2, and hnRNPCL2/RALY, as well as RNA-binding motif protein (RBMX), and the mitochondrial 39S ribosomal protein L37 (MRPL37). Members of the hnRNP family have been linked to tumorigenesis (Chaudhury et al., 2010), and hnRNPC has been linked to increased metastasis in glioblastoma cells (Park et al., 2012). Other co-immunoprecipitated proteins include matrin-3 (MATR3), cell division cycle 5-like protein (CDC5L), and centrosome-associated protein CEP250 (CEP250/Cnap1). MATR3 is a nuclear matrix protein which stabilises mRNA (Salton et al., 2011), CDC5L is involved in cell cycle control and may be oncogenic in osteosarcoma (Lu et al., 2008), and CEP250 is important in centrosome cohesion (Mayor et al., 2000). Interestingly, lactate dehydrogenase B chain (LDHB) was also co-immunoprecipitated, the LDHs catalyse the interconversion of pyruvate and lactate, and although LDHB can

perform the reversible reaction, kinetically it favours conversion of lactate into pyruvate, and therefore the promotion of oxidative phosphorylation. Though this may seem in contrast to RCCs high glycolytic rate, some oxidative phosphorylation still occurs in these tumours (Simonnet et al., 2002). Furthermore, recent studies have shown LDHB to be a downstream target of mTOR (Zha et al., 2011), which is activated downstream of IRS2. The absence of further previously identified interactors is puzzling. Although the study was performed in the presence of protease inhibitors, it may be necessary to induce IRS2 signalling through insulin stimulation. Nevertheless, the co-immunoprecipitated proteins were biologically interesting, and further studies are warranted to further investigate these interactions.

It was not possible to determine if IRS2 was elevated in clinical samples, due to the high amount of non-specific binding to the tissue samples used. It was also discovered during the analysis of all five VHL mutant cell lines that IRS2 had reduced expression in the RCC forming cell line RCC4/2B compared to the VHL-negative cell line RCC4/T, and also had expression in the non-RCC forming cell lines RCC4/2A and RCC4/2C. There is therefore a risk that the expression of this protein may be linked to VHL mutation, and is not RCC-specific. Regardless, this protein has interesting biology which is aligned with the tumourigenesis of RCC, and it is therefore possible that the IRS2 upregulation observed *in vitro* is clinically relevant, however an alternative technique such as immunohistochemistry or multiple reaction monitoring will need to be used to determine this. Alternatively, as IRS2 has been detected previously in serum (Liu et al., 2007, Li et al., 2008, Omenn et al., 2005, Tanaka et al., 2006), it is possible that this protein could be investigated as a fluid-based biomarker, which would improve the clinical utility of this protein.

Finally, IRS2 may serve as a therapeutic target and studies in this area have already begun investigating inhibitors, whereby IRS2 was targeted for destruction through increasing serine phosphorylation (Reuveni et al., 2013).

4.7.1.2. Additional differentially expressed proteins

The remaining differentially expressed proteins were biologically diverse and included proteins involved in metabolism, chromatin remodelling, signalling, and cellular structure. These have not been validated and their expression levels are therefore not confirmed, however this exploratory analysis indicates that a large number of biologically relevant proteins appear to change in response to VHL inactivation, including proteins that impact on metabolism, metastasis, and proliferation; all key processes in a developing tumour. Further research is warranted to delineate their potential role in RCC pathogenesis.

Multiple metabolic changes occur in RCC tumourigenesis, most notably the decreased reliance on oxidative phosphorylation and increased traffic through glycolysis, a mechanism known as the Warburg effect for which RCC is pathognomonic (Warburg, 1956). Multiple proteins with links to metabolism were found to be differentially regulated in this study. Conventional RCC has a characteristically high amount of cytoplasmic lipids, and three proteins with a link to lipid metabolism were differentially regulated: IRS2 (discussed earlier), acyl-CoA dehydrogenase (ACADS), and prolow-density lipoprotein receptor-related protein 1 (LRP1). ACADS catalyses the first step in the β -oxidation of short chain fatty acids in the mitochondria (Thorpe and Kim, 1995), thus enabling the cell to liberate fat supplies as a source of energy. LRP1, which is

a target of HIF (Semenza, 2003) has roles in lipid homeostasis, membrane trafficking, and intracellular signalling (Spuch et al., 2012). Interestingly, LRP1 is also required for signal transducer and activator of transcription (STAT3) activation (Liu et al., 2011), a transcription factor that has a role in multiple cancers (Yu and Jove, 2004), including RCC (Horiguchi et al., 2002). Proteins with a metabolic link were also found to be downregulated by the VHL negative cell line (upregulated in WTHAB6), with the greatest downregulation shown by CA2, TBC1D4, and PDPR. Carbonic anhydrase 2, like CA9, performs the reversible hydration of carbon dioxide and therefore contributes to the maintenance of intracellular pH. It is expressed by the normal kidney, however it has also been found in renal cancer cells (Parkkila et al., 2000), and its loss from RCC4/T may be due to a switch to CA9 in this cell line. Two other RCC4/T downregulated proteins with metabolic roles were TBC1 domain family member 4 (TBC1D4), which is expressed in the normal kidney and serves to enhance glucose transport through GLUT4 (Stockli et al., 2008), and the regulatory subunit of pyruvate dehydrogenase phosphatase (PDP-1), which inhibits the activity of pyruvate dehydrogenase kinase (PDK-1). PDK-1, which was expressed in the VHL negative cell line but was absent from the wild type cell line (data not shown), is a target of HIF (Kim et al., 2006) and functions to downregulate oxidative phosphorylation. The downregulation of PDP-1 in the VHL negative cell line, therefore promoting the activity of PDK-1, could potentially be a mechanism to promote inhibition of oxidative phosphorylation and the HIF-induced mechanisms of the Warburg effect.

Chromatin biology has recently been recognised as an important process in the development of RCC, with the identification of multiple chromatin modelling genes that accrue mutations during pathogenesis (Gossage et al.,

2014). Two proteins involved in transcriptional modulation were found to be highly altered in this plus/minus VHL comparison, including a VHL-mediated upregulation of the transcriptional co-repressor Nuclear Receptor Corepressor 2 (NCOR2), and a downregulation of splicing factor 3B subunit 4 (SF3B4). Interestingly, the transcriptional co-repressor Nuclear Receptor Corepressor 2 (NCOR2), which has roles in chromatin modelling (Battaglia et al., 2010), functions to downregulate a variety of genes through recruitment of histone deacetylase 3 (HDAC3) (Guenther et al., 2001), of which one target is HIF-1 α (He et al., 2011). RCC4 cells express both HIF-1 α and HIF-2 α , and indeed HIF-1 α levels were demonstrated by Western blot in this study, however HIF-1 α has been shown to be anti-tumourigenic (Raval et al., 2005) and NCOR2 may therefore function in the VHL negative cells to limit the transcriptional activity of HIF-1 α .

Multiple proteins involved in signalling cascades were identified, with ITPR2 and ITPR3 demonstrating the greatest upregulation by VHL inactivation. These proteins are involved in binding to inositol 1,4,5-triphosphate, a key second messenger of intracellular signalling, which modulates the release of intracellular calcium. ITPR3 especially is upregulated in both breast cancer (Mound et al., 2013) and colorectal cancer (Shibao et al., 2010), where it has been linked to increased proliferation and aggressiveness, respectively. Upregulation of adenosine deaminase (ADA) in RCC4/T may serve to promote invasive capability, through its regulation of extracellular adenosine. Adenosine has been shown to increase during hypoxia (Saito et al., 1999), and has also been shown to inhibit tumour cell invasion (Virtanen et al., 2014). Deamination of adenosine may support the developing tumour's invasive capabilities. ADA interacts with the plasma membrane situated dipeptidyl

peptidase 4 (DPP4/CD26) (Eltzschig et al., 2006), which is a target of HIF (Dang et al., 2008), and serves to locate ADA to the plasma membrane to aid adenosine catabolism. Slightly baffling is the apparent downregulation of DPP4 in the VHL negative cell line, though DPP4 is also a positive regulator of T cell activation (Ikushima et al., 2000), and perhaps a downregulation of this protein serves to aid immune escape.

Local invasion and the formation of distant metastases by a cancer are the sum results of multiple steps allowing cell motility, requiring input from the actin cytoskeleton, cell surface receptors, and interactions with the extracellular matrix (ECM). To this end, the deregulation of a number of motility-related proteins could be expected in RCC4/T. Tensin (TNS-1) has a key role in the formation of focal adhesions (Lo et al., 1994), which are important intracellular structures involved in cellular interaction with the ECM, and are therefore important in cancer cell migration (Nagano et al., 2012). An upregulation of TNS-1 was observed in RCC4/T, and though there is no confirmation that TNS-1 is regulated by HIF, genomic screening for HIF responsive elements (HRE) revealed a HIF binding site slightly upstream of TNS-1 (Schodel et al., 2011). RCC4/T downregulated structural-related proteins included neurofilament medium polypeptide (NEFM), fibulin-1 (FBLN1), fibronectin (FN1), and tissue factor pathway inhibitor 2 (TFPI2). Fibronectin is a target of HIF (Semenza, 2003), and its downregulation in the VHL negative cell line is puzzling, but may be down to some so far unexplained mechanism. Interestingly, fibronectin associates with fibulin-1, which was shown to have tumour suppressor qualities by limiting tumour cell migration (Hayashido et al., 1998, Twal et al., 2001). Fibulin demonstrated a strong downregulation in the VHL negative cell line, and may therefore

function to control fibronectin activity in the VHL positive cell line. NEFM is a structural protein found predominantly in the neurons, it is reportedly upregulated in some cancers (Hofsli et al., 2008, Perez et al., 1990), and it is also reported as methylated in RCC where its methylation is associated with good prognosis (Ricketts et al., 2013). Finally, TFPI2, which was downregulated in the VHL negative cell line, has been implicated in matrix remodelling and the inhibition of metastasis (Chand et al., 2004, Sierko et al., 2007).

Other differentially expressed proteins include the Alpha N-terminal protein methyltransferase 1A (METTL11A), which is important in spindle formation (Tooley et al., 2010), and the E3 ubiquitin ligases ZC3HC1 and listerin (LTN1). All of these were upregulated in RCC4/T, indicating they may be controlled by VHL. ZC3HC1 forms an integral part of the SCF E3 ubiquitin ligase complex SCFNIPA, which has been implicated in the timing of mitotic entry by degrading cyclin B1 during interphase (Bassermann et al., 2005) and in protecting against apoptosis (Ouyang et al., 2003), whereas LTN1 is involved in protein quality control (Bengtson and Joazeiro, 2010). Protein Niban (FAM129A/NIBAN) was highly downregulated by the absence of VHL. This protein was first discovered when it was found to be upregulated in the TSC2 Eker rat model of renal cell carcinoma (Adachi et al., 2004, Majima et al., 2000). The RCCs that form in this model occur independently of the VHL mutation status, and the expression of this stress-related protein in WTHAB6 does not therefore contradict earlier studies. Finally, upregulation was also demonstrated by the proteins PM20D and SPATS2, the former is a protease (Veiga-da-Cunha et al., 2014) and the latter is involved in spermatogenesis (Senoo et al., 2002). Relatively little is also known about the Echinoderm

microtubule-associated protein-like 2 (EML2), which was downregulated in the VHL negative cell line, other than its potential link to microtubule assembly (Eichenmuller et al., 2002). Importantly, VHL also has a role in preventing microtubule disassembly. Though very little is known on the function of these proteins, they may have roles in cancer biology which are yet to be determined.

4.7.2. Proteomic comparison of the VHL disease-cell lines

A comparison of four cell lines carrying VHL disease mutations, plus a wild type control, was carried out as an exploratory investigation into the effect of different VHL disease mutations on the cellular proteome. Specifically, the study aimed to identify proteins that were dysregulated by the Type 1 (RCC4/T) and Type 2B (RCC4/2B) VHL disease cell lines, as these two carry VHL mutations relevant to the development of RCC. Due to time limitations, no validation was carried out of these proteins, the expression level of these proteins therefore cannot be confirmed, and their function in this setting can only be hypothesised upon. In total, 4680 proteins were confidently identified, of which 62.5% were common to all five cell lines. A previous gene expression microarray investigating differentially expressed genes in these five cell lines revealed 19 differentially expressed transcripts (Abdulrahman et al., 2007), however none of these were found to be differentially expressed in this study. This should not call into question the reliability of the study, as a number of investigations have demonstrated that transcript levels do not necessarily reflect protein levels, due to posttranscriptional and posttranslational control (Vogel and Marcotte, 2012). The RCC marker CA9 was found only in the type 1 (RCC4/T) cell line, however low levels of CA9 were detected in the remaining VHL mutant cell lines by Western blot, which is a more sensitive

technique, in support of a hypoxic response occurring in all of these cell lines. Interestingly, HMOX1 was found to be upregulated in both of the RCC forming cell lines, indicating this previously identified protein (Banerjee et al., 2012) might be unique to RCC, as opposed to a pan-VHL effect.

To identify proteins that were differentially expressed in the RCC forming cell lines two methods of data analysis were used: heat maps and data filtering. The heat maps revealed a high degree of variability in the data, possibly because many of the significantly different proteins were at the limit of detection. The variability in mass spectrometry analyses and the risk of undersampling a protein means heat maps of peptide data must be used with caution, as proteins that are close to the limit of detection have a greater chance of fluctuating between on and off, and this may lead to misinterpretation of the data. The heat maps generated using LFQ data appeared to be less variable, most likely due to the in-built normalisation of this value, and this quantification method was therefore used for all further heat map analyses. Out of the five proteins that clustered and were significantly upregulated in both the RCC forming cell lines, CDK2 was selected as a candidate for potential downstream investigation (discussed later). A limitation of this technique was the use of significance values on which to filter the proteins; this does not give a measure of the level of quantification and as such, many of the significant proteins were identified with very few peptides. Furthermore, as the study was moderately underpowered (n=3 for each cell line) many proteins did not reach significance; heat maps would therefore be much more useful in a highly powered study. Nevertheless, the heat maps did provide a useful tool for visualising all the data and looking for trends, therefore in an underpowered study, instead of focussing on

significant proteins it may be useful to look at fold changes, combined with an increased minimum threshold of peptides required for a confident identification.

Six further candidate proteins were shortlisted by filtering the data using both peptide number and LFQ intensity data, including three upregulated and three downregulated proteins in the RCC forming cell lines. Though these were not analysed any further in this study, they may well be investigated in the future. Absent in melanoma 1 (AIM1), chloride channel CLIC-like protein 1 (CLCC1), and the membrane receptor neuropilin-1 (NRP1) were all downregulated in the RCC-forming cell lines. The cell cycle control proteins cyclin dependent kinase 2 (CDK2) and cyclin dependent kinase 4 (CDK4), and the sialylation enzyme Bifunctional UDP-N-acetylglucosamine 2-epimerase/N-acetylmannosamine kinase (GNE) were all upregulated in the RCC forming cell lines.

AIM1 demonstrated the largest downregulation in the RCC forming cell lines based on peptide data, furthermore it had an on/off response in the RCC forming/non-RCC forming cell lines respectively, based on LFQ intensities. Very little is known about this protein, however it has previously been shown to be downregulated in melanoma where it may function to inhibit tumorigenicity. Its similarity to other cytoskeletal proteins suggests it may achieve this through interaction with actin network (Ray et al., 1997). The two remaining downregulated proteins, NRP-1 and CLCC1, did not demonstrate such a large downregulation. Non-tyrosine kinase receptor neuropilin-1 (NRP-1) is a receptor for the VEGF-A isoform VEGF-165 (Soker et al., 2002) and it is upregulated in multiple cancers (Ellis, 2006). The downregulation of NRP-1

in the RCC-forming cell lines may therefore be a tissue-specific effect. As with AIM1, very little is known about CLCC1, which is a protein of unknown function but according to a Uniprot annotation it may function as a chloride channel. The upregulated proteins all have roles in promoting tumour growth. The cyclin-dependent kinases are a family of protein kinases involved in cell cycle regulation, their overactivity has been reported in multiple cancers, and CDK inhibitors are currently in development as a cancer therapy (Cicenas and Valius, 2011, Shapiro, 2006). Both CDK2 and CDK4 are early cell cycle CDKs; CDK2 is involved in the transition from G1 to S phase through its interaction with cyclin E (Koff et al., 1992), and CDK4 is also responsible for G1 progression and transition into the S phase, it is activated by cyclin D. Interestingly CDK2 appears to be dispensable for cell cycle progression whereas CDK4 is not, possibly reflecting some redundancy in the cyclins (Tetsu and McCormick, 2003). CDK2 and CDK4 function together to control *cdc2/CDK1* (Berthet and Kaldis, 2006), and to phosphorylate the retinoblastoma protein (Rb) (Berthet et al., 2006) – both key cell cycle regulators that allow mitotic progression. The other upregulated protein, GNE, is an important enzyme in sialic acid biosynthesis, a process which is important in tumourigenesis and metastasis (Passaniti and Hart, 1988). Upregulation has been reported in various cancer cell lines (Krause et al., 2005, Kemmner et al., 2012), and its silencing induces apoptosis (Kemmner et al., 2012). Most of these differentially expressed proteins have biologically plausible expression patterns, and it will be interesting to validate their expression in a clinical cohort of samples to determine if they have potential for clinical utility in the management of RCC.

4.7.3. Concluding remarks

This study has uncovered multiple proteins with biologically plausible expression patterns, in the context of tumour development and progression. Although it is not possible from the scope of this study to know if the novel deregulated proteins are downstream of HIF or not, these proteins may provide clues into understanding the early stages of RCC pathogenesis.

A significant limitation in this study is the lack of validation in cell lines for many of the identified proteins, and in clinical samples for IRS2; this is a major step that must be achieved before their clinical utility can be assessed. The *in vitro* nature of this study was both a strength and a limitation. Using cell lines allows the impact of point mutations to be closely scrutinised, however cell lines are not representative of tissues, particularly as they are grown as a monoculture; cells *in situ* exist as a collection of cells with complex interactions, and growing cells in solitude is therefore not reflective of the complex environment found in a tissue. The ability of VHL to act as a TSG has also been shown to differ based on whether the cells are grown as a 2D monoculture, or in a 3D spheroid (Lieubeau-Teillet et al., 1998). Growing cells in 3D co-cultures is more representative of the native tumour environment, but these techniques are highly technical and require specialised equipment. Furthermore, the risk for tissue culture artefacts is significant, and validation in clinical samples is therefore essential before conclusions can be drawn about the translational significance of any findings.

Using mutations specific to VHL disease is another limitation of this study; these mutations will not fully reflect the genetic landscape of sporadic RCC,

because we now know multiple genes are involved in the development of sporadic RCC (Gossage et al., 2014). The mutations pertaining to VHL disease have been heavily investigated, and this resulted in the categorisation of patients into VHL disease subtypes depending on their specific mutation, and therefore predisposition, to RCC, haemangioblastomas, and pheochromocytomas (Crossey et al., 1994, Zbar et al., 1996). Type 1 VHL disease kindreds most frequently display deletions and truncations of the *VHL* gene, whereas those with type 2 VHL disease tend to harbour point mutations (Maher et al., 2011). In contrast, the mutations found in sporadic RCC cover a broad range of mutational types including missense, frameshift, deletions, insertions, truncations, and nonsense mutations, as well as epigenetic modifications such as promoter hypermethylation (Young et al., 2009). Furthermore, sporadic mutations are found across the full coding region of VHL, whereas familial mutations found in different regions tend to predispose to a different type of VHL disease. In sporadic RCC, mutations or epigenetic silencing of *VHL* occur in most clear cell cases, biallelic inactivation of *VHL* occurs mostly through loss of heterozygosity, with the remainder picked up mostly by promoter hypermethylation. In a study of 177 pathologically confirmed conventional RCC cases mutation was observed in 74.6%, methylation in 31.3%, and loss of heterozygosity in 89.2% of cases. An absence of *VHL* involvement was found in only 3.4% of cases (Young et al., 2009). A further study found mutations in 82.4% and methylation in a further 8.3% of cases, in a study of 2085 patient samples (Nickerson et al., 2008). These mutations therefore do not necessarily match the mutations observed in VHL disease, and this must be considered when analysing data from cell lines harbouring VHL disease-specific mutations. Furthermore, it must be considered that whilst using RCC4 as a backdrop is powerful for investigating

VHL, transfection of the wild type gene into WTHAB6 does not make this cell line 'normal', as it still carries other RCC4-specific mutations. Finally, forced overexpression of a protein may impact upon the normal functioning of a cell line. To this end future studies may also consider transfecting the parental cell line with VHL, rather than using an empty vector, to ensure that any impact on the cell lines through protein overexpression is equal across all the cell lines. Despite these limitations, some potentially novel targets of VHL have been uncovered in this study and they may assist in understanding the early stages of RCC progression. Validation in clinical samples may focus on using small tumours that are more relevant to early RCC development.

5. Using FFPE tissue as a source for discovering predictive biomarkers

5.1 Introduction

Multiple studies have used proteomics to investigate biomarkers predictive of response to sunitinib. These have largely been hypothesis driven approaches, based on analysis of preselected targets by immunohistochemistry, or the use of an array-based platform which focuses on biologically reasoned targets. The use of a non-hypothesis driven approach, whereby the tissue is mined for potential biomarkers by analysing the proteome, may allow the identification of protein changes that would not otherwise have been predicted. Furthermore, by using interactive network analysis tools, this type of approach may also shed light on resistance mechanisms, through the integrated analysis of expression data which draws on experimentally determined protein networks to determine if there is over-representation of particular biochemical networks. While frozen tissue is often not readily available, FFPE tissues, which are routinely acquired during clinical management of cancer patients for pathological assessment, provide a large archive of specimens for analysis. Though the fixation process results in chemical cross-linking of the proteins, recent advances in methods to extract these proteins have made possible the proteomic analysis of these samples (Craven et al., 2013a, Nirmalan et al., 2011). Access to larger repositories of samples has made the design of biomarker studies considerably easier than it was a few years ago, and FFPE tissue blocks dating back at least 10 years have been successfully used to identify differentially expressed proteins (Craven et al., 2013a). This study

aimed to use stored FFPE primary tumour samples to identify potential baseline predictors of response, by comparing sunitinib responding and non-responding patients.

5.1.1. Aims

- Compare the proteomes of FFPE primary renal masses from sunitinib responding and non-responding patients.
- Further investigate the patterns of protein expression through analysis of their respective biological networks.
- Validate the expression of candidate biomarkers in the discovery set of patients.

5.2 Patient selection

Seventeen patients – nine responders (R1-R9) and eight non-responders (NR1-NR8) – were selected, based on best response and duration on sunitinib, and FFPE samples were obtained from the pathology archive. The patients were dichotomised based on radiologically determined best response and duration on therapy: patients with a partial response by RECIST 1.1 criteria and at least 500 days on therapy (responders) were compared to patients with disease progression and less than 200 days on therapy (non-responders) (Table 5.0.1). One responder (R3) was later dropped from the mass spectrometry study due to the poor quality of the obtained mass spectrometric data, resulting in eight responders and eight non-responders suitable for comparative analysis. Patients were matched as much as possible for age, gender, grade, and stage. However, differences in the average IMDC (Heng) or MSKCC scores were unavoidable due to differences in the patient

population, which may indicate a difference in prognosis. Where patients were still receiving sunitinib, the period of time on sunitinib was calculated according to the last follow up pre-study initiation.

Table 5.0.1: Characteristics of patients in the FFPE study

Clinical data was available for all the patients. Values are reported as absolute number (n) of patients, and percentage. MSKCC (Motzer et al., 2002) and Heng (Heng et al., 2009) scoring, 0 = favourable, 1-2 = intermediate, 3+ = poor. Unknown = data unavailable.

		Responders	Non-responders
Best response, n (%)	<i>PR</i>	9 (100)	0 (0)
	<i>PD</i>	0 (0)	8 (100)
Gender, n (%)	<i>Male</i>	6 (75)	6 (75)
	<i>Female</i>	3 (25)	2 (25)
Age, y	<i>Median (range)</i>	62 (52 - 82)	62 (48 - 73)
Duration on sunitinib, y	<i>Median (range)</i>	1.91 (1.38 - 3.97)	0.35 (0.20 - 0.54)
	<i>Average (± SE)</i>	2.41 (± 0.31)	0.34 (± 0.11)
Fuhrman grade, n (%)	<i>1</i>	0 (0)	0 (0)
	<i>2</i>	1 (11.1)	0 (0)
	<i>3</i>	4 (44.4)	3 (37.5)
	<i>4</i>	3 (33.3)	5 (62.5)
	<i>Unknown</i>	1 (11.1)	0 (0)
	<i>T1a/T1b</i>	2 (22.2)	1 (12.5)
Pathology stage, n (%)	<i>T2a/T2b</i>	2 (22.2)	0 (0)
	<i>T3a/T3b</i>	4 (44.4)	7 (87.5)
	<i>T4</i>	1 (11.1)	0 (0)
	<i>Favourable</i>	5 (55.5)	1 (12.5)

	<i>Intermediate</i>	3 (33.3)	7 (87.5)
	<i>Poor</i>	1 (11.1)	0 (0)
Heng score, n (%)	<i>Favourable</i>	5 (55.5)	1 (12.5)
	<i>Intermediate</i>	3 (33.3)	3 (37.5)
	<i>Poor</i>	1 (11.1)	4 (50)
Metastases, n (%)	<i>Synchronous</i>	3 (33.3)	5 (62.5)
	<i>Metachronous</i>	6 (66.6)	3 (37.5)
Performance status, n (%)	<i>0</i>	4 (44.4)	1 (12.5)
	<i>1</i>	5 (55.5)	7 (87.5)
Dose reduction, n (%)	<i>Yes</i>	4 (44.4)	6 (75)
	<i>No</i>	5 (55.5)	2 (25)
Previous lines of therapy, n (%)	<i>Yes</i>	2 (22.2)	0 (0)
	<i>No</i>	7 (77.7)	8 (100)

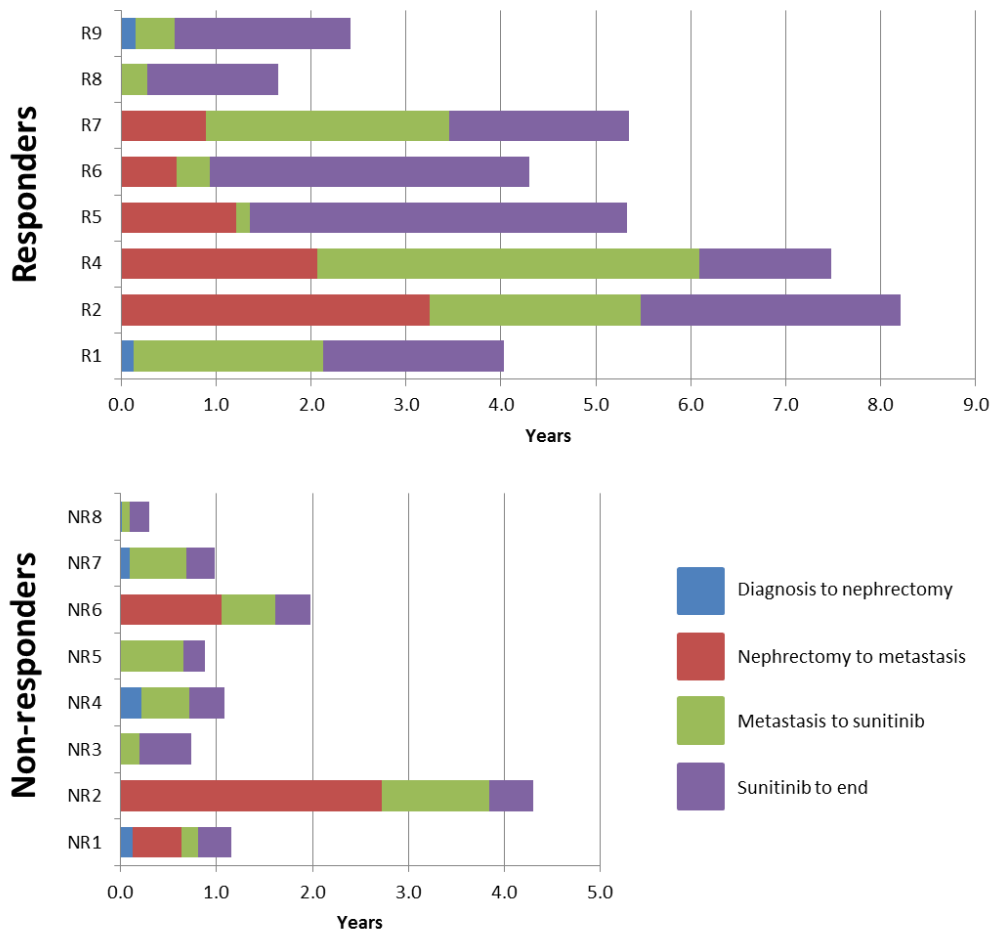
5.2.1. Patient timelines

The individual clinical timelines of the 16 patients, from diagnosis to last follow up, were compared across four time points: diagnosis to nephrectomy, nephrectomy to metastasis, metastasis to sunitinib initiation, and duration on sunitinib (Figure 5.0.1), to enable visualisation of the clinical course of their disease. Three out of eight responders and five out of eight non-responders had synchronous metastases; in cases of metachronous metastases the period to relapse ranged from 0.58-3.25 years for responders and 0.50-2.73 years for non-responders. A difference in the duration from metastasis to the start of sunitinib therapy was observed between the two groups, this ranged 0.15-4.02 years (median=1.20) for responders, and 0.08-1.11 years (median=0.53) for non-responders. Of note, only 3/8 responders, compared to 7/8 non-responders, were diagnosed post 2008 – the year when sunitinib was

introduced to the UK. The shorter period from metastasis to sunitinib treatment initiation for many of the non-responders may therefore reflect the availability of sunitinib, rather than a more rapidly advancing disease.

Figure 5.0.1: Timelines for the responding and non-responding patients.

Duration is plotted in years. Time lines are shown for responders (top panel) and non-responders (bottom panel). Data shows duration from diagnosis to nephrectomy (blue), nephrectomy to metastasis (red), metastasis to sunitinib (green), and duration on sunitinib (purple). NB, age of blocks, 5-11 years for responders, 1-7 years for non-responders.

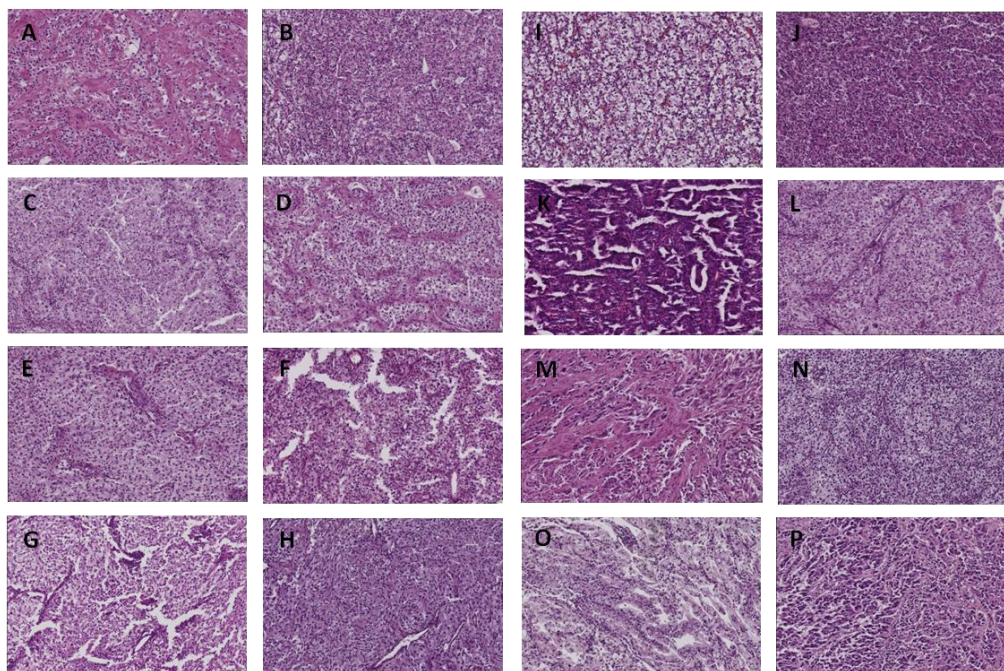


5.2.2. Pathological review of FFPE tissue blocks

To ensure the most suitable FFPE block for each patient was used for downstream analysis, pathological review was carried out on multiple blocks (range 4-16 per patient, based on availability). Blocks were sectioned (3µm), haematoxylin/eosin (H&E) stained, and reviewed by a consultant pathologist (Dr. Patricia Harnden). One representative block per patient was chosen based on tumour quality and grade, and to minimise the presence of inflammation, necrosis, and haemorrhage. In most cases it was necessary for the pathologist to mark off areas for further macrodissection, to improve the quality of the tissue used for analysis. A representative area of each chosen block is shown in Figure 5.0.2. All tumours were confirmed to be of clear cell origin; blocks H, K, M, O, and P were indicated to have sarcomatoid changes. The re-grading performed during pathological review indicated that the sections were mostly matched, with one responder and one-non-responder at grade 2 and 3 respectively, and all remaining blocks at grade 4.

Figure 5.0.2: FFPE H&E stained sections for pathological review

Representative areas from all eight responders (A-H) and all eight non-responders (I-P) used in the mass spectrometry discovery study are shown.



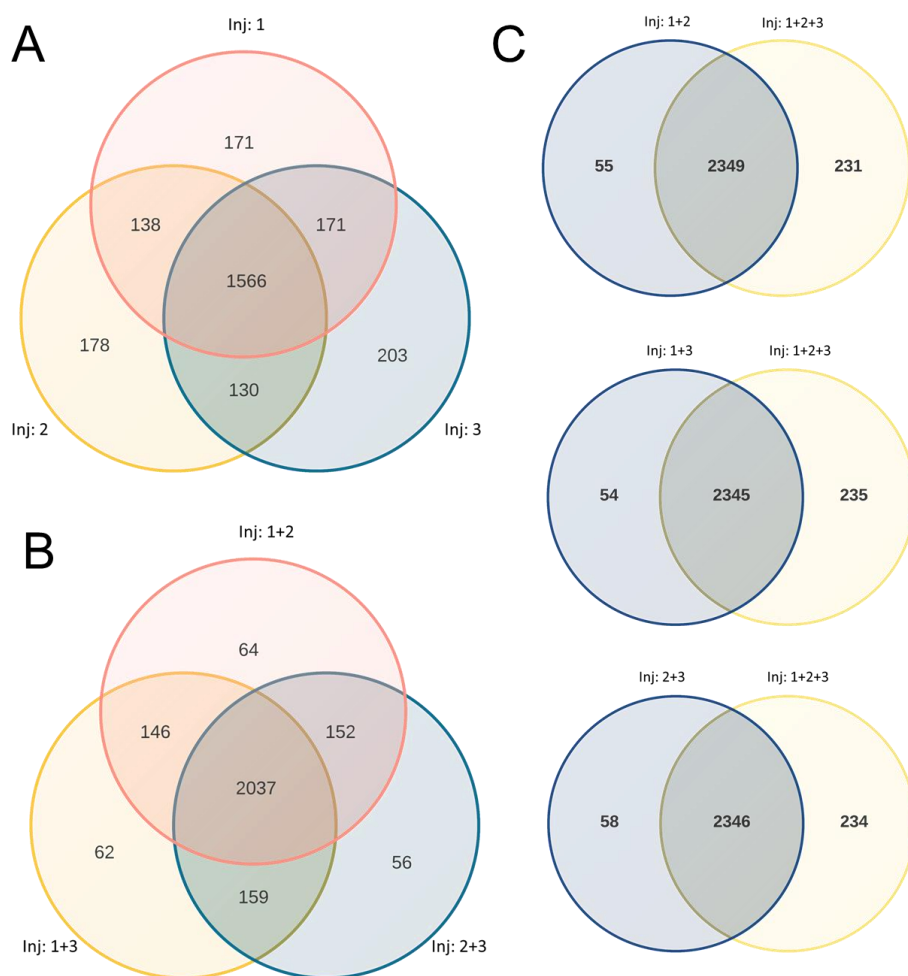
5.3. Optimisation of sample injection number

In-house studies in our laboratory routinely employed three injections of each sample onto the mass spectrometer, although it was not known what improvement in the number of protein identifications was brought about by using three injections over two injections. Performing three injections is a time-consuming process, with each sample requiring 12 hours of acquisition time, and a pilot study was therefore conducted to allow optimisation of injection number for downstream studies. Three injections of one FFPE sample were analysed by mass spectrometry, the raw files then were analysed by MaxQuant in all possible combinations. MaxQuant allows raw files to be analysed independently and, therefore, in comparison against one another,

and this can be done in independent analyses, or together in a combined analysis. Furthermore, MaxQuant allows samples to be grouped together into one sample, whereby the data from all the submitted raw files is used together to yield a single set of quantified protein identities. Exploiting this ability, all seven potential combinations of one, two, or three injections were analysed independently in seven MaxQuant analyses, with each analysis yielding a single set of protein identities, to investigate the hypothesised increase in identifications from one to three injections. In addition, these seven combinations were analysed concurrently in one combined MaxQuant analysis, thus yielding seven sets of protein quantities but only one set of protein IDs. Calculation of LFQ intensities was not possible for this mini-study, as most of the analyses generated a single set of quantitative values; LFQ requires a minimum of two.

Figure 5.0.3: Overlap in identifications between multiple LFQ injections

Overlap in identifications across individual injections (A), between two injections (B) and between two and three injections (C). The majority of proteins were common to all injections, with only a minor increase in unique proteins when all three injections were used.



All three injections had a similar number of unique and shared proteins (Figure 5.0.3), indicating that no single injection had a significantly larger number of identifications than any other. A large increase in identifications was observed

when the number of repeat injections was increased from one to two (Table 5.0.2), with an average percent increase of 17.62 ± 0.59 in the peptide data. As expected, the percent increase from two to three injections was smaller, with an average percent increase of 7.39 ± 0.07 in the peptide data. The results for intensity were almost identical. On this basis, two injections were selected for the forthcoming study due to a combination of the large increase in identification and a balancing of machine time. Correlation of the quantitative values (peptides, intensity) measured for two injections versus three injections (Figure 5.0.4) indicated that no further quantitative information was gained in the peptide dataset. This was demonstrated by the values falling on the line of equality, i.e. the measured values were the same for two injections and for three injections. Interestingly the quantitative values were not the same for the intensity values, with the two injection values falling on the $y=2/3x$ line, indicating they were generally 30% lower than the three injection dataset.

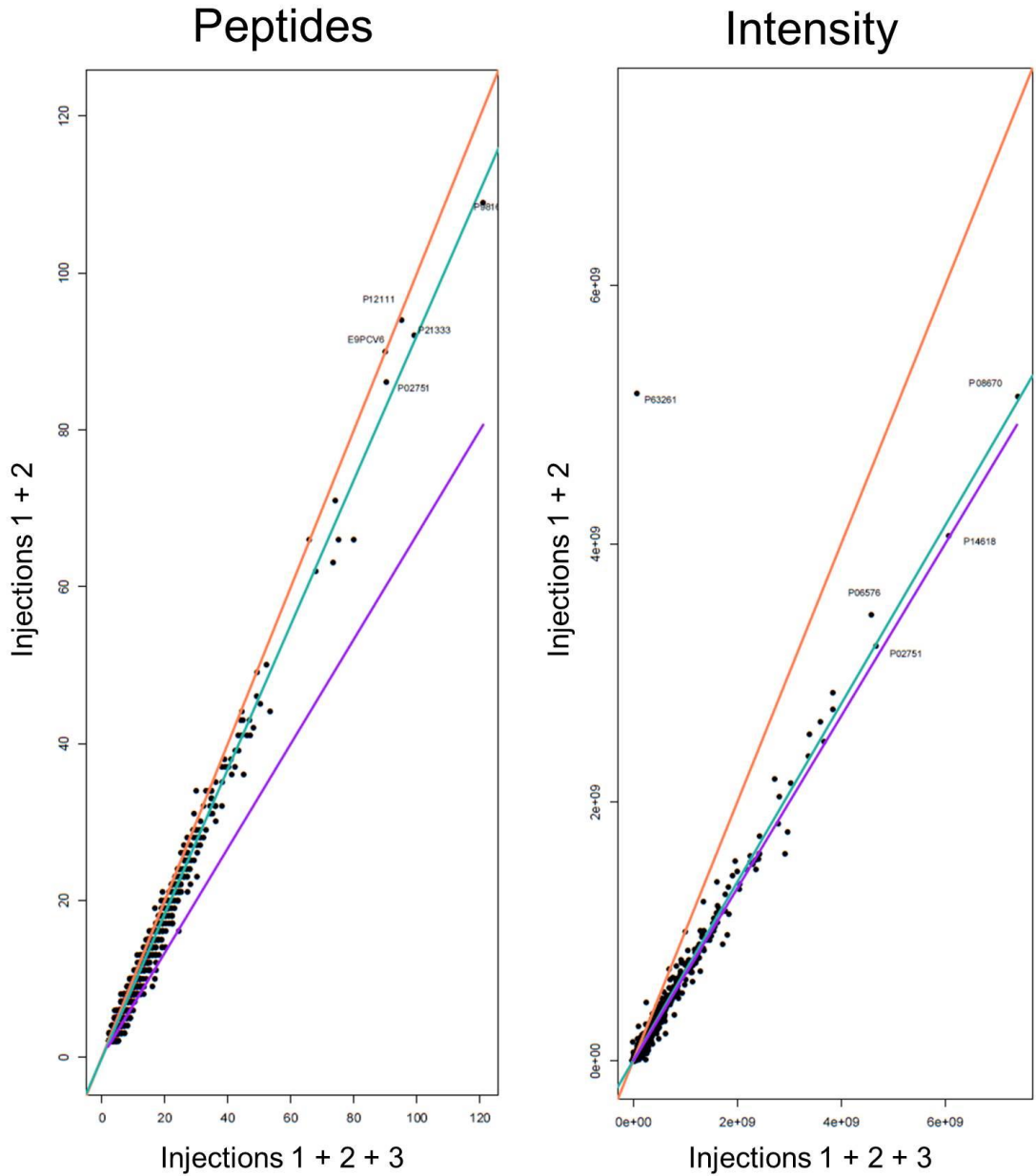
Table 5.0.2: Increase in number of identifications per injection number

Percent increase in number of identifications between single, double, and triple injection combined MaxQuant analyses. Results are average percentage change \pm standard error.

Quantitation value	Single to double	Double to triple	Single to triple
Peptides	17.62 ± 0.60	7.40 ± 0.07	26.32 ± 1.04
Intensity	17.69 ± 0.61	7.51 ± 0.09	26.52 ± 1.08

Figure 5.0.4: Correlation of quantitation values for 2 and 3 injections

Correlation of peptide and intensity values for two versus three injections, one representative analysis is shown. Data shows line of equality (coral), line of best fit (green), and $y=2/3x$ (purple).



There was also a large increase in the number of identifications in the joint MaxQuant analysis compared to the individual MaxQuant analyses (Table 5.0.3), with an 18-21% average increase when comparing the single injection data, and a 7-8% average increase in the double injection dataset. MaxQuant has in-built features ('second peptides' and 'match between runs') which improve the number of identifications based on peptide mass fingerprinting data and peptide retention time; the larger the dataset the more data there is to allow matching between datasets, there is therefore an increased ability for MaxQuant to identify 'unknowns' from each individual dataset. Interestingly there was no increase in quantitative values in the joint MaxQuant data; correlations of the intensity and peptide values for proteins found in both the individual and joint MaxQuant analyses demonstrated high Spearman's rank correlation coefficients (range 0.97-0.99), and for all correlations the points were on the line of equality, indicating the values were equal to one another (data not shown).

Table 5.0.3: Increase in identifications between independent and combined MaxQuant analysis

Percent increase in identifications in the joint MQ analysis as compared to the individual MQ analyses, for a single injection, double injection, and triple injection. Results are average percent increases \pm standard error.

Quantitation value	Single injection	Double injection	Triple injection
Peptides	21.52 \pm 0.88	7.92 \pm 0.19	1.09
Intensity	18.37 \pm 0.77	6.96 \pm 0.14	0.93

5.4. Mass spectrometric analysis of FFPE samples

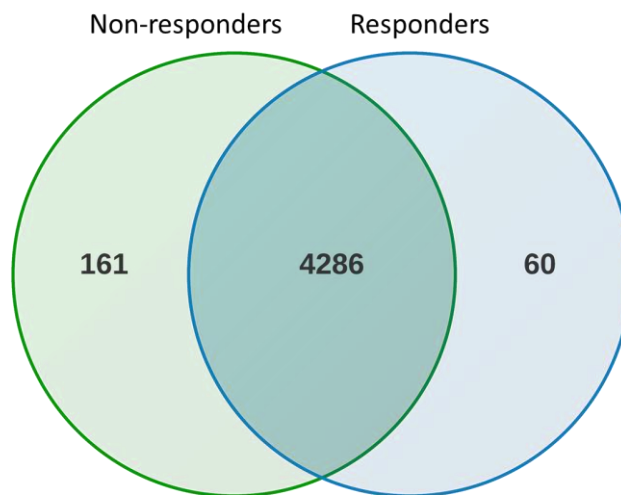
Sections (10µm) were cut from the nine responders and eight non-responders; a minimum of 5cm² total analysable surface area was cut, to ensure enough protein could be extracted for mass spectrometric analysis. Sections were dewaxed, proteins were extracted, and concentrations were measured using the spectrofluorometer and checked by 1D-PAGE, as described in materials and methods. Correlating the protein recovery against the original starting surface area revealed an average recovery of 75µg/cm², indicating that for future studies 3cm² would most likely be sufficient.

FFPE tissue samples (100µg) were digested using the in house FASP method, and analysed by mass spectrometry; two four-hour injections were performed. Peak lists were analysed using MaxQuant and searched against the human UniProt database. Except for R3, all samples had over 3000 identifications, ranging 3187-3544 in the responders, and 3010-3527 in the non-responders. Sample R3 had only 1846 identifications, of which the top hits were haemoglobin, human serum albumin, and complement components – abundant blood proteins – indicating a significant blood component to the sample. This was confirmed by the presence of multiple large vessels in the H&E stained slide (data not shown), and this sample was excluded from the subsequent discovery analysis. In total, 4507 proteins were identified across the remaining sixteen patient samples, of which 21.3% were identified with ≤3 peptides, and were therefore at the limit of detection. Pairwise comparisons between the data revealed that 4286 (95.1%) of proteins were common to both groups of patients, based on peptide data (Figure 5.0.5). The complete

set of raw and analysed data can be found in supplementary data files S12, S13, and S14.

Figure 5.0.5: Proteins unique and shared by responders and non-responders in FFPE tissue

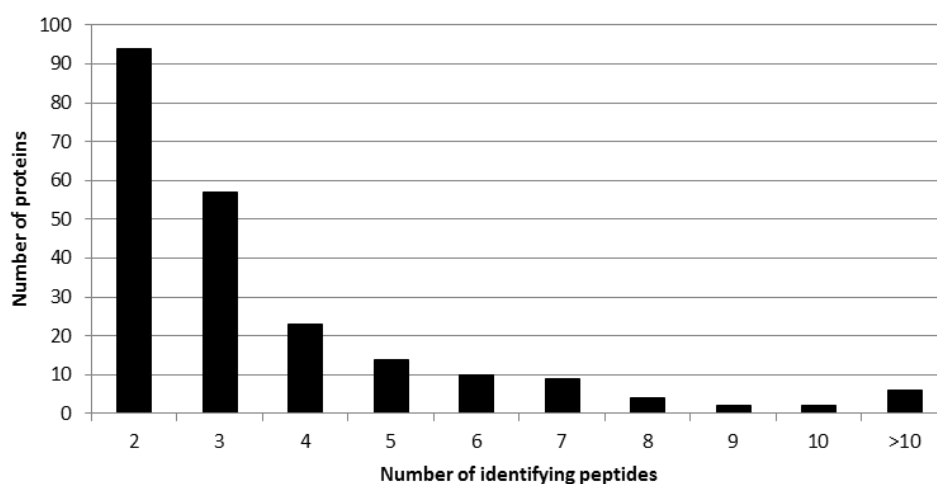
Overlap between responders (blue) and non-responders (green), indicating 95.1% of proteins were common to both groups, based on peptide results.



There were 242 and 43 significantly different proteins between the responders and non-responders, at the $P < 0.05$ and $P < 0.01$ levels respectively. Of the 221 proteins that were unique to either the responders or the non-responders, 27 were found to be significantly different ($p \leq 0.05$), and 154 (69.7%) were identified with ≤ 3 peptides (Figure 5.0.6), indicating that many of these unique identifications were at the limit of detection. Many of these present/absent proteins were not uniformly expressed across patients within a group,

explaining why they did not reach significance. When LFQ data was considered, 1476 proteins were found to be unique to either patient group, however only 30 of these were found to be significantly different ($p \leq 0.05$). Of the unique LFQ identifications, 744 (50.4%) were identified with ≤ 3 peptides. In total, 183 and 36 proteins demonstrated a significant difference between the responders and the non-responders, at the $P < 0.05$ and $P < 0.01$ levels respectively.

Figure 5.0.6: Unique protein identifications in responders and non-responders based on peptide number



Panther analysis of the entire dataset revealed the presence of a broad range of protein families, as expected for a whole tissue extract. Furthermore, the proteins were predicted to come from multiple locations including membranes, cell junction, organelles, and the extracellular matrix. Over half the proteins were annotated with either cell junction (GO:0030054) or cell part (GO:0044464).

5.4.1. Proteins elevated in FFPE tissue from non-responders

By focussing on fold changes, 78 and 100 proteins demonstrated a ≥ 5 fold change in the non-responders compared to responders, based on peptide and LFQ data, respectively. Of these, 21 and 17 proteins demonstrated a significant difference between the two groups, respectively (Table 5.0.4). Proteins were shortlisted based on fold change (≥ 2.5 fold), significance ($p < 0.05$), and concordance between the LFQ and peptide datasets, with 18 proteins matching this criteria (Table 5.0.5).

Table 5.0.4: Number of protein fold changes in the non-responders

The number of proteins demonstrating a ≥ 2.5 , ≥ 5 , or ≥ 10 fold change in non-responders, overall, and those which were found to be significant at $P \leq 0.05$.

		On/off	≥ 10 fold	≥ 5 fold	≥ 2.5 fold
Peptides	Total	-	16	78	245
	Significant	23	10	21	35
LFQ	Total	-	39	100	282
	Significant	15	10	17	30

Significantly different proteins demonstrating the highest fold changes in non-responders versus responders were UBTF, hCAP18, MMP9, PRTN3, and NGAL. A few erythrocyte-based proteins were also found to be highly upregulated in non-responders, including ANK1, SPTA, SPTB, and EPB42 (Table 5.0.5), however the non-responders were not observed to be more vascular than the responders when CD31 stained sections were inspected (data not shown). Figure 5.0.7 shows bar graphs of the LFQ data for the five

most highly upregulated proteins. When these shortlisted proteins were searched against an in-house prognostic (as opposed to predictive) dataset, containing tissue proteomic data on patients with an intermediate Leibovich score, none of these proteins were found to be significantly different. Two of the erythrocyte proteins (SPTA1 and EPB42) were however highly upregulated in the patients with a poorer prognosis and tended towards significance ($P < 0.07$), which may indicate that these proteins are not specifically upregulated in a predictive fashion. Of note, the band 4.1 superfamily member moesin was identified as upregulated in the baseline serum analysis of the non-responding patients.

Figure 5.0.7: Elevated FFPE tissue proteins in the non-responders

The five highest upregulated proteins found in non-responders as compared to responders. Values for mean LFQ intensity are shown. Bars represent SEM.

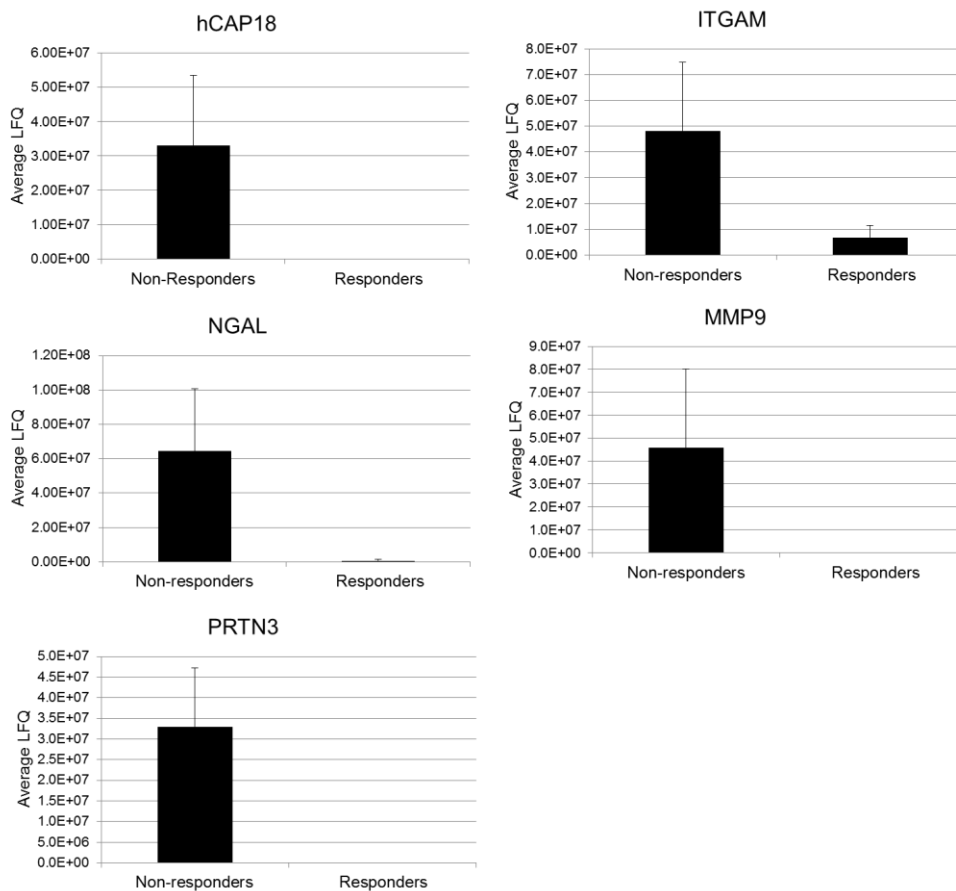


Table 5.0.5: Proteins upregulated in the non-responders

Differentially expressed proteins in non-responders versus responders, based on peptide and LFQ data. Proteins were shortlisted based on fold change (≥ 2.5 fold), significance ($p < 0.05$), and biological interest.

Gene	Name	Uniprot ID	Peptide fold	Peptide P val	LFQ Fold	LFQ P val
AZU1	Azurocidin	P20160	5.75	0.018	-	0.013
hCAP18	Cathelicidin antimicrobial peptide	J3KNB4	-	0.005	-	0.013
CTSG	Cathepsin G	P08311	3.04	0.003	11.55	0.005
DLG1	Disks large homolog 1	Q12959-2	7.00	0.018	-	0.013
ITGAM	Integrin alpha-M	P11215-2	5.00	0.002	7.11	0.010
LCN2	Neutrophil gelatinase-associated lipocalin	H9KV70	8.33	0.007	93.98	0.009
LTF	Lactotransferrin	P02788	3.16	0.020	10.83	0.024
MMP9	Matrix metalloproteinase-9	P14780	20.00	0.009	-	0.032
MPO	Myeloperoxidase	P05164-3	2.80	0.005	9.19	0.003
PRTN3	Proteinase 3	P24158	15.00	0.003	-	0.013
SEPHS2	Selenide, water dikinase 2	J3KR58	2.60	0.047	-	0.032

UBFD1	Ubiquitin domain-containing protein UBFD1	O14562	4.00	0.017	-	0.032
UBR4	E3 ubiquitin-protein ligase UBR4	Q5T4S7-2	3.47	0.028	6.38	0.018
UBTF	Nucleolar transcription factor 1	P17480	-	0.004	-	0.032
ANK1	Ankyrin-1	P16157-14	13.00	0.001	30.18	0.001
EPB42	Erythrocyte membrane protein band 4.2	P16452-2	4.63	0.002	21.23	0.001
SPTA1	Spectrin alpha chain, erythrocyte	P02549	57.00	0.004	-	0.005
SPTB	Spectrin beta chain, erythrocyte	P11277-2	6.23	0.010	-	0.013

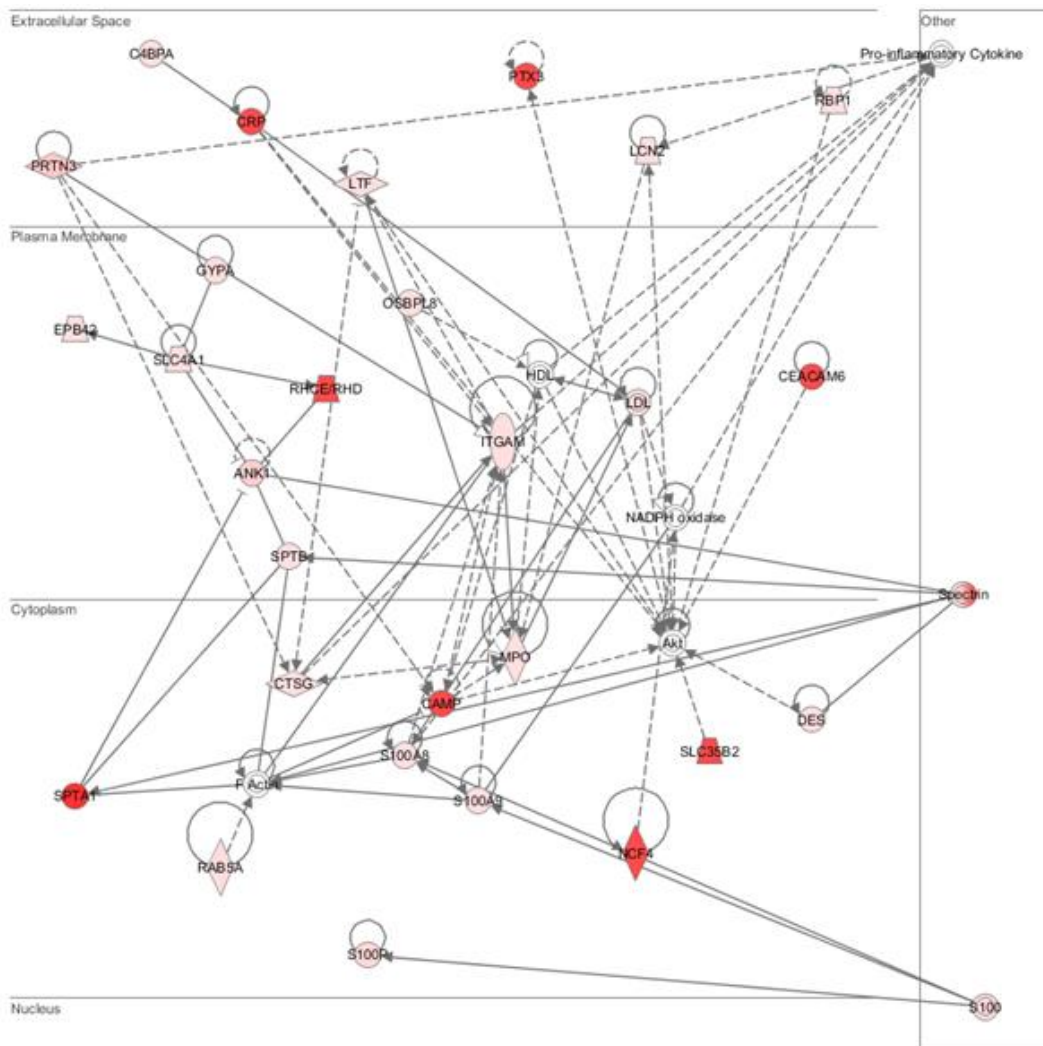
Analysis by Ingenuity Pathways Analysis (IPA) of the non-responder elevated proteins showed the most highly upregulated network was 'Cell-to-cell signalling and interaction; Tissue development; Cellular function and maintenance' (Table 5.0.6), with 27 of the input proteins having associations with this network including hCAP18, PRTN3, and ITGAM (Figure 5.0.8). Many of the proteins in this network act on the RAC-alpha serine/threonine-protein kinase (Akt1), which was also found to be moderately elevated in the non-responder dataset, however this was not significant (data not shown). Interestingly, there were also 20 input proteins with associations to drug metabolism, and this included the multidrug resistance associated protein 1 (ABCC1). Finally, 15 proteins had associations with carbohydrate and lipid metabolism, which is interesting as RCC is a lipid rich tumour. The most highly significant over-represented molecular functions included 'Cell death and survival', 'Cell movement', and 'Cell morphology' (Table 5.0.6). Through observation of the data it was noted that a large number of immunological proteins were upregulated in the non-responder dataset, and analysis by IPA revealed 24 proteins were significantly associated with immunological disease ($P=7.60 \times 10^{-11}$). These included AZU1, hCAP18, LCN2, ITGAM, PRTN3, CTSG, and SPTA1, all of which were the most highly upregulated proteins in the non-responders dataset.

Table 5.0.6: Upregulated pathways in non-responder elevated proteins

Top diseases and functions	Number of proteins	Score
Cell-to-cell signalling and interaction; Tissue development; Cellular function and maintenance	27	62
Protein synthesis; Cardiovascular system development and function; Organ development	20	41
Drug metabolism; Molecular transport; Organismal injury and abnormalities	20	39
Cellular development; Carbohydrate metabolism; Lipid metabolism	15	28
DNA replication, recombination, and repair; Nucleic acid metabolism; Small molecule biochemistry	5	7
Top molecular and cellular functions	Number of proteins	Probability value
Cell death and survival	32	7.76×10^{-12} - 1.37×10^{-2}
Cell-to-cell signalling and interaction	25	1.64×10^{-10} - 1.37×10^{-2}
Cellular movement	21	3.67×10^{-9} - 1.37×10^{-2}
Cellular function and maintenance	31	4.55×10^{-7} - 1.37×10^{-2}
Cell morphology	16	1.67×10^{-6} - 9.17×10^{-3}

Figure 5.0.8: Cell-to-cell signalling interaction network containing proteins elevated in non-responders

Analysis of proteins upregulated by non-responding patients using IPA, pink-red proteins were identified in this cell-to-cell interaction network, with red proteins showing the highest levels and pink showing the lowest levels of expression. Key: dashed line (indirect relationship), solid line with arrow (acts on), diamond (enzyme), vertical oval (transmembrane receptor), trapezoid (transporter)



5.4.2. Proteins elevated in FFPE tissue from the responders

Compared to the non-responders, 59 and 70 proteins demonstrated a ≥ 5 fold change in the responders, based on peptide and LFQ data respectively, of which 20 and 10 demonstrated a significant difference between the two patient groups (Table 5.0.7). Proteins were initially shortlisted for further investigation based on fold change (≥ 2.5 fold) and significance ($p < 0.05$), with twelve proteins matching the shortlist criteria in both the peptide and LFQ dataset (Table 5.0.8). The most highly upregulated proteins were ADCK3, CDH1, CD70, ABP1 and VCAM1 (Figure 5.0.9). Fewer proteins were found to be upregulated in the responders compared to the non-responders.

Table 5.0.7: Number of protein fold changes in the responders

The number of proteins demonstrating a ≥ 2.5 , ≥ 5 , or ≥ 10 fold change in responders; overall, and those which were found to be significant at $P \leq 0.05$.

		On/off	≥ 10 fold	≥ 5 fold	≥ 2.5 fold
Peptides	Total	-	10	59	227
	Significant	4	5	20	52
LFQ	Total	-	18	70	223
	Significant	15	3	10	22

When the initial responder shortlisted proteins were searched against an in-house prognostic dataset containing tissue proteomic data on patients with an intermediate Leibovich score, two proteins were found to be significantly elevated in the patients with a better prognosis ($P < 0.05$), indicating these are not specifically upregulated in the responders in a predictive fashion, and these were dropped from further shortlisting.

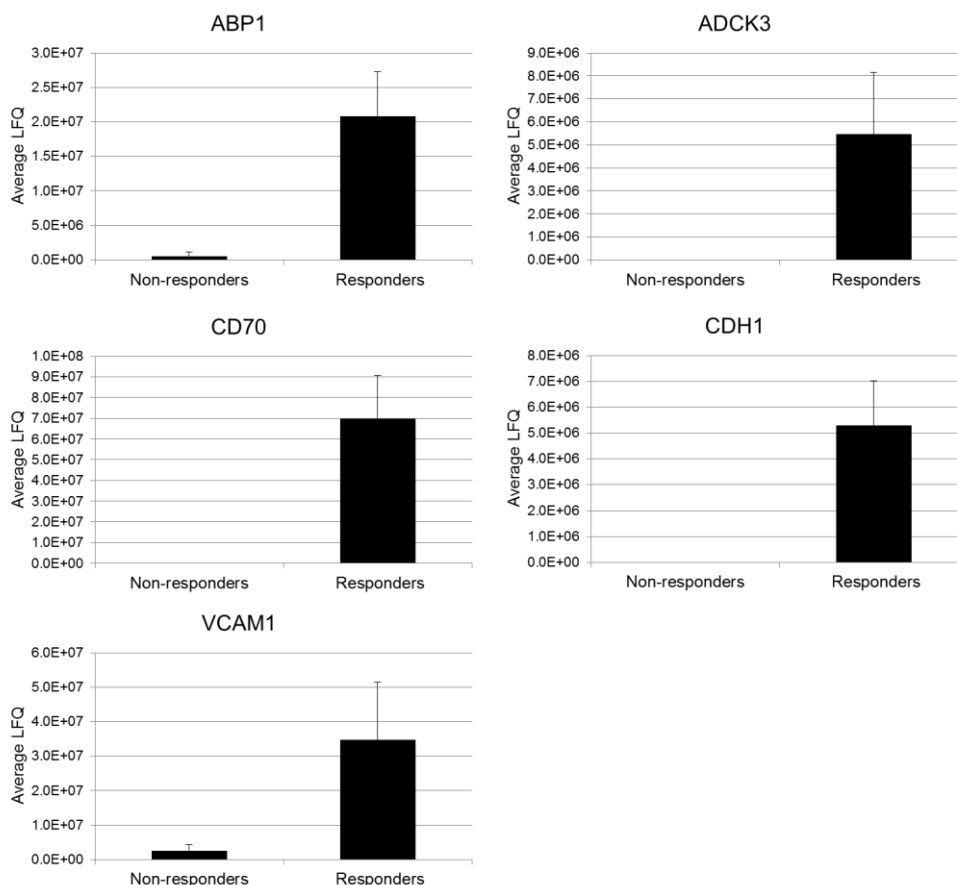
Table 5.0.8: Proteins upregulated in the FFPE tissue of responders

Differentially expressed proteins in responders versus non-responders, based on peptide and LFQ data, see main text for details.

Gene	Name	Uniprot	Peptide fold	Peptide P val	LFQ Fold	LFQ P val
ABP1	Amine oxidase	C9J690	7.250	0.028	37.81	0.009
ACY3	Aspartoacylase-2	Q96HD9	5.167	0.006	4.83	0.032
ADCK3	Chaperone activity of bc1 complex-like, mitochondrial	Q8NI60	-	0.004	-	0.032
ADSSL1	Adenylosuccinate synthetase isozyme 1	Q8N142	3.478	0.001	5.57	0.031
CD70	CD70 antigen	P32970	13.500	0.016	-	0.005
CDH1	Cadherin-1	P12830	14.000	0.030	-	0.013
FGL2	Fibroleukin	Q14314	3.286	0.023	5.66	0.007
LRP1	Pro-low-density lipoprotein receptor-related protein 1	Q07954	2.513	0.002	2.71	0.007
MVD	Diphosphomevalonate decarboxylase	P53602	3.000	0.029	-	0.032
NDUFA4L2	NADH dehydrogenase [ubiquinone] 1 alpha subcomplex subunit 4-like 2	Q9NRX3	3.300	0.012	3.77	0.024
SHPK	Sedoheptulokinase	Q9UJH6	2.786	0.011	3.41	0.040
VCAM1	Vascular cell adhesion protein 1	P19320	4.900	0.032	13.16	0.050

Figure 5.0.9: Proteins elevated in the FFPE tissue of responders

The highest upregulated proteins found in responders as compared to non-responders. Values for LFQ intensity (right panel) are shown. Bars represent SEM.



Analysis of the proteins elevated in the responders by IPA indicated multiple networks were upregulated in this dataset (Table 5.0.9), the most predominant of which was the cell-to-cell interaction and cardiovascular disease network (Figure 5.0.10), with 18 proteins found to participate in this network. The T cell regulator CD70 is involved in this network, with indirect links to both the T cell receptor and the P38 MAPK. Furthermore, analysis of the upregulated molecular and cellular functions revealed cell-to-cell signalling and interaction was heavily upregulated here, with 7 proteins involved in this function. Four of the shortlisted proteins were involved in this network; these were CD70,

CDH1, LRP1, and VCAM1. Other upregulated biological functions included cell cycle and cell morphology. Interestingly, amino acid and nucleotide metabolic canonical pathways appeared to be upregulated in this dataset, including Glycine betaine degradation ($P = 6.85 \times 10^{-4}$), methionine salvage ($P = 1.19 \times 10^{-2}$), uracil degradation II ($P = 1.58 \times 10^{-2}$), thymine degradation ($P = 1.58 \times 10^{-2}$), and lysine degradation V ($P = 1.97 \times 10^{-2}$).

5.4.3. Cross-over of candidate proteins between the FFPE and serum analyses

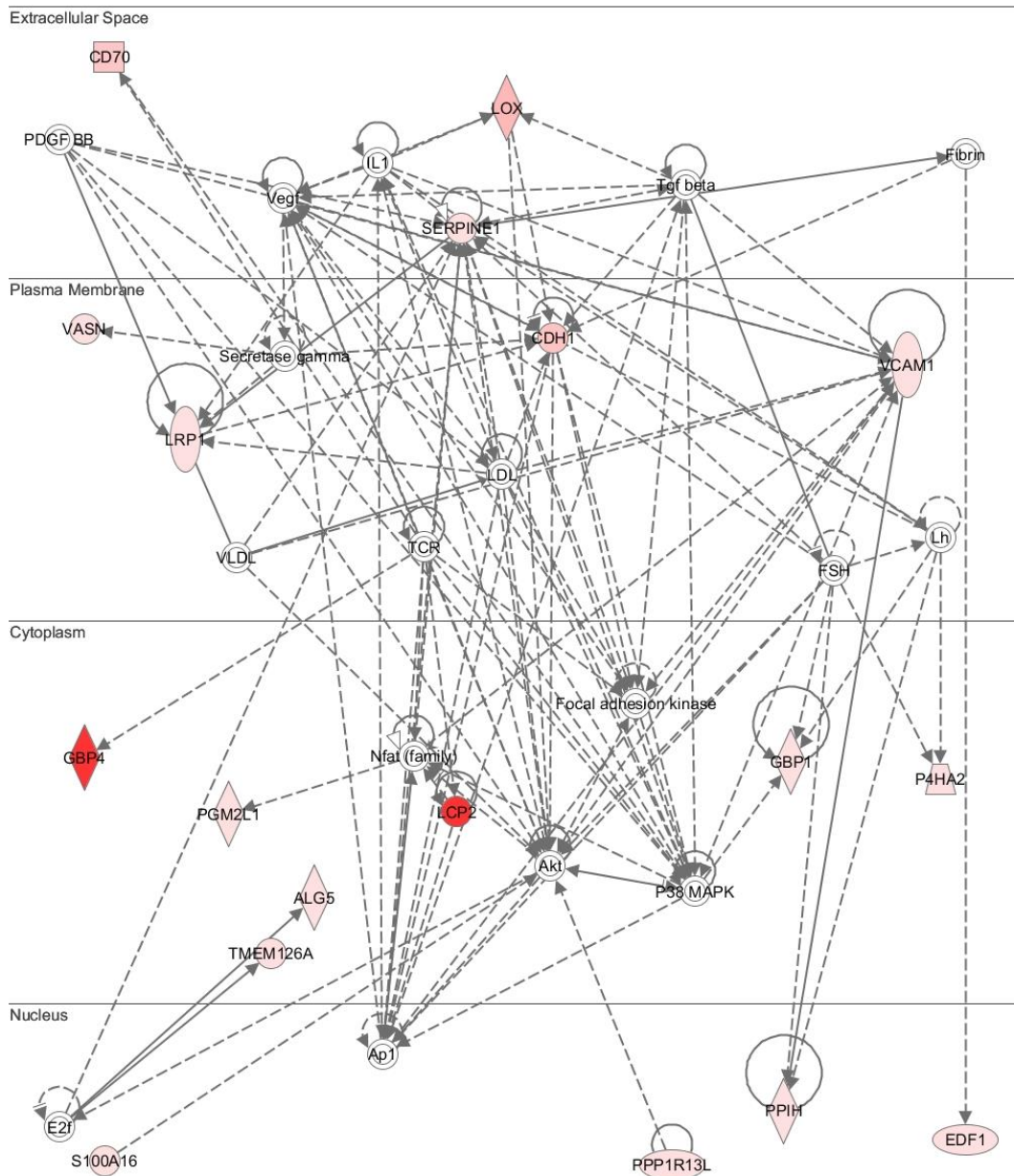
There was some cross-over of proteins between the FFPE tissue and the serum analyses. Expression of LRP1, VCAM1, AZU, CTSG, NGAL, MMP9, LTF, and MPO was found in the serum analysis, however no difference in expression was observed between the responders and the non-responders. The inflammatory protein hCAP18 was found to be upregulated in non-responders in both the serum and FFPE analyses, and the cell adhesion molecule CDH1 was found to be upregulated in the responders in both the serum and FFPE datasets.

Table 5.0.9: Upregulated pathways amongst proteins elevated in responding patients

Top diseases and functions	Number of proteins	Score
Cell-to-cell signalling and interaction; Cardiovascular disease	18	32
Connective tissue disorders	16	30
Hereditary disorder; Metabolic disease; Cellular assembly and organisation	15	29
Cancer; Endocrine system disorders; Neurological disease	14	26
Cell-to-cell signalling and interaction; Inflammatory response; Antigen presentation	13	23
Cellular growth and proliferation; Cell death and survival	7	11
Top molecular and cellular functions	Number of proteins	Probability value
Cell-to-cell signalling and interaction	7	$9.27 \times 10^{-5} - 4.66 \times 10^{-2}$
Amino acid metabolism	2	$3.97 \times 10^{-3} - 7.92 \times 10^{-3}$
Antigen Presentation	1	$3.97 \times 10^{-3} - 3.97 \times 10^{-3}$
Cell cycle	7	$3.97 \times 10^{-3} - 4.28 \times 10^{-2}$
Cell morphology	7	$3.97 \times 10^{-3} - 4.66 \times 10^{-2}$

Figure 5.0.10: Cell-to-cell signalling interaction network containing proteins elevated in responders

Analysis of proteins upregulated by non-responding patients using IPA, pink-red proteins were identified in this cell-to-cell interaction network, with red proteins showing the highest levels and pink showing the lowest levels of expression. Key: dashed line (indirect relationship), solid line with arrow (acts on), diamond (enzyme), square (cytokine), vertical oval (transmembrane receptor), trapezoid (transporter)



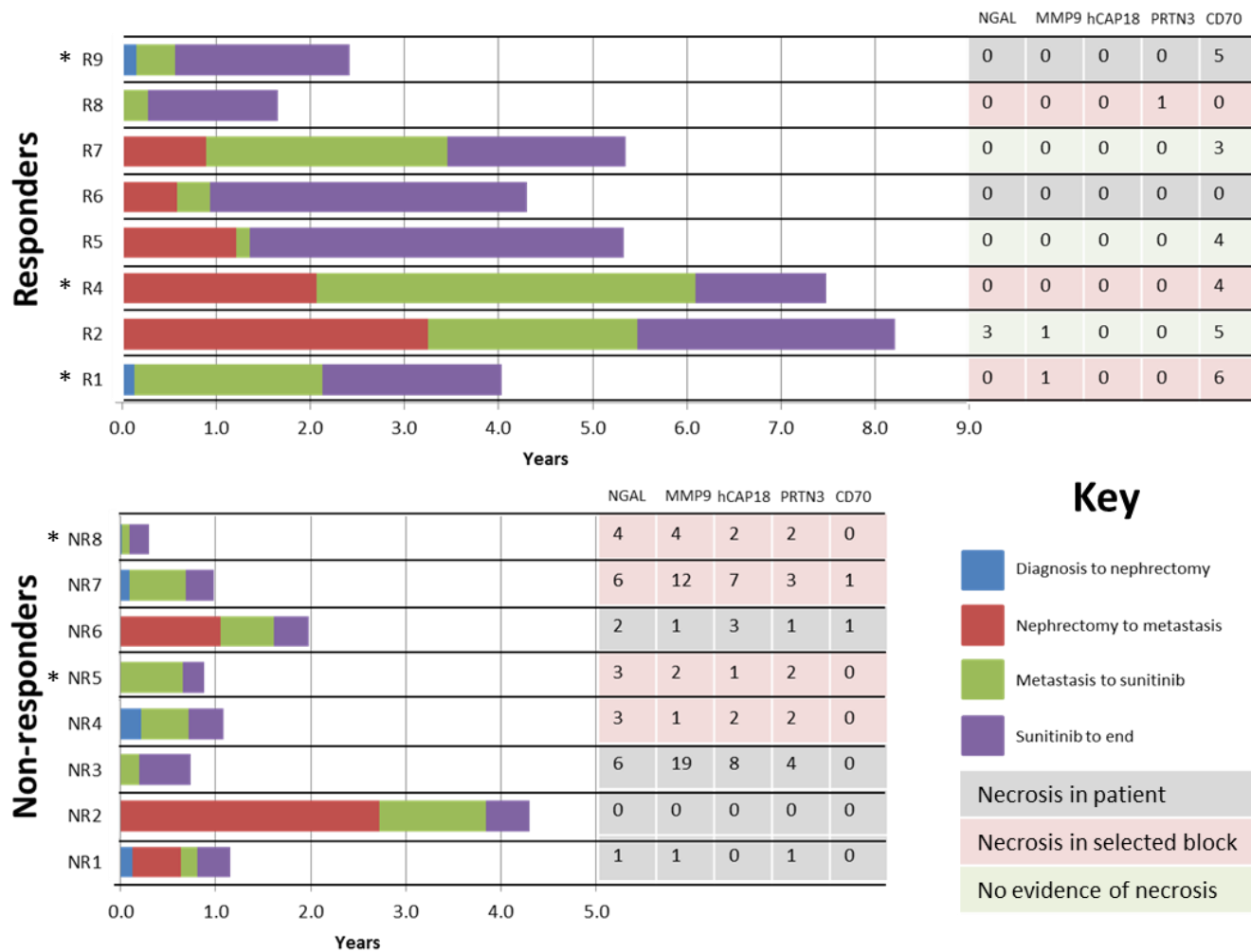
5.5. Validation of protein expression patterns

5.5.1. Candidate biomarkers

Proteins were selected for downstream validation based on level of upregulation, statistical significance, biological function, and availability of reagents. In the non-responders a large number of the shortlisted proteins were noted to be linked to neutrophil biology, either through an involvement in chemotaxis or through being directly expressed by neutrophils, including myeloblastin (PRTN3), cathelicidin (CAMP), azurocidin (AZU1), cathepsin G (CTSG), myeloperoxidase (MPO), neutrophil gelatinase associated lipocalin (NGAL), and matrix metalloproteinase 9 (MMP9). Upregulation of these proteins did not appear to be correlated with inflammation or necrosis in the selected block (Figure 5.0.11). The proteins PRTN3 and hCAP18 were chosen for downstream validation due to their high upregulation in the non-responders. Importantly, hCAP18 was also found to be moderately upregulated in the serum of non-responders, versus responders (Chapter 3).

In the responders no single group of proteins appeared to be upregulated, with upregulated proteins involved in a wide variety of functions, including cell adhesion, angiogenesis, mitochondrial metabolism, and T-cell activation. The T-cell activator CD70 was chosen for downstream investigation. The upregulation of this protein did not appear to be correlated with inflammatory infiltrate or necrosis within the sections (Figure 5.0.11).

Figure 5.0.11: Clinical features of patients and quantitative levels of target proteins



Patient timelines (coloured bars) and the presence of necrosis (colour bands) and/or inflammation (*) were not found to be linked to peptide levels of the proteins NGAL, MMP9, hCAP18, PRTN3, or CD70 in either responders or non-responders. Necrosis in patient - pathology report of necrosis in a different block to the one analysed.

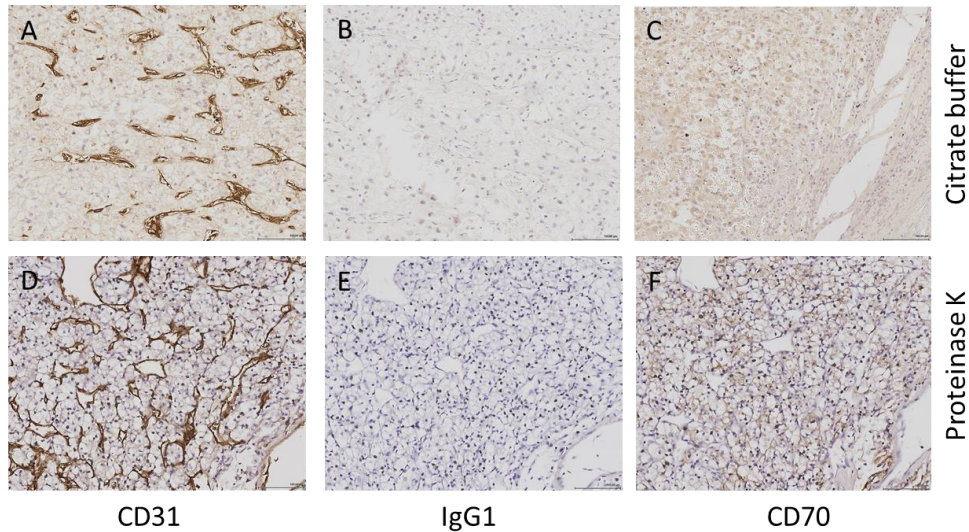
5.5.2. Validation of CD70 expression pattern

The expression of CD70 was investigated using immunohistochemistry. To determine which staining system should be used, a head-to-head comparison of the Dako EnVision kit with the Leica Novolink kit was performed, by staining normal kidney sections for CD31. The Dako method was quicker as it only involves two antibody incubation steps – the primary and the secondary antibodies. The Novolink kit is a three-tier system and is therefore a slower method to perform, however it was found to give a stronger, cleaner signal (data not shown). The Novolink kit was therefore used in all downstream immunohistochemistry studies.

The CD70 antibody was first titrated using IHC with OCT-embedded frozen sections from a responding patient in the discovery set, to optimise the antibody concentration and confirm the staining pattern. Following this, two antigen retrieval methods for FFPE tissue were compared; citrate buffer and proteinase-K (Figure 5.0.12). In the absence of antigen retrieval with FFPE tissue, CD70 staining had a very high background and did not demonstrate any specificity (data not shown), and with citrate acid buffer retrieval, no CD70 staining was observed. Proteinase-K retrieval was found to yield strong, specific staining which was strongest at the plasma membrane, but also had diffuse intracellular staining, and this antigen retrieval method was used for all future CD70 IHC FFPE studies.

Figure 5.0.12: Antigen retrieval for CD70 staining on FFPE

Citrate buffer retrieval (A-C) and proteinase K retrieval (D-F) were compared. Sections were stained for CD31 (A,D), mouse IgG1 as negative control (B,E), and CD70 (C,F). Bar represents 100µm.



To initially validate the mass spectrometry data, immunohistochemistry was performed on the set of blocks used for the discovery study (Figure 5.0.13). Sections (4µm) were cut and probed based on the optimised antigen retrieval and antibody conditions. Stained sections were reviewed by a consultant pathologist, and scored based on staining intensity. A score of 0-3 was given based on the following criteria: 0 - negative staining; 1 - up to 25% cells positive; 2 - 25-50% cells positive; 3 - over 50% cells positive. Two negative controls were concurrently performed on all sections: absent primary and IgG₁, for which no specific staining was observed on any section. Staining with the vessel endothelial marker CD31 revealed strong positivity in all sections (Figure 5.0.13).

Review of the stained sections revealed that 5/9 responders and 1/8 non-responders were positive for CD70 staining (Figure 5.0.13, Table 5.0.10). Amongst the responders, negative staining was seen in R3, R6, R7 and R8. Weak (<25%) or focal staining was found in R1, where approximately 10% of cells were positive. Mid-level (25-50%) staining was demonstrated by R5, where 30-40% of cells were weakly positive. Strong staining was demonstrated by R2, R4, and R9, with strong positivity in 70-80% of cells in all three cases. The R9 sections also contained some rhabdoid cells and these were noticeably less stained than the clear cells. The IHC data correlated relatively well with the mass spectrometry data, two of the four patients that were CD70 negative by IHC were also negative by MS (a further patient (R3) had no MS data as they were removed from the analysis). All of the CD70 positive patients by IHC were also positive by MS with some similarity in levels of expression, except for patient R1 who had high levels by MS but low levels by IHC (Figure 5.0.13). In terms of the non-responders, the MS and IHC data correlated well, five of the seven patients that were negative by IHC were also negative by MS, and the remaining two patients (NR6 and NR7) had very low levels by MS. The only patient to demonstrate any staining was NR3, which had weak positivity in 30% of the cells, which is in contradiction to the MS data, for which this patient had no detectable CD70.

Table 5.0.10: CD70 staining intensity of responders and non-responders

Staining intensity values: 0 - negative staining; 1 - up to 25% cells positive; 2 - 25-50% cells positive; 3 - over 50% cells positive.

Staining intensity	0	1	2	3
Responders	4	1	1	3
Non-responders	7	0	1	0

Figure 5.0.13: IHC validation of CD70 expression

Responders (R1-R9) and non-responders (NR1-NR8) are shown. Representative control sections are also shown (from patient R9), control staining was performed for CD31, IgG, and absent primary (neg). Bar represents 100µm.

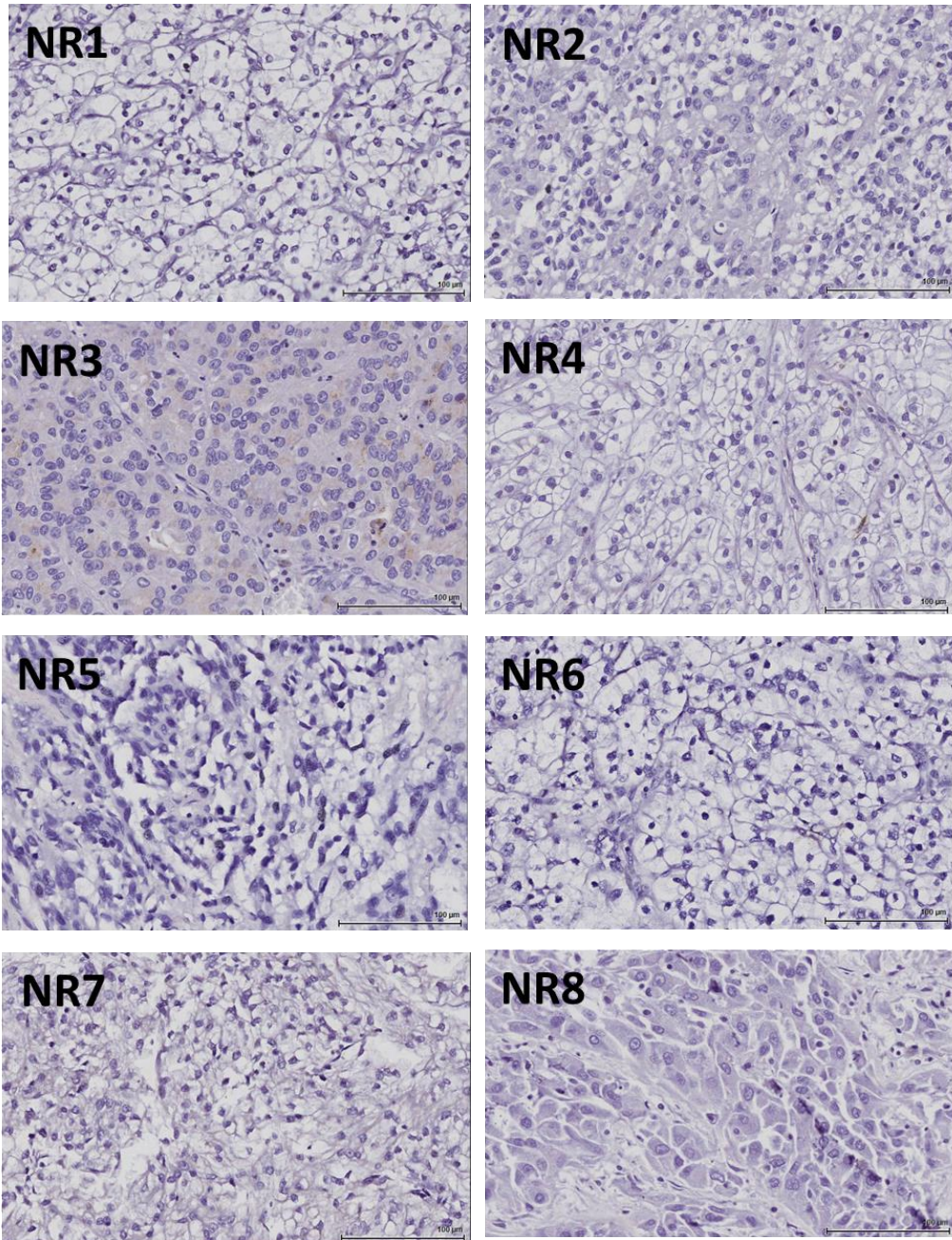
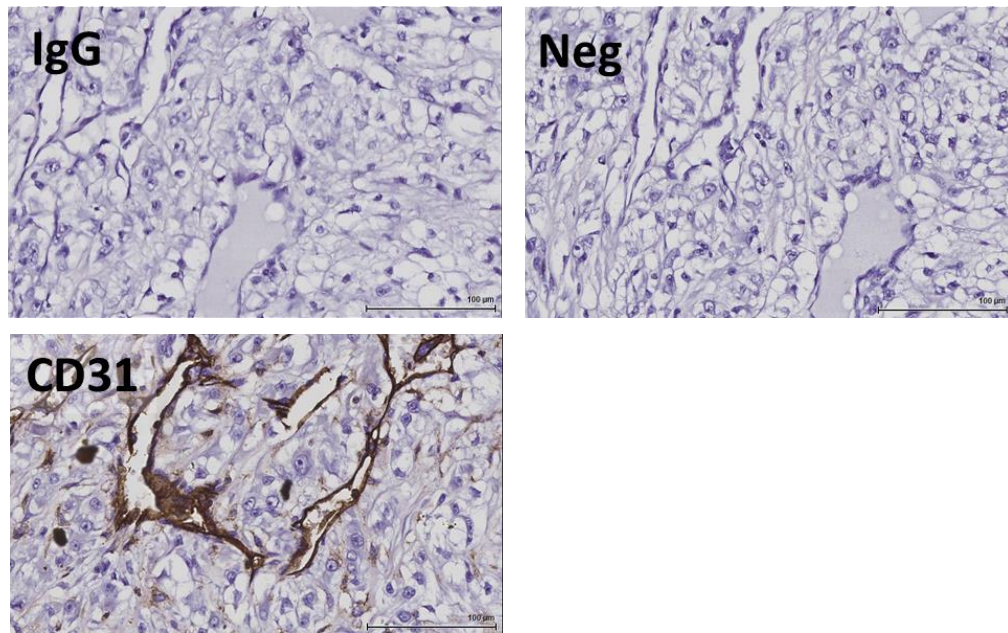


Figure 5.0.13: IHC validation of CD70 expression



5.5.2.1. Analysis of the heterogeneity of CD70 expression

To investigate if there was heterogeneity in the expression of CD70 across different patient blocks, two further blocks for each patient were selected from the pathology archive for analysis by IHC. Blocks were selected to ensure they were not from adjacent tissue to the original block used in the discovery analysis. Sections (4µm) were cut, probed, and analysed as described above. One negative control was completed for each section (IgG₁), which showed no specific binding. Three of the sections stained in the first validation study were repeated as positive controls, and these demonstrated the same staining pattern in both studies. The results are overviewed in Table 5.0.11, which contains the results for the original CD70 validation study completed in Section 5.5.2 (Block 1) and the two additional blocks (Block 2 and Block 3).

Table 5.0.11: CD70 expression in different blocks in responders and non-responders

FFPE sections were stained for CD70 and scored. Score values: 0 - negative staining; 1 - up to 25% cells positive; 2 - 25-50% cells positive; 3 - over 50% cells positive.

		Score			
		0	1	2	3
Responders	Block 1	4	1	1	3
	Block 2	6	0	1	1
	Block 3	4	0	3	2
Non-responders	Block 1	7	1	0	0
	Block 2	8	0	0	0
	Block 3	8	0	0	0

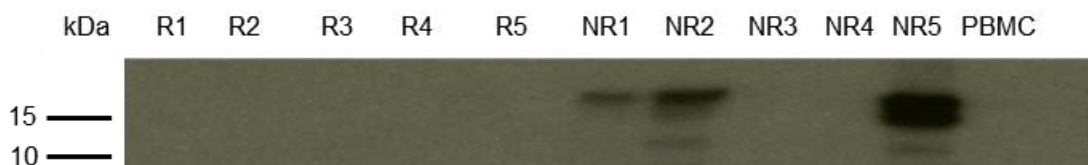
This study revealed there were a low level of heterogeneity in CD70 expression. Of note, a few of the blocks had staining on <1% of cells (3 responders, 2 non-responders), for the purposes of the study these were given a negative score. Compared to the initial validation study on the discovery sections, 7/7 non-responders remained negative for CD70, and the non-responder with positive CD70 staining in block 1 was negative for CD70 in the two additional blocks. Out of the responders, 4/5 of the responders (R2, R4, R5, R9) with positive staining in block 1 also had positive staining in blocks 2 and 3. The remaining responder with positive staining in block 1 (R1) had negative staining in blocks 2 and 3, though of note, the staining intensity was low in block 1. Of the remaining responders, three (R3, R6, R8) remained negative for CD70 in blocks 2 and 3, and one (R7) had strong (score 3) staining in block 3 only.

5.5.3. Investigation of hCAP18 and PRTN3 expression

To investigate the hCAP18 and PRTN3 results obtained by mass spectrometry, the expression of these proteins was investigated by Western blot and immunohistochemistry. FFPE lysates (10ug) of five responders (R1-R5) and five non-responders (NR1-NR5) were separated by 1D SDS-PAGE, proteins levels were checked for normality by parallel Coomassie (data not shown). Investigations into the levels of PRTN3 were hampered by the poor quality of the antibody (data not shown), with no detectable bands observed by Western blot. Probing of the Western blot membrane with a monoclonal antibody specific to hCAP18 revealed upregulated levels of hCAP18 in all the non-responders, with especially high levels in NR1, NR2 and NR5 (Figure 5.0.14), which correlated with the mass spectrometry data. Due to the high levels of expression in NR5 it was necessary to titrate the signal intensity in the Western blot, however there was visible expression of hCAP18 in NR3, NR4, and the positive controls (PBMCs) (data not shown). There were a few high molecular weight non-specific bands observed with this antibody, they were uniform across the samples and did not impact upon the ability to detect hCAP18, however this reinforces the poor quality of the antibody, and an antibody of higher quality is required for further analyses.

Figure 5.0.14: Western blot of hCAP18 in responders and non-responders

Expression of hCAP18 was investigated in five responders (R1-R5), five non-responders (NR1-NR5), and peripheral blood mononuclear cells (PBMCs). A parallel coomassie was used to check normalisation.



When the expression of hCAP18 was investigated using immunohistochemistry, staining was limited and restricted to inflammatory cells. To investigate if the staining was entirely a result of inflammation, a highly inflamed frozen renal tumour tissue was stained alongside tissue from a frozen non-responder. Review of the stained sections by a consultant pathologist indicated the staining was non-specific in all cases, due to high background staining found in the kidney samples. To try to improve the quality of the staining, immunofluorescence of frozen tissue sections was performed. Autofluorescence from the kidney is a known problem with immunofluorescence studies and to counteract this problem, two fluorescent secondary antibodies were investigated, Alexa-568 and Alexa-594. Furthermore, Sudan Black B was used as a counterstain, to investigate whether it could be used to block the autofluorescence. The autofluorescence appeared stronger when using the far red dye Alexa-594, and no improvement was seen by counterstaining with Sudan Black B (data not shown). A low amount of specific staining was observed with the Alexa-568 dye. However this did not give a clean enough signal to resolve the problem. Further investigation of this protein would require an alternative technique such as multiple reaction monitoring (MRM) or microdissected tissues.

5.6. Discussion

The search for biomarkers to predict response to sunitinib has included proteomic and genomic studies of serum, urine, and *in vitro* cell lines, as well as comparative studies of clinical and anatomical features of the patient and tumour. Although some promise has been shown by VEGFR-3 protein in both serum and tissue (Deprimo et al., 2007, Rini et al., 2008, Harmon et al., 2014, Garcia-Donas et al.,

2013, Dornbusch et al., 2013) and IL-8 protein in serum (Harmon et al., 2014), as yet none of these have been validated in a large, prospective study. The development of drug-induced hypertension has so far demonstrated the greatest level of predictive power. However this feature is a *post-hoc* test and there remains the need for a sensitive and specific biomarker that will predict response to sunitinib ahead of therapy. By comparing primary tumour specimens from sunitinib responding and non-responding patients, this study aimed to identify tissue baseline predictors of response. Two proteins especially – CD70 and hCAP18 – demonstrated early promise in this setting and further research is warranted to fully validate their predictive potential.

Differences in the patient population were unavoidable. Whilst every care was taken to normalise for clinical features such as stage, age, and grade, a difference in the prognostic nomogram scores by MSKCC and IMDC (Heng) remained, with a tendency towards higher scores (and hence higher risk) in the non-responding group of patients. A comparison of the clinical timelines of the patients revealed that the non-responding patients more frequently had synchronous metastases and a shorter period between metastasis and the initiation of sunitinib therapy, however this latter point is likely explained by the date of relapse; most of the non-responding patients relapsed after 2008, the date when sunitinib became available in the UK, and they would therefore have received sunitinib as frontline therapy following metastasis. Despite these differences, when the dataset was checked for known prognostic markers (CA9, B7H1, IMP3, Ki67, HIF, VEGF, MMP2, MMP9, CXCR3, CXCR4, and survivin), these proteins were either not identified or no difference was observed, providing confidence that the clinical features were normalised sufficiently to minimise the risk of solely identifying markers of prognosis.

5.6.1. Mass spectrometry optimisation

The use of tissue for biomarker studies, though not as accessible as serum or urine, provides a rich source of tumour-derived molecules. A variety of techniques to allow proteomic biomarker mining in tissue have been developed in recent years, including tissue microarrays, antibody arrays, and improved protein separation and extraction techniques. With techniques recently developed to extract proteins from formalin fixed-paraffin embedded tissue blocks, a much larger repertoire of samples is now available (Nirmalan et al., 2011, Craven et al., 2013a). However biological samples are highly complex, and variation brought about by interpatient variability is a major challenge for proteomic studies. Increasing both the confidence in identification and number of identifications would increase the chances of identifying clinically useful biomarkers. In mass spectrometric analysis, this may be achieved by increasing the length of the separation through increasing the physical length of the column, by increasing the amount of pre-fractionation (for example by employing an orthogonal pre-fractionation method), or by increasing the number of injections of the sample. Though each of these methods have been successfully used to increase coverage, the increased processing time and/or mass spectrometry analysis time required means these methods are not always feasible in a clinical research laboratory, which generally handles large numbers of samples. With each injection of sample onto the mass spectrometer, there is hypothesised to be a sloping increase in sample identifications due to the random selection of peptides. There is therefore room for optimisation of sample injection, to maximise the number of confident identifications, with the analysis time taken to analyse each sample. In this study an increase in the number of identifications was observed with increasing number of injections; an increase of approximately 17% was achieved between one and two injections, with a lower increase of around 7% between two and three injections. Interestingly, no additional peptide quantitative information was

achieved through increasing the number of injections, however the intensity values were around 30% higher when comparing three injections to two injections. Though it was not possible to assess the impact on LFQ values, as the LFQ value is computed from the intensity value it is likely there would have been a concomitant increase in LFQ scores as well. In terms of absolute number of identifications, the increased analysis time required for a third injection does not warrant this step when machine time is limited. However if particularly low abundance targets are of interest, it may be worth considering a third injection to improve the chances of observing these proteins at sufficiently high intensity for a confident identification.

5.6.2. Differentially expressed proteins in responders and non-responders

A total of 4507 proteins were identified, which is consistent with other FFPE studies (Craven et al., 2013a), and most of these were common to both responders and non-responders. Out of the potential predictive biomarkers previously reported in the literature, most were not identified or were identified with very low levels in this dataset. This is most likely due to the more sensitive techniques used to examine these markers in focussed analyses, such as ELISA and immunohistochemistry; mass spectrometry is currently less sensitive than these techniques. Interestingly, two proteins that have previously been reported as elevated in the serum of non-responding patients – MMP9 and NGAL (Porta et al., 2010, Perez-Gracia et al., 2009) – were found to be elevated in the tissue of non-responders in this study, indicating they may have use as a baseline tissue predictor of response. Interestingly however, MMP9 and NGAL were not found to be differentially expressed in the serum of responding and non-responding patients, in contrast to previous studies (Porta et al., 2010, Perez-Gracia et al., 2009).

5.6.2.1. Elevated proteins in the FFPE tissue of non-responders

IPA analysis of non-responder elevated proteins indicated that there was a high enrichment of cell-to-cell signalling proteins, which included the shortlisted biomarker candidate proteins hCAP18 and PRTN3. Many of these proteins appear to act upstream of, or directly upon, Akt1, which is part of the PI3K/Akt/mTOR cascade. Interestingly, Akt1 inhibition was shown to overcome sunitinib resistance in renal cancer cell lines (Makhov et al., 2012), and this may therefore represent a resistance mechanism. Furthermore, there was an association with drug resistance pathways; the presence of the ABCC1 transporter in the non-responders dataset may assist in cellular export of sunitinib thereby promoting resistance, due to its role in drug resistance (Munoz et al., 2007),

The most highly upregulated proteins in the non-responders were all neutrophil derived proteins, most of which can be found in the azurophilic granule, one of a few granules which is released during degranulation (Faurischou and Borregaard, 2003). These proteins included cathelicidin (hCAP18/LL37), proteinase 3 (PRTN3), azurocidin (AZU1), cathepsin G (CTSG), and myeloperoxidase (MPO). Western blot analysis of hCAP18 expression in ten of the discovery patients (five responders and five non-responders) confirmed the pattern observed by mass spectrometry, and importantly, it was also found to be elevated in the serum of non-responding patients, suggesting this protein could be investigated as a fluid biomarker. Individually, many of these proteins have been associated with cancer progression. Expression of the antimicrobial peptide hCAP18 is elevated in a number of cancers including breast (Heilborn et al., 2005), lung (Li et al., 2014), ovarian (Coffelt et al., 2008), and prostate (Hensel et al., 2011), where it drives proliferation and invasiveness, whereas proteinase 3 has roles in invasiveness and inflammation (Pezzato et al., 2003). Pro-metastasis and invasive functions are also demonstrated

by the serine protease CTSG (Morimoto-Kamata et al., 2012), which appears to function with PRTN3 to activate MMP2 (Shamamian et al., 2001). MPO, which is involved in the neutrophil respiratory burst, may act to protect against apoptosis (Saed et al., 2010). Interestingly, MPO functions to convert hydrogen peroxide, made within the phagolysosomes of neutrophils, into hypochlorous acid which has mutagenic properties and may therefore support genotoxicity in cancer progression (Gregory and Houghton, 2011, Gungor et al., 2010).

Aside from the independent roles of these proteins, neutrophils themselves have been associated with tumour progression through promoting proliferation, angiogenesis, and metastasis; effects that have been attributed to the release of ECM-degrading proteases (Gregory and Houghton, 2011), and cytokines such as VEGF (Webb et al., 1998). Neutrophils have been shown to form NETs (Neutrophil Extracellular Traps), which are mesh like structures that contain chromatin and antimicrobial proteins (Brinkmann et al., 2004), including the azurophilic proteins listed previously (Papayannopoulos and Zychlinsky, 2009). NETs have recently been implicated in trapping circulating cancer cells and promoting metastasis (Cools-Lartigue et al., 2013). Interestingly, IL-8, a protein which has been heavily implicated in anti-angiogenic therapy resistance (Huang et al., 2010), induces neutrophil chemotaxis (Hammond et al., 1995) and activation (Baggiolini et al., 1989), and this activation may support the promotion of metastasis by neutrophils (De Larco et al., 2004).

Although neutrophil NETs have been shown to drive metastasis, other routes through which neutrophils can aid metastasis and angiogenesis is through the release of ECM-degrading proteins, such as the matrix metalloproteinases (MMPs)

(Gialeli et al., 2011). MMP-9, which forms a heterodimeric complex with neutrophil gelatinase-associated lipocalin (NGAL) (Yan et al., 2001), has been implicated in promoting several stages of cancer progression including angiogenesis, proliferation, and metastasis (Gialeli et al., 2011). Both NGAL and MMP-9 were significantly elevated in the non-responders dataset, which is consistent with other tissue studies reporting elevated levels in RCC (Barresi et al., 2010, Kallakury et al., 2001). Furthermore, serum levels of both NGAL and MMP9 have previously been shown to be associated with poor response to sunitinib (Porta et al., 2010, Perez-Gracia et al., 2009). Certainly the pre-treatment neutrophil to lymphocyte ratio (NLR) has been reported as predictive for sunitinib outcome (Keizman et al., 2011, Keizman et al., 2012), however this is a systemic effect and does not guarantee the presence of intratumoural neutrophils. Validation of the expression of these proteins is necessary to further investigate their contribution to sunitinib resistance, and a properly controlled study is essential to ensure these proteins are predictive rather than prognostic, especially when considering a previous study linking intratumoural neutrophils to prognosis in RCC patients (Jensen et al., 2009). Intratumoural neutrophils could be indicative of an inflammatory response occurring in the non-responders, a manifestation that is associated with aggressive cancer. Further studies would be needed to determine if this was the case, however there did not appear to be any correlation between the levels of these proteins and the presence of inflammation, when the pathology comments for each block were compared to the achieved results.

Another immune related protein that was elevated in this dataset was ITGAM (CD11b). This protein is expressed on a number of leukocytes, and interestingly is expressed on neutrophils (Miller et al., 1987). Myeloid cells that are CD11b+ Gr+ are found in patient tumours, and coinjection of tumours with these cells increased

vascularity and decreased necrosis. Furthermore, high levels of MMP9 were observed to be expressed by these cells (Yang et al., 2004). Interestingly CD11b+ Gr1+ myeloid cells have been shown to promote refractoriness to anti-angiogenic therapy (Shojaei et al., 2007), and sunitinib has been shown to induce an influx of these cells (Panka et al., 2013). Finally, lactotransferrin (LTF) is a further neutrophil-derived protein, where it appears to be involved in preventing neutrophil apoptosis (Francis et al., 2011). In this study LTF was found to be upregulated in the non-responders; it was also found to be moderately elevated in the serum of non-responders. With so many neutrophil-related proteins upregulated in the non-responding patients it certainly seems there could be a potential link with sunitinib resistance mechanisms through the modulation of neutrophil activity, and further biochemical testing is necessary to investigate this hypothesis.

Other proteins upregulated by the non-responders include SEPHS2 which is involved in selenoprotein biosynthesis (Xu et al., 2007), UBFD1 which may have a role in regulating NF- κ B (Fenner et al., 2009), UBR4 which has roles in anchorage independent growth (Huh et al., 2005) and cellular structure (Nakatani et al., 2005), and UBTF which is involved in ribosomal RNA synthesis (Bell et al., 1988) and is upregulated in hepatocellular carcinoma (Huang et al., 2002). Disks large homolog 1 (DLG1), had a mild upregulation in the non-responders, this protein has conflicting *in vitro* studies regarding its role in cancer, with evidence for both increased cell migration (O'Neill et al., 2011), and possible tumour suppressor qualities (Humbert et al., 2003). Finally, a few erythrocyte proteins were also found to be highly upregulated in the non-responders, these were spectrin alpha, spectrin beta, ankyrin 1, and erythrocyte membrane protein band 4.2. Due to the highly ubiquitous nature of these proteins, their upregulation is not likely to be specifically

predictive of sunitinib efficacy, especially considering two of these (SPTA1 and EPB42) were also found to be upregulated in an independent prognostic dataset.

5.6.2.2. Elevated proteins in the FFPE tissue of responders

Twelve proteins demonstrated a significant upregulation in the responders, based on peptide and LFQ data. Analysis of all the peptide and LFQ upregulated proteins by IPA indicated that the most prominent upregulated pathways, like the non-responders, was also cell-to-cell signalling, however a different set of proteins were upregulated. In this pathway many proteins were associated with cadherin 1 (CDH1) and the p38 MAPK, interestingly, CDH1 has been shown to have anti-metastatic properties (Birchmeier and Behrens, 1994), and the P38 MAPK has a role in regulating apoptosis (Wada and Penninger, 2004), both of which may therefore serve to limit tumour growth in the responding patients.

The protein demonstrating the highest consistent upregulation in the peptide and LFQ datasets was the T cell activator CD70 (CD27L). This protein was significantly upregulated in both peptide ($P = 0.016$) and LFQ ($P = 0.005$) values. 6/8 responders and 2/8 non-responders expressed this protein, furthermore the CD70 expressing non-responders had only low levels based on peptide data, and these values were normalised out in the LFQ dataset, indicating their levels were much lower than those observed in the responders. When the levels of CD70 were compared to the patient's clinical timelines, indications of inflammation, and indications of necrosis, there did not appear to be any correlation with any of these features, nor was there any correlation with the MSKCC or Heng scores (data not shown). During analysis of CD70 levels by IHC, it was found that 7/8 of the non-responders were negative for CD70 expression, and 5/9 responders were positive

for CD70 expression. This did not fully match the mass spectrometry data, where 6/8 responders were positive for CD70 expression, however there was reasonable consistency between the mass spectrometry and the IHC data, providing reassurance in the mass spectrometry data.

Localised heterogeneity is an important point for consideration in tumour tissue studies, due to localised differences in tumour morphology, as well as proteomic and genomic differences (Gerlinger et al., 2012). To determine if there was heterogeneity in CD70 expression, an additional study was conducted whereby two further blocks from each patient were stained for CD70. From this study it was found that there was a low level of heterogeneity in expression, with only 2/9 responders and 1/8 non-responders displaying a different expression pattern in the two further blocks. From these results, CD70 appears to have a strong negative predictive power, with most of the non-responders not demonstrating any expression. Further studies are warranted to fully test the potential utility of this protein, and plans are currently being made for a larger in house study looking at sunitinib responders and non-responders, followed by a collaborative case-controlled study to properly assess whether CD70 may be predictive or prognostic.

Interestingly, CD70 is a member of the Tumour Necrosis Factor (TNF) superfamily, and is a cytokine involved in proliferation and activation of costimulated T cells (Goodwin et al., 1993), and in the induction of T cell driven B cell antibody production (Arens et al., 2004). It is a transmembrane receptor that is transiently expressed on activated B and T cells, and mature dendritic cells (Borst et al., 2005, Tesselaar et al., 2003), and this cell membrane location is consistent with the cellular location observed during the IHC staining performed in this study. The

cognate receptor for CD70 is CD27, a Tumour Necrosis Factor Receptor (TNFR) family member which is constitutively found on the majority of T cells and thymocytes, and on some natural killer (NK) and haematopoietic stem cells (Wiesmann et al., 2000, van Lier et al., 1987). CD70 is also expressed in a number of cancers including brain tumours (Held-Feindt and Mentlein, 2002), multiple lymphomas (Lens et al., 1999), thymic carcinoma (Hishima et al., 2000), and breast cancer (Petrau et al., 2014), and it is therefore being investigated as a potential drug target (Grewal, 2008). CD70 has been found in renal cancer in multiple studies, where it appears to be expressed by both the primary and the metastatic lesions. In a small IHC and mRNA study of 10 ccRCC patients, positive CD70 mRNA and protein expression was found in 8/10 patients and 10/10 patients respectively (Diegmann et al., 2005). Expression of CD70 protein was found in all ccRCC specimens (41/41) and no expression in the adjacent normal tissue in a larger IHC study (Junker et al., 2005). Another study investigated CD70 protein in both primary and metastatic lesions, whereby expression was found in 16/30 and 8/11 samples respectively (Adam et al., 2006). Clear cell histologies express higher levels than other RCC types (Jilaveanu et al., 2012), and its absence from normal tissue has led to its suggested use as a diagnostic marker (Diegmann et al., 2005). However it does not appear to have any prognostic utility (Jilaveanu et al., 2012), a large TMA with 234 ccRCC samples found variable levels of CD70, 49% of patients had expression levels of CD70 above the 95% percentile of that measured in the matched normal tissue, and this was not associated with survival in multivariate analysis (Jilaveanu et al., 2012).

Interaction between CD27 and CD70 can lead to lymphocyte activation, proliferation, differentiation, and control of cell survival (Gruss and Dower, 1995). CD70 seems to be capable of inducing lymphoid apoptosis in peripheral blood

mononuclear cells (PBMCs) incubated with a glioma cell line (Wischhusen et al., 2002) and in lymphocytes incubated with renal cell carcinoma cell lines (Diegmann et al., 2006), and this has therefore been proposed as an immune escape mechanism for developing cancers. Alternatively, as CD70 stimulates activation of the cytotoxic CD8+ T cells (Brown et al., 1995) and promotes their survival (van Oosterwijk et al., 2007), a number of studies have indicated the potential for CD70 in anti-tumour activity (Lorenz et al., 1999, Couderc et al., 1998, Nieland et al., 1998). With both stimulatory and regulatory roles, CD70 clearly has a dichotomy in function, and many other molecules and proteins are likely to be involved in deciding cell fate.

Of note, VCAM1, which was also elevated in the responders and is involved in cell-cell recognition and leukocyte-endothelial cell adhesion, is also able to co-induce T cell proliferation (Burkly et al., 1991), and is also able to activate CD4+ T cells (Damle and Aruffo, 1991). These in turn are able to induce expression of VCAM1 (Yarwood et al., 2000, Damle et al., 1991). In cancer VCAM1 has been proposed to confer a survival advantage (Chen et al., 2011). This link between VCAM1 and T cell activation is interesting, considering CD70 has a role in regulating T cells, and it may be that this T cell regulation has a role in promoting the effects of sunitinib, or preventing resistance, through an as yet unidentified mechanism. Finally, another immune-related protein found at higher levels in the responders which may also be involved is sedoheptulosekinase (SHPK). This is a kinase involved in phosphorylating the sugar sedoheptulose (Kardon et al., 2008) and in activating macrophages (Haschemi et al., 2012).

In addition to CD70, other proteins found at higher levels in the responders included proteins involved in metabolism and cellular structure. Proteins with a link to metabolism included the aarF domain-containing protein kinase 3 (ADCK3), which is involved in the biosynthesis of coenzyme Q (ubiquinone) and is a component of the electron transport chain (Xie et al., 2011b), NADH dehydrogenase [ubiquinone] 1 alpha subcomplex subunit 4-like 2 (NDUFA4L2), which is also involved in the functioning of the electron transport chain and is induced by HIF (Tello et al., 2011), adenylosuccinate synthetase isozyme 1 (ADSSL1), which is involved in purine biosynthesis (Borza et al., 2003), and amine oxidase (ABP1) which is involved in polyamine degradation and appears to be dysregulated in colorectal cancer (Linsalata et al., 1993). The link to the electron transport chain is interesting as oxidative phosphorylation is affected during RCC pathogenesis, where its decreased functioning is linked with tumour aggressiveness (Simonnet et al., 2002). Two proteins involved in lipid metabolism were also significantly upregulated. These were diphosphomevalonate decarboxylase (MVD) and prolow-density lipoprotein receptor-related protein 1 (LRP1), the latter of which was also found to be upregulated in the VHL-negative cell line RCC4/T. MVD is involved in cholesterol biosynthesis (Krepkiy and Miziorko, 2004), whereas LRP1 is involved in lipid homeostasis (Spuch et al., 2012) and is HIF activated. Finally, the enzyme aminoacylase-3 (ACY3) is involved in deacetylating mercapturic acids in the kidney proximal tubule, a process that can lead to nephrotoxicity (Pushkin et al., 2004). This protein is upregulated in neuroblastoma, where its elevated expression is associated with poor prognosis (Long et al., 2011). These metabolic proteins may be linked to a tumour phenotype that is less nutrient starved, and therefore less metastatic and invasive. The presence of HIF activated proteins is interesting, as HIF upregulation has previously been shown to predict a favourable response to sunitinib (Patel et al., 2008, Saez et al., 2012, Garcia-Donas et al., 2013).

Proteins with a link to cellular structure and signalling that were detected at higher levels in the responders patient group were cadherin-1 (CDH1), and fibroleukin (FGL2). CDH1 is a cell adhesion molecule which may have tumour suppressor qualities properties (Birchmeier and Behrens, 1994), this protein was also found to be upregulated in the responders patient group in the baseline serum study. Loss of this protein has been linked with the epithelial-mesenchymal transition, a step widely regarded as pivotal in metastasis. The presence of this protein in the responders may therefore aid in limiting metastatic spread, and may indicate a tumour with a decreased ability to drive invasion, one mechanism which has previously been suggested as a resistance mechanism for anti-angiogenic therapy (Bergers and Hanahan, 2008). FGL2 is expressed on activated macrophages and is also secreted by CD4+ and CD8+ T lymphocytes (Su et al., 2008, Marazzi et al., 1998), it is able to modulate activity of the adaptive immune system (Chan et al., 2003) and appears to be upregulated in multiple cancers (Rabizadeh et al., 2014, Su et al., 2008).

5.6.3. Concluding remarks and study limitations

By utilising a combination of mass spectrometry, bioinformatics, and immunohistochemistry, this study has identified a number of proteins that may assist in identifying a clinically relevant biomarker in the primary tumour to predict response to sunitinib in the metastatic setting. Furthermore, it is possible that the enriched networks identified in this study may shed light on sunitinib resistance mechanisms. The identification of CD70, which has not previously been associated with sunitinib response, is an exciting development that has shown early promise and is currently being investigated in a larger cohort of patient samples. The association between this protein and the immune system is particularly interesting, as it may function to assist in immune system priming to promote the effects of

sunitinib. Furthermore a number of other proteins, especially those associated with neutrophil biology and EMT such as CDH1, have extremely interesting biology and further investigation of their expression is being pursued.

One of the largest problems impacting upon studies utilising clinical samples, particularly tissue samples, is gaining access to sufficient quantities of sample to allow for a properly controlled and sufficiently powered study. Considerations for any biomarker study must therefore focus not simply on the numbers of samples, but also on minimising the inter-patient variability as much as possible, to increase the chance of identifying biomarkers with clinical utility. If the differences in the patient population are numerous enough to dichotomise the cohort, the validity of the study may be called into question. Normalising for these factors is a difficult task; although this is made easier by access to large tissue banks, it remains a confounding factor in many studies. Aside from the biological variation, every step must be taken to minimise the effects of technical variation – through sample collection, processing, storage, extraction, to mass spectrometric analysis.

Bioinformatic analysis must be used with caution, using it only to provide a testable hypothesis rather than a means on which to make assertions about protein expression patterns and roles. A further consideration of this study lies in the fact that the primary renal masses were used to predict response in metastatic disease, which in some cases occurred many years after the primary tumour was resected, and this may be too much to ask of a primary tumour. Future studies may measure CD70 levels in matched primary and metastatic lesions, to investigate if there is concordance in the levels of this protein. Nevertheless, if primary renal masses can

be used to predict response in metastatic disease, this would be a significant advantage, as metastatic tissue is infrequently collected.

The risk of identifying a prognostic as opposed to a predictive biomarker is very real, especially given the unavoidable prognostic differences in the discovery patient cohort. The next steps for this study therefore involve extensive validation of CD70 in a large patient cohort, followed by validation in a case controlled study (using a treated and untreated patient population) to fully assess the potential predictive nature of this protein. Finally, given their similar mode of action, it is possible that any marker identified that can predict for sunitinib efficacy may also predict for clinical response to other TKIs, such as pazopanib, which is being used with increasing frequency in the clinic.

6. Final Discussion

The clinical management of RCC would be significantly assisted by the identification of biomarkers. These could impact upon all stages of patient care, from diagnosis and prognosis, to the prediction of therapeutic benefit and monitoring response to therapy. Renal cell carcinoma is a complex malignancy with multiple genetic aberrations (Sato et al., 2013, Gossage et al., 2014), and many genetic studies have been performed to identify biomarkers, find new drug targets, and understand the mechanism of disease (Vasudev et al., 2012), however these studies cannot determine the protein expression level of these genes. Transcriptomic studies may allow for some information of protein expression to be garnered, but it is not known how well this translates into protein levels (Vogel and Marcotte, 2012). With protein based studies comes not only the ability to investigate the protein content of a tissue, cell, organelle, or membrane, it also provides the ability to research protein interactions, regulation, and post-translational modifications. Mass spectrometry has now started to come of age, with multiple studies reporting interactomes and novel PTMS, as well as validated biomarkers and targets (Collinson et al., 2013, Welberry Smith et al., 2013). The use of mass spectrometry for protein mining is a powerful technique that makes very few assumptions about the type of protein that will be identified.

This study employed the quick and cheap label-free quantification technique, a technique that is most powerful when used as a tool for discovery, where accurate quantification is less important than the ability to analyse multiple samples. Although LFQ quantification has pitfalls, proteins with validated differential expression patterns were identified in the three different sample types analysed in

this study. Out of the three sample types analysed here, serum was the most problematic, with 10 fold fewer proteins identified in this sample compared to the cell lysates and FFPE tissue extracts, despite hypotheses of similar numbers of proteins present in the sample (Anderson, 2002, Archakov et al., 2007). Historically, serum and fluids generally have been difficult samples to analyse by mass spectrometry, and though pre-fractionation has increased the number of possible identifications, considerable method development is still required for this sample type to fully tap the depths of the serum proteome. Nevertheless, interesting biological changes were found in this study and recent successes using similar techniques to those employed here provide confidence in the proteomic analysis of serum for biomarkers (Collinson et al., 2013, Welberry Smith et al., 2013, Timms et al., 2014). In comparison, many more proteins were identified in the cell line and FFPE tissue extract studies, and one protein from each of these studies was successfully validated in their respective discovery samples. The differentially expressed proteins identified between sunitinib responding and non-responding patients in the FFPE study included a number of pro-inflammatory and pro-invasive proteins. These results were supported by similar findings in the serum study, where multiple proteins involved in the regulation of invasiveness were identified. The crossover between the serum and FFPE studies was low, however there is no guarantee that the tumour proteins present in the tissue are released or shed into the serum. Investigation of the proteomic differences between the five VHL disease cell lines indicated that a large number of proteins change in response to VHL mutation, although the potential for cell line artefacts must be considered, and there is therefore a risk that these proteins may not translate into a clinically useful finding. Although IRS2 expression was found in a further VHL cell lines pair, suggesting this expression pattern is not a cell culture artefact, however there is still no guarantee that this expression pattern remains valid in a tissue environment. It is

also important to remember that many studies in the literature are focussed on tumour-normal differences, a scenario where there are frequently large differences due to the significant morphological and karyotypic differences that occur during tumourigenesis. It is generally more difficult to find large proteomic differences when performing tumour-tumour comparisons, such as those conducted in this study, as the samples are often far more similar.

The steps taken in this study to validate the differential protein expression patterns involved the use of Western blotting and immunohistochemistry. Proteins identified in the serum study were not successfully validated, due partly to the poor quality of the available antibodies, and also due to the planned MRM validation being delayed, however steps are currently in place to validate CDH1 and IGFBP5, using ELISA and Luminex. IRS2, identified in the cell line study as regulated by VHL, was validated in the discovery cell line using Western blot. Although this technique is sensitive, it is prone to many sources of error (Ghosh et al., 2014) and a less subjective and more sensitive technique should be used for further validation studies, such as MRM, ELISA, or IHC. CD70, identified in the FFPE predictive biomarker study, was validated using immunohistochemistry. This sensitive technique that is routinely used in the clinic, and proved powerful in validating the mass spectrometry findings. These early studies of CD70 have warranted further investigation of this protein, for which studies are currently underway. The difficulty in measuring hCAP18 levels using IHC was a result of an inadequate antibody; this represents a common problem in proteomic studies. Validation of candidate proteins is frequently hampered by reagent availability, and even if antibodies are available there is no guarantee they will be suitable or of sufficient quality.

Confirmation of the expression pattern of each of these proteins must now be completed in larger, carefully selected patient cohorts, using sensitive and specific techniques such as MRM, ELISA, or IHC. Investigation of IGFBP5 and CDH1 levels will initially focus on serum from the discovery sample set, followed by validation in a larger group of responders and non-responders. The validation of these markers would be highly beneficial to RCC management due to their presence in serum, a simple ELISA of blood samples would allow a clinician to make decisions about the correct course of therapy. Further investigation into the expression of IRS2 must be performed in a clinical setting to determine if this protein has clinical utility, either as a biomarker candidate or a druggable target. In addition, research into its functional role in RCC may help us to understand more about the early stages of RCC pathogenesis. Having already achieved initial validation of CD70, the next step would be to investigate levels in a wider cohort of responders and non-responders. This would be followed by a case-controlled study, whereby the levels of CD70 would be tested in both a treated and untreated patient cohort, to assess its predictive power. We have already approached a potential collaborator regarding access to samples that would allow this analysis to be completed. Additionally it would also be interesting to determine if CD70 is leaked into the serum, though no evidence has yet been found for this, the presence of soluble CD70 would allow the use of this protein as a soluble biomarker. Finally, determining if the expression of these proteins predicts for sensitivity to other tyrosine kinase inhibitors, such as pazopanib, would be a useful future step, given the similar mode of action this is not unfeasible.

List of References

- ABDULRAHMAN, M., MAINA, E. N., MORRIS, M. R., ZATYKA, M., RAVAL, R. R., BANKS, R. E., WIESENER, M. S., RICHARDS, F. M., JOHNSON, C. M., LATIF, F. & MAHER, E. R. 2007. Identification of novel VHL targets that are associated with the development of renal cell carcinoma. *Oncogene*, 26, 1661-72.
- ABEL, E. J., CULP, S. H., TANNIR, N. M., TAMBOLI, P., MATIN, S. F. & WOOD, C. G. 2011. Early primary tumor size reduction is an independent predictor of improved overall survival in metastatic renal cell carcinoma patients treated with sunitinib. *European urology*, 60, 1273-9.
- ADACHI, H., MAJIMA, S., KON, S., KOBAYASHI, T., KAJINO, K., MITANI, H., HIRAYAMA, Y., SHIINA, H., IGAWA, M. & HINO, O. 2004. Niban gene is commonly expressed in the renal tumors: a new candidate marker for renal carcinogenesis. *Oncogene*, 23, 3495-500.
- ADAM, P. J., TERRETT, J. A., STEERS, G., STOCKWIN, L., LOADER, J. A., FLETCHER, G. C., LU, L. S., LEACH, B. I., MASON, S., STAMPS, A. C., BOYD, R. S., PEZZELLA, F., GATTER, K. C. & HARRIS, A. L. 2006. CD70 (TNFSF7) is expressed at high prevalence in renal cell carcinomas and is rapidly internalised on antibody binding. *Br J Cancer*, 95, 298-306.
- ADOTEVI, O., PERE, H., RAVEL, P., HAICHEUR, N., BADOUAL, C., MERILLON, N., MEDIONI, J., PEYRARD, S., RONCELIN, S., VERKARRE, V., MEJEAN, A., FRIDMAN, W. H., OUDARD, S. & TARTOUR, E. 2010. A decrease of regulatory T cells correlates with overall survival after sunitinib-based antiangiogenic therapy in metastatic renal cancer patients. *J Immunother*, 33, 991-8.
- AGGELIS, V., CRAVEN, R. A., PENG, J., HARNDEN, P., CAIRNS, D. A., MAHER, E. R., TONGE, R., SELBY, P. J. & BANKS, R. E. 2009. Proteomic identification of differentially expressed plasma membrane proteins in renal cell carcinoma by stable isotope labelling of a von Hippel-Lindau transfectant cell line model. *Proteomics*, 9, 2118-30.
- AKKARI, L., GOCHEVA, V., KESTER, J. C., HUNTER, K. E., QUICK, M. L., SEVENICH, L., WANG, H. W., PETERS, C., TANG, L. H., KLIMSTRA, D. S., REINHECKEL, T. & JOYCE, J. A. 2014. Distinct functions of macrophage-derived and cancer cell-derived cathepsin Z combine to promote tumor malignancy via interactions with the extracellular matrix. *Genes & development*, 28, 2134-50.
- AL-SARRAF, N., REIFF, J. N., HINRICHSEN, J., MAHMOOD, S., TEH, B. T., MCGOVERN, E., DE MEYTS, P., O'BYRNE K, J. & GRAY, S. G. 2007. DOK4/IRS-5 expression is altered in clear cell renal cell carcinoma. *Int J Cancer*, 121, 992-8.
- ANDERSON, N. L. 2002. The Human Plasma Proteome: History, Character, and Diagnostic Prospects. *Molecular & Cellular Proteomics*, 1, 845-867.
- ANG, S. O., CHEN, H., HIROTA, K., GORDEUK, V. R., JELINEK, J., GUAN, Y., LIU, E., SERGUEEVA, A. I., MIASNIKOVA, G. Y., MOLE, D., MAXWELL, P. H., STOCKTON, D. W., SEMENZA, G. L. & PRCHAL, J. T. 2002. Disruption of oxygen homeostasis underlies congenital Chuvash polycythemia. *Nat Genet*, 32, 614-21.
- ARCHAKOV, A. I., IVANOV, Y. D., LISITSA, A. V. & ZGODA, V. G. 2007. AFM fishing nanotechnology is the way to reverse the Avogadro number in proteomics. *Proteomics*, 7, 4-9.

- ARENS, R., NOLTE, M. A., TESSELAAR, K., HEEMSKERK, B., REEDQUIST, K. A., VAN LIER, R. A. & VAN OERS, M. H. 2004. Signaling through CD70 regulates B cell activation and IgG production. *J Immunol*, 173, 3901-8.
- ARMSTRONG, A. J., GEORGE, D. J. & HALABI, S. 2012. Serum lactate dehydrogenase predicts for overall survival benefit in patients with metastatic renal cell carcinoma treated with inhibition of mammalian target of rapamycin. *Journal of Clinical Oncology*, 30, 3402-7.
- ARMSTRONG, B. & DOLL, R. 1975. Environmental factors and cancer incidence and mortality in different countries, with special reference to dietary practices. *International journal of cancer. Journal international du cancer*, 15, 617-31.
- ATKINS, M. B., HIDALGO, M., STADLER, W. M., LOGAN, T. F., DUTCHER, J. P., HUDES, G. R., PARK, Y., LIOU, S. H., MARSHALL, B., BONI, J. P., DUKART, G. & SHERMAN, M. L. 2004. Randomized phase II study of multiple dose levels of CCI-779, a novel mammalian target of rapamycin kinase inhibitor, in patients with advanced refractory renal cell carcinoma. *Journal of clinical oncology : official journal of the American Society of Clinical Oncology*, 22, 909-18.
- ATRIH, A., MUDALIAR, M. A., ZAKIKHANI, P., LAMONT, D. J., HUANG, J. T., BRAY, S. E., BARTON, G., FLEMING, S. & NABI, G. 2014. Quantitative proteomics in resected renal cancer tissue for biomarker discovery and profiling. *Br J Cancer*, 110, 1622-33.
- BACHERT, C., FIMMEL, C. & LINSTEDT, A. D. 2007. Endosomal trafficking and proprotein convertase cleavage of cis Golgi protein GP73 produces marker for hepatocellular carcinoma. *Traffic*, 8, 1415-23.
- BAGGIOLINI, M., WALZ, A. & KUNKEL, S. L. 1989. Neutrophil-activating peptide-1/interleukin 8, a novel cytokine that activates neutrophils. *J Clin Invest*, 84, 1045-9.
- BAMIAS, A., TZANNIS, K., BEUSELINCK, B., OUDARD, S., ESCUDIER, B., DIOSYNOPOULOS, D., PAPAZISIS, K., LANG, H., WOLTER, P., DE GUILLEBON, E., STRAVODIMOS, K., CHRISOFOFOS, M., FOUNTZILAS, G., ELAIDI, R. T., DIMOPOULOS, M. A. & BAMIA, C. 2013. Development and validation of a prognostic model in patients with metastatic renal cell carcinoma treated with sunitinib: a European collaboration. *British journal of cancer*, 109, 332-41.
- BANERJEE, P., BASU, A., WEGIEL, B., OTTERBEIN, L. E., MIZUMURA, K., GASSER, M., WAAGA-GASSER, A. M., CHOI, A. M. & PAL, S. 2012. Heme oxygenase-1 promotes survival of renal cancer cells through modulation of apoptosis- and autophagy-regulating molecules. *J Biol Chem*, 287, 32113-23.
- BARNEA, E., SORKIN, R., ZIV, T., BEER, I. & ADMON, A. 2005. Evaluation of prefractionation methods as a preparatory step for multidimensional based chromatography of serum proteins. *Proteomics*, 5, 3367-75.
- BARRESI, V., IENI, A., BOLIGNANO, D., MAGNO, C., BUEMI, M. & BARRESI, G. 2010. Neutrophil gelatinase-associated lipocalin immunoexpression in renal tumors: correlation with histotype and histological grade. *Oncology reports*, 24, 305-10.
- BASAPPA, N. S., ELSON, P., GOLSHAYAN, A. R., WOOD, L., GARCIA, J. A., DREICER, R. & RINI, B. I. 2011. The impact of tumor burden characteristics in patients with metastatic renal cell carcinoma treated with sunitinib. *Cancer*, 117, 1183-9.
- BASSERMANN, F., PESCHEL, C. & DUUYSTER, J. 2005. Mitotic entry: a matter of oscillating destruction. *Cell Cycle*, 4, 1515-7.

- BATTAGLIA, S., MAGUIRE, O. & CAMPBELL, M. J. 2010. Transcription factor co-repressors in cancer biology: roles and targeting. *Int J Cancer*, 126, 2511-9.
- BELL, S. P., LEARNED, R. M., JANTZEN, H. M. & TJIAN, R. 1988. Functional cooperativity between transcription factors UBF1 and SL1 mediates human ribosomal RNA synthesis. *Science*, 241, 1192-7.
- BELLEI, E., BERGAMINI, S., MONARI, E., FANTONI, L. I., CUOGHI, A., OZBEN, T. & TOMASI, A. 2011. High-abundance proteins depletion for serum proteomic analysis: concomitant removal of non-targeted proteins. *Amino acids*, 40, 145-56.
- BENGTSON, M. H. & JOAZEIRO, C. A. 2010. Role of a ribosome-associated E3 ubiquitin ligase in protein quality control. *Nature*, 467, 470-3.
- BERGERS, G. & HANAHAN, D. 2008. Modes of resistance to anti-angiogenic therapy. *Nature reviews. Cancer*, 8, 592-603.
- BERTHET, C. & KALDIS, P. 2006. Cdk2 and Cdk4 cooperatively control the expression of Cdc2. *Cell Div*, 1, 10.
- BERTHET, C., KLARMANN, K. D., HILTON, M. B., SUH, H. C., KELLER, J. R., KIYOKAWA, H. & KALDIS, P. 2006. Combined loss of Cdk2 and Cdk4 results in embryonic lethality and Rb hypophosphorylation. *Dev Cell*, 10, 563-73.
- BERX, G. & VAN ROY, F. 2009. Involvement of members of the cadherin superfamily in cancer. *Cold Spring Harb Perspect Biol*, 1, a003129.
- BEUSELINCK, B., KARADIMOU, A., LAMBRECHTS, D., CLAES, B., WOLTER, P., COUCHY, G., BERKERS, J., PARIDAENS, R., SCHOFFSKI, P., MEJEAN, A., VERKARRE, V., LERUT, E., DE LA TAILLE, A., TOURANI, J. M., BIGOT, P., LINASSIER, C., NEGRIER, S., BERGER, J., PATARD, J. J., ZUCMAN-ROSSI, J. & OUDARD, S. 2013. Single-nucleotide polymorphisms associated with outcome in metastatic renal cell carcinoma treated with sunitinib. *British journal of cancer*, 108, 887-900.
- BEUSELINCK, B., KARADIMOU, A., LAMBRECHTS, D., CLAES, B., WOLTER, P., COUCHY, G., BERKERS, J., VAN POPPEL, H., PARIDAENS, R., SCHOFFSKI, P., MEJEAN, A., VERKARRE, V., LERUT, E., JOLY, F., LEBRET, T., GRAVIS, G., DEPLANQUE, G., DESCAZEAUD, A., LECLERCQ, N. R., MOLINIE, V., PATARD, J. J., TEGHOM, C., ELAIDI, R., ZUCMAN-ROSSI, J. & OUDARD, S. 2014. VEGFR1 single nucleotide polymorphisms associated with outcome in patients with metastatic renal cell carcinoma treated with sunitinib - a multicentric retrospective analysis. *Acta Oncol*, 53, 103-12.
- BHARGAVA, P. E., B.; AL-ADHAMI, M.; NOSOV, D.; LIPATOV, O.N.; LYULKO, A.A.; ANISCHENKO, A.A.; CHACKO, R.T.; SLICHENMYER, W.J. 2010. Effect of hypertension, nephrectomy, and prior treatment on the efficacy of tivozanib (AV-951) in a phase II randomized discontinuation trial (RDT) in patients with renal cell carcinoma (RCC). *Poster presented at the American Society of Clinical Oncology Genitourinary Cancers Symposium (Abstract 342)*.
- BIRCH, A. H., QUINN, M. C., FILALI-MOUHIM, A., PROVENCHER, D. M., MES-MASSON, A. M. & TONIN, P. N. 2008. Transcriptome analysis of serous ovarian cancers identifies differentially expressed chromosome 3 genes. *Molecular carcinogenesis*, 47, 56-65.
- BIRCHMEIER, W. & BEHRENS, J. 1994. Cadherin expression in carcinomas: role in the formation of cell junctions and the prevention of invasiveness. *Biochim Biophys Acta*, 1198, 11-26.
- BOEHM, S., ROTHERMUNDT, C., HESS, D. & JOERGER, M. 2010. Antiangiogenic drugs in oncology: a focus on drug safety and the elderly - a mini-review. *Gerontology*, 56, 303-9.

- BOISSAN, M., BEUREL, E., WENDUM, D., REY, C., LECLUSE, Y., HOUSSET, C., LACOMBE, M. L. & DESBOIS-MOUTHON, C. 2005. Overexpression of insulin receptor substrate-2 in human and murine hepatocellular carcinoma. *Am J Pathol*, 167, 869-77.
- BONO, P., RAUTIOLA, J., UTRIAINEN, T. & JOENSUU, H. 2011. Hypertension as predictor of sunitinib treatment outcome in metastatic renal cell carcinoma. *Acta Oncol*, 50, 569-73.
- BORST, J., HENDRIKS, J. & XIAO, Y. 2005. CD27 and CD70 in T cell and B cell activation. *Curr Opin Immunol*, 17, 275-81.
- BORZA, T., IANCU, C. V., PIKE, E., HONZATKO, R. B. & FROMM, H. J. 2003. Variations in the response of mouse isozymes of adenylosuccinate synthetase to inhibitors of physiological relevance. *J Biol Chem*, 278, 6673-9.
- BRAEUER, R. R., ZIGLER, M., VILLARES, G. J., DOBROFF, A. S. & BAR-ELI, M. 2011. Transcriptional control of melanoma metastasis: the importance of the tumor microenvironment. *Semin Cancer Biol*, 21, 83-8.
- BRANNON, A. R. & RATHMELL, W. K. 2010. Renal cell carcinoma: where will the state-of-the-art lead us? *Current oncology reports*, 12, 193-201.
- BRIAUD, I., DICKSON, L. M., LINGOHR, M. K., MCCUAIG, J. F., LAWRENCE, J. C. & RHODES, C. J. 2005. Insulin receptor substrate-2 proteasomal degradation mediated by a mammalian target of rapamycin (mTOR)-induced negative feedback down-regulates protein kinase B-mediated signaling pathway in beta-cells. *J Biol Chem*, 280, 2282-93.
- BRINKMANN, V., REICHARD, U., GOOSMANN, C., FAULER, B., UHLEMANN, Y., WEISS, D. S., WEINRAUCH, Y. & ZYCHLINSKY, A. 2004. Neutrophil extracellular traps kill bacteria. *Science*, 303, 1532-5.
- BROUTIN, S., AMEUR, N., LACROIX, L., ROBERT, T., PETIT, B., OUMATA, N., TALBOT, M., CAILLOU, B., SCHLUMBERGER, M., DUPUY, C. & BIDART, J. M. 2011. Identification of soluble candidate biomarkers of therapeutic response to sunitinib in medullary thyroid carcinoma in preclinical models. *Clin Cancer Res*, 17, 2044-54.
- BROUXHON, S. M., KYRKANIDES, S., TENG, X., ATHAR, M., GHAZIZADEH, S., SIMON, M., O'BANION, M. K. & MA, L. 2014. Soluble E-cadherin: a critical oncogene modulating receptor tyrosine kinases, MAPK and PI3K/Akt/mTOR signaling. *Oncogene*, 33, 225-35.
- BROWN, G. R., MEEK, K., NISHIOKA, Y. & THIELE, D. L. 1995. CD27-CD27 ligand/CD70 interactions enhance alloantigen-induced proliferation and cytolytic activity in CD8+ T lymphocytes. *J Immunol*, 154, 3686-95.
- BROWN, L. M., HELMKE, S. M., HUNSUCKER, S. W., NETEA-MAIER, R. T., CHIANG, S. A., HEINZ, D. E., SHROYER, K. R., DUNCAN, M. W. & HAUGEN, B. R. 2006. Quantitative and qualitative differences in protein expression between papillary thyroid carcinoma and normal thyroid tissue. *Mol Carcinog*, 45, 613-26.
- BRUNING, J. C., WINNAY, J., CHEATHAM, B. & KAHN, C. R. 1997. Differential signaling by insulin receptor substrate 1 (IRS-1) and IRS-2 in IRS-1-deficient cells. *Mol Cell Biol*, 17, 1513-21.
- BUI, M. H., SELIGSON, D., HAN, K. R., PANTUCK, A. J., DOREY, F. J., HUANG, Y., HORVATH, S., LEBOVICH, B. C., CHOPRA, S., LIAO, S. Y., STANBRIDGE, E., LERMAN, M. I., PALOTIE, A., FIGLIN, R. A. & BELLDEGRUN, A. S. 2003. Carbonic anhydrase IX is an independent predictor of survival in advanced renal clear cell carcinoma: implications for prognosis and therapy. *Clin Cancer Res*, 9, 802-11.
- BUKHOLM, I. K., NESLAND, J. M. & BORRESEN-DALE, A. L. 2000. Re-expression of E-cadherin, alpha-catenin and beta-catenin, but not of

- gamma-catenin, in metastatic tissue from breast cancer patients [seecomments]. *J Pathol*, 190, 15-9.
- BURKLY, L. C., JAKUBOWSKI, A., NEWMAN, B. M., ROSA, M. D., CHI-ROSSO, G. & LOBB, R. R. 1991. Signaling by vascular cell adhesion molecule-1 (VCAM-1) through VLA-4 promotes CD3-dependent T cell proliferation. *Eur J Immunol*, 21, 2871-5.
- BYRON, S. A., HORWITZ, K. B., RICHER, J. K., LANGE, C. A., ZHANG, X. & YEE, D. 2006. Insulin receptor substrates mediate distinct biological responses to insulin-like growth factor receptor activation in breast cancer cells. *Br J Cancer*, 95, 1220-8.
- C, D. A., PORTELLA, L., OTTAIANO, A., RIZZO, M., CARTENI, G., PIGNATA, S., FACCHINI, G., PERDONA, S., DI LORENZO, G., AUTORINO, R., FRANCO, R., LA MURA, A., NAPPI, O., CASTELLO, G. & SCALA, S. 2012. High CXCR4 expression correlates with sunitinib poor response in metastatic renal cancer. *Curr Cancer Drug Targets*, 12, 693-702.
- CAIRNS, P. 2010. Renal cell carcinoma. *Cancer Biomark*, 9, 461-73.
- CARME LIET, P. & JAIN, R. K. 2011. Molecular mechanisms and clinical applications of angiogenesis. *Nature*, 473, 298-307.
- CASANOVAS, O., HICKLIN, D. J., BERGERS, G. & HANAHAN, D. 2005. Drug resistance by evasion of antiangiogenic targeting of VEGF signaling in late-stage pancreatic islet tumors. *Cancer cell*, 8, 299-309.
- CHAN, C. W., KAY, L. S., KHADAROO, R. G., CHAN, M. W., LAKATOO, S., YOUNG, K. J., ZHANG, L., GORCZYNSKI, R. M., CATTRAL, M., ROTSTEIN, O. & LEVY, G. A. 2003. Soluble fibrinogen-like protein 2/fibroleukin exhibits immunosuppressive properties: suppressing T cell proliferation and inhibiting maturation of bone marrow-derived dendritic cells. *J Immunol*, 170, 4036-44.
- CHAND, H. S., DU, X., MA, D., INZUNZA, H. D., KAMEI, S., FOSTER, D., BRODIE, S. & KISIEL, W. 2004. The effect of human tissue factor pathway inhibitor-2 on the growth and metastasis of fibrosarcoma tumors in athymic mice. *Blood*, 103, 1069-77.
- CHARAFE-JAUFFRET, E., MONVILLE, F., BERTUCCI, F., ESTERNI, B., GINESTIER, C., FINETTI, P., CERVERA, N., GENEIX, J., HASSANEIN, M., RABAYROL, L., SOBOL, H., TARANGER-CHARPIN, C., XERRI, L., VIENS, P., BIRNBAUM, D. & JACQUEMIER, J. 2007. Moesin expression is a marker of basal breast carcinomas. *International journal of cancer. Journal international du cancer*, 121, 1779-85.
- CHAUDHURY, A., CHANDER, P. & HOWE, P. H. 2010. Heterogeneous nuclear ribonucleoproteins (hnRNPs) in cellular processes: Focus on hnRNP E1's multifunctional regulatory roles. *RNA*, 16, 1449-62.
- CHEN, Q., ZHANG, X. H. & MASSAGUE, J. 2011. Macrophage binding to receptor VCAM-1 transmits survival signals in breast cancer cells that invade the lungs. *Cancer Cell*, 20, 538-49.
- CHOI, H., CHARNSANGAVEJ, C., FARIA, S. C., MACAPINLAC, H. A., BURGESS, M. A., PATEL, S. R., CHEN, L. L., PODOLOFF, D. A. & BENJAMIN, R. S. 2007. Correlation of computed tomography and positron emission tomography in patients with metastatic gastrointestinal stromal tumor treated at a single institution with imatinib mesylate: proposal of new computed tomography response criteria. *Journal of Clinical Oncology*, 25, 1753-9.
- CHOUERI, T. K., VAZIRI, S. A., JAEGER, E., ELSON, P., WOOD, L., BHALLA, I. P., SMALL, E. J., WEINBERG, V., SEIN, N., SIMKO, J., GOLSHAYAN, A. R., SERCIA, L., ZHOU, M., WALDMAN, F. M., RINI, B. I., BUKOWSKI, R. M. & GANAPATHI, R. 2008. von Hippel-Lindau gene status and response to

- vascular endothelial growth factor targeted therapy for metastatic clear cell renal cell carcinoma. *J Urol*, 180, 860-5; discussion 865-6.
- CHOW, J. Y., LI, Z. J., WU, W. K. & CHO, C. H. 2013. Cathelicidin a potential therapeutic peptide for gastrointestinal inflammation and cancer. *World J Gastroenterol*, 19, 2731-5.
- CHOW, W. H., DONG, L. M. & DEVESA, S. S. 2010. Epidemiology and risk factors for kidney cancer. *Nature reviews. Urology*, 7, 245-57.
- CICENAS, J. & VALIUS, M. 2011. The CDK inhibitors in cancer research and therapy. *J Cancer Res Clin Oncol*, 137, 1409-18.
- CIRIELLO, G., MILLER, M. L., AKSOY, B. A., SENBABAOGU, Y., SCHULTZ, N. & SANDER, C. 2013. Emerging landscape of oncogenic signatures across human cancers. *Nat Genet*, 45, 1127-1133.
- CLIFFORD, S. C., COCKMAN, M. E., SMALLWOOD, A. C., MOLE, D. R., WOODWARD, E. R., MAXWELL, P. H., RATCLIFFE, P. J. & MAHER, E. R. 2001. Contrasting effects on HIF-1alpha regulation by disease-causing pVHL mutations correlate with patterns of tumorigenesis in von Hippel-Lindau disease. *Human molecular genetics*, 10, 1029-38.
- COFFELT, S. B., WATERMAN, R. S., FLOREZ, L., HONER ZU BENTRUP, K., ZWEZDARYK, K. J., TOMCHUCK, S. L., LAMARCA, H. L., DANKA, E. S., MORRIS, C. A. & SCANDURRO, A. B. 2008. Ovarian cancers overexpress the antimicrobial protein hCAP-18 and its derivative LL-37 increases ovarian cancer cell proliferation and invasion. *International journal of cancer. Journal international du cancer*, 122, 1030-9.
- COLLINSON, F., HUTCHINSON, M., CRAVEN, R. A., CAIRNS, D. A., ZOUGMAN, A., WIND, T. C., GAHIR, N., MESSENGER, M. P., JACKSON, S., THOMPSON, D., ADUSEI, C., LEDERMANN, J. A., HALL, G., JAYSON, G. C., SELBY, P. J. & BANKS, R. E. 2013. Predicting response to bevacizumab in ovarian cancer: a panel of potential biomarkers informing treatment selection. *Clin Cancer Res*, 19, 5227-39.
- COOLS-LARTIGUE, J., SPICER, J., MCDONALD, B., GOWING, S., CHOW, S., GIANNIAS, B., BOURDEAU, F., KUBES, P. & FERRI, L. 2013. Neutrophil extracellular traps sequester circulating tumor cells and promote metastasis. *J Clin Invest*.
- COPPIN, C., PORZSOLT, F., AWA, A., KUMPF, J., COLDMAN, A. & WILT, T. 2005. Immunotherapy for advanced renal cell cancer. *Cochrane Database Syst Rev*, CD001425.
- COSTA, V. L., HENRIQUE, R., DANIELSEN, S. A., EKNAES, M., PATRICIO, P., MORAIS, A., OLIVEIRA, J., LOTHE, R. A., TEIXEIRA, M. R., LIND, G. E. & JERONIMO, C. 2011. TCF21 and PCDH17 methylation: An innovative panel of biomarkers for a simultaneous detection of urological cancers. *Epigenetics*, 6, 1120-30.
- COUDERC, B., ZITVOGEL, L., DOUIN-ECHINARD, V., DJENNANE, L., TAHARA, H., FAVRE, G., LOTZE, M. T. & ROBBINS, P. D. 1998. Enhancement of antitumor immunity by expression of CD70 (CD27 ligand) or CD154 (CD40 ligand) costimulatory molecules in tumor cells. *Cancer Gene Ther*, 5, 163-75.
- COWEY, C. L., FIELDING, J. R. & RATHMELL, W. K. 2010. The loss of radiographic enhancement in primary renal cell carcinoma tumors following multitargeted receptor tyrosine kinase therapy is an additional indicator of response. *Urology*, 75, 1108-13 e1.
- COX, J. & MANN, M. 2008a. MaxQuant enables high peptide identification rates, individualized p.p.b.-range mass accuracies and proteome-wide protein quantification. *Nature biotechnology*, 26, 1367-72.

- COX, J. & MANN, M. 2008b. MaxQuant enables high peptide identification rates, individualized p.p.b.-range mass accuracies and proteome-wide protein quantification. *Nat Biotechnol*, 26, 1367-72.
- COX, J., MATIC, I., HILGER, M., NAGARAJ, N., SELBACH, M., OLSEN, J. V. & MANN, M. 2009. A practical guide to the MaxQuant computational platform for SILAC-based quantitative proteomics. *Nat Protoc*, 4, 698-705.
- CRAVEN, R. A., CAIRNS, D. A., ZOUGMAN, A., HARNDEN, P., SELBY, P. J. & BANKS, R. E. 2013a. Proteomic analysis of formalin-fixed paraffin-embedded renal tissue samples by label-free MS: assessment of overall technical variability and the impact of block age. *Proteomics Clin Appl*, 7, 273-82.
- CRAVEN, R. A., HANRAHAN, S., TOTTY, N., HARNDEN, P., STANLEY, A. J., MAHER, E. R., HARRIS, A. L., TRIMBLE, W. S., SELBY, P. J. & BANKS, R. E. 2006. Proteomic identification of a role for the von Hippel Lindau tumour suppressor in changes in the expression of mitochondrial proteins and septin 2 in renal cell carcinoma. *Proteomics*, 6, 3880-93.
- CRAVEN, R. A., VASUDEEV, N. S. & BANKS, R. E. 2013b. Proteomics and the search for biomarkers for renal cancer. *Clin Biochem*, 46, 456-65.
- CROSS, S. S., HAMDY, F. C., DELOULME, J. C. & REHMAN, I. 2005. Expression of S100 proteins in normal human tissues and common cancers using tissue microarrays: S100A6, S100A8, S100A9 and S100A11 are all overexpressed in common cancers. *Histopathology*, 46, 256-69.
- CROSSEY, P. A., RICHARDS, F. M., FOSTER, K., GREEN, J. S., PROWSE, A., LATIF, F., LERMAN, M. I., ZBAR, B., AFFARA, N. A., FERGUSON-SMITH, M. A. & ET AL. 1994. Identification of intragenic mutations in the von Hippel-Lindau disease tumour suppressor gene and correlation with disease phenotype. *Human molecular genetics*, 3, 1303-8.
- DALGLIESH, G. L., FURGE, K., GREENMAN, C., CHEN, L., BIGNELL, G., BUTLER, A., DAVIES, H., EDKINS, S., HARDY, C., LATIMER, C., TEAGUE, J., ANDREWS, J., BARTHORPE, S., BEARE, D., BUCK, G., CAMPBELL, P. J., FORBES, S., JIA, M., JONES, D., KNOTT, H., KOK, C. Y., LAU, K. W., LEROY, C., LIN, M. L., MCBRIDE, D. J., MADDISON, M., MAGUIRE, S., MCLAY, K., MENZIES, A., MIRONENKO, T., MULDERRIG, L., MUDIE, L., O'MEARA, S., PLEASANCE, E., RAJASINGHAM, A., SHEPHERD, R., SMITH, R., STEBBINGS, L., STEPHENS, P., TANG, G., TARPEY, P. S., TURRELL, K., DYKEMA, K. J., KHOO, S. K., PETILLO, D., WONDERGEM, B., ANEMA, J., KAHNOSKI, R. J., TEH, B. T., STRATTON, M. R. & FUTREAL, P. A. 2010. Systematic sequencing of renal carcinoma reveals inactivation of histone modifying genes. *Nature*, 463, 360-3.
- DAMLE, N. K. & ARUFFO, A. 1991. Vascular cell adhesion molecule 1 induces T-cell antigen receptor-dependent activation of CD4+T lymphocytes. *Proc Natl Acad Sci U S A*, 88, 6403-7.
- DAMLE, N. K., EBERHARDT, C. & VAN DER VIEREN, M. 1991. Direct interaction with primed CD4+ CD45R0+ memory T lymphocytes induces expression of endothelial leukocyte adhesion molecule-1 and vascular cell adhesion molecule-1 on the surface of vascular endothelial cells. *Eur J Immunol*, 21, 2915-23.
- DANG, D. T., CHUN, S. Y., BURKITT, K., ABE, M., CHEN, S., HAVRE, P., MABJEESH, N. J., HEATH, E. I., VOGELZANG, N. J., CRUZ-CORREA, M., BLAYNEY, D. W., ENSMINGER, W. D., ST CROIX, B., DANG, N. H. & DANG, L. H. 2008. Hypoxia-inducible factor-1 target genes as indicators of tumor vessel response to vascular endothelial growth factor inhibition. *Cancer Res*, 68, 1872-80.

- DAVIDOWITZ, E. J., SCHOENFELD, A. R. & BURK, R. D. 2001. VHL induces renal cell differentiation and growth arrest through integration of cell-cell and cell-extracellular matrix signaling. *Mol Cell Biol*, 21, 865-74.
- DAVIS, M. P., FIGLIN, R. A., HUTSON, T. E., GOLDSTEIN, D., LI, S., PERKINS, J. & MOTZER, R. J. 2011. Asthenia and Fatigue as Potential Biomarkers of Sunitinib Efficacy in Metastatic Renal Cell Carcinoma. *European journal of cancer*, 47, S135-S135.
- DE BOCK, K., MAZZONE, M. & CARMELIET, P. 2011. Antiangiogenic therapy, hypoxia, and metastasis: risky liaisons, or not? *Nature reviews. Clinical oncology*, 8, 393-404.
- DE LARCO, J. E., WUERTZ, B. R. & FURCHT, L. T. 2004. The potential role of neutrophils in promoting the metastatic phenotype of tumors releasing interleukin-8. *Clin Cancer Res*, 10, 4895-900.
- DEARTH, R. K., CUI, X., KIM, H. J., HADSELL, D. L. & LEE, A. V. 2007. Oncogenic transformation by the signaling adaptor proteins insulin receptor substrate (IRS)-1 and IRS-2. *Cell Cycle*, 6, 705-13.
- DEL PUERTO-NEVADO, L., ROJO, F., ZAZO, S., CARAMES, C., RUBIO, G., VEGA, R., CHAMIZO, C., CASADO, V., MARTINEZ-USEROS, J., RINCON, R., RODRIGUEZ-REMIREZ, M., BORRERO-PALACIOS, A., CRISTOBAL, I., MADOZ-GURPIDE, J., AGUILERA, O. & GARCIA-FONCILLAS, J. 2014. Active angiogenesis in metastatic renal cell carcinoma predicts clinical benefit to sunitinib-based therapy. *British journal of cancer*, 110, 2700-7.
- DEPRIMO, S. E., BELLO, C. L., SMERAGLIA, J., BAUM, C. M., SPINELLA, D., RINI, B. I., MICHAELSON, M. D. & MOTZER, R. J. 2007. Circulating protein biomarkers of pharmacodynamic activity of sunitinib in patients with metastatic renal cell carcinoma: modulation of VEGF and VEGF-related proteins. *Journal of translational medicine*, 5, 32.
- DIEGMANN, J., JUNKER, K., GERSTMAYER, B., BOSIO, A., HINDERMANN, W., ROSENHAHN, J. & VON EGGELING, F. 2005. Identification of CD70 as a diagnostic biomarker for clear cell renal cell carcinoma by gene expression profiling, real-time RT-PCR and immunohistochemistry. *European journal of cancer*, 41, 1794-801.
- DIEGMANN, J., JUNKER, K., LONCAREVIC, I. F., MICHEL, S., SCHIMMEL, B. & VON EGGELING, F. 2006. Immune escape for renal cell carcinoma: CD70 mediates apoptosis in lymphocytes. *Neoplasia*, 8, 933-8.
- DIRICAN, A., KUCUKZEYBEK, Y., SOMALI, I., ERTEN, C., DEMIR, L., CAN, A., BAHRIYE PAYZIN, K., VEDAT BAYOGLU, I., AKYOL, M., KOSEOGLU, M., ALACACIOGLU, A. & OKTAY TARHAN, M. 2013. The association of hematologic parameters on the prognosis of patients with metastatic renal cell carcinoma. *J BUON*, 18, 413-9.
- DONSKOV, F., MICHAELSON, M. D., PUZANOV, I., DAVIS, M. P., BJARNASON, G. A., MOTZER, R. J., LIN, X., COHEN, D. P., WILTSHIRE, R. & RINI, B. I. 2012. Comparative Assessment of Sunitinib-Associated Adverse Events (Aes) as Potential Biomarkers of Efficacy in Metastatic Renal Cell Carcinoma (Mrcc). *Annals of Oncology*, 23, 259-259.
- DORNBUSCH, J., ZACHARIS, A., MEINHARDT, M., ERDMANN, K., WOLFF, I., FROEHNER, M., WIRTH, M. P., ZASTROW, S. & FUESSEL, S. 2013. Analyses of potential predictive markers and survival data for a response to sunitinib in patients with metastatic renal cell carcinoma. *PloS one*, 8, e76386.
- DU, R., LU, K. V., PETRITSCH, C., LIU, P., GANSS, R., PASSEGUE, E., SONG, H., VANDENBERG, S., JOHNSON, R. S., WERB, Z. & BERGERS, G. 2008. HIF1alpha induces the recruitment of bone marrow-derived vascular

- modulatory cells to regulate tumor angiogenesis and invasion. *Cancer cell*, 13, 206-20.
- DU, S., GUAN, Z., HAO, L., SONG, Y., WANG, L., GONG, L., LIU, L., QI, X., HOU, Z. & SHAO, S. 2014. Fructose-bisphosphate aldolase a is a potential metastasis-associated marker of lung squamous cell carcinoma and promotes lung cell tumorigenesis and migration. *PloS one*, 9, e85804.
- EBOS, J. M., LEE, C. R., CHRISTENSEN, J. G., MUTSAERS, A. J. & KERBEL, R. S. 2007. Multiple circulating proangiogenic factors induced by sunitinib malate are tumor-independent and correlate with antitumor efficacy. *Proceedings of the National Academy of Sciences of the United States of America*, 104, 17069-74.
- EBOS, J. M., LEE, C. R., CRUZ-MUNOZ, W., BJARNASON, G. A., CHRISTENSEN, J. G. & KERBEL, R. S. 2009. Accelerated metastasis after short-term treatment with a potent inhibitor of tumor angiogenesis. *Cancer cell*, 15, 232-9.
- ECKERICH, C., ZAPF, S., ULBRICHT, U., MÜLLER, S., FILLBRANDT, R., WESTPHAL, M. & LAMSZUS, K. 2006. Contactin is expressed in human astrocytic gliomas and mediates repulsive effects. *Glia*, 53, 1-12.
- EECHOUTE, K., VAN DER VELDT, A. A., OOSTING, S., KAPPERS, M. H., WESSELS, J. A., GELDERBLOM, H., GUCHELAAR, H. J., REYNERS, A. K., VAN HERPEN, C. M., HAANEN, J. B., MATHIJSSSEN, R. H. & BOVEN, E. 2012. Polymorphisms in endothelial nitric oxide synthase (eNOS) and vascular endothelial growth factor (VEGF) predict sunitinib-induced hypertension. *Clin Pharmacol Ther*, 92, 503-10.
- EICHELBERG, C., JUNKER, K., LJUNGBERG, B. & MOCH, H. 2009. Diagnostic and prognostic molecular markers for renal cell carcinoma: a critical appraisal of the current state of research and clinical applicability. *European urology*, 55, 851-63.
- EICHENMULLER, B., EVERLEY, P., PALANGE, J., LEPLEY, D. & SUPRENANT, K. A. 2002. The human EMAP-like protein-70 (ELP70) is a microtubule destabilizer that localizes to the mitotic apparatus. *J Biol Chem*, 277, 1301-9.
- EISENHAUER, E. A., THERASSE, P., BOGAERTS, J., SCHWARTZ, L. H., SARGENT, D., FORD, R., DANCEY, J., ARBUCK, S., GWYTHYER, S., MOONEY, M., RUBINSTEIN, L., SHANKAR, L., DODD, L., KAPLAN, R., LACOMBE, D. & VERWEIJ, J. 2009. New response evaluation criteria in solid tumours: revised RECIST guideline (version 1.1). *European journal of cancer*, 45, 228-47.
- ELLIS, L. M. 2006. The role of neuropilins in cancer. *Mol Cancer Ther*, 5, 1099-107.
- ELTZSCHIG, H. K., FAIGLE, M., KNAPP, S., KARHAUSEN, J., IBLA, J., ROSENBERGER, P., ODEGARD, K. C., LAUSSEN, P. C., THOMPSON, L. F. & COLGAN, S. P. 2006. Endothelial catabolism of extracellular adenosine during hypoxia: the role of surface adenosine deaminase and CD26. *Blood*, 108, 1602-10.
- ERBER, R., THURNHER, A., KATSEN, A. D., GROTH, G., KERGER, H., HAMMES, H. P., MENGER, M. D., ULLRICH, A. & VAJKOCZY, P. 2004. Combined inhibition of VEGF and PDGF signaling enforces tumor vessel regression by interfering with pericyte-mediated endothelial cell survival mechanisms. *The FASEB journal : official publication of the Federation of American Societies for Experimental Biology*, 18, 338-40.
- ESCUDIER, B., EISEN, T., STADLER, W. M., SZCZYLIK, C., OUDARD, S., SIEBELS, M., NEGRIER, S., CHEVREAU, C., SOLSKA, E., DESAI, A. A., ROLLAND, F., DEMKOW, T., HUTSON, T. E., GORE, M., FREEMAN, S., SCHWARTZ, B., SHAN, M., SIMANTOV, R. & BUKOWSKI, R. M. 2007a.

- Sorafenib in advanced clear-cell renal-cell carcinoma. *The New England journal of medicine*, 356, 125-34.
- ESCUДИER, B., EISEN, T., STADLER, W. M., SZCZYLIK, C., OUDARD, S., STAEHLER, M., NEGRIER, S., CHEVREAU, C., DESAI, A. A., ROLLAND, F., DEMKOW, T., HUTSON, T. E., GORE, M., ANDERSON, S., HOFILENA, G., SHAN, M., PENA, C., LATHIA, C. & BUKOWSKI, R. M. 2009a. Sorafenib for treatment of renal cell carcinoma: Final efficacy and safety results of the phase III treatment approaches in renal cancer global evaluation trial. *Journal of clinical oncology : official journal of the American Society of Clinical Oncology*, 27, 3312-8.
- ESCUДИER, B. & GORE, M. 2011. Axitinib for the management of metastatic renal cell carcinoma. *Drugs R D*, 11, 113-26.
- ESCUДИER, B., GOUPIL, M. G., MASSARD, C. & FIZAZI, K. 2009b. Sequential therapy in renal cell carcinoma. *Cancer*, 115, 2321-6.
- ESCUДИER, B., PLUZANSKA, A., KORALEWSKI, P., RAVAUD, A., BRACARDA, S., SZCZYLIK, C., CHEVREAU, C., FILIPEK, M., MELICHAR, B., BAJETTA, E., GORBUNOVA, V., BAY, J. O., BODROGI, I., JAGIELLOGRUSZFELD, A. & MOORE, N. 2007b. Bevacizumab plus interferon alfa-2a for treatment of metastatic renal cell carcinoma: a randomised, double-blind phase III trial. *Lancet*, 370, 2103-11.
- ESTECHA, A., SANCHEZ-MARTIN, L., PUIG-KROGER, A., BARTOLOME, R. A., TEIXIDO, J., SAMANIEGO, R. & SANCHEZ-MATEOS, P. 2009. Moesin orchestrates cortical polarity of melanoma tumour cells to initiate 3D invasion. *J Cell Sci*, 122, 3492-501.
- FAIVRE SJ, R. E., DOUILLARD J, BOUCHER E, LIM HY, KIM JS, LANZALONE & S, L. M., SHERMAN L, CHENG A 2007. Assessment of safety and drug-induced tumor necrosis with sunitinib in patients (pts) with unresectable hepatocellular carcinoma (HCC). *Journal of clinical oncology : official journal of the American Society of Clinical Oncology*, 25.
- FARACE, F., GROSS-GOUPIL, M., TOURNAY, E., TAYLOR, M., VIMOND, N., JACQUES, N., BILLIOT, F., MAUGUEN, A., HILL, C. & ESCUDIER, B. 2011. Levels of circulating CD45(dim)CD34(+)VEGFR2(+) progenitor cells correlate with outcome in metastatic renal cell carcinoma patients treated with tyrosine kinase inhibitors. *British journal of cancer*, 104, 1144-50.
- FAURSCHOU, M. & BORREGAARD, N. 2003. Neutrophil granules and secretory vesicles in inflammation. *Microbes Infect*, 5, 1317-27.
- FENNER, B. J., SCANNELL, M. & PREHN, J. H. 2009. Identification of polyubiquitin binding proteins involved in NF-kappaB signaling using protein arrays. *Biochim Biophys Acta*, 1794, 1010-6.
- FERLAY J, S. I., ERVIK M, DIKSHIT R, ESER S, MATHERS C, REBELO M, PARKIN DM, FORMAN D, BRAY, F. 2013. *GLOBOCAN 2012 v1.0, Cancer Incidence and Mortality Worldwide: IARC CancerBase No. 11 [Internet]* [Online]. Lyon, France: International Agency for Research on Cancer. Available: <http://globocan.iarc.fr> [Accessed 5th August 2014].
- FIGLIN, R. A., KAUFMANN, I. & BRECHBIEL, J. 2013. Targeting PI3K and mTORC2 in metastatic renal cell carcinoma: new strategies for overcoming resistance to VEGFR and mTORC1 inhibitors. *International journal of cancer. Journal international du cancer*, 133, 788-96.
- FOLKMAN, J. 1971. Tumor angiogenesis: therapeutic implications. *N Engl J Med*, 285, 1182-6.
- FOLKMAN, J. 2007. Angiogenesis: an organizing principle for drug discovery? *Nature reviews. Drug discovery*, 6, 273-86.
- FRANCIS, N., WONG, S. H., HAMPSON, P., WANG, K., YOUNG, S. P., DEIGNER, H. P., SALMON, M., SCHEEL-TOELLNER, D. & LORD, J. M.

2011. Lactoferrin inhibits neutrophil apoptosis via blockade of proximal apoptotic signaling events. *Biochim Biophys Acta*, 1813, 1822-6.
- FRANK, I., BLUTE, M. L., CHEVILLE, J. C., LOHSE, C. M., WEAVER, A. L. & ZINCKE, H. 2002. An outcome prediction model for patients with clear cell renal cell carcinoma treated with radical nephrectomy based on tumor stage, size, grade and necrosis: the SSIGN score. *J Urol*, 168, 2395-400.
- FUJITA, T., IWAMURA, M., ISHII, D., TABATA, K., MATSUMOTO, K., YOSHIDA, K. & BABA, S. 2012. C-reactive protein as a prognostic marker for advanced renal cell carcinoma treated with sunitinib. *International journal of urology : official journal of the Japanese Urological Association*, 19, 908-13.
- FUJITA, T., WAKATABE, Y., MATSUMOTO, K., TABATA, K., YOSHIDA, K. & IWAMURA, M. 2014. Leukopenia as a biomarker of sunitinib outcome in advanced renal cell carcinoma. *Anticancer Res*, 34, 3781-7.
- FUNAKOSHI, T., LEE, C. H. & HSIEH, J. J. 2014. A systematic review of predictive and prognostic biomarkers for VEGF-targeted therapy in renal cell carcinoma. *Cancer Treat Rev*, 40, 533-47.
- FUZERY, A. K., LEVIN, J., CHAN, M. M. & CHAN, D. W. 2013. Translation of proteomic biomarkers into FDA approved cancer diagnostics: issues and challenges. *Clin Proteomics*, 10, 13.
- GAMEZ-POZO, A., ANTON-APARICIO, L. M., BAYONA, C., BORREGA, P., GALLEGOS SANCHO, M. I., GARCIA-DOMINGUEZ, R., DE PORTUGAL, T., RAMOS-VAZQUEZ, M., PEREZ-CARRION, R., BOLOS, M. V., MADERO, R., SANCHEZ-NAVARRO, I., FRESNO VARA, J. A. & ESPINOSA ARRANZ, E. 2012. MicroRNA expression profiling of peripheral blood samples predicts resistance to first-line sunitinib in advanced renal cell carcinoma patients. *Neoplasia*, 14, 1144-52.
- GARCIA-DONAS, J., ESTEBAN, E., LEANDRO-GARCIA, L. J., CASTELLANO, D. E., DEL ALBA, A. G., CLIMENT, M. A., ARRANZ, J. A., GALLARDO, E., PUENTE, J., BELLMUNT, J., MELLADO, B., MARTINEZ, E., MORENO, F., FONT, A., ROBLEDO, M. & RODRIGUEZ-ANTONA, C. 2011. Single nucleotide polymorphism associations with response and toxic effects in patients with advanced renal-cell carcinoma treated with first-line sunitinib: a multicentre, observational, prospective study. *Lancet Oncol*, 12, 1143-50.
- GARCIA-DONAS, J., LEANDRO-GARCIA, L. J., GONZALEZ DEL ALBA, A., MORENTE, M., ALEMANY, I., ESTEBAN, E., ARRANZ, J. A., CLIMENT, M. A., GALLARDO, E., CASTELLANO, D. E., BELLMUNT, J., MELLADO, B., PUENTE, J., MORENO, F., FONT, A., HERNANDO, S., ROBLEDO, M. & RODRIGUEZ-ANTONA, C. 2013. Prospective study assessing hypoxia-related proteins as markers for the outcome of treatment with sunitinib in advanced clear-cell renal cell carcinoma. *Annals of oncology : official journal of the European Society for Medical Oncology / ESMO*, 24, 2409-14.
- GERLINGER, M., ROWAN, A. J., HORSWELL, S., LARKIN, J., ENDESFELDER, D., GRONROOS, E., MARTINEZ, P., MATTHEWS, N., STEWART, A., TARPEY, P., VARELA, I., PHILLIMORE, B., BEGUM, S., MCDONALD, N. Q., BUTLER, A., JONES, D., RAINE, K., LATIMER, C., SANTOS, C. R., NOHADANI, M., EKLUND, A. C., SPENCER-DENE, B., CLARK, G., PICKERING, L., STAMP, G., GORE, M., SZALLASI, Z., DOWNWARD, J., FUTREAL, P. A. & SWANTON, C. 2012. Intratumor heterogeneity and branched evolution revealed by multiregion sequencing. *N Engl J Med*, 366, 883-92.
- GHOSH, R., GILDA, J. E. & GOMES, A. V. 2014. The necessity of and strategies for improving confidence in the accuracy of western blots. *Expert Rev Proteomics*, 11, 549-60.

- GIALELI, C., THEOCHARIS, A. D. & KARAMANOS, N. K. 2011. Roles of matrix metalloproteinases in cancer progression and their pharmacological targeting. *FEBS J*, 278, 16-27.
- GIBSON, U. E., HEID, C. A. & WILLIAMS, P. M. 1996. A novel method for real time quantitative RT-PCR. *Genome Res*, 6, 995-1001.
- GLENN, S. T., JONES, C. A., LIANG, P., KAUSHIK, D., GROSS, K. W. & KIM, H. L. 2007. Expression profiling of archival renal tumors by quantitative PCR to validate prognostic markers. *Biotechniques*, 43, 639-40, 642-3, 647.
- GNARRA, J. R., ZHOU, S., MERRILL, M. J., WAGNER, J. R., KRUMM, A., PAPAVALASSILIOU, E., OLDFIELD, E. H., KLAUSNER, R. D. & LINEHAN, W. M. 1996. Post-transcriptional regulation of vascular endothelial growth factor mRNA by the product of the VHL tumor suppressor gene. *Proceedings of the National Academy of Sciences of the United States of America*, 93, 10589-94.
- GOODWIN, R. G., ALDERSON, M. R., SMITH, C. A., ARMITAGE, R. J., VANDENBOS, T., JERZY, R., TOUGH, T. W., SCHOENBORN, M. A., DAVIS-SMITH, T., HENNEN, K. & ET AL. 1993. Molecular and biological characterization of a ligand for CD27 defines a new family of cytokines with homology to tumor necrosis factor. *Cell*, 73, 447-56.
- GOSSAGE, L., MURTAZA, M., SLATTER, A. F., LICHTENSTEIN, C. P., WARREN, A., HAYNES, B., MARASS, F., ROBERTS, I., SHANAHAN, S. J., CLAAS, A., DUNHAM, A., MAY, A. P., ROSENFELD, N., FORSHEW, T. & EISEN, T. 2014. Clinical and pathological impact of VHL, PBRM1, BAP1, SETD2, KDM6A, and JARID1c in clear cell renal cell carcinoma. *Genes Chromosomes Cancer*, 53, 38-51.
- GREGORY, A. D. & HOUGHTON, A. M. 2011. Tumor-associated neutrophils: new targets for cancer therapy. *Cancer Res*, 71, 2411-6.
- GREWAL, I. S. 2008. CD70 as a therapeutic target in human malignancies. *Expert Opin Ther Targets*, 12, 341-51.
- GRUENWALD, V., BEUTEL, G., SCHUCH-JANTSCH, S., REUTER, C., IVANYI, P., GANSER, A. & HAUBITZ, M. 2010. Circulating endothelial cells are an early predictor in renal cell carcinoma for tumor response to sunitinib. *BMC cancer*, 10, 695.
- GRUSS, H. J. & DOWER, S. K. 1995. Tumor necrosis factor ligand superfamily: involvement in the pathology of malignant lymphomas. *Blood*, 85, 3378-404.
- GUENTHER, M. G., BARAK, O. & LAZAR, M. A. 2001. The SMRT and N-CoR corepressors are activating cofactors for histone deacetylase 3. *Mol Cell Biol*, 21, 6091-101.
- GUNDRY, R. L., FU, Q., JELINEK, C. A., VAN EYK, J. E. & COTTER, R. J. 2007. Investigation of an albumin-enriched fraction of human serum and its albuminome. *Proteomics. Clinical applications*, 1, 73-88.
- GUNGOR, N., KNAAPEN, A. M., MUNNIA, A., PELUSO, M., HAENEN, G. R., CHIU, R. K., GODSCHALK, R. W. & VAN SCHOOTEN, F. J. 2010. Genotoxic effects of neutrophils and hypochlorous acid. *Mutagenesis*, 25, 149-54.
- HAMBERG, P., VERWEIJ, J. & SLEIJFER, S. 2010. (Pre-)clinical pharmacology and activity of pazopanib, a novel multikinase angiogenesis inhibitor. *The oncologist*, 15, 539-47.
- HAMMERS HJ, P. E., JEFFREY R. INFANTE, MARC S. ERNSTOFF, BRIAN I. RINI, DAVID F. MCDERMOTT, ALBIRUNI R. A. RAZAK, SUMANTA KUMAR PAL, MARTIN HENNER VOSS, PADMANEE SHARMA, CHRISTIAN K. KOLLMANNBERGER, DANIEL YICK CHIN HENG, JENNIFER L. SPRATLIN, YUN SHEN, JOHN F. KURLAND, PAUL GAGNIER, ASIM AMIN 2014. Phase I study of nivolumab in combination

- with ipilimumab in metastatic renal cell carcinoma (mRCC). *Journal of clinical oncology : official journal of the American Society of Clinical Oncology*, 32.
- HAMMOND, M. E., LAPOINTE, G. R., FEUCHT, P. H., HILT, S., GALLEGOS, C. A., GORDON, C. A., GIEDLIN, M. A., MULLENBACH, G. & TEKAMP-OLSON, P. 1995. IL-8 induces neutrophil chemotaxis predominantly via type I IL-8 receptors. *J Immunol*, 155, 1428-33.
- HANKE, S. & MANN, M. 2009. The phosphotyrosine interactome of the insulin receptor family and its substrates IRS-1 and IRS-2. *Mol Cell Proteomics*, 8, 519-34.
- HARMON, C. S., DEPRIMO, S. E., FIGLIN, R. A., HUDES, G. R., HUTSON, T. E., MICHAELSON, M. D., NEGRIER, S., KIM, S. T., HUANG, X., WILLIAMS, J. A., EISEN, T. & MOTZER, R. J. 2014. Circulating proteins as potential biomarkers of sunitinib and interferon-alpha efficacy in treatment-naive patients with metastatic renal cell carcinoma. *Cancer Chemother Pharmacol*, 73, 151-61.
- HARMON, C. S., DEPRIMO, S. E., RAYMOND, E., CHENG, A. L., BOUCHER, E., DOUILLARD, J. Y., LIM, H. Y., KIM, J. S., LECHUGA, M. J., LANZALONE, S., LIN, X. & FAIVRE, S. 2011. Mechanism-related circulating proteins as biomarkers for clinical outcome in patients with unresectable hepatocellular carcinoma receiving sunitinib. *Journal of translational medicine*, 9, 120.
- HASCHEMI, A., KOSMA, P., GILLE, L., EVANS, C. R., BURANT, C. F., STARKL, P., KNAPP, B., HAAS, R., SCHMID, J. A., JANDL, C., AMIR, S., LUBEC, G., PARK, J., ESTERBAUER, H., BILBAN, M., BRIZUELA, L., POSPISILIK, J. A., OTTERBEIN, L. E. & WAGNER, O. 2012. The sedoheptulose kinase CARL directs macrophage polarization through control of glucose metabolism. *Cell Metab*, 15, 813-26.
- HAYASHIDO, Y., LUCAS, A., ROUGEOT, C., GODYNA, S., ARGRAVES, W. S. & ROCHEFORT, H. 1998. Estradiol and fibulin-1 inhibit motility of human ovarian- and breast-cancer cells induced by fibronectin. *Int J Cancer*, 75, 654-8.
- HE, Q., GAO, Z., YIN, J., ZHANG, J., YUN, Z. & YE, J. 2011. Regulation of HIF-1{alpha} activity in adipose tissue by obesity-associated factors: adipogenesis, insulin, and hypoxia. *Am J Physiol Endocrinol Metab*, 300, E877-85.
- HEILBORN, J. D., NILSSON, M. F., JIMENEZ, C. I., SANDSTEDT, B., BORREGAARD, N., THAM, E., SORENSEN, O. E., WEBER, G. & STAHL, M. 2005. Antimicrobial protein hCAP18/LL-37 is highly expressed in breast cancer and is a putative growth factor for epithelial cells. *International journal of cancer. Journal international du cancer*, 114, 713-9.
- HELD-FEINDT, J. & MENTLEIN, R. 2002. CD70/CD27 ligand, a member of the TNF family, is expressed in human brain tumors. *Int J Cancer*, 98, 352-6.
- HENG, D. Y., KOLLMANNBERGER, C. & CHI, K. N. 2010. Targeted therapy for metastatic renal cell carcinoma: current treatment and future directions. *Therapeutic advances in medical oncology*, 2, 39-49.
- HENG, D. Y., XIE, W., REGAN, M. M., WARREN, M. A., GOLSHAYAN, A. R., SAHI, C., EIGL, B. J., RUETHER, J. D., CHENG, T., NORTH, S., VENNER, P., KNOX, J. J., CHI, K. N., KOLLMANNBERGER, C., MCDERMOTT, D. F., OH, W. K., ATKINS, M. B., BUKOWSKI, R. M., RINI, B. I. & CHOUERI, T. K. 2009. Prognostic factors for overall survival in patients with metastatic renal cell carcinoma treated with vascular endothelial growth factor-targeted agents: results from a large, multicenter study. *Journal of Clinical Oncology*, 27, 5794-9.

- HENSEL, J. A., CHANDA, D., KUMAR, S., SAWANT, A., GRIZZLE, W. E., SIEGAL, G. P. & PONNAZHAGAN, S. 2011. LL-37 as a therapeutic target for late stage prostate cancer. *Prostate*, 71, 659-70.
- HERBERS, J., SCHULLERUS, D., CHUDEK, J., BUGERT, P., KANAMARU, H., ZEISLER, J., LJUNGBERG, B., AKHTAR, M. & KOVACS, G. 1998. Lack of genetic changes at specific genomic sites separates renal oncocytomas from renal cell carcinomas. *J Pathol*, 184, 58-62.
- HERGOVICH, A., LISZTAN, J., BARRY, R., BALLSCHMIETER, P. & KREK, W. 2003. Regulation of microtubule stability by the von Hippel-Lindau tumour suppressor protein pVHL. *Nat Cell Biol*, 5, 64-70.
- HIDAKA, S., YASUTAKE, T., TAKESHITA, H., KONDO, M., TSUJI, T., NANASHIMA, A., SAWAI, T., YAMAGUCHI, H., NAKAGOE, T., AYABE, H. & TAGAWA, Y. 2000. Differences in 20q13.2 copy number between colorectal cancers with and without liver metastasis. *Clin Cancer Res*, 6, 2712-7.
- HILLMAN, G. G., SINGH-GUPTA, V., ZHANG, H., AL-BASHIR, A. K., KATKURI, Y., LI, M., YUNKER, C. K., PATEL, A. D., ABRAMS, J. & HAACKE, E. M. 2009. Dynamic contrast-enhanced magnetic resonance imaging of vascular changes induced by sunitinib in papillary renal cell carcinoma xenograft tumors. *Neoplasia*, 11, 910-20.
- HIRATSUKA, S., WATANABE, A., ABURATANI, H. & MARU, Y. 2006. Tumour-mediated upregulation of chemoattractants and recruitment of myeloid cells predetermines lung metastasis. *Nature cell biology*, 8, 1369-75.
- HISHIMA, T., FUKAYAMA, M., HAYASHI, Y., FUJII, T., Ooba, T., FUNATA, N. & KOIKE, M. 2000. CD70 expression in thymic carcinoma. *Am J Surg Pathol*, 24, 742-6.
- HOANG, C. D., ZHANG, X., SCOTT, P. D., GUILLAUME, T. J., MADDAUS, M. A., YEE, D. & KRATZKE, R. A. 2004. Selective activation of insulin receptor substrate-1 and -2 in pleural mesothelioma cells: association with distinct malignant phenotypes. *Cancer Res*, 64, 7479-85.
- HOEBEN, A., LANDUYT, B., HIGHLEY, M. S., WILDIERS, H., VAN OOSTEROM, A. T. & DE BRUIJN, E. A. 2004. Vascular endothelial growth factor and angiogenesis. *Pharmacological reviews*, 56, 549-80.
- HOFFMAN, M. A., OHH, M., YANG, H., KLCO, J. M., IVAN, M. & KAELIN, W. G., JR. 2001. von Hippel-Lindau protein mutants linked to type 2C VHL disease preserve the ability to downregulate HIF. *Human molecular genetics*, 10, 1019-27.
- HOFFMANN, N. E., SHEININ, Y., LOHSE, C. M., PARKER, A. S., LEIBOVICH, B. C., JIANG, Z. & KWON, E. D. 2008. External validation of IMP3 expression as an independent prognostic marker for metastatic progression and death for patients with clear cell renal cell carcinoma. *Cancer*, 112, 1471-9.
- HOFSLI, E., WHEELER, T. E., LANGAAS, M., LAEGREID, A. & THOMMESEN, L. 2008. Identification of novel neuroendocrine-specific tumour genes. *Br J Cancer*, 99, 1330-9.
- HOLLINGSWORTH, J. M., MILLER, D. C., DAIGNAULT, S. & HOLLENBECK, B. K. 2007. Five-year survival after surgical treatment for kidney cancer: a population-based competing risk analysis. *Cancer*, 109, 1763-8.
- HORIGUCHI, A., OYA, M., SHIMADA, T., UCHIDA, A., MARUMO, K. & MURAI, M. 2002. Activation of signal transducer and activator of transcription 3 in renal cell carcinoma: a study of incidence and its association with pathological features and clinical outcome. *J Urol*, 168, 762-5.
- HUANG, D., DING, Y., ZHOU, M., RINI, B. I., PETILLO, D., QIAN, C. N., KAHNOSKI, R., FUTREAL, P. A., FURGE, K. A. & TEH, B. T. 2010.

- Interleukin-8 mediates resistance to antiangiogenic agent sunitinib in renal cell carcinoma. *Cancer research*, 70, 1063-71.
- HUANG, D. W., SHERMAN, B. T. & LEMPICKI, R. A. 2009a. Systematic and integrative analysis of large gene lists using DAVID bioinformatics resources. *Nat Protoc*, 4, 44-57.
- HUANG, D. W., SHERMAN, B. T., ZHENG, X., YANG, J., IMAMICHI, T., STEPHENS, R. & LEMPICKI, R. A. 2009b. Extracting biological meaning from large gene lists with DAVID. *Curr Protoc Bioinformatics*, Chapter 13, Unit 13 11.
- HUANG, R., WU, T., XU, L., LIU, A., JI, Y. & HU, G. 2002. Upstream binding factor up-regulated in hepatocellular carcinoma is related to the survival and cisplatin-sensitivity of cancer cells. *FASEB J*, 16, 293-301.
- HUDES, G., CARDUCCI, M., TOMCZAK, P., DUTCHER, J., FIGLIN, R., KAPOOR, A., STAROSLAWSKA, E., SOSMAN, J., MCDERMOTT, D., BODROGI, I., KOVACEVIC, Z., LESOVOY, V., SCHMIDT-WOLF, I. G., BARBARASH, O., GOKMEN, E., O'TOOLE, T., LUSTGARTEN, S., MOORE, L. & MOTZER, R. J. 2007. Temsirolimus, interferon alfa, or both for advanced renal-cell carcinoma. *The New England journal of medicine*, 356, 2271-81.
- HUGHES, M. D., KAPLLANI, E., ALEXANDER, A. E., BURK, R. D. & SCHOENFELD, A. R. 2007. HIF-2alpha downregulation in the absence of functional VHL is not sufficient for renal cell differentiation. *Cancer Cell Int*, 7, 13.
- HUH, K. W., DEMASI, J., OGAWA, H., NAKATANI, Y., HOWLEY, P. M. & MUNGER, K. 2005. Association of the human papillomavirus type 16 E7 oncoprotein with the 600-kDa retinoblastoma protein-associated factor, p600. *Proc Natl Acad Sci U S A*, 102, 11492-7.
- HUMBERT, P., RUSSELL, S. & RICHARDSON, H. 2003. Dlg, Scribble and Lgl in cell polarity, cell proliferation and cancer. *Bioessays*, 25, 542-53.
- HUNT, J. D., VAN DER HEL, O. L., MCMILLAN, G. P., BOFFETTA, P. & BRENNAN, P. 2005. Renal cell carcinoma in relation to cigarette smoking: meta-analysis of 24 studies. *International journal of cancer. Journal international du cancer*, 114, 101-8.
- IKUSHIMA, H., MUNAKATA, Y., ISHII, T., IWATA, S., TERASHIMA, M., TANAKA, H., SCHLOSSMAN, S. F. & MORIMOTO, C. 2000. Internalization of CD26 by mannose 6-phosphate/insulin-like growth factor II receptor contributes to T cell activation. *Proc Natl Acad Sci U S A*, 97, 8439-44.
- ILIOPOULOS, O., KIBEL, A., GRAY, S. & KAELIN, W. G., JR. 1995. Tumour suppression by the human von Hippel-Lindau gene product. *Nat Med*, 1, 822-6.
- ISHIHAMA, Y., RAPPSILBER, J. & MANN, M. 2006. Modular stop and go extraction tips with stacked disks for parallel and multidimensional Peptide fractionation in proteomics. *Journal of proteome research*, 5, 988-94.
- JAGDEV, S. P., GREGORY, W., VASUDEV, N. S., HARNDEN, P., SIM, S., THOMPSON, D., CARTLEDGE, J., SELBY, P. J. & BANKS, R. E. 2010. Improving the accuracy of pre-operative survival prediction in renal cell carcinoma with C-reactive protein. *British journal of cancer*, 103, 1649-56.
- JAYSON, M. & SANDERS, H. 1998. Increased incidence of serendipitously discovered renal cell carcinoma. *Urology*, 51, 203-5.
- JENSEN, H. K., DONSKOV, F., MARCUSSEN, N., NORDSMARK, M., LUNDBECK, F. & VON DER MAASE, H. 2009. Presence of intratumoral neutrophils is an independent prognostic factor in localized renal cell carcinoma. *J Clin Oncol*, 27, 4709-17.
- JIANG, F., RICHTER, J., SCHRAML, P., BUBENDORF, L., GASSER, T., SAUTER, G., MIHATSCH, M. J. & MOCH, H. 1998. Chromosomal imbalances in

- papillary renal cell carcinoma: genetic differences between histological subtypes. *Am J Pathol*, 153, 1467-73.
- JILAVEANU, L. B., SZNOL, J., AZIZ, S. A., DUCHEN, D., KLUGER, H. M. & CAMP, R. L. 2012. CD70 expression patterns in renal cell carcinoma. *Hum Pathol*, 43, 1394-9.
- JUNG, M., RAMANKULOV, A., ROIGAS, J., JOHANNSEN, M., RINGSDORF, M., KRISTIANSEN, G. & JUNG, K. 2007. In search of suitable reference genes for gene expression studies of human renal cell carcinoma by real-time PCR. *BMC Mol Biol*, 8, 47.
- JUNKER, K., HINDERMANN, W., VON EGGELING, F., DIEGMANN, J., HAESSLER, K. & SCHUBERT, J. 2005. CD70: a new tumor specific biomarker for renal cell carcinoma. *J Urol*, 173, 2150-3.
- KAKIZOE, M., YAO, M., TATEISHI, U., MINAMIMOTO, R., UENO, D., NAMURA, K., MAKIYAMA, K., HAYASHI, N., SANO, F., KISHIDA, T., KOBAYASHI, K., NOGUCHI, S., IKEDA, I., OHGO, Y., TAGURI, M., MORITA, S., INOUE, T., KUBOTA, Y. & NAKAIGAWA, N. 2014. The early response of renal cell carcinoma to tyrosine kinase inhibitors evaluated by FDG PET/CT was not influenced by metastatic organ. *BMC cancer*, 14, 390.
- KALLAKURY, B. V., KARIKEHALLI, S., HAHOLU, A., SHEEHAN, C. E., AZUMI, N. & ROSS, J. S. 2001. Increased expression of matrix metalloproteinases 2 and 9 and tissue inhibitors of metalloproteinases 1 and 2 correlate with poor prognostic variables in renal cell carcinoma. *Clin Cancer Res*, 7, 3113-9.
- KAMURA, T., SATO, S., HAQUE, D., LIU, L., KAELIN, W. G., JR., CONAWAY, R. C. & CONAWAY, J. W. 1998. The Elongin BC complex interacts with the conserved SOCS-box motif present in members of the SOCS, ras, WD-40 repeat, and ankyrin repeat families. *Genes Dev*, 12, 3872-81.
- KANEKURA, T. & CHEN, X. 2010. CD147/basigin promotes progression of malignant melanoma and other cancers. *J Dermatol Sci*, 57, 149-54.
- KANESVARAN, R. & TAN, M. H. 2014. Targeted therapy for renal cell carcinoma: The next lap. *J Carcinog*, 13, 3.
- KARAKIEWICZ, P. I., BRIGANTI, A., CHUN, F. K., TRINH, Q. D., PERROTTE, P., FICARRA, V., CINDOLO, L., DE LA TAILLE, A., TOSTAIN, J., MULDER, P. F., SALOMON, L., ZIGEUNER, R., PRAYER-GALETTO, T., CHAUTARD, D., VALERI, A., LECHEVALLIER, E., DESCOTES, J. L., LANG, H., MEJEAN, A. & PATARD, J. J. 2007a. Multi-institutional validation of a new renal cancer-specific survival nomogram. *J Clin Oncol*, 25, 1316-22.
- KARAKIEWICZ, P. I., HUTTERER, G. C., TRINH, Q. D., JELDRES, C., PERROTTE, P., GALLINA, A., TOSTAIN, J. & PATARD, J. J. 2007b. C-reactive protein is an informative predictor of renal cell carcinoma-specific mortality: a European study of 313 patients. *Cancer*, 110, 1241-7.
- KARAMAN, M. W., HERRGARD, S., TREIBER, D. K., GALLANT, P., ATTERIDGE, C. E., CAMPBELL, B. T., CHAN, K. W., CICERI, P., DAVIS, M. I., EDEEN, P. T., FARAONI, R., FLOYD, M., HUNT, J. P., LOCKHART, D. J., MILANOV, Z. V., MORRISON, M. J., PALLARES, G., PATEL, H. K., PRITCHARD, S., WODICKA, L. M. & ZARRINKAR, P. P. 2008. A quantitative analysis of kinase inhibitor selectivity. *Nature biotechnology*, 26, 127-32.
- KARDON, T., STROOBANT, V., VEIGA-DA-CUNHA, M. & SCHAFTINGEN, E. V. 2008. Characterization of mammalian sedoheptulokinase and mechanism of formation of erythritol in sedoheptulokinase deficiency. *FEBS Lett*, 582, 3330-4.
- KAWASHIMA, A., TSUJIMURA, A., TAKAYAMA, H., ARAI, Y., NIN, M., TANIGAWA, G., UEMURA, M., NAKAI, Y., NISHIMURA, K., NONOMURA, N. & CARCINOMA, O. R. C. 2012. Impact of hyponatremia on survival of

- patients with metastatic renal cell carcinoma treated with molecular targeted therapy. *International Journal of Urology*, 19, 1050-1057.
- KE, Q. & COSTA, M. 2006. Hypoxia-inducible factor-1 (HIF-1). *Molecular pharmacology*, 70, 1469-80.
- KEIZMAN, D., ISH-SHALOM, M., HUANG, P., EISENBERGER, M. A., PILI, R., HAMMERS, H. & CARDUCCI, M. A. 2011. The association of pre-treatment neutrophil to lymphocyte ratio with response rate, progression free survival and overall survival of patients treated with sunitinib for metastatic renal cell carcinoma. *European journal of cancer (Oxford, England : 1990)*.
- KEIZMAN, D., ISH-SHALOM, M., HUANG, P., EISENBERGER, M. A., PILI, R., HAMMERS, H. & CARDUCCI, M. A. 2012. The association of pre-treatment neutrophil to lymphocyte ratio with response rate, progression free survival and overall survival of patients treated with sunitinib for metastatic renal cell carcinoma. *European journal of cancer*, 48, 202-8.
- KEMMNER, W., KESSEL, P., SANCHEZ-RUDERISCH, H., MOLLER, H., HINDERLICH, S., SCHLAG, P. M. & DETJEN, K. 2012. Loss of UDP-N-acetylglucosamine 2-epimerase/N-acetylmannosamine kinase (GNE) induces apoptotic processes in pancreatic carcinoma cells. *FASEB J*, 26, 938-46.
- KERBEL, R. S. 2008. Tumor angiogenesis. *The New England journal of medicine*, 358, 2039-49.
- KERKHOFF, C., KLEMPT, M. & SORG, C. 1998. Novel insights into structure and function of MRP8 (S100A8) and MRP14 (S100A9). *Biochimica et biophysica acta*, 1448, 200-11.
- KIM, H. A., SEO, K. H., KANG, Y. R., KO, H. M., KIM, K. J., BACK, H. K., LEE, H. K. & IM, S. Y. 2011. Mechanisms of platelet-activating factor-induced enhancement of VEGF expression. *Cell Physiol Biochem*, 27, 55-62.
- KIM, H. J., LV, D., ZHANG, Y., PENG, T. & MA, X. 2012a. Golgi phosphoprotein 2 in physiology and in diseases. *Cell Biosci*, 2, 31.
- KIM, H. L., SELIGSON, D., LIU, X., JANZEN, N., BUI, M. H., YU, H., SHI, T., BELLDEGRUN, A. S., HORVATH, S. & FIGLIN, R. A. 2005. Using tumor markers to predict the survival of patients with metastatic renal cell carcinoma. *J Urol*, 173, 1496-501.
- KIM, H. L., SELIGSON, D., LIU, X., JANZEN, N., BUI, M. H., YU, H., SHI, T., FIGLIN, R. A., HORVATH, S. & BELLDEGRUN, A. S. 2004. Using protein expressions to predict survival in clear cell renal carcinoma. *Clin Cancer Res*, 10, 5464-71.
- KIM, J. J., RINI, B. I. & HANSEL, D. E. 2010. Von Hippel Lindau syndrome. *Adv Exp Med Biol*, 685, 228-49.
- KIM, J. J., VAZIRI, S. A., RINI, B. I., ELSON, P., GARCIA, J. A., WIRKA, R., DREICER, R., GANAPATHI, M. K. & GANAPATHI, R. 2012b. Association of VEGF and VEGFR2 single nucleotide polymorphisms with hypertension and clinical outcome in metastatic clear cell renal cell carcinoma patients treated with sunitinib. *Cancer*, 118, 1946-54.
- KIM, J. W., TCHERNYSHYOV, I., SEMENZA, G. L. & DANG, C. V. 2006. HIF-1-mediated expression of pyruvate dehydrogenase kinase: a metabolic switch required for cellular adaptation to hypoxia. *Cell Metab*, 3, 177-85.
- KIM, M. S., PINTO, S. M., GETNET, D., NIRUJOGI, R. S., MANDA, S. S., CHAERKADY, R., MADUGUNDU, A. K., KELKAR, D. S., ISSERLIN, R., JAIN, S., THOMAS, J. K., MUTHUSAMY, B., LEAL-ROJAS, P., KUMAR, P., SAHASRABUDDHE, N. A., BALAKRISHNAN, L., ADVANI, J., GEORGE, B., RENUSE, S., SELVAN, L. D., PATIL, A. H., NANJAPPA, V., RADHAKRISHNAN, A., PRASAD, S., SUBBANNAYYA, T., RAJU, R., KUMAR, M., SREENIVASAMURTHY, S. K., MARIMUTHU, A., SATHE, G.

- J., CHAVAN, S., DATTA, K. K., SUBBANNAYYA, Y., SAHU, A., YELAMANCHI, S. D., JAYARAM, S., RAJAGOPALAN, P., SHARMA, J., MURTHY, K. R., SYED, N., GOEL, R., KHAN, A. A., AHMAD, S., DEY, G., MUDGAL, K., CHATTERJEE, A., HUANG, T. C., ZHONG, J., WU, X., SHAW, P. G., FREED, D., ZAHARI, M. S., MUKHERJEE, K. K., SHANKAR, S., MAHADEVAN, A., LAM, H., MITCHELL, C. J., SHANKAR, S. K., SATISHCHANDRA, P., SCHROEDER, J. T., SIRDESHMUKH, R., MAITRA, A., LEACH, S. D., DRAKE, C. G., HALUSHKA, M. K., PRASAD, T. S., HRUBAN, R. H., KERR, C. L., BADER, G. D., IACOBUZIO-DONAHUE, C. A., GOWDA, H. & PANDEY, A. 2014. A draft map of the human proteome. *Nature*, 509, 575-81.
- KIM, W. Y. & KAE LIN, W. G. 2004. Role of VHL gene mutation in human cancer. *J Clin Oncol*, 22, 4991-5004.
- KLEAVELAND, B., ZHENG, X., LIU, J. J., BLUM, Y., TUNG, J. J., ZOU, Z., SWEENEY, S. M., CHEN, M., GUO, L., LU, M. M., ZHOU, D., KITAJEWSKI, J., AFFOLTER, M., GINSBERG, M. H. & KAHN, M. L. 2009. Regulation of cardiovascular development and integrity by the heart of glass-cerebral cavernous malformation protein pathway. *Nature medicine*, 15, 169-76.
- KOBAYASHI, H., SAGARA, J., KURITA, H., MORIFUJI, M., OHISHI, M., KURASHINA, K. & TANIGUCHI, S. 2004. Clinical significance of cellular distribution of moesin in patients with oral squamous cell carcinoma. *Clin Cancer Res*, 10, 572-80.
- KOFF, A., GIORDANO, A., DESAI, D., YAMASHITA, K., HARPER, J. W., ELLEDGE, S., NISHIMOTO, T., MORGAN, D. O., FRANZA, B. R. & ROBERTS, J. M. 1992. Formation and activation of a cyclin E-cdk2 complex during the G1 phase of the human cell cycle. *Science*, 257, 1689-94.
- KOLLMANNNSBERGER, C., SOULIERES, D., WONG, R., SCALERA, A., GASPO, R. & BJARNASON, G. 2007. Sunitinib therapy for metastatic renal cell carcinoma: recommendations for management of side effects. *Canadian Urological Association journal = Journal de l'Association des urologues du Canada*, 1, S41-54.
- KONDO, K., KIM, W. Y., LECHPAMMER, M. & KAE LIN, W. G., JR. 2003. Inhibition of HIF2alpha is sufficient to suppress pVHL-defective tumor growth. *PLoS Biol*, 1, E83.
- KONDO, K., KLCO, J., NAKAMURA, E., LECHPAMMER, M. & KAE LIN, W. G., JR. 2002. Inhibition of HIF is necessary for tumor suppression by the von Hippel-Lindau protein. *Cancer cell*, 1, 237-46.
- KONTOVINIS, L. F., PAPA ZISIS, K. T., TOUPLIKIOTI, P., ANDREADIS, C., MOURATIDOU, D. & KORTSARIS, A. H. 2009. Sunitinib treatment for patients with clear-cell metastatic renal cell carcinoma: clinical outcomes and plasma angiogenesis markers. *BMC cancer*, 9, 82.
- KORN MANN, M., MARUYAMA, H., BERGMANN, U., TANGVORANUNTAKUL, P., BEGER, H. G., WHITE, M. F. & KORC, M. 1998. Enhanced expression of the insulin receptor substrate-2 docking protein in human pancreatic cancer. *Cancer Res*, 58, 4250-4.
- KOVACS, G., AKHTAR, M., BECKWITH, B. J., BUGERT, P., COOPER, C. S., DELAHUNT, B., EBLE, J. N., FLEMING, S., LJUNGBERG, B., MEDEIROS, L. J., MOCH, H., REUTER, V. E., RITZ, E., ROOS, G., SCHMIDT, D., SRIGLEY, J. R., STORKEL, S., VAN DEN BERG, E. & ZBAR, B. 1997. The Heidelberg classification of renal cell tumours. *J Pathol*, 183, 131-3.
- KRAUSE, S., HINDERLICH, S., AMSILI, S., HORSTKORTE, R., WIENDL, H., ARGOV, Z., MITRANI-ROSENBAUM, S. & LOCHMULLER, H. 2005. Localization of UDP-GlcNAc 2-epimerase/ManAc kinase (GNE) in the Golgi complex and the nucleus of mammalian cells. *Exp Cell Res*, 304, 365-79.

- KREPKIY, D. & MIZIORKO, H. M. 2004. Identification of active site residues in mevalonate diphosphate decarboxylase: implications for a family of phosphotransferases. *Protein Sci*, 13, 1875-81.
- KRUEGER, S., KALINSKI, T., HUNDERTMARK, T., WEX, T., KUSTER, D., PEITZ, U., EBERT, M., NAGLER, D. K., KELLNER, U., MALFERTHEINER, P., NAUMANN, M., ROCKEN, C. & ROESSNER, A. 2005. Up-regulation of cathepsin X in *Helicobacter pylori* gastritis and gastric cancer. *J Pathol*, 207, 32-42.
- KULAK, N. A., PICHLER, G., PARON, I., NAGARAJ, N. & MANN, M. 2014. Minimal, encapsulated proteomic-sample processing applied to copy-number estimation in eukaryotic cells. *Nat Methods*, 11, 319-24.
- KUME, K. & SHIMIZU, T. 1997. Platelet-activating factor (PAF) induces growth stimulation, inhibition, and suppression of oncogenic transformation in NRK cells overexpressing the PAF receptor. *J Biol Chem*, 272, 22898-904.
- KUST, D., PRPIC, M., MURGIC, J., JAZVIC, M., JAKSIC, B., KRILIC, D., BOLANCA, A. & KUSIC, Z. 2014. Hypothyroidism as a predictive clinical marker of better treatment response to sunitinib therapy. *Anticancer Res*, 34, 3177-84.
- KUZNETSOVA, A. V., MELLER, J., SCHNELL, P. O., NASH, J. A., IGNACAK, M. L., SANCHEZ, Y., CONAWAY, J. W., CONAWAY, R. C. & CZYZYK-KRZESKA, M. F. 2003. von Hippel-Lindau protein binds hyperphosphorylated large subunit of RNA polymerase II through a proline hydroxylation motif and targets it for ubiquitination. *Proceedings of the National Academy of Sciences of the United States of America*, 100, 2706-11.
- KWON, W. A., CHO, I. C., YU, A., NAM, B. H., JOUNG, J. Y., SEO, H. K., LEE, K. H. & CHUNG, J. 2013. Validation of the MSKCC and Heng risk criteria models for predicting survival in patients with metastatic renal cell carcinoma treated with sunitinib. *Ann Surg Oncol*, 20, 4397-404.
- LAMBRECHTS, D., CLAES, B., DELMAR, P., REUMERS, J., MAZZONE, M., YESILYURT, B. T., DEVLIEGER, R., VERSLYPE, C., TEJPAR, S., WILDIERS, H., DE HAAS, S., CARMELIET, P., SCHERER, S. J. & VAN CUTSEM, E. 2012. VEGF pathway genetic variants as biomarkers of treatment outcome with bevacizumab: an analysis of data from the AViTA and AVOREN randomised trials. *Lancet Oncol*, 13, 724-33.
- LAMURAGLIA, M., ESCUDIER, B., CHAMI, L., SCHWARTZ, B., LECLERE, J., ROCHE, A. & LASSAU, N. 2006. To predict progression-free survival and overall survival in metastatic renal cancer treated with sorafenib: pilot study using dynamic contrast-enhanced Doppler ultrasound. *European journal of cancer*, 42, 2472-9.
- LANGNER, C., RATSCHKEK, M., REHAK, P., SCHIPS, L. & ZIGEUNER, R. 2004. Expression of MUC1 (EMA) and E-cadherin in renal cell carcinoma: a systematic immunohistochemical analysis of 188 cases. *Mod Pathol*, 17, 180-8.
- LASSEIGNE, B. N., BURWELL, T. C., PATIL, M. A., ABSHER, D. M., BROOKS, J. D. & MYERS, R. M. 2014. DNA methylation profiling reveals novel diagnostic biomarkers in renal cell carcinoma. *BMC Med*, 12, 235.
- LATIF, F., TORY, K., GNARRA, J., YAO, M., DUH, F. M., ORCUTT, M. L., STACKHOUSE, T., KUZMIN, I., MODI, W., GEIL, L. & ET AL. 1993. Identification of the von Hippel-Lindau disease tumor suppressor gene. *Science*, 260, 1317-20.
- LAURSEN, L. S., OVERGAARD, M. T., SOE, R., BOLDT, H. B., SOTTRUP-JENSEN, L., GIUDICE, L. C., CONOVER, C. A. & OXVIG, C. 2001. Pregnancy-associated plasma protein-A (PAPP-A) cleaves insulin-like

growth factor binding protein (IGFBP)-5 independent of IGF: implications for the mechanism of IGFBP-4 proteolysis by PAPP-A. *FEBS letters*, 504, 36-40.

- LEE, J. E., MANNISTO, S., SPIEGELMAN, D., HUNTER, D. J., BERNSTEIN, L., VAN DEN BRANDT, P. A., BURING, J. E., CHO, E., ENGLISH, D. R., FLOOD, A., FREUDENHEIM, J. L., GILES, G. G., GIOVANNUCCI, E., HAKANSSON, N., HORN-ROSS, P. L., JACOBS, E. J., LEITZMANN, M. F., MARSHALL, J. R., MCCULLOUGH, M. L., MILLER, A. B., ROHAN, T. E., ROSS, J. A., SCHATZKIN, A., SCHOUTEN, L. J., VIRTAMO, J., WOLK, A., ZHANG, S. M. & SMITH-WARNER, S. A. 2009. Intakes of fruit, vegetables, and carotenoids and renal cell cancer risk: a pooled analysis of 13 prospective studies. *Cancer Epidemiol Biomarkers Prev*, 18, 1730-9.
- LEMMON, M. A. & SCHLESSINGER, J. 2010. Cell signaling by receptor tyrosine kinases. *Cell*, 141, 1117-34.
- LENS, S. M., DRILLENBURG, P., DEN DRIJVER, B. F., VAN SCHIJNDEL, G., PALS, S. T., VAN LIER, R. A. & VAN OERS, M. H. 1999. Aberrant expression and reverse signalling of CD70 on malignant B cells. *Br J Haematol*, 106, 491-503.
- LI, D., BEISSWENGER, C., HERR, C., SCHMID, R. M., GALLO, R. L., HAN, G., ZAKHARKINA, T. & BALS, R. 2014. Expression of the antimicrobial peptide cathelicidin in myeloid cells is required for lung tumor growth. *Oncogene*, 33, 2709-16.
- LI, J. L., SAINSON, R. C., OON, C. E., TURLEY, H., LEEK, R., SHELDON, H., BRIDGES, E., SHI, W., SNELL, C., BOWDEN, E. T., WU, H., CHOWDHURY, P. S., RUSSELL, A. J., MONTGOMERY, C. P., POULSOM, R. & HARRIS, A. L. 2011. DLL4-Notch signaling mediates tumor resistance to anti-VEGF therapy in vivo. *Cancer research*, 71, 6073-83.
- LI, R. X., CHEN, H. B., TU, K., ZHAO, S. L., ZHOU, H., LI, S. J., DAI, J., LI, Q. R., NIE, S., LI, Y. X., JIA, W. P., ZENG, R. & WU, J. R. 2008. Localized-statistical quantification of human serum proteome associated with type 2 diabetes. *PLoS One*, 3, e3224.
- LI, Z., NA, X., WANG, D., SCHOEN, S. R., MESSING, E. M. & WU, G. 2002a. Ubiquitination of a novel deubiquitinating enzyme requires direct binding to von Hippel-Lindau tumor suppressor protein. *J Biol Chem*, 277, 4656-62.
- LI, Z., WANG, D., NA, X., SCHOEN, S. R., MESSING, E. M. & WU, G. 2002b. Identification of a deubiquitinating enzyme subfamily as substrates of the von Hippel-Lindau tumor suppressor. *Biochem Biophys Res Commun*, 294, 700-9.
- LIEUBEAU-TEILLET, B., RAK, J., JOTHY, S., ILIOPOULOS, O., KAELIN, W. & KERBEL, R. S. 1998. von Hippel-Lindau gene-mediated growth suppression and induction of differentiation in renal cell carcinoma cells grown as multicellular tumor spheroids. *Cancer research*, 58, 4957-62.
- LINEHAN, W. M., PINTO, P. A., BRATSLAVSKY, G., PFAFFENROTH, E., MERINO, M., VOCKE, C. D., TORO, J. R., BOTTARO, D., NECKERS, L., SCHMIDT, L. S. & SRINIVASAN, R. 2009. Hereditary kidney cancer: unique opportunity for disease-based therapy. *Cancer*, 115, 2252-61.
- LINSALATA, M., RUSSO, F., CAVALLINI, A., BERLOCO, P. & DI LEO, A. 1993. Polyamines, diamine oxidase, and ornithine decarboxylase activity in colorectal cancer and in normal surrounding mucosa. *Dis Colon Rectum*, 36, 662-7.
- LIU, Q., ZHANG, J., ZERBINATTI, C., ZHAN, Y., KOLBER, B. J., HERZ, J., MUGLIA, L. J. & BU, G. 2011. Lipoprotein receptor LRP1 regulates leptin signaling and energy homeostasis in the adult central nervous system. *PLoS Biol*, 9, e1000575.

- LIU, X., VALENTINE, S. J., PLASENCIA, M. D., TRIMPIN, S., NAYLOR, S. & CLEMMER, D. E. 2007. Mapping the human plasma proteome by SCX-LC-IMS-MS. *Journal of the American Society for Mass Spectrometry*, 18, 1249-64.
- LIVAK, K. J., FLOOD, S. J., MARMARO, J., GIUSTI, W. & DEETZ, K. 1995. Oligonucleotides with fluorescent dyes at opposite ends provide a quenched probe system useful for detecting PCR product and nucleic acid hybridization. *PCR Methods Appl*, 4, 357-62.
- LIVAK, K. J. & SCHMITTGEN, T. D. 2001. Analysis of relative gene expression data using real-time quantitative PCR and the 2(-Delta Delta C(T)) Method. *Methods*, 25, 402-8.
- LJUNGBERG, B., COWAN, N. C., HANBURY, D. C., HORA, M., KUCZYK, M. A., MERSEBURGER, A. S., PATARD, J. J., MULDER, P. F. & SINESCU, I. C. 2010. EAU guidelines on renal cell carcinoma: the 2010 update. *European urology*, 58, 398-406.
- LO, S. H., WEISBERG, E. & CHEN, L. B. 1994. Tensin: a potential link between the cytoskeleton and signal transduction. *Bioessays*, 16, 817-23.
- LONG, P. M., STRADECKI, H. M., MINTURN, J. E., WESLEY, U. V. & JAWORSKI, D. M. 2011. Differential aminoacylase expression in neuroblastoma. *Int J Cancer*, 129, 1322-30.
- LORENZ, M. G., KANTOR, J. A., SCHLOM, J. & HODGE, J. W. 1999. Anti-tumor immunity elicited by a recombinant vaccinia virus expressing CD70 (CD27L). *Hum Gene Ther*, 10, 1095-103.
- LU, X. Y., LU, Y., ZHAO, Y. J., JAEWEON, K., KANG, J., XIAO-NAN, L., GE, G., MEYER, R., PERLAKY, L., HICKS, J., CHINTAGUMPALA, M., CAI, W. W., LADANYI, M., GORLICK, R., LAU, C. C., PATI, D., SHELDON, M. & RAO, P. H. 2008. Cell cycle regulator gene CDC5L, a potential target for 6p12-p21 amplicon in osteosarcoma. *Mol Cancer Res*, 6, 937-46.
- LU, Y., YI, Y., LIU, P., WEN, W., JAMES, M., WANG, D. & YOU, M. 2007. Common human cancer genes discovered by integrated gene-expression analysis. *PLoS one*, 2, e1149.
- LUBENSKY, I. A., GNARRA, J. R., BERTHEAU, P., WALTHER, M. M., LINEHAN, W. M. & ZHUANG, Z. 1996. Allelic deletions of the VHL gene detected in multiple microscopic clear cell renal lesions in von Hippel-Lindau disease patients. *Am J Pathol*, 149, 2089-94.
- LYNCH, T. J., BELL, D. W., SORDELLA, R., GURUBHAGAVATULA, S., OKIMOTO, R. A., BRANNIGAN, B. W., HARRIS, P. L., HASERLAT, S. M., SUPKO, J. G., HALUSKA, F. G., LOUIS, D. N., CHRISTIANI, D. C., SETTLEMAN, J. & HABER, D. A. 2004. Activating mutations in the epidermal growth factor receptor underlying responsiveness of non-small-cell lung cancer to gefitinib. *The New England journal of medicine*, 350, 2129-39.
- MAHER, E. R., NEUMANN, H. P. & RICHARD, S. 2011. von Hippel-Lindau disease: a clinical and scientific review. *Eur J Hum Genet*, 19, 617-23.
- MAJIMA, S., KAJINO, K., FUKUDA, T., OTSUKA, F. & HINO, O. 2000. A novel gene "Niban" upregulated in renal carcinogenesis: cloning by the cDNA-amplified fragment length polymorphism approach. *Jpn J Cancer Res*, 91, 869-74.
- MAKHOV, P. B., GOLOVINE, K., KUTIKOV, A., TEPER, E., CANTER, D. J., SIMHAN, J., UZZO, R. G. & KOLENKO, V. M. 2012. Modulation of Akt/mTOR signaling overcomes sunitinib resistance in renal and prostate cancer cells. *Mol Cancer Ther*, 11, 1510-7.
- MANOLA, J., ROYSTON, P., ELSON, P., MCCORMACK, J. B., MAZUMDAR, M., NEGRIER, S., ESCUDIER, B., EISEN, T., DUTCHER, J., ATKINS, M.,

- HENG, D. Y., CHOUEIRI, T. K., MOTZER, R. & BUKOWSKI, R. 2011. Prognostic model for survival in patients with metastatic renal cell carcinoma: results from the international kidney cancer working group. *Clin Cancer Res*, 17, 5443-50.
- MARAZZI, S., BLUM, S., HARTMANN, R., GUNDERSEN, D., SCHREYER, M., ARGRAVES, S., VON FLIEDNER, V., PYTELA, R. & RUEGG, C. 1998. Characterization of human fibroleukin, a fibrinogen-like protein secreted by T lymphocytes. *J Immunol*, 161, 138-47.
- MARDILOVICH, K. & SHAW, L. M. 2009. Hypoxia regulates insulin receptor substrate-2 expression to promote breast carcinoma cell survival and invasion. *Cancer Res*, 69, 8894-901.
- MARRERO, J. A., ROMANO, P. R., NIKOLAEVA, O., STEEL, L., MEHTA, A., FIMMEL, C. J., COMUNALE, M. A., D'AMELIO, A., LOK, A. S. & BLOCK, T. M. 2005. GP73, a resident Golgi glycoprotein, is a novel serum marker for hepatocellular carcinoma. *J Hepatol*, 43, 1007-12.
- MASUI, O., WHITE, N. M., DESOUZA, L. V., KRAKOVSKA, O., MATTA, A., METIAS, S., KHALIL, B., ROMASCHIN, A. D., HONEY, R. J., STEWART, R., PACE, K., BJARNASON, G. A., SIU, K. W. & YOUSEF, G. M. 2013. Quantitative proteomic analysis in metastatic renal cell carcinoma reveals a unique set of proteins with potential prognostic significance. *Mol Cell Proteomics*, 12, 132-44.
- MATHEW, A., DEVESA, S. S., FRAUMENI, J. F., JR. & CHOW, W. H. 2002. Global increases in kidney cancer incidence, 1973-1992. *Eur J Cancer Prev*, 11, 171-8.
- MAXWELL, P. H., WIESENER, M. S., CHANG, G. W., CLIFFORD, S. C., VAUX, E. C., COCKMAN, M. E., WYKOFF, C. C., PUGH, C. W., MAHER, E. R. & RATCLIFFE, P. J. 1999. The tumour suppressor protein VHL targets hypoxia-inducible factors for oxygen-dependent proteolysis. *Nature*, 399, 271-5.
- MAYOR, T., STIERHOF, Y. D., TANAKA, K., FRY, A. M. & NIGG, E. A. 2000. The centrosomal protein C-Nap1 is required for cell cycle-regulated centrosome cohesion. *J Cell Biol*, 151, 837-46.
- MEHTA, A. I., ROSS, S., LOWENTHAL, M. S., FUSARO, V., FISHMAN, D. A., PETRICOIN, E. F., 3RD & LIOTTA, L. A. 2003. Biomarker amplification by serum carrier protein binding. *Dis Markers*, 19, 1-10.
- MENDEL, D. B., LAIRD, A. D., XIN, X., LOUIE, S. G., CHRISTENSEN, J. G., LI, G., SCHRECK, R. E., ABRAMS, T. J., NGAI, T. J., LEE, L. B., MURRAY, L. J., CARVER, J., CHAN, E., MOSS, K. G., HAZNEDAR, J. O., SUKBUNTERNG, J., BLAKE, R. A., SUN, L., TANG, C., MILLER, T., SHIRAZIAN, S., MCMAHON, G. & CHERRINGTON, J. M. 2003. In vivo antitumor activity of SU11248, a novel tyrosine kinase inhibitor targeting vascular endothelial growth factor and platelet-derived growth factor receptors: determination of a pharmacokinetic/pharmacodynamic relationship. *Clinical cancer research : an official journal of the American Association for Cancer Research*, 9, 327-37.
- MIAO, P., SHENG, S., SUN, X., LIU, J. & HUANG, G. 2013. Lactate dehydrogenase A in cancer: a promising target for diagnosis and therapy. *IUBMB Life*, 65, 904-10.
- MIKHAYLOVA, O., IGNACAK, M. L., BARANKIEWICZ, T. J., HARBAUGH, S. V., YI, Y., MAXWELL, P. H., SCHNEIDER, M., VAN GEYTE, K., CARMELIET, P., REVELO, M. P., WYDER, M., GREIS, K. D., MELLER, J. & CZYZYK-KRZESKA, M. F. 2008. The von Hippel-Lindau tumor suppressor protein and Egl-9-Type proline hydroxylases regulate the large subunit of RNA polymerase II in response to oxidative stress. *Mol Cell Biol*, 28, 2701-17.

- MILLER, L. J., BAINTON, D. F., BORREGAARD, N. & SPRINGER, T. A. 1987. Stimulated mobilization of monocyte Mac-1 and p150,95 adhesion proteins from an intracellular vesicular compartment to the cell surface. *J Clin Invest*, 80, 535-44.
- MILLIONI, R., TOLIN, S., PURICELLI, L., SBRIGNADELLO, S., FADINI, G. P., TESSARI, P. & ARRIGONI, G. 2011. High abundance proteins depletion vs low abundance proteins enrichment: comparison of methods to reduce the plasma proteome complexity. *PloS one*, 6, e19603.
- MINAMIDA, S., IWAMURA, M., KODERA, Y., KAWASHIMA, Y., TABATA, K., MATSUMOTO, K., FUJITA, T., SATOH, T., MAEDA, T. & BABA, S. 2011. 14-3-3 protein beta/alpha as a urinary biomarker for renal cell carcinoma: proteomic analysis of cyst fluid. *Anal Bioanal Chem*, 401, 245-52.
- MISCHAK, H., IOANNIDIS, J. P., ARGILES, A., ATTWOOD, T. K., BONGCAM-RUDLOFF, E., BROENSTRUP, M., CHARONIS, A., CHROUSOS, G. P., DELLES, C., DOMINICZAK, A., DYLAG, T., EHRICH, J., EGIDO, J., FINDEISEN, P., JANKOWSKI, J., JOHNSON, R. W., JULIEN, B. A., LANKISCH, T., LEUNG, H. Y., MAAHS, D., MAGNI, F., MANNS, M. P., MANOLIS, E., MAYER, G., NAVIS, G., NOVAK, J., ORTIZ, A., PERSSON, F., PETER, K., RIESE, H. H., ROSSING, P., SATTAR, N., SPASOVSKI, G., THONGBOONKERD, V., VANHOLDER, R., SCHANSTRA, J. P. & VLAHOU, A. 2012. Implementation of proteomic biomarkers: making it work. *Eur J Clin Invest*, 42, 1027-36.
- MIYAKE, H., NISHIKAWA, M., TEI, H., FURUKAWA, J., HARADA, K. & FUJISAWA, M. 2014. Significance of circulating matrix metalloproteinase-9 to tissue inhibitor of metalloproteinases-2 ratio as a predictor of disease progression in patients with metastatic renal cell carcinoma receiving sunitinib. *Urologic oncology*, 32, 584-8.
- MOLINA, A. M., LIN, X., KORYTOWSKY, B., MATCZAK, E., LECHUGA, M. J., WILTSHIRE, R. & MOTZER, R. J. 2014. Sunitinib objective response in metastatic renal cell carcinoma: analysis of 1059 patients treated on clinical trials. *European journal of cancer*, 50, 351-8.
- MORIMOTO-KAMATA, R., MIZOGUCHI, S., ICHISUGI, T. & YUI, S. 2012. Cathepsin G induces cell aggregation of human breast cancer MCF-7 cells via a 2-step mechanism: catalytic site-independent binding to the cell surface and enzymatic activity-dependent induction of the cell aggregation. *Mediators Inflamm*, 2012, 456462.
- MORRISSEY, J. J., LONDON, A. N., LUO, J. & KHARASCH, E. D. 2010. Urinary biomarkers for the early diagnosis of kidney cancer. *Mayo Clin Proc*, 85, 413-21.
- MORRISSEY, J. J., MOBLEY, J., SONG, J., VETTER, J., LUO, J., BHAYANI, S., FIGENSHAU, R. S. & KHARASCH, E. D. 2014. Urinary concentrations of aquaporin-1 and perilipin-2 in patients with renal cell carcinoma correlate with tumor size and stage but not grade. *Urology*, 83, 256 e9-14.
- MOTZER, R. B. I. R., DAVID F. MCDERMOTT, BRUCE G. REDMAN, TIMOTHY KUZEL, MICHAEL ROGER HARRISON, ULKA N. VAISHAMPAYAN, HARRY A. DRABKIN, SABY GEORGE, THEODORE F. LOGAN, KIM ALLYSON MARGOLIN, ELIZABETH R. PLIMACK, IAN WAXMAN, ALEXANDRE LAMBERT, HANS J. HAMMERS 2014. Nivolumab for metastatic renal cell carcinoma (mRCC): Results of a randomized, dose-ranging phase II trial. *Journal of clinical oncology : official journal of the American Society of Clinical Oncology*, 32.
- MOTZER, R. J., BACIK, J., MURPHY, B. A., RUSSO, P. & MAZUMDAR, M. 2002. Interferon-alfa as a comparative treatment for clinical trials of new therapies

- against advanced renal cell carcinoma. *Journal of clinical oncology : official journal of the American Society of Clinical Oncology*, 20, 289-96.
- MOTZER, R. J., ESCUDIER, B., OUDARD, S., HUTSON, T. E., PORTA, C., BRACARDA, S., GRUNWALD, V., THOMPSON, J. A., FIGLIN, R. A., HOLLAENDER, N., KAY, A. & RAVAUD, A. 2010. Phase 3 trial of everolimus for metastatic renal cell carcinoma : final results and analysis of prognostic factors. *Cancer*, 116, 4256-65.
- MOTZER, R. J., ESCUDIER, B., TOMCZAK, P., HUTSON, T. E., MICHAELSON, M. D., NEGRIER, S., OUDARD, S., GORE, M. E., TARAZI, J., HARIHARAN, S., CHEN, C., ROSBROOK, B., KIM, S. & RINI, B. I. 2013a. Axitinib versus sorafenib as second-line treatment for advanced renal cell carcinoma: overall survival analysis and updated results from a randomised phase 3 trial. *Lancet Oncol*, 14, 552-62.
- MOTZER, R. J., HUTSON, T. E., CELLA, D., REEVES, J., HAWKINS, R., GUO, J., NATHAN, P., STAEHLER, M., DE SOUZA, P., MERCHAN, J. R., BOLETI, E., FIFE, K., JIN, J., JONES, R., UEMURA, H., DE GIORGI, U., HARMENBERG, U., WANG, J., STERNBERG, C. N., DEEN, K., MCCANN, L., HACKSHAW, M. D., CRESCENZO, R., PANDITE, L. N. & CHOUERI, T. K. 2013b. Pazopanib versus sunitinib in metastatic renal-cell carcinoma. *N Engl J Med*, 369, 722-31.
- MOTZER, R. J., HUTSON, T. E., HUDES, G. R., FIGLIN, R. A., MARTINI, J. F., ENGLISH, P. A., HUANG, X., VALOTA, O. & WILLIAMS, J. A. 2014. Investigation of novel circulating proteins, germ line single-nucleotide polymorphisms, and molecular tumor markers as potential efficacy biomarkers of first-line sunitinib therapy for advanced renal cell carcinoma. *Cancer Chemother Pharmacol*.
- MOTZER, R. J., HUTSON, T. E., TOMCZAK, P., MICHAELSON, M. D., BUKOWSKI, R. M., RIXE, O., OUDARD, S., NEGRIER, S., SZCZYLIK, C., KIM, S. T., CHEN, I., BYCOTT, P. W., BAUM, C. M. & FIGLIN, R. A. 2007. Sunitinib versus interferon alfa in metastatic renal-cell carcinoma. *The New England journal of medicine*, 356, 115-24.
- MOTZER, R. J., MICHAELSON, M. D., REDMAN, B. G., HUDES, G. R., WILDING, G., FIGLIN, R. A., GINSBERG, M. S., KIM, S. T., BAUM, C. M., DEPRIMO, S. E., LI, J. Z., BELLO, C. L., THEUER, C. P., GEORGE, D. J. & RINI, B. I. 2006. Activity of SU11248, a multitargeted inhibitor of vascular endothelial growth factor receptor and platelet-derived growth factor receptor, in patients with metastatic renal cell carcinoma. *Journal of clinical oncology : official journal of the American Society of Clinical Oncology*, 24, 16-24.
- MOUND, A., RODAT-DESPOIX, L., BOUGARN, S., OUAJID-AHIDOUCH, H. & MATIFAT, F. 2013. Molecular interaction and functional coupling between type 3 inositol 1,4,5-trisphosphate receptor and BKCa channel stimulate breast cancer cell proliferation. *Eur J Cancer*, 49, 3738-51.
- MUKHOPADHYAY, D., KNEBELMANN, B., COHEN, H. T., ANANTH, S. & SUKHATME, V. P. 1997. The von Hippel-Lindau tumor suppressor gene product interacts with Sp1 to repress vascular endothelial growth factor promoter activity. *Mol Cell Biol*, 17, 5629-39.
- MUNOZ, M., HENDERSON, M., HABER, M. & NORRIS, M. 2007. Role of the MRP1/ABCC1 multidrug transporter protein in cancer. *IUBMB Life*, 59, 752-7.
- MURIEL LOPEZ, C., ESTEBAN, E., ASTUDILLO, A., PARDO, P., BERROS, J. P., IZQUIERDO, M., CRESPO, G., FONSECA, P. J., SANMAMED, M. & MARTINEZ-CAMBLOR, P. 2012. Predictive factors for response to treatment in patients with advanced renal cell carcinoma. *Invest New Drugs*, 30, 2443-9.

- NA, X., DUAN, H. O., MESSING, E. M., SCHOEN, S. R., RYAN, C. K., DI SANT'AGNESE, P. A., GOLEMIS, E. A. & WU, G. 2003. Identification of the RNA polymerase II subunit hsRPB7 as a novel target of the von Hippel-Lindau protein. *EMBO J*, 22, 4249-59.
- NAGANO, M., HOSHINO, D., KOSHIKAWA, N., AKIZAWA, T. & SEIKI, M. 2012. Turnover of focal adhesions and cancer cell migration. *Int J Cell Biol*, 2012, 310616.
- NAGARAJ, N., WISNIEWSKI, J. R., GEIGER, T., COX, J., KIRCHER, M., KELSO, J., PAABO, S. & MANN, M. 2011. Deep proteome and transcriptome mapping of a human cancer cell line. *Mol Syst Biol*, 7, 548.
- NAKAMURA, E., ABREU-E-LIMA, P., AWAKURA, Y., INOUE, T., KAMOTO, T., OGAWA, O., KOTANI, H., MANABE, T., ZHANG, G. J., KONDO, K., NOSE, V. & KAELIN, W. G., JR. 2006. Clusterin is a secreted marker for a hypoxia-inducible factor-independent function of the von Hippel-Lindau tumor suppressor protein. *Am J Pathol*, 168, 574-84.
- NAKATANI, Y., KONISHI, H., VASSILEV, A., KUROOKA, H., ISHIGURO, K., SAWADA, J., IKURA, T., KORSMEYER, S. J., QIN, J. & HERLITZ, A. M. 2005. p600, a unique protein required for membrane morphogenesis and cell survival. *Proc Natl Acad Sci U S A*, 102, 15093-8.
- NAMURA, K., MINAMIMOTO, R., YAO, M., MAKIYAMA, K., MURAKAMI, T., SANO, F., HAYASHI, N., TATEISHI, U., ISHIGAKI, H., KISHIDA, T., MIURA, T., KOBAYASHI, K., NOGUCHI, S., INOUE, T., KUBOTA, Y. & NAKAIGAWA, N. 2010. Impact of maximum standardized uptake value (SUVmax) evaluated by 18-Fluoro-2-deoxy-D-glucose positron emission tomography/computed tomography (18F-FDG-PET/CT) on survival for patients with advanced renal cell carcinoma: a preliminary report. *BMC cancer*, 10, 667.
- NANJAPPA, V., THOMAS, J. K., MARIMUTHU, A., MUTHUSAMY, B., RADHAKRISHNAN, A., SHARMA, R., AHMAD KHAN, A., BALAKRISHNAN, L., SAHASRABUDDHE, N. A., KUMAR, S., JHAVERI, B. N., SHETH, K. V., KUMAR KHATANA, R., SHAW, P. G., SRIKANTH, S. M., MATHUR, P. P., SHANKAR, S., NAGARAJA, D., CHRISTOPHER, R., MATHIVANAN, S., RAJU, R., SIRDESHMUKH, R., CHATTERJEE, A., SIMPSON, R. J., HARSHA, H. C., PANDEY, A. & PRASAD, T. S. 2014. Plasma Proteome Database as a resource for proteomics research: 2014 update. *Nucleic acids research*, 42, D959-65.
- NEUKAMM, S. S., TOOTH, R., MORRICE, N., CAMPBELL, D. G., MACKINTOSH, C., LEHMANN, R., HAERING, H. U., SCHLEICHER, E. D. & WEIGERT, C. 2012. Identification of the amino acids 300-600 of IRS-2 as 14-3-3 binding region with the importance of IGF-1/insulin-regulated phosphorylation of Ser-573. *PLoS One*, 7, e43296.
- NICKERSON, M. L., JAEGER, E., SHI, Y., DUROCHER, J. A., MAHURKAR, S., ZARIDZE, D., MATVEEV, V., JANOUT, V., KOLLAROVA, H., BENCKO, V., NAVRATILOVA, M., SZESZENIA-DABROWSKA, N., MATES, D., MUKERIA, A., HOLCATOVA, I., SCHMIDT, L. S., TORO, J. R., KARAMI, S., HUNG, R., GERARD, G. F., LINEHAN, W. M., MERINO, M., ZBAR, B., BOFFETTA, P., BRENNAN, P., ROTHMAN, N., CHOW, W. H., WALDMAN, F. M. & MOORE, L. E. 2008. Improved identification of von Hippel-Lindau gene alterations in clear cell renal tumors. *Clin Cancer Res*, 14, 4726-34.
- NIELAND, J. D., GRAUS, Y. F., DORTMANS, Y. E., KREMERS, B. L. & KRUISBEEK, A. M. 1998. CD40 and CD70 co-stimulate a potent in vivo antitumor T cell response. *J Immunother*, 21, 225-36.
- NIRMALAN, N. J., HUGHES, C., PENG, J., MCKENNA, T., LANGRIDGE, J., CAIRNS, D. A., HARNDEN, P., SELBY, P. J. & BANKS, R. E. 2011. Initial

- development and validation of a novel extraction method for quantitative mining of the formalin-fixed, paraffin-embedded tissue proteome for biomarker investigations. *Journal of proteome research*, 10, 896-906.
- O'CONNOR, J. P. & JAYSON, G. C. 2012. Do imaging biomarkers relate to outcome in patients treated with VEGF inhibitors? *Clin Cancer Res*, 18, 6588-98.
- O'FARRELL, A. M., ABRAMS, T. J., YUEN, H. A., NGAI, T. J., LOUIE, S. G., YEE, K. W., WONG, L. M., HONG, W., LEE, L. B., TOWN, A., SMOLICH, B. D., MANNING, W. C., MURRAY, L. J., HEINRICH, M. C. & CHERRINGTON, J. M. 2003. SU11248 is a novel FLT3 tyrosine kinase inhibitor with potent activity in vitro and in vivo. *Blood*, 101, 3597-605.
- O'NEILL, A. K., GALLEGOS, L. L., JUSTILIEN, V., GARCIA, E. L., LEITGES, M., FIELDS, A. P., HALL, R. A. & NEWTON, A. C. 2011. Protein kinase Calpha promotes cell migration through a PDZ-dependent interaction with its novel substrate discs large homolog 1 (DLG1). *J Biol Chem*, 286, 43559-68.
- OHH, M., YAUCH, R. L., LONERGAN, K. M., WHALEY, J. M., STEMMER-RACHAMIMOV, A. O., LOUIS, D. N., GAVIN, B. J., KLEY, N., KAELIN, W. G., JR. & ILIOPOULOS, O. 1998. The von Hippel-Lindau tumor suppressor protein is required for proper assembly of an extracellular fibronectin matrix. *Mol Cell*, 1, 959-68.
- OKUDA, H., SAITOH, K., HIRAI, S., IWAI, K., TAKAKI, Y., BABA, M., MINATO, N., OHNO, S. & SHUIN, T. 2001. The von Hippel-Lindau tumor suppressor protein mediates ubiquitination of activated atypical protein kinase C. *J Biol Chem*, 276, 43611-7.
- OLSSON, A. K., DIMBERG, A., KREUGER, J. & CLAESSION-WELSH, L. 2006. VEGF receptor signalling - in control of vascular function. *Nature reviews. Molecular cell biology*, 7, 359-71.
- OMENN, G. S., STATES, D. J., ADAMSKI, M., BLACKWELL, T. W., MENON, R., HERMJAKOB, H., APWEILER, R., HAAB, B. B., SIMPSON, R. J., EDDES, J. S., KAPP, E. A., MORITZ, R. L., CHAN, D. W., RAI, A. J., ADMON, A., AEBERSOLD, R., ENG, J., HANCOCK, W. S., HEFTA, S. A., MEYER, H., PAIK, Y.-K., YOO, J.-S., PING, P., POUNDS, J., ADKINS, J., QIAN, X., WANG, R., WASINGER, V., WU, C. Y., ZHAO, X., ZENG, R., ARCHAKOV, A., TSUGITA, A., BEER, I., PANDEY, A., PISANO, M., ANDREWS, P., TAMMEN, H., SPEICHER, D. W. & HANASH, S. M. 2005. Overview of the HUPO Plasma Proteome Project: results from the pilot phase with 35 collaborating laboratories and multiple analytical groups, generating a core dataset of 3020 proteins and a publicly-available database. *Proteomics*, 5, 3226-45.
- OOSTERWIJK, E., RUITER, D. J., HOEDEMAEKER, P. J., PAUWELS, E. K., JONAS, U., ZWARTENDIJK, J. & WARNAAR, S. O. 1986. Monoclonal antibody G 250 recognizes a determinant present in renal-cell carcinoma and absent from normal kidney. *Int J Cancer*, 38, 489-94.
- OUYANG, T., BAI, R. Y., BASSERMANN, F., VON KLITZING, C., KLUMPEN, S., MIETHING, C., MORRIS, S. W., PESCHEL, C. & DUYSER, J. 2003. Identification and characterization of a nuclear interacting partner of anaplastic lymphoma kinase (NIPA). *J Biol Chem*, 278, 30028-36.
- OVERGAARD, M. T., HAANING, J., BOLDT, H. B., OLSEN, I. M., LAURSEN, L. S., CHRISTIANSEN, M., GLEICH, G. J., SOTTRUP-JENSEN, L., CONOVER, C. A. & OXVIG, C. 2000. Expression of recombinant human pregnancy-associated plasma protein-A and identification of the proform of eosinophil major basic protein as its physiological inhibitor. *J Biol Chem*, 275, 31128-33.

- OZCAN, A., DE LA ROZA, G., RO, J. Y., SHEN, S. S. & TRUONG, L. D. 2012. PAX2 and PAX8 expression in primary and metastatic renal tumors: a comprehensive comparison. *Arch Pathol Lab Med*, 136, 1541-51.
- PAEZ, J. G., JANNE, P. A., LEE, J. C., TRACY, S., GREULICH, H., GABRIEL, S., HERMAN, P., KAYE, F. J., LINDEMAN, N., BOGGON, T. J., NAOKI, K., SASAKI, H., FUJII, Y., ECK, M. J., SELLERS, W. R., JOHNSON, B. E. & MEYERSON, M. 2004. EGFR mutations in lung cancer: correlation with clinical response to gefitinib therapy. *Science*, 304, 1497-500.
- PAEZ-RIBES, M., ALLEN, E., HUDOCK, J., TAKEDA, T., OKUYAMA, H., VINALS, F., INOUE, M., BERGERS, G., HANAHAN, D. & CASANOVAS, O. 2009. Antiangiogenic therapy elicits malignant progression of tumors to increased local invasion and distant metastasis. *Cancer cell*, 15, 220-31.
- PAL, S., CLAFFEY, K. P., COHEN, H. T. & MUKHOPADHYAY, D. 1998. Activation of Sp1-mediated vascular permeability factor/vascular endothelial growth factor transcription requires specific interaction with protein kinase C zeta. *J Biol Chem*, 273, 26277-80.
- PAL, S., CLAFFEY, K. P., DVORAK, H. F. & MUKHOPADHYAY, D. 1997. The von Hippel-Lindau gene product inhibits vascular permeability factor/vascular endothelial growth factor expression in renal cell carcinoma by blocking protein kinase C pathways. *J Biol Chem*, 272, 27509-12.
- PANCHENKO, M. V., ZHOU, M. I. & COHEN, H. T. 2004. von Hippel-Lindau partner Jade-1 is a transcriptional co-activator associated with histone acetyltransferase activity. *J Biol Chem*, 279, 56032-41.
- PANKA, D. J., LIU, Q., GEISLER, A. K. & MIER, J. W. 2013. Effects of HDM2 antagonism on sunitinib resistance, p53 activation, SDF-1 induction, and tumor infiltration by CD11b+/Gr-1+ myeloid derived suppressor cells. *Mol Cancer*, 12, 17.
- PANKRATZ, S. L., TAN, E. Y., FINE, Y., MERCURIO, A. M. & SHAW, L. M. 2009. Insulin receptor substrate-2 regulates aerobic glycolysis in mouse mammary tumor cells via glucose transporter 1. *J Biol Chem*, 284, 2031-7.
- PANTUCK, A. J., AN, J., LIU, H. & RETTIG, M. B. 2010. NF-kappaB-dependent plasticity of the epithelial to mesenchymal transition induced by Von Hippel-Lindau inactivation in renal cell carcinomas. *Cancer research*, 70, 752-61.
- PAO, W., WANG, T. Y., RIELY, G. J., MILLER, V. A., PAN, Q., LADANYI, M., ZAKOWSKI, M. F., HEELAN, R. T., KRIS, M. G. & VARMUS, H. E. 2005. KRAS mutations and primary resistance of lung adenocarcinomas to gefitinib or erlotinib. *PLoS medicine*, 2, e17.
- PAPAYANNOPOULOS, V. & ZYCHLINSKY, A. 2009. NETs: a new strategy for using old weapons. *Trends Immunol*, 30, 513-21.
- PAPAZISIS, K. T., KONTOVINIS, L. F., PAPANDREOU, C. N., KOUVATSEAS, G., LAFARAS, C., ANTONAKIS, E., CHRISTOPOULOU, M., ANDREADIS, C., MOURATIDOU, D. & KORTSARIS, A. H. 2010. Brain natriuretic peptide precursor (NT-pro-BNP) levels predict for clinical benefit to sunitinib treatment in patients with metastatic renal cell carcinoma. *BMC cancer*, 10, 489.
- PARK, Y. H., KU, J. H., KWAK, C. & KIM, H. H. 2014. Post-treatment neutrophil-to-lymphocyte ratio in predicting prognosis in patients with metastatic clear cell renal cell carcinoma receiving sunitinib as first line therapy. *Springerplus*, 3, 243.
- PARK, Y. M., HWANG, S. J., MASUDA, K., CHOI, K. M., JEONG, M. R., NAM, D. H., GOROSPE, M. & KIM, H. H. 2012. Heterogeneous nuclear ribonucleoprotein C1/C2 controls the metastatic potential of glioblastoma by regulating PDCD4. *Mol Cell Biol*, 32, 4237-44.

- PARKKILA, S., RAJANIEMI, H., PARKKILA, A. K., KIVELA, J., WAHEED, A., PASTOREKOVA, S., PASTOREK, J. & SLY, W. S. 2000. Carbonic anhydrase inhibitor suppresses invasion of renal cancer cells in vitro. *Proc Natl Acad Sci U S A*, 97, 2220-4.
- PASSANITI, A. & HART, G. W. 1988. Cell surface sialylation and tumor metastasis. Metastatic potential of B16 melanoma variants correlates with their relative numbers of specific penultimate oligosaccharide structures. *J Biol Chem*, 263, 7591-603.
- PATEL, B. B., BARRERO, C. A., BRAVERMAN, A., KIM, P. D., JONES, K. A., CHEN, D. E., BOWLER, R. P., MERALI, S., KELSEN, S. G. & YEUNG, A. T. 2012. Assessment of two immunodepletion methods: off-target effects and variations in immunodepletion efficiency may confound plasma proteomics. *Journal of proteome research*, 11, 5947-58.
- PATEL, P. H., CHADALAVADA, R. S., ISHILL, N. M., PATIL, S., REUTER, V. E., MOTZER, R. J. & CHAGANTI, R. S. 2008. Hypoxia-inducible factor (HIF) 1 alpha and 2 alpha levels in cell lines and human tumor predicts response to sunitinib in renal cell carcinoma (RCC). *Journal of Clinical Oncology*, 26.
- PECINA-SLAUS, N. 2003. Tumor suppressor gene E-cadherin and its role in normal and malignant cells. *Cancer Cell Int*, 3, 17.
- PENA-LLOPIS, S., VEGA-RUBIN-DE-CELIS, S., LIAO, A., LENG, N., PAVIA-JIMENEZ, A., WANG, S., YAMASAKI, T., ZHREBKER, L., SIVANAND, S., SPENCE, P., KINCH, L., HAMBUCH, T., JAIN, S., LOTAN, Y., MARGULIS, V., SAGALOWSKY, A. I., SUMMEROUR, P. B., KABBANI, W., WONG, S. W., GRISHIN, N., LAURENT, M., XIE, X. J., HAUDENSCHILD, C. D., ROSS, M. T., BENTLEY, D. R., KAPUR, P. & BRUGAROLAS, J. 2012. BAP1 loss defines a new class of renal cell carcinoma. *Nat Genet*, 44, 751-9.
- PEREZ, M. A., SAUL, S. H. & TROJANOWSKI, J. Q. 1990. Neurofilament and chromogranin expression in normal and neoplastic neuroendocrine cells of the human gastrointestinal tract and pancreas. *Cancer*, 65, 1219-27.
- PEREZ-GRACIA, J. L., PRIOR, C., GUILLÉN-GRIMA, F., SEGURA, V., GONZALEZ, A., PANIZO, A., MELERO, I., GRANDE-PULIDO, E., GURPIDE, A., GIL-BAZO, I. & CALVO, A. 2009. Identification of TNF-alpha and MMP-9 as potential baseline predictive serum markers of sunitinib activity in patients with renal cell carcinoma using a human cytokine array. *British journal of cancer*, 101, 1876-83.
- PETRAU, C., CORNIC, M., BERTRAND, P., MAINGONNAT, C., MARCHAND, V., PICQUENOT, J. M., JARDIN, F. & CLATOT, F. 2014. CD70: A Potential Target in Breast Cancer? *J Cancer*, 5, 761-4.
- PEZZATO, E., DONA, M., SARTOR, L., DELL'AICA, I., BENELLI, R., ALBINI, A. & GARBISA, S. 2003. Proteinase-3 directly activates MMP-2 and degrades gelatin and Matrigel; differential inhibition by (-)epigallocatechin-3-gallate. *J Leukoc Biol*, 74, 88-94.
- PFLEIDERER, G., THONER, M. & WACHSMUTH, E. D. 1975. Histological examination of the aldolase monomer composition of cells from human kidney and hypernephroid carcinoma. *Beitr Pathol*, 156, 266-79.
- PORT, F. K., RAGHEB, N. E., SCHWARTZ, A. G. & HAWTHORNE, V. M. 1989. Neoplasms in dialysis patients: a population-based study. *American journal of kidney diseases : the official journal of the National Kidney Foundation*, 14, 119-23.
- PORTA, C., PAGLINO, C., DE AMICI, M., QUAGLINI, S., SACCHI, L., IMARISIO, I. & CANIPARI, C. 2010. Predictive value of baseline serum vascular endothelial growth factor and neutrophil gelatinase-associated lipocalin in

- advanced kidney cancer patients receiving sunitinib. *Kidney international*, 77, 809-15.
- POWLES, T. O., S; BERNARD J. ESCUDIER, JANET ELIZABETH BROWN, ROBERT E. HAWKINS, DANIEL E. CASTELLANO, ALAIN RAVAUD, MICHAEL D. STAEHLER, BRIAN I. RINI, WEI LIN, BRIDGET O'KEEFFE, MICHELLE BYRTEK, MARK LACKNER, JILL M SPOERKE, JOSEPH A. WARE, RUI ZHU, ROBERT J. MOTZER 2014. A randomized phase II study of GDC-0980 versus everolimus in metastatic renal cell carcinoma (mRCC) patients (pts) after VEGF-targeted therapy (VEGF-TT). *Journal of clinical oncology : official journal of the American Society of Clinical Oncology*, 32, 4525.
- PRASAD, S. R., HUMPHREY, P. A., CATENA, J. R., NARRA, V. R., SRIGLEY, J. R., CORTEZ, A. D., DALRYMPLE, N. C. & CHINTAPALLI, K. N. 2006. Common and uncommon histologic subtypes of renal cell carcinoma: imaging spectrum with pathologic correlation. *Radiographics*, 26, 1795-806; discussion 1806-10.
- PRIOR, C., PEREZ-GRACIA, J. L., GARCIA-DONAS, J., RODRIGUEZ-ANTONA, C., GURUCEAGA, E., ESTEBAN, E., SUAREZ, C., CASTELLANO, D., DEL ALBA, A. G., LOZANO, M. D., CARLES, J., CLIMENT, M. A., ARRANZ, J. A., GALLARDO, E., PUENTE, J., BELLMUNT, J., GURPIDE, A., LOPEZ-PICAZO, J. M., HERNANDEZ, A. G., MELLADO, B., MARTINEZ, E., MORENO, F., FONT, A. & CALVO, A. 2014. Identification of tissue microRNAs predictive of sunitinib activity in patients with metastatic renal cell carcinoma. *PLoS one*, 9, e86263.
- PUSHKIN, A., CARPENITO, G., ABULADZE, N., NEWMAN, D., TSUPRUN, V., RYAZANTSEV, S., MOTEMOTURU, S., SASSANI, P., SOLOVIEVA, N., DUKKIPATI, R. & KURTZ, I. 2004. Structural characterization, tissue distribution, and functional expression of murine aminoacylase III. *Am J Physiol Cell Physiol*, 286, C848-56.
- PUZANOV, I., MICHAELSON, D., COHEN, D., LI, S., BURNETT, P. & DESAI, J. 2011. Evaluation of Hand-foot Syndrome (HFS) as a Potential Biomarker of Sunitinib (SU) Efficacy in Patients (pts) With Metastatic Renal Cell Carcinoma (mRCC) and Gastrointestinal Stromal Tumour (GIST). *European journal of cancer*, 47, S182-S182.
- RABIZADEH, E., CHERNY, I., WOLACH, O., SHERMAN, S., BINKOVSKI, N., PERETZ, A., LEDERFEIN, D. & INBAL, A. 2014. Increased activity of cell membrane-associated prothrombinase, fibrinogen-like protein 2, in peripheral blood mononuclear cells of B-cell lymphoma patients. *PLoS One*, 9, e109648.
- RAKOFF-NAHOUM, S. 2006. Why cancer and inflammation? *Yale J Biol Med*, 79, 123-30.
- RAMETTA, R., MOZZI, E., DONGIOVANNI, P., MOTTA, B. M., MILANO, M., ROVIARO, G., FARGION, S. & VALENTI, L. 2013. Increased insulin receptor substrate 2 expression is associated with steatohepatitis and altered lipid metabolism in obese subjects. *Int J Obes (Lond)*, 37, 986-92.
- RAVAL, R. R., LAU, K. W., TRAN, M. G., SOWTER, H. M., MANDRIOTA, S. J., LI, J. L., PUGH, C. W., MAXWELL, P. H., HARRIS, A. L. & RATCLIFFE, P. J. 2005. Contrasting properties of hypoxia-inducible factor 1 (HIF-1) and HIF-2 in von Hippel-Lindau-associated renal cell carcinoma. *Mol Cell Biol*, 25, 5675-86.
- RAY, M. E., WISTOW, G., SU, Y. A., MELTZER, P. S. & TRENT, J. M. 1997. AIM1, a novel non-lens member of the betagamma-crystallin superfamily, is associated with the control of tumorigenicity in human malignant melanoma.

- Proceedings of the National Academy of Sciences of the United States of America*, 94, 3229-34.
- RENEHAN, A. G., TYSON, M., EGGER, M., HELLER, R. F. & ZWAHLEN, M. 2008. Body-mass index and incidence of cancer: a systematic review and meta-analysis of prospective observational studies. *Lancet*, 371, 569-78.
- REUVENI, H., FLASHNER-ABRAMSON, E., STEINER, L., MAKEDONSKI, K., SONG, R., SHIR, A., HERLYN, M., BAR-ELI, M. & LEVITZKI, A. 2013. Therapeutic destruction of insulin receptor substrates for cancer treatment. *Cancer Res*, 73, 4383-94.
- RICKETTS, C. J., MORRIS, M. R., GENTLE, D., SHUIB, S., BROWN, M., CLARKE, N., WEI, W., NATHAN, P., LATIF, F. & MAHER, E. R. 2013. Methylation profiling and evaluation of demethylating therapy in renal cell carcinoma. *Clin Epigenetics*, 5, 16.
- RINI, B. I., COHEN, D. P., LU, D. R., CHEN, I., HARIHARAN, S., GORE, M. E., FIGLIN, R. A., BAUM, M. S. & MOTZER, R. J. 2011a. Hypertension as a biomarker of efficacy in patients with metastatic renal cell carcinoma treated with sunitinib. *Journal of the National Cancer Institute*, 103, 763-73.
- RINI, B. I., HALABI, S., ROSENBERG, J. E., STADLER, W. M., VAENA, D. A., ARCHER, L., ATKINS, J. N., PICUS, J., CZAYKOWSKI, P., DUTCHER, J. & SMALL, E. J. 2010a. Phase III Trial of Bevacizumab Plus Interferon Alfa Versus Interferon Alfa Monotherapy in Patients With Metastatic Renal Cell Carcinoma: Final Results of CALGB 90206. *Journal of Clinical Oncology*, 28, 2137-2143.
- RINI, B. I., HALABI, S., ROSENBERG, J. E., STADLER, W. M., VAENA, D. A., ARCHER, L., ATKINS, J. N., PICUS, J., CZAYKOWSKI, P., DUTCHER, J. & SMALL, E. J. 2010b. Phase III trial of bevacizumab plus interferon alfa versus interferon alfa monotherapy in patients with metastatic renal cell carcinoma: final results of CALGB 90206. *Journal of Clinical Oncology*, 28, 2137-43.
- RINI, B. I., JAEGER, E., WEINBERG, V., SEIN, N., CHEW, K., FONG, K., SIMKO, J., SMALL, E. J. & WALDMAN, F. M. 2006. Clinical response to therapy targeted at vascular endothelial growth factor in metastatic renal cell carcinoma: impact of patient characteristics and Von Hippel-Lindau gene status. *BJU Int*, 98, 756-62.
- RINI, B. I., MICHAELSON, M. D., ROSENBERG, J. E., BUKOWSKI, R. M., SOSMAN, J. A., STADLER, W. M., HUTSON, T. E., MARGOLIN, K., HARMON, C. S., DEPRIMO, S. E., KIM, S. T., CHEN, I. & GEORGE, D. J. 2008. Antitumor activity and biomarker analysis of sunitinib in patients with bevacizumab-refractory metastatic renal cell carcinoma. *Journal of clinical oncology : official journal of the American Society of Clinical Oncology*, 26, 3743-8.
- RINI, B. I., SCHILLER, J. H., FRUEHAUF, J. P., COHEN, E. E., TARAZI, J. C., ROSBROOK, B., BAIR, A. H., RICART, A. D., OLSZANSKI, A. J., LETRENT, K. J., KIM, S. & RIXE, O. 2011b. Diastolic blood pressure as a biomarker of axitinib efficacy in solid tumors. *Clinical cancer research : an official journal of the American Association for Cancer Research*, 17, 3841-9.
- RIXE, O., BILLEMONT, B. & IZZEDINE, H. 2007. Hypertension as a predictive factor of Sunitinib activity. *Annals of oncology : official journal of the European Society for Medical Oncology / ESMO*, 18, 1117.
- ROBERTS, E. L. & ROBERTS, O. T. 2012. Plasma adenosine deaminase isoform 2 in cancer patients undergoing chemotherapy. *Br J Biomed Sci*, 69, 11-3.

- ROE, J. S., KIM, H., LEE, S. M., KIM, S. T., CHO, E. J. & YOUN, H. D. 2006. p53 stabilization and transactivation by a von Hippel-Lindau protein. *Mol Cell*, 22, 395-405.
- ROSSI, E., FASSAN, M., AIETA, M., ZILIO, F., CELADIN, R., BORIN, M., GRASSI, A., TROIANI, L., BASSO, U., BARILE, C., SAVA, T., LANZA, C., MIATELLO, L., JIRILLO, A., RUGGE, M., INDRACCOLO, S., CRISTOFANILLI, M., AMADORI, A. & ZAMARCHI, R. 2012. Dynamic changes of live/apoptotic circulating tumour cells as predictive marker of response to sunitinib in metastatic renal cancer. *British journal of cancer*, 107, 1286-94.
- RUI, L., YUAN, M., FRANTZ, D., SHOELSON, S. & WHITE, M. F. 2002. SOCS-1 and SOCS-3 block insulin signaling by ubiquitin-mediated degradation of IRS1 and IRS2. *J Biol Chem*, 277, 42394-8.
- SAED, G. M., ALI-FEHMI, R., JIANG, Z. L., FLETCHER, N. M., DIAMOND, M. P., ABU-SOUD, H. M. & MUNKARAH, A. R. 2010. Myeloperoxidase serves as a redox switch that regulates apoptosis in epithelial ovarian cancer. *Gynecol Oncol*, 116, 276-81.
- SAEZ, M. I., PEREZ, J. M. T., PEREZ-RIVAS, L. G., PEREZ-VILLA, L., VILLATORO, R., MONTESA, A., CID, J. I., LEON, M., DE LUQUE, V., FERNANDEZ, C., QUERO, C., PAJARES, B. & ALBA, E. 2012. Hypoxia-inducible factor (HIF) 1 alpha and 2 alpha as predictive markers of outcome to VEGFR tyrosine kinase inhibitors (TKI) in renal cell carcinoma (RCC). *Journal of Clinical Oncology*, 30.
- SAITO, H., NISHIMURA, M., SHINANO, H., MAKITA, H., TSUJINO, I., SHIBUYA, E., SATO, F., MIYAMOTO, K. & KAWAKAMI, Y. 1999. Plasma concentration of adenosine during normoxia and moderate hypoxia in humans. *Am J Respir Crit Care Med*, 159, 1014-8.
- SALEM, M. E., SHAH, S. N., ELSON, P., GARCIA, J. A., WOOD, L. S., MEDSINGE, A., CAMPBELL, S., DREICER, R. & RINI, B. I. 2014. Computed tomography characteristics of unresectable primary renal cell carcinoma treated with neoadjuvant sunitinib. *Clinical genitourinary cancer*, 12, 117-23.
- SALTON, M., ELKON, R., BORODINA, T., DAVYDOV, A., YASPO, M. L., HALPERIN, E. & SHILOH, Y. 2011. MatrIn 3 binds and stabilizes mRNA. *PLoS One*, 6, e23882.
- SANFORD, T., CHUNG, P. H., REINISH, A., VALERA, V., SRINIVASAN, R., LINEHAN, W. M. & BRATSLAVSKY, G. 2011. Molecular sub-classification of renal epithelial tumors using meta-analysis of gene expression microarrays. *PloS one*, 6, e21260.
- SATO, Y., YOSHIZATO, T., SHIRAISHI, Y., MAEKAWA, S., OKUNO, Y., KAMURA, T., SHIMAMURA, T., SATO-OTSUBO, A., NAGAE, G., SUZUKI, H., NAGATA, Y., YOSHIDA, K., KON, A., SUZUKI, Y., CHIBA, K., TANAKA, H., NIIDA, A., FUJIMOTO, A., TSUNODA, T., MORIKAWA, T., MAEDA, D., KUME, H., SUGANO, S., FUKAYAMA, M., ABURATANI, H., SANADA, M., MIYANO, S., HOMMA, Y. & OGAWA, S. 2013. Integrated molecular analysis of clear-cell renal cell carcinoma. *Nat Genet*, 45, 860-7.
- SAWYERS, C. L. 2008. The cancer biomarker problem. *Nature*, 452, 548-52.
- SCARTOZZI, M., BIANCONI, M., FALOPPI, L., LORETELLI, C., BITTONI, A., DEL PRETE, M., GIAMPIERI, R., MACCARONI, E., NICOLETTI, S., BURATTINI, L., MINARDI, D., MUZZONIGRO, G., MONTIRONI, R. & CASCINU, S. 2013. VEGF and VEGFR polymorphisms affect clinical outcome in advanced renal cell carcinoma patients receiving first-line sunitinib. *British journal of cancer*, 108, 1126-32.

- SCHMIDINGER, M., VOGL, U. M., BOJIC, M., LAMM, W., HEINZL, H., HAITEL, A., CLODI, M., KRAMER, G. & ZIELINSKI, C. C. 2011. Hypothyroidism in Patients With Renal Cell Carcinoma Blessing or Curse? *Cancer*, 117, 534-544.
- SCHODEL, J., OIKONOMOPOULOS, S., RAGOSSIS, J., PUGH, C. W., RATCLIFFE, P. J. & MOLE, D. R. 2011. High-resolution genome-wide mapping of HIF-binding sites by ChIP-seq. *Blood*, 117, e207-17.
- SCHOENFELD, A., DAVIDOWITZ, E. J. & BURK, R. D. 1998. A second major native von Hippel-Lindau gene product, initiated from an internal translation start site, functions as a tumor suppressor. *Proceedings of the National Academy of Sciences of the United States of America*, 95, 8817-22.
- SCUMACI, D., GASPARI, M., SACCOMANNO, M., ARGIRO, G., QUARESIMA, B., FANIELLO, C. M., RICCI, P., COSTANZO, F. & CUDA, G. 2011. Assessment of an ad hoc procedure for isolation and characterization of human albuminome. *Anal Biochem*, 418, 161-3.
- SEMENZA, G. L. 1998. Hypoxia-inducible factor 1: master regulator of O₂ homeostasis. *Current opinion in genetics & development*, 8, 588-94.
- SEMENZA, G. L. 2003. Targeting HIF-1 for cancer therapy. *Nat Rev Cancer*, 3, 721-32.
- SENOO, M., HOSHINO, S., MOCHIDA, N., MATSUMURA, Y. & HABU, S. 2002. Identification of a novel protein p59(scr), which is expressed at specific stages of mouse spermatogenesis. *Biochem Biophys Res Commun*, 292, 992-8.
- SESTI, G., FEDERICI, M., HRIBAL, M. L., LAURO, D., SBRACCIA, P. & LAURO, R. 2001. Defects of the insulin receptor substrate (IRS) system in human metabolic disorders. *FASEB J*, 15, 2099-111.
- SEVENICH, L., SCHURIGT, U., SACHSE, K., GAJDA, M., WERNER, F., MULLER, S., VASILJEVA, O., SCHWINDE, A., KLEMM, N., DEUSSING, J., PETERS, C. & REINHECKEL, T. 2010. Synergistic antitumor effects of combined cathepsin B and cathepsin Z deficiencies on breast cancer progression and metastasis in mice. *Proceedings of the National Academy of Sciences of the United States of America*, 107, 2497-502.
- SHAMAMIAN, P., SCHWARTZ, J. D., POCOCK, B. J., MONEA, S., WHITING, D., MARCUS, S. G. & MIGNATTI, P. 2001. Activation of progelatinase A (MMP-2) by neutrophil elastase, cathepsin G, and proteinase-3: a role for inflammatory cells in tumor invasion and angiogenesis. *J Cell Physiol*, 189, 197-206.
- SHAPIRO, G. I. 2006. Cyclin-dependent kinase pathways as targets for cancer treatment. *J Clin Oncol*, 24, 1770-83.
- SHAW, L. M. 2001. Identification of insulin receptor substrate 1 (IRS-1) and IRS-2 as signaling intermediates in the alpha6beta4 integrin-dependent activation of phosphoinositide 3-OH kinase and promotion of invasion. *Mol Cell Biol*, 21, 5082-93.
- SHIBAO, K., FIEDLER, M. J., NAGATA, J., MINAGAWA, N., HIRATA, K., NAKAYAMA, Y., IWAKIRI, Y., NATHANSON, M. H. & YAMAGUCHI, K. 2010. The type III inositol 1,4,5-trisphosphate receptor is associated with aggressiveness of colorectal carcinoma. *Cell Calcium*, 48, 315-23.
- SHOJAEI, F., WU, X., MALIK, A. K., ZHONG, C., BALDWIN, M. E., SCHANZ, S., FUH, G., GERBER, H. P. & FERRARA, N. 2007. Tumor refractoriness to anti-VEGF treatment is mediated by CD11b+Gr1+ myeloid cells. *Nat Biotechnol*, 25, 911-20.
- SIERKO, E., WOJTUKIEWICZ, M. Z. & KISIEL, W. 2007. The role of tissue factor pathway inhibitor-2 in cancer biology. *Semin Thromb Hemost*, 33, 653-9.

- SIERRA, J. R., CEPERO, V. & GIORDANO, S. 2010. Molecular mechanisms of acquired resistance to tyrosine kinase targeted therapy. *Molecular cancer*, 9, 75.
- SIM, S. H., MESSENGER, M. P., GREGORY, W. M., WIND, T. C., VASUDEV, N. S., CARTLEDGE, J., THOMPSON, D., SELBY, P. J. & BANKS, R. E. 2012. Prognostic utility of pre-operative circulating osteopontin, carbonic anhydrase IX and CRP in renal cell carcinoma. *British journal of cancer*, 107, 1131-7.
- SIMONNET, H., ALAZARD, N., PFEIFFER, K., GALLOU, C., BEROUD, C., DEMONT, J., BOUVIER, R., SCHAGGER, H. & GODINOT, C. 2002. Low mitochondrial respiratory chain content correlates with tumor aggressiveness in renal cell carcinoma. *Carcinogenesis*, 23, 759-68.
- SIRAJ, M. A., PICHON, C., RADU, A. & GHINEA, N. 2012. Endothelial follicle stimulating hormone receptor in primary kidney cancer correlates with subsequent response to sunitinib. *J Cell Mol Med*, 16, 2010-6.
- SITOHY, B., NAGY, J. A. & DVORAK, H. F. 2012. Anti-VEGF/VEGFR therapy for cancer: reassessing the target. *Cancer research*, 72, 1909-14.
- SLATTERY, M. L., SAMOWITZ, W., CURTIN, K., MA, K. N., HOFFMAN, M., CAAN, B. & NEUHAUSEN, S. 2004. Associations among IRS1, IRS2, IGF1, and IGF1R3 genetic polymorphisms and colorectal cancer. *Cancer Epidemiol Biomarkers Prev*, 13, 1206-14.
- SMITH, A. D., LIEBER, M. L. & SHAH, S. N. 2010a. Assessing tumor response and detecting recurrence in metastatic renal cell carcinoma on targeted therapy: importance of size and attenuation on contrast-enhanced CT. *AJR Am J Roentgenol*, 194, 157-65.
- SMITH, A. D., SHAH, S. N., RINI, B. I., LIEBER, M. L. & REMER, E. M. 2010b. Morphology, Attenuation, Size, and Structure (MASS) criteria: assessing response and predicting clinical outcome in metastatic renal cell carcinoma on antiangiogenic targeted therapy. *AJR Am J Roentgenol*, 194, 1470-8.
- SMITH, M. P., WOOD, S. L., ZOUGMAN, A., HO, J. T., PENG, J., JACKSON, D., CAIRNS, D. A., LEWINGTON, A. J., SELBY, P. J. & BANKS, R. E. 2011a. A systematic analysis of the effects of increasing degrees of serum immunodepletion in terms of depth of coverage and other key aspects in top-down and bottom-up proteomic analyses. *Proteomics*, 11, 2222-35.
- SMITH, M. P. W., WOOD, S. L., ZOUGMAN, A., HO, J. T. C., PENG, J., JACKSON, D., CAIRNS, D. A., LEWINGTON, A. J. P., SELBY, P. J. & BANKS, R. E. 2011b. A systematic analysis of the effects of increasing degrees of serum immunodepletion in terms of depth of coverage and other key aspects in top-down and bottom-up proteomic analyses. *Proteomics*, 11, 2222-35.
- SMITH, M. W., YUE, Z. N., GEISS, G. K., SADOVNIKOVA, N. Y., CARTER, V. S., BOIX, L., LAZARO, C. A., ROSENBERG, G. B., BUMGARNER, R. E., FAUSTO, N., BRUIX, J. & KATZE, M. G. 2003. Identification of novel tumor markers in hepatitis C virus-associated hepatocellular carcinoma. *Cancer research*, 63, 859-64.
- SOBIN, L. H., GOSPODAROWICZ, M. K. & WITTEKIND, C. (eds.) 2009. *International Union Against Cancer (UICC) TNM Classification of Malignant Tumors, 7th ed*, Oxford, UK: Wiley-Blackwell.
- SOKER, S., MIAO, H.-Q., NOMI, M., TAKASHIMA, S. & KLAGSBRUN, M. 2002. VEGF 165 Mediates Formation of Complexes Containing VEGFR-2 and Neuropilin-1 That Enhance VEGF 165 -Receptor Binding. *Journal of Cellular Biochemistry*, 368.

- SPUCH, C., ORTOLANO, S. & NAVARRO, C. 2012. LRP-1 and LRP-2 receptors function in the membrane neuron. Trafficking mechanisms and proteolytic processing in Alzheimer's disease. *Front Physiol*, 3, 269.
- STERNBERG, C. N., DAVIS, I. D., MARDIAK, J., SZCZYLIK, C., LEE, E., WAGSTAFF, J., BARRIOS, C. H., SALMAN, P., GLADKOV, O. A., KAVINA, A., ZARBA, J. J., CHEN, M., MCCANN, L., PANDITE, L., ROYCHOWDHURY, D. F. & HAWKINS, R. E. 2010. Pazopanib in locally advanced or metastatic renal cell carcinoma: results of a randomized phase III trial. *J Clin Oncol*, 28, 1061-8.
- STEWART, G. D., O'MAHONY, F. C., LAIRD, A., RASHID, S., MARTIN, S. A., EORY, L., LUBBOCK, A. L., NANDA, J., O'DONNELL, M., MACKAY, A., MULLEN, P., MCNEILL, S. A., RIDDICK, A. C., AITCHISON, M., BERNEY, D., BEX, A., OVERTON, I. M., HARRISON, D. J. & POWLES, T. 2014. Carbonic Anhydrase 9 Expression Increases with Vascular Endothelial Growth Factor-Targeted Therapy and Is Predictive of Outcome in Metastatic Clear Cell Renal Cancer. *European urology*.
- STOCKLI, J., DAVEY, J. R., HOHNEN-BEHRENS, C., XU, A., JAMES, D. E. & RAMM, G. 2008. Regulation of glucose transporter 4 translocation by the Rab guanosine triphosphatase-activating protein AS160/TBC1D4: role of phosphorylation and membrane association. *Mol Endocrinol*, 22, 2703-15.
- STOREY, J. D. 2002. A direct approach to false discovery rates. *Journal of the Royal Statistical Society Series B-Statistical Methodology*, 64, 479-498.
- SU, J.-L., YANG, C.-Y., SHIH, J.-Y., WEI, L.-H., HSIEH, C.-Y., JENG, Y.-M., WANG, M.-Y., YANG, P.-C. & KUO, M.-L. 2006. Knockdown of contactin-1 expression suppresses invasion and metastasis of lung adenocarcinoma. *Cancer research*, 66, 2553-61.
- SU, K., CHEN, F., YAN, W. M., ZENG, Q. L., XU, L., XI, D., PI, B., LUO, X. P. & NING, Q. 2008. Fibrinogen-like protein 2/fibroleukin prothrombinase contributes to tumor hypercoagulability via IL-2 and IFN-gamma. *World J Gastroenterol*, 14, 5980-9.
- SU KIM, D., CHOI, Y. D., MOON, M., KANG, S., LIM, J. B., KIM, K. M., PARK, K. M. & CHO, N. H. 2013. Composite three-marker assay for early detection of kidney cancer. *Cancer Epidemiol Biomarkers Prev*, 22, 390-8.
- SUN, M., SHARIAT, S. F., CHENG, C., FICARRA, V., MURAI, M., OUDARD, S., PANTUCK, A. J., ZIGEUNER, R. & KARAKIEWICZ, P. I. 2011. Prognostic factors and predictive models in renal cell carcinoma: a contemporary review. *European urology*, 60, 644-61.
- SUN, X. J., ROTHENBERG, P., KAHN, C. R., BACKER, J. M., ARAKI, E., WILDEN, P. A., CAHILL, D. A., GOLDSTEIN, B. J. & WHITE, M. F. 1991. Structure of the insulin receptor substrate IRS-1 defines a unique signal transduction protein. *Nature*, 352, 73-7.
- SUN, X. J., WANG, L. M., ZHANG, Y., YENUSH, L., MYERS, M. G., JR., GLASHEEN, E., LANE, W. S., PIERCE, J. H. & WHITE, M. F. 1995. Role of IRS-2 in insulin and cytokine signalling. *Nature*, 377, 173-7.
- SUNDELIN, J. P., STAHLMAN, M., LUNDQVIST, A., LEVIN, M., PARINI, P., JOHANSSON, M. E. & BOREN, J. 2012. Increased expression of the very low-density lipoprotein receptor mediates lipid accumulation in clear-cell renal cell carcinoma. *PLoS One*, 7, e48694.
- SURESHBABU, A., OKAJIMA, H., YAMANAKA, D., TONNER, E., SHASTRI, S., MAYCOCK, J., SZYMANOWSKA, M., SHAND, J., TAKAHASHI, S., BEATTIE, J., ALLAN, G. & FLINT, D. 2012. IGFBP5 induces cell adhesion, increases cell survival and inhibits cell migration in MCF-7 human breast cancer cells. *J Cell Sci*, 125, 1693-705.

- SZMIT, S., LANGIEWICZ, P., ZLNIEREK, J., NURZYNSKI, P., ZABOROWSKA, M., FILIPIAK, K. J., OPOLSKI, G. & SZCZYLIK, C. 2012. Hypertension as a predictive factor for survival outcomes in patients with metastatic renal cell carcinoma treated with sunitinib after progression on cytokines. *Kidney Blood Press Res*, 35, 18-25.
- TAKASHI, M., ZHU, Y., NAKANO, Y., MIYAKE, K. & KATO, K. 1992. Elevated levels of serum aldolase A in patients with renal cell carcinoma. *Urol Res*, 20, 307-11.
- TAN, P. H., CHENG, L., RIOUX-LECLERCQ, N., MERINO, M. J., NETTO, G., REUTER, V. E., SHEN, S. S., GRIGNON, D. J., MONTIRONI, R., EGEVAD, L., SRIGLEY, J. R., DELAHUNT, B. & MOCH, H. 2013. Renal tumors: diagnostic and prognostic biomarkers. *Am J Surg Pathol*, 37, 1518-31.
- TANAKA, Y., AKIYAMA, H., KURODA, T., JUNG, G., TANAHASHI, K., SUGAYA, H., UTSUMI, J., KAWASAKI, H. & HIRANO, H. 2006. A novel approach and protocol for discovering extremely low-abundance proteins in serum. *Proteomics*, 6, 4845-55.
- TANIGUCHI, C. M., UEKI, K. & KAHN, R. 2005. Complementary roles of IRS-1 and IRS-2 in the hepatic regulation of metabolism. *J Clin Invest*, 115, 718-27.
- TEAM, R. D. C. 2011. R: A language and environment for statistical computing. Vienna, Austria.: R Development Core Team.
- TELLO, D., Balsa, E., ACOSTA-IBORRA, B., FUERTES-YEBRA, E., ELORZA, A., ORDONEZ, A., CORRAL-ESCARIZ, M., SORO, I., LOPEZ-BERNARDO, E., PERALES-CLEMENTE, E., MARTINEZ-RUIZ, A., ENRIQUEZ, J. A., ARAGONES, J., CADENAS, S. & LANDAZURI, M. O. 2011. Induction of the mitochondrial NDUFA4L2 protein by HIF-1alpha decreases oxygen consumption by inhibiting Complex I activity. *Cell Metab*, 14, 768-79.
- TENG, P. N., HOOD, B. L., SUN, M., DHIR, R. & CONRADS, T. P. 2011. Differential proteomic analysis of renal cell carcinoma tissue interstitial fluid. *J Proteome Res*, 10, 1333-42.
- TERAKAWA, T., MIYAKE, H., KUSUDA, Y. & FUJISAWA, M. 2013. Expression level of vascular endothelial growth factor receptor-2 in radical nephrectomy specimens as a prognostic predictor in patients with metastatic renal cell carcinoma treated with sunitinib. *Urologic oncology*, 31, 493-8.
- TESSELAAR, K., XIAO, Y., ARENS, R., VAN SCHIJNDEL, G. M., SCHUURHUIS, D. H., MEBIUS, R. E., BORST, J. & VAN LIER, R. A. 2003. Expression of the murine CD27 ligand CD70 in vitro and in vivo. *J Immunol*, 170, 33-40.
- TETSU, O. & MCCORMICK, F. 2003. Proliferation of cancer cells despite CDK2 inhibition. *Cancer Cell*, 3, 233-45.
- THERASSE, P., ARBUCK, S. G., EISENHAUER, E. A., WANDERS, J., KAPLAN, R. S., RUBINSTEIN, L., VERWEIJ, J., VAN GLABBEKE, M., VAN OOSTEROM, A. T., CHRISTIAN, M. C. & GWYTHYER, S. G. 2000. New guidelines to evaluate the response to treatment in solid tumors. European Organization for Research and Treatment of Cancer, National Cancer Institute of the United States, National Cancer Institute of Canada. *J Natl Cancer Inst*, 92, 205-16.
- THIAM, R., FOURNIER, L. S., TRINQUART, L., MEDIONI, J., CHATELLIER, G., BALVAY, D., ESCUDIER, B., DROMAIN, C., CUENOD, C. A. & OUDARD, S. 2010. Optimizing the size variation threshold for the CT evaluation of response in metastatic renal cell carcinoma treated with sunitinib. *Annals of oncology : official journal of the European Society for Medical Oncology / ESMO*, 21, 936-41.
- THOMA, C. R., TOSO, A., GUTBRODT, K. L., REGGI, S. P., FREW, I. J., SCHRAML, P., HERGOVICH, A., MOCH, H., MERALDI, P. & KREK, W.

2009. VHL loss causes spindle misorientation and chromosome instability. *Nat Cell Biol*, 11, 994-1001.
- THOMAS, J. C., MATAK-VINKOVIC, D., VAN MOLLE, I. & CIULLI, A. 2013. Multimeric complexes among ankyrin-repeat and SOCS-box protein 9 (ASB9), ElonginBC, and Cullin 5: insights into the structure and assembly of ECS-type Cullin-RING E3 ubiquitin ligases. *Biochemistry*, 52, 5236-46.
- THOMAS, R. K., BAKER, A. C., DEBIASI, R. M., WINCKLER, W., LAFRAMBOISE, T., LIN, W. M., WANG, M., FENG, W., ZANDER, T., MACCONAILL, L., LEE, J. C., NICOLETTI, R., HATTON, C., GOYETTE, M., GIRARD, L., MAJMUDAR, K., ZIAUGRA, L., WONG, K. K., GABRIEL, S., BEROUKHIM, R., PEYTON, M., BARRETINA, J., DUTT, A., EMERY, C., GREULICH, H., SHAH, K., SASAKI, H., GAZDAR, A., MINNA, J., ARMSTRONG, S. A., MELLINGHOFF, I. K., HODI, F. S., DRANOFF, G., MISCHER, P. S., CLOUGHESY, T. F., NELSON, S. F., LIAU, L. M., MERTZ, K., RUBIN, M. A., MOCH, H., LODA, M., CATALONA, W., FLETCHER, J., SIGNORETTI, S., KAYE, F., ANDERSON, K. C., DEMETRI, G. D., DUMMER, R., WAGNER, S., HERLYN, M., SELLERS, W. R., MEYERSON, M. & GARRAWAY, L. A. 2007. High-throughput oncogene mutation profiling in human cancer. *Nat Genet*, 39, 347-51.
- THOMPSON, R. H., GILLETT, M. D., CHEVILLE, J. C., LOHSE, C. M., DONG, H., WEBSTER, W. S., KREJCI, K. G., LOBO, J. R., SENGUPTA, S., CHEN, L., ZINCKE, H., BLUTE, M. L., STROME, S. E., LEIBOVICH, B. C. & KWON, E. D. 2004. Costimulatory B7-H1 in renal cell carcinoma patients: Indicator of tumor aggressiveness and potential therapeutic target. *Proceedings of the National Academy of Sciences of the United States of America*, 101, 17174-9.
- THORPE, C. & KIM, J. J. 1995. Structure and mechanism of action of the acyl-CoA dehydrogenases. *FASEB J*, 9, 718-25.
- TIMMS, J. F., ARSLAN-LOW, E., KABIR, M., WORTHINGTON, J., CAMUZEAX, S., SINCLAIR, J., SZAUB, J., AFROUGH, B., PODUST, V. N., FOURKALA, E. O., CUBIZOLLES, M., KRONENBERG, F., FUNG, E. T., GENTRY-MAHARAJ, A., MENON, U. & JACOBS, I. 2014. Discovery of serum biomarkers of ovarian cancer using complementary proteomic profiling strategies. *Proteomics Clin Appl*, 8, 982-93.
- TOOLEY, C. E., PETKOWSKI, J. J., MURATORE-SCHROEDER, T. L., BALSBAUGH, J. L., SHABANOWITZ, J., SABAT, M., MINOR, W., HUNT, D. F. & MACARA, I. G. 2010. NRMT is an alpha-N-methyltransferase that methylates RCC1 and retinoblastoma protein. *Nature*, 466, 1125-8.
- TOSTAIN, J., LI, G., GENTIL-PERRET, A. & GIGANTE, M. 2010. Carbonic anhydrase 9 in clear cell renal cell carcinoma: a marker for diagnosis, prognosis and treatment. *European journal of cancer*, 46, 3141-8.
- TRAN, H. T., LIU, Y., ZURITA, A. J., LIN, Y., BAKER-NEBLETT, K. L., MARTIN, A. M., FIGLIN, R. A., HUTSON, T. E., STERNBERG, C. N., AMADO, R. G., PANDITE, L. N. & HEYMACH, J. V. 2012. Prognostic or predictive plasma cytokines and angiogenic factors for patients treated with pazopanib for metastatic renal-cell cancer: a retrospective analysis of phase 2 and phase 3 trials. *Lancet Oncol*, 13, 827-37.
- TRUONG, L. D. & SHEN, S. S. 2011. Immunohistochemical diagnosis of renal neoplasms. *Arch Pathol Lab Med*, 135, 92-109.
- TU, C., RUDNICK, P. A., MARTINEZ, M. Y., CHEEK, K. L., STEIN, S. E., SLEBOS, R. J. & LIEBLER, D. C. 2010. Depletion of abundant plasma proteins and limitations of plasma proteomics. *Journal of proteome research*, 9, 4982-91.

- TWAL, W. O., CZIROK, A., HEGEDUS, B., KNAAK, C., CHINTALAPUDI, M. R., OKAGAWA, H., SUGI, Y. & ARGRAVES, W. S. 2001. Fibulin-1 suppression of fibronectin-regulated cell adhesion and motility. *J Cell Sci*, 114, 4587-98.
- UENO, D., YAO, M., TATEISHI, U., MINAMIMOTO, R., MAKIYAMA, K., HAYASHI, N., SANO, F., MURAKAMI, T., KISHIDA, T., MIURA, T., KOBAYASHI, K., NOGUCHI, S., IKEDA, I., OHGO, Y., INOUE, T., KUBOTA, Y. & NAKAIGAWA, N. 2012. Early assessment by FDG-PET/CT of patients with advanced renal cell carcinoma treated with tyrosine kinase inhibitors is predictive of disease course. *BMC cancer*, 12, 162.
- VAINIO, P., LEHTINEN, L., MIRTITI, T., HILVO, M., SEPPANEN-LAAKSO, T., VIRTANEN, J., SANKILA, A., NORDLING, S., LUNDIN, J., RANNIKKO, A., ORESIC, M., KALLIONIEMI, O. & ILJIN, K. 2011. Phospholipase PLA2G7, associated with aggressive prostate cancer, promotes prostate cancer cell migration and invasion and is inhibited by statins. *Oncotarget*, 2, 1176-90.
- VALERA, V. A. & MERINO, M. J. 2011. Misdiagnosis of clear cell renal cell carcinoma. *Nature reviews. Urology*, 8, 321-33.
- VAN DEN ELSEN, J. M., KUNTZ, D. A. & ROSE, D. R. 2001. Structure of Golgi alpha-mannosidase II: a target for inhibition of growth and metastasis of cancer cells. *EMBO J*, 20, 3008-17.
- VAN DER VELDT, A. A., DE BOER, M. P., BOVEN, E., ERINGA, E. C., VAN DEN EERTWEGH, A. J., VAN HINSBERGH, V. W., SMULDERS, Y. M. & SERNE, E. H. 2010a. Reduction in skin microvascular density and changes in vessel morphology in patients treated with sunitinib. *Anticancer Drugs*, 21, 439-46.
- VAN DER VELDT, A. A., ECHOUTE, K., GELDERBLOM, H., GIETEMA, J., GUCHELAAR, H. J., VAN ERP, N. P., VAN DEN EERTWEGH, A. J., HAANEN, J. B., MATHIJSSSEN, R. H. & WESSELS, J. A. 2011. Genetic polymorphisms associated with a prolonged progression-free survival in patients with metastatic renal cell cancer treated with sunitinib. *Clin Cancer Res*, 17, 620-9.
- VAN DER VELDT, A. A., MEIJERINK, M. R., VAN DEN EERTWEGH, A. J., HAANEN, J. B. & BOVEN, E. 2010b. Choi response criteria for early prediction of clinical outcome in patients with metastatic renal cell cancer treated with sunitinib. *British journal of cancer*, 102, 803-9.
- VAN LIER, R. A., BORST, J., VROOM, T. M., KLEIN, H., VAN MOURIK, P., ZEIJLEMAKER, W. P. & MELIEF, C. J. 1987. Tissue distribution and biochemical and functional properties of Tp55 (CD27), a novel T cell differentiation antigen. *J Immunol*, 139, 1589-96.
- VAN OOSTERWIJK, M. F., JUWANA, H., ARENS, R., TESSELAAR, K., VAN OERS, M. H., ELDERING, E. & VAN LIER, R. A. 2007. CD27-CD70 interactions sensitise naive CD4+ T cells for IL-12-induced Th1 cell development. *Int Immunol*, 19, 713-8.
- VARAMBALLY, S., LAXMAN, B., MEHRA, R., CAO, Q., DHANASEKARAN, S. M., TOMLINS, S. A., GRANGER, J., VELLAICHAMY, A., SREEKUMAR, A., YU, J., GU, W., SHEN, R., GHOSH, D., WRIGHT, L. M., KLDNEY, R. D., KUEFER, R., RUBIN, M. A., FIMMEL, C. J. & CHINNAIYAN, A. M. 2008. Golgi protein GOLM1 is a tissue and urine biomarker of prostate cancer. *Neoplasia*, 10, 1285-94.
- VARELA, I., TARPEY, P., RAINE, K., HUANG, D., ONG, C. K., STEPHENS, P., DAVIES, H., JONES, D., LIN, M. L., TEAGUE, J., BIGNELL, G., BUTLER, A., CHO, J., DALGLIESH, G. L., GALAPPATHTHIGE, D., GREENMAN, C., HARDY, C., JIA, M., LATIMER, C., LAU, K. W., MARSHALL, J., MCLAREN, S., MENZIES, A., MUDIE, L., STEBBINGS, L., LARGAESPADA, D. A., WESSELS, L. F., RICHARD, S., KAHNOSKI, R. J., ANEMA, J., TUVESON,

- D. A., PEREZ-MANCERA, P. A., MUSTONEN, V., FISCHER, A., ADAMS, D. J., RUST, A., CHAN-ON, W., SUBIMERB, C., DYKEMA, K., FURGE, K., CAMPBELL, P. J., TEH, B. T., STRATTON, M. R. & FUTREAL, P. A. 2011. Exome sequencing identifies frequent mutation of the SWI/SNF complex gene PBRM1 in renal carcinoma. *Nature*, 469, 539-42.
- VASUDEV, N. S., GOH, V., JUTTLA, J. K., THOMPSON, V. L., LARKIN, J. M., GORE, M., NATHAN, P. D. & REYNOLDS, A. R. 2013. Changes in tumour vessel density upon treatment with anti-angiogenic agents: relationship with response and resistance to therapy. *British journal of cancer*, 109, 1230-42.
- VASUDEV, N. S. & REYNOLDS, A. R. 2014. Anti-angiogenic therapy for cancer: current progress, unresolved questions and future directions. *Angiogenesis*, 17, 471-94.
- VASUDEV, N. S., SELBY, P. J. & BANKS, R. E. 2012. Renal cancer biomarkers: the promise of personalized care. *BMC Med*, 10, 112.
- VEIGA-DA-CUNHA, M., CHEVALIER, N., STROOBANT, V., VERTOMMEN, D. & VAN SCHAFTINGEN, E. 2014. Metabolite proofreading in carnosine and homocarnosine synthesis: molecular identification of PM20D2 as beta-alanyl-lysine dipeptidase. *J Biol Chem*, 289, 19726-36.
- VIRTANEN, S. S., KUKKONEN-MACCHI, A., VAINIO, M., ELIMA, K., HARKONEN, P. L., JALKANEN, S. & YEGUTKIN, G. G. 2014. Adenosine Inhibits Tumor Cell Invasion via Receptor-Independent Mechanisms. *Mol Cancer Res*.
- VOGEL, C. & MARCOTTE, E. M. 2012. Insights into the regulation of protein abundance from proteomic and transcriptomic analyses. *Nat Rev Genet*, 13, 227-32.
- VON HAUSSEN, J., KOCZULLA, R., SHAYKHIEV, R., HERR, C., PINKENBURG, O., REIMER, D., WIEWRODT, R., BIESTERFELD, S., AIGNER, A., CZUBAYKO, F. & BALS, R. 2008. The host defence peptide LL-37/hCAP-18 is a growth factor for lung cancer cells. *Lung Cancer*, 59, 12-23.
- WADA, T. & PENNINGER, J. M. 2004. Mitogen-activated protein kinases in apoptosis regulation. *Oncogene*, 23, 2838-49.
- WANG, G. L., JIANG, B. H., RUE, E. A. & SEMENZA, G. L. 1995. Hypoxia-inducible factor 1 is a basic-helix-loop-helix-PAS heterodimer regulated by cellular O₂ tension. *Proceedings of the National Academy of Sciences of the United States of America*, 92, 5510-4.
- WANG, J., CHEN, L., LI, Y. & GUAN, X. Y. 2011. Overexpression of cathepsin Z contributes to tumor metastasis by inducing epithelial-mesenchymal transition in hepatocellular carcinoma. *PLoS one*, 6, e24967.
- WARBURG, O. 1956. On the origin of cancer cells. *Science*, 123, 309-14.
- WARDE-FARLEY, D., DONALDSON, S. L., COMES, O., ZUBERI, K., BADRAWI, R., CHAO, P., FRANZ, M., GROUIOS, C., KAZI, F., LOPES, C. T., MAITLAND, A., MOSTAFAVI, S., MONTOJO, J., SHAO, Q., WRIGHT, G., BADER, G. D. & MORRIS, Q. 2010. The GeneMANIA prediction server: biological network integration for gene prioritization and predicting gene function. *Nucleic Acids Res*, 38, W214-20.
- WEBB, N. J., MYERS, C. R., WATSON, C. J., BOTTOMLEY, M. J. & BRENCHLEY, P. E. 1998. Activated human neutrophils express vascular endothelial growth factor (VEGF). *Cytokine*, 10, 254-7.
- WEI, K., PIECEWICZ, S. M., MCGINNIS, L. M., TANIGUCHI, C. M., WIEGAND, S. J., ANDERSON, K., CHAN, C. W., MULLIGAN, K. X., KUO, D., YUAN, J., VALLON, M., MORTON, L. C., LEFAL, E., SIMON, M. C., MAHER, J. J., MITHIEUX, G., RAJAS, F., ANNES, J. P., MCGUINNESS, O. P., THURSTON, G., GIACCIA, A. J. & KUO, C. J. 2013. A liver Hif-2alpha-Irs2 pathway sensitizes hepatic insulin signaling and is modulated by Vegf inhibition. *Nat Med*, 19, 1331-7.

- WEIGEL, M. T. & DOWSETT, M. 2010. Current and emerging biomarkers in breast cancer: prognosis and prediction. *Endocr Relat Cancer*, 17, R245-62.
- WEIKERT, S., BOEING, H., PISCHON, T., WEIKERT, C., OLSEN, A., TJONNELAND, A., OVERVAD, K., BECKER, N., LINSEISEN, J., TRICHOPOULOU, A., MOUNTOKALAKIS, T., TRICHOPOULOS, D., SIERI, S., PALLI, D., VINEIS, P., PANICO, S., PEETERS, P. H., BUENO-DE-MESQUITA, H. B., VERSCHUREN, W. M., LJUNGBERG, B., HALLMANS, G., BERGLUND, G., GONZALEZ, C. A., DORRONSORO, M., BARRICARTE, A., TORMO, M. J., ALLEN, N., RODDAM, A., BINGHAM, S., KHAW, K. T., RINALDI, S., FERRARI, P., NORAT, T. & RIBOLI, E. 2008. Blood pressure and risk of renal cell carcinoma in the European prospective investigation into cancer and nutrition. *American journal of epidemiology*, 167, 438-46.
- WEINSTEIN, J. N., COLLISSON, E. A., MILLS, G. B., SHAW, K. R., OZENBERGER, B. A., ELLROTT, K., SHMULEVICH, I., SANDER, C. & STUART, J. M. 2013. The Cancer Genome Atlas Pan-Cancer analysis project. *Nat Genet*, 45, 1113-20.
- WELBERRY SMITH, M. P., ZOUGMAN, A., CAIRNS, D. A., WILSON, M., WIND, T., WOOD, S. L., THOMPSON, D., MESSENGER, M. P., MOONEY, A., SELBY, P. J., LEWINGTON, A. J. & BANKS, R. E. 2013. Serum aminoacylase-1 is a novel biomarker with potential prognostic utility for long-term outcome in patients with delayed graft function following renal transplantation. *Kidney Int*, 84, 1214-25.
- WHITE, M. F. 1998. The IRS-signalling system: a network of docking proteins that mediate insulin action. *Mol Cell Biochem*, 182, 3-11.
- WHITE, M. F. 2002. IRS proteins and the common path to diabetes. *Am J Physiol Endocrinol Metab*, 283, E413-22.
- WIESMANN, A., PHILLIPS, R. L., MOJICA, M., PIERCE, L. J., SEARLES, A. E., SPANGRUDE, G. J. & LEMISCHKA, I. 2000. Expression of CD27 on murine hematopoietic stem and progenitor cells. *Immunity*, 12, 193-9.
- WILHELM, M., SCHLEGL, J., HAHNE, H., MOGHADDAS GHOLAMI, A., LIEBERENZ, M., SAVITSKI, M. M., ZIEGLER, E., BUTZMANN, L., GESSULAT, S., MARX, H., MATHIESON, T., LEMEER, S., SCHNATBAUM, K., REIMER, U., WENSCHUH, H., MOLLENHAUER, M., SLOTTA-HUSPENINA, J., BOESE, J. H., BANTSCHIEFF, M., GERSTMAYER, A., FAERBER, F. & KUSTER, B. 2014. Mass-spectrometry-based draft of the human proteome. *Nature*, 509, 582-7.
- WISCHHUSEN, J., JUNG, G., RADOVANOVIC, I., BEIER, C., STEINBACH, J. P., RIMNER, A., HUANG, H., SCHULZ, J. B., OHGAKI, H., AGUZZI, A., RAMMENSEE, H. G. & WELLER, M. 2002. Identification of CD70-mediated apoptosis of immune effector cells as a novel immune escape pathway of human glioblastoma. *Cancer Res*, 62, 2592-9.
- WISNIEWSKI, J. R., ZOUGMAN, A., NAGARAJ, N. & MANN, M. 2009. Universal sample preparation method for proteome analysis. *Nat Methods*, 6, 359-62.
- WOLTER, P., STEFAN, C., DECALLONNE, B., DUMEZ, H., FIEUWS, S., WILDIERS, H., CLEMENT, P., DEBAERE, D., VAN OOSTEROM, A. & SCHOFFSKI, P. 2008. Evaluation of thyroid dysfunction as a candidate surrogate marker for efficacy of sunitinib in patients (pts) with advanced renal cell cancer (RCC). *Journal of Clinical Oncology*, 26.
- WOOD, S. L., KNOWLES, M. A., THOMPSON, D., SELBY, P. J. & BANKS, R. E. 2013. Proteomic studies of urinary biomarkers for prostate, bladder and kidney cancers. *Nat Rev Urol*, 10, 206-18.
- XIE, C., MAO, X., HUANG, J., DING, Y., WU, J., DONG, S., KONG, L., GAO, G., LI, C. Y. & WEI, L. 2011a. KOBAS 2.0: a web server for annotation and

- identification of enriched pathways and diseases. *Nucleic Acids Res*, 39, W316-22.
- XIE, L. X., HSIEH, E. J., WATANABE, S., ALLAN, C. M., CHEN, J. Y., TRAN, U. C. & CLARKE, C. F. 2011b. Expression of the human atypical kinase ADCK3 rescues coenzyme Q biosynthesis and phosphorylation of Coq polypeptides in yeast *coq8* mutants. *Biochim Biophys Acta*, 1811, 348-60.
- XU, C., REICHERT, E. C., NAKANO, T., LOHSE, M., GARDNER, A. A., REVELO, M. P., TOPHAM, M. K. & STAFFORINI, D. M. 2013. Deficiency of phospholipase A2 group 7 decreases intestinal polyposis and colon tumorigenesis in *Apc(Min/+)* mice. *Cancer research*, 73, 2806-16.
- XU, H. N., KADLECECK, S., PROFKA, H., GLICKSON, J. D., RIZI, R. & LI, L. Z. 2014. Is higher lactate an indicator of tumor metastatic risk? A pilot MRS study using hyperpolarized (¹³C)-pyruvate. *Acad Radiol*, 21, 223-31.
- XU, X. M., CARLSON, B. A., IRONS, R., MIX, H., ZHONG, N., GLADYSHEV, V. N. & HATFIELD, D. L. 2007. Selenophosphate synthetase 2 is essential for selenoprotein biosynthesis. *Biochem J*, 404, 115-20.
- XU, Z. G., DU, J. J., ZHANG, X., CHENG, Z. H., MA, Z. Z., XIAO, H. S., YU, L., WANG, Z. Q., LI, Y. Y., HUO, K. K. & HAN, Z. G. 2003. A novel liver-specific zona pellucida domain containing protein that is expressed rarely in hepatocellular carcinoma. *Hepatology*, 38, 735-44.
- YAMAUCHI, T., KABURAGI, Y., UEKI, K., TSUJI, Y., STARK, G. R., KERR, I. M., TSUSHIMA, T., AKANUMA, Y., KOMURO, I., TOBE, K., YAZAKI, Y. & KADOWAKI, T. 1998. Growth hormone and prolactin stimulate tyrosine phosphorylation of insulin receptor substrate-1, -2, and -3, their association with p85 phosphatidylinositol 3-kinase (PI3-kinase), and concomitantly PI3-kinase activation via JAK2 kinase. *J Biol Chem*, 273, 15719-26.
- YAN, B., ZHANG, Z. Z., HUANG, L. Y., SHEN, H. L. & HAN, Z. G. 2012. OIT3 deficiency impairs uric acid reabsorption in renal tubule. *FEBS letters*, 586, 760-5.
- YAN, L., BORREGAARD, N., KJELDSSEN, L. & MOSES, M. A. 2001. The high molecular weight urinary matrix metalloproteinase (MMP) activity is a complex of gelatinase B/MMP-9 and neutrophil gelatinase-associated lipocalin (NGAL). Modulation of MMP-9 activity by NGAL. *J Biol Chem*, 276, 37258-65.
- YANG, J., YANG, J., GAO, Y., ZHAO, L., LIU, L., QIN, Y., WANG, X., SONG, T. & HUANG, C. 2014. Identification of potential serum proteomic biomarkers for clear cell renal cell carcinoma. *PLoS One*, 9, e111364.
- YANG, L., DEBUSK, L. M., FUKUDA, K., FINGLETON, B., GREEN-JARVIS, B., SHYR, Y., MATRISIAN, L. M., CARBONE, D. P. & LIN, P. C. 2004. Expansion of myeloid immune suppressor Gr⁺CD11b⁺ cells in tumor-bearing host directly promotes tumor angiogenesis. *Cancer Cell*, 6, 409-21.
- YANG, Z. Z. & ZOU, A. P. 2001. Transcriptional regulation of heme oxygenases by HIF-1 α in renal medullary interstitial cells. *Am J Physiol Renal Physiol*, 281, F900-8.
- YAO, M., HUANG, Y., SHIOI, K., HATTORI, K., MURAKAMI, T., NAKAIGAWA, N., KISHIDA, T., NAGASHIMA, Y. & KUBOTA, Y. 2007. Expression of adipose differentiation-related protein: a predictor of cancer-specific survival in clear cell renal carcinoma. *Clin Cancer Res*, 13, 152-60.
- YAO, M., TABUCHI, H., NAGASHIMA, Y., BABA, M., NAKAIGAWA, N., ISHIGURO, H., HAMADA, K., INAYAMA, Y., KISHIDA, T., HATTORI, K., YAMADA-OKABE, H. & KUBOTA, Y. 2005. Gene expression analysis of renal carcinoma: adipose differentiation-related protein as a potential diagnostic and prognostic biomarker for clear-cell renal carcinoma. *The Journal of pathology*, 205, 377-87.

- YARWOOD, H., MASON, J. C., MAHIOUZ, D., SUGARS, K. & HASKARD, D. O. 2000. Resting and activated T cells induce expression of E-selectin and VCAM-1 by vascular endothelial cells through a contact-dependent but CD40 ligand-independent mechanism. *J Leukoc Biol*, 68, 233-42.
- YOU, D., SONG, S. H., CHO, Y. M., LEE, J. L., JEONG, I. G., SONG, C., HONG, J. H., KIM, C. S. & AHN, H. 2014. Predictive role of tissue-based molecular markers in patients treated with sunitinib for metastatic renal cell carcinoma. *World journal of urology*.
- YOUNG, A. C., CRAVEN, R. A., COHEN, D., TAYLOR, C., BOOTH, C., HARNDEN, P., CAIRNS, D. A., ASTUTI, D., GREGORY, W., MAHER, E. R., KNOWLES, M. A., JOYCE, A., SELBY, P. J. & BANKS, R. E. 2009. Analysis of VHL Gene Alterations and their Relationship to Clinical Parameters in Sporadic Conventional Renal Cell Carcinoma. *Clinical cancer research : an official journal of the American Association for Cancer Research*, 15, 7582-7592.
- YOUSSEF, Y. M., WHITE, N. M., GRIGULL, J., KRIZOVA, A., SAMY, C., MEJIA-GUERRERO, S., EVANS, A. & YOUSEF, G. M. 2011. Accurate molecular classification of kidney cancer subtypes using microRNA signature. *European urology*, 59, 721-30.
- YU, H. & JOVE, R. 2004. The STATs of cancer--new molecular targets come of age. *Nat Rev Cancer*, 4, 97-105.
- YUASA, T., URAKAMI, S., YAMAMOTO, S., YONESE, J., NAKANO, K., KODAIRA, M., TAKAHASHI, S., HATAKE, K., INAMURA, K., ISHIKAWA, Y. & FUKUI, I. 2011. Tumor size is a potential predictor of response to tyrosine kinase inhibitors in renal cell cancer. *Urology*, 77, 831-5.
- ZBAR, B., KISHIDA, T., CHEN, F., SCHMIDT, L., MAHER, E. R., RICHARDS, F. M., CROSSEY, P. A., WEBSTER, A. R., AFFARA, N. A., FERGUSON-SMITH, M. A., BRAUCH, H., GLAVAC, D., NEUMANN, H. P., TISHERMAN, S., MULVIHILL, J. J., GROSS, D. J., SHUIN, T., WHALEY, J., SEIZINGER, B., KLEY, N., OLSCHWANG, S., BOISSON, C., RICHARD, S., LIPS, C. H., LERMAN, M. & ET AL. 1996. Germline mutations in the Von Hippel-Lindau disease (VHL) gene in families from North America, Europe, and Japan. *Hum Mutat*, 8, 348-57.
- ZHA, X., WANG, F., WANG, Y., HE, S., JING, Y., WU, X. & ZHANG, H. 2011. Lactate dehydrogenase B is critical for hyperactive mTOR-mediated tumorigenesis. *Cancer Res*, 71, 13-8.
- ZHANG, J. G., FARLEY, A., NICHOLSON, S. E., WILLSON, T. A., ZUGARO, L. M., SIMPSON, R. J., MORITZ, R. L., CARY, D., RICHARDSON, R., HAUSMANN, G., KILE, B. J., KENT, S. B., ALEXANDER, W. S., METCALF, D., HILTON, D. J., NICOLA, N. A. & BACA, M. 1999. The conserved SOCS box motif in suppressors of cytokine signaling binds to elongins B and C and may couple bound proteins to proteasomal degradation. *Proc Natl Acad Sci U S A*, 96, 2071-6.
- ZHAO, Z., WU, F., DING, S., SUN, L., LIU, Z., DING, K. & LU, J. 2014. Label-free quantitative proteomic analysis reveals potential biomarkers and pathways in renal cell carcinoma. *Tumour Biol*.
- ZHOU, M. I., FOY, R. L., CHITALIA, V. C., ZHAO, J., PANCHENKO, M. V., WANG, H. & COHEN, H. T. 2005. Jade-1, a candidate renal tumor suppressor that promotes apoptosis. *Proceedings of the National Academy of Sciences of the United States of America*, 102, 11035-40.
- ZHOU, M. I., WANG, H., FOY, R. L., ROSS, J. J. & COHEN, H. T. 2004. Tumor suppressor von Hippel-Lindau (VHL) stabilization of Jade-1 protein occurs through plant homeodomains and is VHL mutation dependent. *Cancer research*, 64, 1278-86.

- ZHUANG, Z., BERTHEAU, P., EMMERT-BUCK, M. R., LIOTTA, L. A., GNARRA, J., LINEHAN, W. M. & LUBENSKY, I. A. 1995. A microdissection technique for archival DNA analysis of specific cell populations in lesions < 1 mm in size. *Am J Pathol*, 146, 620-5.
- ZISMAN, A., PANTUCK, A. J., DOREY, F., SAID, J. W., SHVARTS, O., QUINTANA, D., GITLITZ, B. J., DEKERNION, J. B., FIGLIN, R. A. & BELLDEGRUN, A. S. 2001. Improved prognostication of renal cell carcinoma using an integrated staging system. *J Clin Oncol*, 19, 1649-57.
- ZOUGMAN, A., SELBY, P. J. & BANKS, R. E. 2014. Suspension trapping (STrap) sample preparation method for bottom-up proteomics analysis. *Proteomics*, 14, 1006-0.

Appendix 1

List of Suppliers

Abcam plc

330 Cambridge Science Park
Cambridge
CB4 0FL

Agilent Technologies UK Ltd

Mead road
Yarnton
Kidlington
OX5 1QU

Dako

Cambridge House
St Thomas Place
Ely
Cambridgeshire
CB7 4EX

Eppendorf UK Ltd

Eppendorf House
Gateway 1000 Whittle Way
Arlington Business Park
Stevenage
SG1 2FP

GE Healthcare Life Sciences

Amersham Place
Little Chalfont
Buckinghamshire

Affymetrix UK Ltd

Voyager, Mercury Park,
Wycombe Lane Wooburn Green,
High Wycombe
HP10 0HH

BioRad

Bio-Rad Laboratories Ltd.
Bio-Rad House, Maxted Road
Hemel Hempstead
Hertfordshire HP2 7DX

EMD Millipore

Suite 3 & 5, Building 6, Croxley Green
Business Park
Watford
Hertfordshire
WD18 8YH

Eurogentec

Old Headmasters House
Unit 1, Building 1
Forest Business Centre
Fawley Road, Fawley
Southampton
SO45 1FJ

Greiner BioOne Ltd

Brunel Way
Stroudwater Business Park
Stonehouse

HP7 9NA UK

GL10 3 SX

Jasco

Oak Industrial Park
Chelmsford Road
Dunmow
CM6 1XN

Konica Minolta

Medical and Graphic Imaging
Barford road
Banbury
OX15 4FF

Leica Biosystems Ltd

Balliol Business Park West
Newcastle Upon Tyne
NE12 8EW

Life Technologies Ltd

3 Fountain Drive
Inchinnan Business Park
Paisley
PA4 9RF

Molecular Devices, LLC

1311 Orleans Drive
Sunnyvale CA 94089
USA

Munktell Filter ab

Box 1003
S-791 10 Falun
Sweden

MSE (UK) Ltd

Worsley Bridge Road
Lower Sydenham
London
SE26 5AZ

Pall Life Sciences

5 Harbourgate Business Park
Southampton Road
Portsmouth
PO6 4BQ

Promega UK

Delta House
Southampton Science Park
Southampton
SO16 7NS

Qiagen

House Fleming Way
Crawley
West Sussex
RH10 9NQ

Roche Diagnostics

Charles Avenue
Burgess Hill
West Sussex
RH15 9RY

SDIX

Corporate Headquarters
111 Pencader Drive
Newark
Delaware 19702

USA

Sigma-Aldrich Company Ltd

Fancy Rd
Poole
Dorset
BH12 4QH

SoftGenetics

100 Oakwood Ave
Suite 350
State College
PA 16803
USA

Sterlitech Corporation

22027 70th Avenue South
Kent
WA 98032
USA

Thermo Fisher UK Ltd

Stafford House
Boundary Way
Hemel Hempstead
HP2 7GE

Vector Laboratories

3, Ascent Park
Bakewell road
Orton Southgate
Peterborough
PE2 6XS